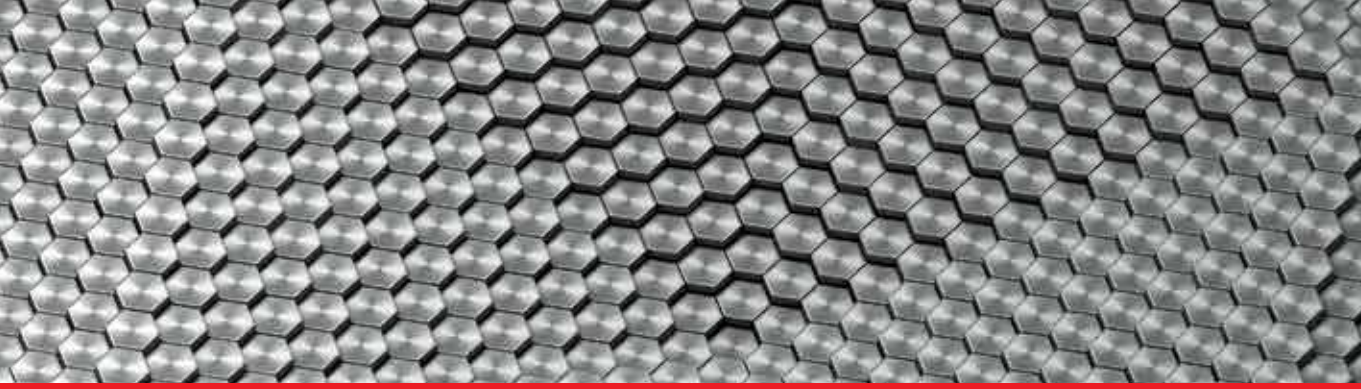

IntechOpen

Nanomaterials

Toxicity and Risk Assessment

Edited by Sonia Soloneski and Marcelo L. Larramendy

NANOMATERIALS - TOXICITY AND RISK ASSESSMENT

Edited by **Sonia Soloneski** and **Marcelo L. Larramendy**

Nanomaterials - Toxicity and Risk Assessment
http://dx.doi.org/10.5772/59381
Edited by Sonia Soloneski and Marcelo L. Larramendy

Contributors

Tifeng Jiao, Simona Clichici, Gabriela Adriana Filip, Manuel Fuentes, Guoan Xiang, Anton Ficai, Denisa Ficai, Ecaterina Andronescu, Eleonore Fröhlich, Claudia Meindl, Denis Girard, Tao Chen, Xiaoqing Guo, Krzysztof Siemianowicz, Wirginia Likus, Jarosław Markowski

Notice

First published in Croatia, 2015 by INTECH d.o.o.
eBook (PDF) Published by IN TECH d.o.o.
Place and year of publication of eBook (PDF): Rijeka, 2019.
IntechOpen is the global imprint of IN TECH d.o.o.
Printed in Croatia

Legal deposit, Croatia: National and University Library in Zagreb

Additional hard and PDF copies can be obtained from orders@intechopen.com

Nanomaterials - Toxicity and Risk Assessment
Edited by Sonia Soloneski and Marcelo L. Larramendy

p. cm.

ISBN 978-953-51-2143-5

eBook (PDF) ISBN 978-953-51-4219-5

Meet the editors

Sonia Soloneski is PhD in Natural Sciences and Professor Assistant of Molecular Cell Biology at the Faculty of Natural Sciences and Museum of La Plata, National University of La Plata, Argentina. She became a member of the National Scientific and Technological Research Council (CONICET) of Argentina in Genetic Toxicology field. Presently, she is member of the Latin American Association of Environmental Mutagenesis, Teratogenesis and Carcinogenesis (ALAMCTA), the Argentinian Society of Toxicology (ATA), and the Argentinian Society of Genetics (SAG). She is author of more than 270 scientific publications in the field, including scientific publications in research papers, reviewed journals, and conferences worldwide. She is a regular lecturer at the international A. Hollaender Courses by the International Association of Environmental Mutagen Societies (IAEMS). She is a referent for issues related to Mutagenesis, Genetic Toxicology, and Ecotoxicology field.

Marcelo L. Larramendy, PhD, serves as Professor of Molecular Cell Biology at the School of Natural Sciences and Museum (National University of La Plata, Argentina). He is appointed as Senior Researcher of the National Scientific and Technological Research Council of Argentina. He is also a former member of the Executive Committee of the Latin American Association of Environmental Mutagensis, Teratogenesis and Carcinogenesis. He is author of more than 450 contributions, including scientific publications, research communications, and conferences worldwide. Dr. Larramendy has received several national and international awards. Dr. Larramendy is a regular lecturer at the international A. Hollaender Courses organized by the International Association of Environmental Mutagenesis Societies and former guest scientist at National Institutes of Health (USA) and University of Helsinki (Finland). He is expert in Genetic Toxicology and has been referee for more than 20 international scientific journals.

Contents

Preface

The nanoscience revolution started in the 1990s, with this emerging area of science having the potential to generate radical new products and processes. It has been estimated that production of nanomaterials will increase by 2020 to 25 times what it is today. Nanoparticles have dimensions ranging from 1 to 100 nanometers, and they present physicochemical characteristics and coatings that impart upon them unique electrical, thermal, mechanical, and imaging properties that make them highly attractive for applications within the commercial, pharmaceutical, medical, food packaging, cosmetics, household appliance, and environmental sectors. Today, the challenge to create awareness and gain acceptance of the use of nanomaterials in an extensive range of available products, including specifically those engineered for applications in human welfare, has issued serious public concern, mostly related to their use. Potential occupational and public exposure to nanomaterials will increase considerably due to the ability of nanoparticles to improve the quality and the performance of many daily consumer products as well as the development of medical therapies and tests that use nanoparticles. Now, they represent an imperative research target for discovering whether they represent a potential hazard to human health and the environment.

In recent years, proactive multidisciplinary research initiatives have been established by regulatory institutions such as the US Environmental Protection Agency, the National Institute of Environmental Health, and the International Agency of Research on Cancer that are charged with the protection of human health and the environment, ensuring that the employment of engineered nanotechnological products can occur without unreasonable harm to either. Concerns as to the risk of natural and anthropogenic nanomaterials on numerous parameters, such as physical and chemical properties, uptake, distribution, absorption, and interactions with organs, the immune system, and the environment, require that the adequacy of current toxicity bioassays for nanoscale materials be assessed to develop an effective approach for further evaluation of nanomaterial toxicity. Workers who use nanomaterials in research or in nanotechnology-related industries may be exposed to several nanoparticles through dermal contact, inhalation, or ingestion, depending upon how these workers use and handle them. Occupational health risks associated with manufacturing and using nanomaterials are not yet clearly understood. Minimal information is currently available on dominant exposure routes, potential exposure levels, and material toxicity of nanoscale materials. Although the potential health effects of such exposure are not entirely understood at this time, research investigations indicate that at least some of these nanomaterials are biologically active and may readily penetrate intact human epithelium, and they have produced toxicological reactions in the lungs of exposed experimental animals. There is general recognition that the in vitro, in vivo, and in silico testing strategies and safety assessments currently in place can be used as well for nanomaterials as for any other chemicals to obtain

relevant data to develop guidelines for regulating the exposure of nanomaterials in the environment.

Research in the field of emerging nanomaterials and nanotechnologies is of increasing importance; most scientific databases reveal increasing numbers of publications such as books, papers, reviews, and even patents, and there is an increasing market share of nanotechnology products in the thousands of billon US dollars worldwide. Furthermore, the number of publications on the topic of nanomaterials has increased at an almost exponential rate since the early 1990s, reaching about 192,000 in the year 2014, as indicated by a search on the Scopus database. However, more efforts are clearly needed to improve the toxicity screening of the increasing number of nanomaterials.

This book, *Nanomaterials - Toxicity and Risk Assessment* , consisting of nine chapters, is a collection of current research and information on numerous advances on the toxicity and hazardous effects of nanomaterials, including theoretical and experimental approaches as well as nanotechnology applications in the field of medicine, pharmacology, and the manufacture of nanoscale materials. Based on the large number of nanomaterial applications, a careful understanding of the associated systemic and local toxicity is critically required.

We aimed to compress information from a diversity of sources into a single volume. The first chapter includes details of the advances in the field of nanoparticle-mediated cancer treatment, with special attention devoted to the use of magnetite and silver nanoparticles. The second chapter is a comprehensive review of recent developments and an outline of future strategies for nanotechnology-based medicines requested by the National Cancer Institute, with special attention on in vivo and in vitro trial systems employing biocompatibility and immunological studies. The third chapter provides a good review summarizing the current literature dealing with the direct interaction of nanoparticles with human neutrophils as well as recent data showing the murine air pouch model of inflammation for evaluation of nanoparticle toxicity. The fourth and fifth chapters of this book provide, respectively, an in vitro chronic study on respiratory cells exposed to nanoparticles to study the physiologically relevant exposure of prolonged contact to nanoparticles by respiratory exposure and a detailed update of in vivo and in vitro methodologies in nanomaterial toxicity evaluation, focusing on different testing strategies currently in place to find the appropriate analysis methods and the cautions that should be taken in the design of experiments that will contribute to the better understanding of the mechanisms of nanomaterial toxicity. The sixth chapter provides an in vitro study employing single-walled carbon nanohorns for the estimation of several cytotoxic parameters on human liver cell lines, with special emphasis on the apoptosis mechanism observed in metabolically active liver-like HepG2 cells. The seventh chapter highlights the current progress in the genotoxicity evaluation of engineered nanomaterials with a focus on results from standard genotoxicity bioassays, possible mechanisms underlying the genotoxicity of engineered nanomaterials, the suitability of current genotoxicity bioassays for engineered nanomaterial evaluation, and the application of engineered nanomaterial genotoxicity data for risk assessment. The eighth chapter includes the advances in medical aspects related to the nanomaterial toxicity. Finally, the last chapter addresses investigations into the manufacture of several kinds of nanocomposites, e.g., gold nanoparticles, inorganic–organic hybrid composites, graphene oxide nanocomposites, and supramolecular gels via functionalized imide amphiphiles/binary mixtures, focusing on the potential perspective for the design and fabrication of new nanomaterials and nanocomposites.

This book will serve as a textbook for the research community, academia, and the industry and will provide up-to-date state-of-the-art information presented by recognized international experts in the field of nanotoxicology. They have contributed to the publication of this book of high importance to researchers, scientists, engineers, and graduate students who make use of these different investigations to understand the hazard implications in the use of manufactured and natural nanomaterials. Finally, we expect that the information content in the present book will continue to meet the expectations and needs of all interested in the different aspects of human and environmental risk toxicities associated with exposure to nanomaterials. The publishing Web platform provided by the publisher InTech is gratefully acknowledged.

Sonia Soloneski and Marcelo L. Larramendy
School of Natural Sciences and Museum
National University of La Plata
Argentina

Chapter 1

Advances in Cancer Treatment: Role of Nanoparticles

Denisa Ficai, Anton Ficai and Ecaterina Andronescu

Additional information is available at the end of the chapter

Abstract

This chapter is devoted to the advances in the field of nanoparticles-mediated cancer treatment. A special attention is devoted to the use of magnetite and silver nanoparticles. The synthesis and properties of Fe_3O_4 and Ag nanoparticles as contrast or antitumoral agents as monolith or component of more complex systems such as polymer matrix composite materials based on: polymers (chitosan, collagen, polyethylene glycol, polyacrylates, and polymethacrylates, polylactic acid, etc.) and various antitumoral agents (cytostatics, natural agents and even nanoparticles-magnetite, silver, or gold) are discussed. Special attention is paid for the benefits and risks of using silver and magnetite nanoparticles. In both cases, the discussion focuses on aspects related to diagnosis and treatment of cancer. The influence of size and shape [1-3] is important from the materials characteristics as well as from the biological points of view. The role of magnetite is also analyzed from the point of view of its influence on the delivery of different components of interests (antitumoral components, analgesics/anti-inflammatory agents, etc.). The potentiating effect of the nanoparticles over the cytostatics and natural components is highlighted.

Keywords: cancer, magnetite, silver nanoparticles, diagnosis and treatment, hyperthermia, drug delivery

1. Introduction

Cancer is a real problem of our century and one of the leading causes of death, accounting for one of eight deaths occurring worldwide [4, 5]. Based on the actual data, the International Agency for Research on Cancer (IARC) estimates ~13.1 million deaths associated to cancer by

2030. It is becoming clear for many researchers that the low survival rate is due to the lack of adequate drug delivery systems and not due to the lack of potent, natural, or synthetic antitumoral agents. Therefore, there is a real need to develop carriers and delivery systems which would be able to deliver the chemotherapeutic agents only at the specific target site and improve the efficiency of treatment and consequently limiting the unwanted systemic side effects [6]. Cancer is characterized by rapid, uncontrolled cell differentiation. Due to the fast cell differentiations, the tumor grows fast but the angiogenesis is slower and consequently nonmatured or formative vasculature is characteristic for these tumoral tissues. This is why nanoparticles are able to penetrate the cancer tissue through the leaky vasculature, whereas tight junctions between endothelial cells in healthy tissue do not allow the penetration [7]. Furthermore, cancer tissue lacks a well-formed lymphatic circulation which is responsible for tissue homeostasis. This leads to enhanced retention of particles in cancer tissue. This phenomenon in cancer is called enhanced permeation and retention (EPR) effect. The size of the drug carrier system plays an important role in retention process [8, 9]. Consequently, the use of nanoparticles could be a great opportunity for the treatment of cancer.

Cancer that begins in bone tissue is rare in adults and increases in importance in young people. Bone cancer treatment is a real challenge in this century. It affects especially children and young people/teenagers (10–20 years) – up to 4-7% of all cancers – and rarely appears in old people (less than 0.2% of all cancers) [10-12]. Malignant primary bone tumors are usually associated with an aggressive growth [12]. One of the most common forms of primary bone cancer is osteosarcoma (which counts for ~35.1% of primary bone cancer). In many cases, bone cancer treatment involves surgery, radio- and chemotherapy, even if many unconventional therapies are available; some of the most studied being hyperthermia and photothermia as well as the use of different nanoparticles due too their intrinsic antitumoral activity. Some of our previous works proved the possibility of combining surgery with hyperthermia [13], surgery with chemotherapy [14, 15], as well as surgery with hyperthermia and with antitumoral nanoparticles [16]. The use of these nanoparticles is beneficial because it can lead to a decrease in the amount of cytostatics and consequently lower systemic toxicity due to the use of cytostatics. Beside the treatment, special attention is paid to pain management. In all phases of cancer, the management of pain is present, the analgesics used being gradually changed from mild analgesics to even opioids, especially in the advanced forms of cancer when the treatment is shifted from cure to palliation [17].

Bone cancer treatment involves a different approach compared to other types of cancer especially due to the particularities of the bony tissue. The most important characteristic of the bone tissue, which affects bone cancer treatment, is the low diffusivity of the antitumoral agents inside the tumoral tissue as well as the low penetration ability of different radiations into the bony tissue [18].

Over the past decades, developments in polymer as well as in nanoparticles chemistry have allowed synthesis and conjugation of functionalities which can respond to stimuli. This is an important advance in the field of cancer treatment because it allows not only a passive targeting strategy but also an active targeting strategy by using carrier–monoclonal antibody conjugates and carrier–ligand conjugates, which can be activated at desired moment/site. The stimuli-

responsive polymers can be used in order to design various carrier systems such as micelles, vesicles, liposomes, gels, micro- and nanospheres, micro- and nanoparticles, and core–shell structures [5, 19].

Nanoscience and nanotechnologies are of high interest for researchers from all fields of science allowing exciting opportunities from industry to (nano)medicine, but also unsuspected menace. In most fields, the researches in the field of nanomaterials and nanotechnologies are of increasing importance, the most scientific database revealing increasing number of publications (papers, reviews or even patents) [20, 21], especially increasing market share of the nanotechnology products of thousands of billion Euros [22]. A rational use of the nanotechnologies/nanomaterials must be laid down in order to optimize the opportunities/risks ratio. In the case of cancer and other deadly diseases, higher risks can be assumed in their treatment.

It is well known that there are a lot of "smart polymers" which are stimuli-responsive polymers. They can be "activated" by pH, temperature, light, electric field or even by dual stimuli like pH and ionic strength, pH and redox, pH and temperature, etc. [5, 23], as presented in Scheme 1.

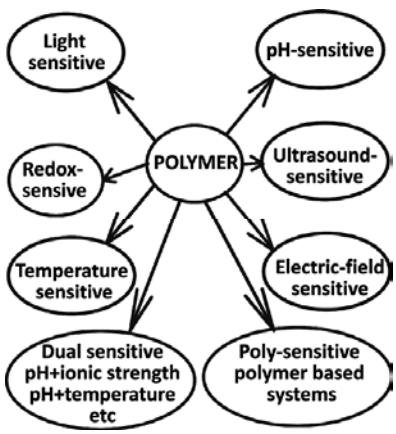

Temperature-responsive polymers:
- Poly(N-isopropylacrylamide);
- Poly(N-vinylcaprolactam);
- Polylactic acid

pH-responsive polymers:
- Poly(acrylic acid);
- Poly(methacrylic acid);
- Poly(lactic-co-glycolic)–polyethylene glycol
- Poly(acetoacetoxyethyl methacrylate);
- Poly[2-(diisopropylamino)ethyl methacrylate];
- Poly(hexyl methacrylate);
- Poly[2-(dimethylamine)ethyl methacrylate)
- poly(methacrylic acid–co-acrylic acid)-co-polyvinyl-pyrrolidone;
- 2-(N,N-diethylamino)ethyl methacrylate;

Light-responsive polymers:
- Poly(N,N-dimethylacrylamide-co-4-phenyl-azophenyl acrylate);
- Poly(N,N-dimethyl acrylamide-co-4-phenyl-azophenyl acrylamide);

Electric field-responsive polymers:
- Poly(dimethylsiloxane);
- Poly[2-(methacryloyloxy)ethyl phosphorylcholine];
- Poly(ethylenediamine-co-1,10-bis(chloro-carbonyl)decane);

Dual-responsive polymers:
- Poly(acrylic acid-graft-vinylidenefluoride) – pH and ionic strength.

Sheme 1. Classes of stimuli-responsive polymers and some of their major representative polymers

However, in most cases, the delivery mechanism is very complex; the contribution of several mechanisms has to be considered. The influence of the temperature, for instance, is important. For instance, even for the non-thermo-sensitive systems the temperature plays an important role, the delivery being influenced. Usually, the temperature can influence the solubility of the drug (usually increasing temperature leads to increased solubility) as well as the mobility/diffusion of the drug (usually these properties increase with the temperature). Similarly, the pH can influence the solubility of the drugs and consequently influence the delivery rate of the active components.

2. Role of magnetite in cancer treatment

Magnetite is widely used in the medical field, being recommended due its native magnetic properties – magnetically guiding possibility, hyperthermia generating property, high loading capacity of many biological active agents, etc. Magnetic systems offer attractive diagnostic and treatment possibilities and consequently there are increasingly studied for a lot of biomedical applications. Superparamagnetic iron oxide nanoparticles (the so-called SPIONs) are usually used for inducing magnetic-field-responsive functionality of drug delivery systems. For this purpose, magnetite and/or maghemite can be further coated with a proper hydrophilic shell. The presence of the shell can dramatically change the properties of the magnetite, making it suitable for a wide range of medical and nonmedical applications. The main applications of magnetite and magnetite-based materials are presented in Scheme 2.

Applications of magnetite and magnetite-based materials

Biomedical applications

- Magnetic resonance imaging (MRI) [24-26]
- Biosensor and bioseparation, including DNA separation and isolation [26, 27]
- Magnetic manipulation of biomolecules [25]
- Drug and gene delivery [28]
- Drug transport [11, 29]
- Cancer therapy by hyperthermia [26] magnetocytolysis
- Tissue engineering [26]

Nonmedical applications

- Permanent magnets
- Ferrofluids for mechano-electrical applications
- Environmental contaminant (organic and inorganic) removal [30, 31]
- Magnetic sealing [32]
- Dampening and cooling mechanisms in loudspeakers

Sheme 2. Applications of magnetite

2.1. Magnetic materials as contrast agents

Iron oxide nanoparticles have been extensively studied as contrast agents for cancer detection and monitoring by MRI. They generally produce enhanced proton relaxation rates at significantly lower doses than paramagnetic ions (Gd^{3+}, for instance) because of their larger magnetic

moment, and they provide negative (dark) contrast by enhancing T_2 relaxivity of water protons.

(Ultrasmall) Super Paramagnetic Iron Oxides are often used for magnetic resonance imaging – MRI. They consist of iron oxide cores, covered by different hydrophilic macromolecules, for example, dextran. Their synthesis is generally realized in one step alkaline precipitation starting from Fe^{2+} and Fe^{3+} aqueous precursors. The shell has three main roles: limit the magnetic core growth during the synthesis, limit the agglomeration due to the sterical repulsion due to the charged nature of the shell, and reduce the *in vivo* opsonization process. In fact, usually these core–shell structures consist of several magnetic cores, more or less aggregated, embedded into a hydrophilic macromolecules, which are sometimes cross-linked in a second step for enhancing the mechanical entrapment [33, 34].

2.2. Magnetic supports for drug delivery systems

Magnetite is widely used for obtaining drug delivery systems because it is a good sorbent; it can be functionalized; and can bind by covalent bonds different drugs, but also because it can be guided in magnetic field into the tumor (tumoral tissue/organ). The magnetically targeted drug delivery involves the loading of the magnetic nanoparticles with the antitumoral drug and the implanting of these magnetite-based nanoparticles into or in the proximity of the tumor or to inject these nanoparticles in the patient body via the circulatory system. Then, the magnetic nanoparticles are concentrated into the tumor by using adequate magnetic field. In this case, the delivery will occur mainly into the tumor and, consequently, the systemic toxicity will be low [35].

The mechanism of delivery can function differently, depending on the internal and external factors, as schematically represented in Scheme 3. These delivery mechanisms can be generally considered for any delivery system as also for magnetic drug delivery systems.

pH-triggered delivery is an essential issue in many medical applications because in many diseases pH changes occur, or once introduced into the body, the delivery must happen at a certain pH which corresponds to the pH of the desired tissue/organ. As presented in Scheme 1, there are a lot of pH-sensitive polymers.

Core–shell structures are often used as drug delivery systems. In the case of magnetite, the extensive use of core–shell structures is explained based on the low chemical stability of the magnetite as well as due to the nonspecific adsorption of plasma proteins and a rapid clearance of the particles by the immune system. The presence of different shells can lead to a strong modification of the surface properties of these micro- and nanostructured particles, which makes these materials suitable for biomedical applications. Both organic and inorganic coatings are extensively studied [41, 42].

Chitosan-based magnetic materials are often used as drug delivery systems of different drugs, including cytostatics. The polycationic structure of chitosan is proved to be effective as an antimicrobial agent as well as carrier and delivery systems. Many chitosan-based magnetic drug delivery systems for cancer treatment were developed during the time. Chitosan-coated magnetite for camptothecin release was obtained via typical precipitation/absorption route.

Delivery mechanism	
Factors affecting the delivery [5, 16, 35-40]	
Osmotic-controlled delivery	The osmotic-controlled delivery is the simplest mechanism of delivery, the drugs being delivered due to the different osmotic concentrations between the drug delivery system and the surrounding environment. Most of the drug delivery systems involve this mechanism, its share in the overall release process being variable.
Enzymatic-triggered delivery	This mechanism is especially important in the case of covalently bonded drugs. In this case, existent enzyme must recognize the support-drug bond and once the bond is broken the drug is free and can manifest its specific antitumoral activity. Proteases, hydrolyses, as well as other enzymes can be involved in the support-drug bond breaking. In certain conditions, the enzyme can be also introduced into the body, since the magnetic materials is accumulated into the desired organ/tissue.
pH-triggered delivery	pH-triggered delivery is often essential for medical applications, especially when the targeted application is related to the digestive tract, including the treatment of different forms of digestive-tube-associated cancers. The pH of the digestive tract is between 1 and 3 (in stomach) and over 8–9. In these conditions, the targeted delivery in stomach or intestines can be induced by designing drug delivery systems with pH-sensitive polymers. Such systems are also used for orally administered cytostatics delivery when protective measures have to be taken because of sensitive cytostatics (proteases from stomach could destroy the antitumoral agent).
Temperature-triggered delivery (including magnetic control due to the produced hyperthermia)	Temperature is an essential factor that influences the delivery of biological active agents, including cytostatics. Many formulations were proposed and tested at preclinical and clinical levels. In cancer, temperature can be considered as an internal factor because the tumor cells are in continuous replication and proliferation and consequently energy release is happen, even if the temperature increase is not very high. Also, especially in cancer treatment, the temperature can be considered external factor/stimuli because the intentionally produced temperature/hyperthermia leads to cancer cells death. In these conditions, the produced temperature is not enough for temperature-responsive systems to be developed. However, under hyperthermia conditions (an increase of 4–8^{o}C) as well as along with the implantation or injection of temperature-sensitive systems (the temperature increase can be upto 20^{o}C), the temperature increase is enough to develop temperature-triggered delivery systems.
Electromagnetic-triggered delivery	External electromagnetic field is applied and, due to the produced hyperthermia, the delivery rate is increased. Lipid matrices containing dispersed superparamagnetic iron oxide (SPIO) or other magnetite-based systems were investigated as magnetic field responsive drug delivery systems. Yi et al. [37] showed that lipid matrices based on myristic alcohol, oleic acid-coated SPIO particles, and umbelliferone, was able to deliver umbelliferone when external magnetic field was applied. The delivery is an indirect process which is due to the heating process and not directly due to the applied alternating magnetic field [38, 39]. In the case of lipid matrices containing dispersed superparamagnetic iron oxide, once heated the delivered heat leads to phase change in the lipid matrix and, along with melting, drug release is dramatically increased. When composite materials based on magnetite and cytostatics are obtained, the delivery is assured by the increasing diffusion induced by the increasing temperature. It was showed that once the alternating electromagnetic field was applied, the delivery rate increased [16].
Dual or poly-sensitive delivery	There are a lot of complex systems able to respond to two or even more factors. Usually, the increasing number of components can lead to an increasing number of factors of controlling the delivery. Usually, combining polymers from two independent classes allows a dual delivery control. The same observation is correct when using magnetic nanoparticles and polymers from certain classes. Magnetic control is very important because can assure "targeted delivery: as well as can be used to intensify the delivery rate.

Sheme 3. Delivery mechanism of magnetite or magnetite-based drug delivery systems of cytostatic drugs

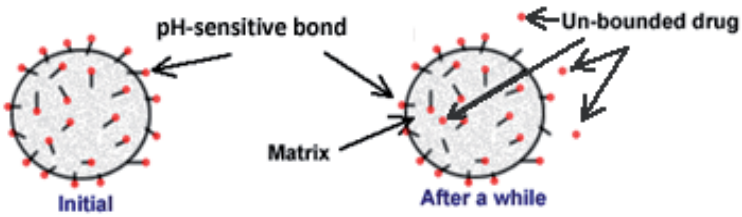

Sheme 4. Schematic representation of the delivery mechanism in pH-sensitive mechanism

Basically, the synthesis consists in magnetite preparation by precipitation followed by chitosan and camptothecin adsorption from aqueous solution. The thus obtained camptothecin-loaded magnetic chitosan nanoparticles have spherical shape and a hydrodynamic radius of 65–280nm and exhibit low cytotoxicity against 7721 liver cancer cells. The in vitro drug release from these polysaccharide modified magnetic nanoparticles exhibited a steady and sustained release profile, after 12 h the overall release of camptothecin being ~20% (in 0.001M PBS, pH = 7.4, temperature or 37°C) [43-46].

Zhang and Misra [47] developed a novel magnetic drug targeting carrier consisting of magnetic nanoparticles encapsulated in dextran-g-poly(N-isopropylacrylamide-co-N,N-dimethylacrylamide). This nanostructured system was obtained by functionalization of the magnetic nanoparticles with 3-mercaptopropionic acid hydrazide ($HSCH_2CH_2CONHNH_2$) via Fe–S covalent bonds. The anticancer therapeutic drug, doxorubicin, was attached to the surface of the functionalized magnetic nanoparticles through an acid-labile hydrazone bond, formed by the reaction of hydrazide group of 3-mercaptopropionic acid hydrazide with the carbonyl group of doxorubicin (see Scheme 5).

The developed system is pH-sensitive and could be a valuable system for cancer treatment when considering the normal pH of the blood (pH=7.4) and the pH of the endosomes of some cancer cells (pH =~5.0–5.5), since the delivery is faster under acidic conditions. This means that targeted delivery will be obtained in the acidic regions corresponding to the tumor sites. Furthermore, due to the presence of magnetite, the magnetic system can be concentrated at the desired tissue/organ and local hyperthermia can be produced. In these conditions, additional temperature control can be applied; once the temperature increases, the cumulative doxorubicin release increases by almost 20%, reaching ~90% after 48 h [47]. The thus designed stimuli-responsive magnetic system has a lower critical solution temperature (LCST) of ~38°C, which makes it suitable as carrier system in cancer treatments of humans.

Drug delivery system	Active component	Delivery mechanism
Polyethylene glycol (linker hydrazone)	Doxorubicin	**pH-sensitive mechanism** of delivery induced by drug–polymer bond breaking (polymer/active component is realized via a third agent called linker)
Poly(amidoamine) dendrimer (linker hydrazone)		
Hyaluronic acid (linker hydrazone)		
Melanolactone– polycaprolactone (linker hydrazone)		

Drug delivery system	Active component	Delivery mechanism
N-(2-hydroxypropyl) methacrylamide (linker hydrazone)		
Poly(amidoamine) dendrimer (linker cis-aconityl)		
Polyacetal (linker acetal)		
Pullalan (amide linker		
Poly(aspartate hydrazide) (linker hydrazone)	Paclitaxel	
Polyethylene glycol (linker hydrazone)		
Dextran (linker hydrazone)	Streptomycin	
Alginate (linker cis-aconityl)	Daunomycin	
Polyethylene glycol and poly(lactic acid)		
Polyethylene glycol and oligocholic acids	Paclitaxel	
Gold nanoparticle-pluronic		
Poly(ε-caprolactone) and poly(ethyl ethylene phosphate)		
Poly(ε -caprolactone), poly(2,4-dinitrophenylthioethyl ethylene phosphate), and polyethylene glycol	Doxorubicin	**redox-responsive drug delivery mechanism** via disulfuric bond breaking
Polyethylene glycol and poly(ε -caprolactone)		
Dextran-lipoic acid derivatives		
Methoxy polyethylene glycol and poly(ε-caprolactone)		
Methacrylic acid and *N*,*N*-bis(acryloyl)cystamine		
Polyethylene glycol and oligocholic acids	Vincristine	
Polyethylene glycol, poly(L-lysine), and poly(L-phenylalanine)	Methotrexate	
Poly(*N*-isopropylacrylamide)	5-Fluorouracil	
Poly(*N*-vinylcaprolactum)		
Pluronic F-127-chitosan	Curcumin	
Hydroxypropyl cellulose		
Poly(*N*-isopropylacrylamide-co-*N*,*N*-dimethylacrylamide), poly(D,L-lactide-co-glycolide), poly(ε -caprolactone)	Doxorubicn	**Temperature-triggered delivery mechanism**
Poly(*N*-isopropylacrylamide-co-acrylamide)-b-poly(D,L-lactide)	Docetaxel	
Poly(*N*-isopropylacrylamide-co-*N*,*N*-dimethylacrylamide)-bpoly(D,L-lactide-co-glycolide)	Paclitaxel	
Poly(*N*-isopropylacrylamide-co-*N*,*N*dimethylacrylamide- co-10-undecenoic acid) nanoparticles	Doxorubicin	**Complex, dual pH/ temperature-responsive** drug delivery **mechanism**
Poly(*N*-isopropylacrylamide-co-acrylic acid)-b-polycaprolactone nanoparticles	Paclitaxel	

Drug delivery system	Active component	Delivery mechanism
Methoxy polyethylene glycol-b-P(*N*-(2-hydroxypropyl) methacrylamide dilactate)-co-(*N*-(2-hydroxypropyl) methacrylamide-co-histidine, methoxy polyethylene glycol-b-poly(lactic acid)	Doxorubicin	
Poly(D,L-lactide)-g-poly(*N*-isopropylacrylamide-comethacrylic acid) nanoparticles	5-Flourouracil	
Methacrylic acid and *N*,*N*-bis(acryloyl)cystamine nanogels	Doxorubicin	
Polyethylene glycol-SS-poly(2,4,6-trimethoxybenzylidene-pentaerythritol carbonate) micelle	Doxorubicin	**Complex, dual pH/redox responsive** drug delivery **mechanism**
Methoxy polyethylene glycol-2-mercaptoethylamine-grafted-poly(L-aspartic acid)-2-(diisopropylamino) ethylamine-graftedpoly(L-aspartic acid) micelles	Doxorubicin	
Polyethylene glycol- Fe_3O_4 nanoparticles	Doxorubicin	
Methoxy polyethylene glycol-b-poly(methacrylic acid)-b-poly(glycerol monomethacrylate) coated Fe_3O_4 nanoparticles	Adriamycin	
Methoxy polyethylene glycol-b-(*N*,*N*-dimethylamino)ethyl methacrylate-b-polyglycidyl methacrylate coated Fe_3O_4 nanoparticles	Chlorambucil and Indomethacin	**Complex, dual pH/ magnetic-responsive** drug delivery **mechanism**
Polyethylene glycol-poly(imidazole L-aspartamide)-2-vinylpyridine coated Fe_3O_4-SiO_2 nanoparticles	Doxorubicin	
1,3,5-Triazaadamantane Fe_3O_4 capped mesoporous silica nanoparticles	Doxorubicin	
Pluronic with Fe_3O_4 nanoparticles	Doxorubicin	**Complex, dual temperature/ magnetic-responsive** drug delivery **mechanism**
Poly(*N*-isopropylacrylamide-acrylamide-allylamine) coated Fe_3O_4 nanoparticles		
DNA-capped MSNs	CPT, floxuridine	**Complex, dual temperature/ enzyme-responsive** drug delivery **mechanism**
Poly(oligo(ethylene glycol) acrylate-co-2-(5,5-dimethyl-1,3-dioxan-2-yloxy)ethyl acrylate) (P(OEGA-co-DMDEA)) nanogels containing bis(2-acryloyloxyethyl) disulfide	Doxorubicin, Paclitaxel	**Complex, ternary temperature/pH/ redox-responsive** drug delivery **mechanism**
Poly(*N*-isopropylacrylamide-co-methacrylic acid) (P(NIPAM-co-MAA)) coated magnetic mesoporous silica nanoparticles	Doxorubicin	**Complex, ternary temperature/pH/ magnetic-responsive** drug delivery **mechanism**
Poly(*N*-isopropylacrylamide)-chitosan magnetic nanohydrogels		

Drug delivery system	Active component	Delivery mechanism
Fe(II) loaded poly(methacrylic acid) microcontainers crosslinked by *N,N*-methylene-bisacrylamide and *N,N*-bis(acryloyl)-cystamine	Daunorubicin	**Complex, ternary pH/redox/magnetic-responsive** drug delivery **mechanism**

Table 1. Most important delivery mechanism of antitumoral agents and some of their most important representatives (based on [5, 48])

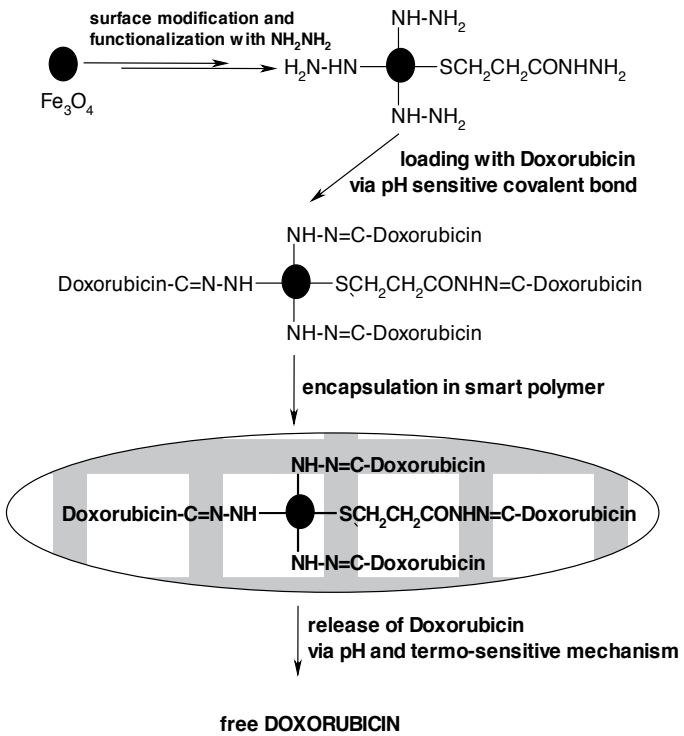

Scheme 5. Synthesis and dual-sensitive magnetic drug delivery system

Bhatnagar and Venuganti [5] realized a very complex review based on stimuli responsive drug delivery systems of over 70 smart delivery systems, classifying them function of the delivery mechanism and active components. Some of the most representative drug delivery systems are presented in Table 1. It can be seen that the mechanism of delivery is very important because it can allow a tighter control of release, which is essential in cancer treatment due to the high toxicity of the cytostatics.

2.3. Magnetic materials as hyperthermia generator

Hyperthermia is an interesting effect of some materials and appears to be of great importance in cancer treatment. Since discovered, over 4000 years ago [49], magnetite was tested for the treatment of different types of cancer from primary (breast, colon, bladder, toque, bone, etc.)

to metastatic cancer [50-56]. The high attractiveness of these materials is related to the easy targeted hyperthermia, these nanoparticles being easy to move using an adequate magnetic field to the desired tissue or organ.

Hyperthermia is a technique of the Ancient Egyptians. Records related to the use of hyperthermia in the treatment of (breast) cancer were reported around 2600 BC and later in 2000 BC and was rediscovered in the late 19th century [53, 57]. In the treatment of cancer, the high expectations of the use of hyperthermia can be justified taking into account the following issues. Cancer cells generally perish above 43^{o}C because the oxygen demand is high while the oxygen transported via the blood is not sufficient (due to incomplete angiogenesis) whereas normal cells are less affected even at higher temperatures. In addition, tumors are more easily heated than the surrounding normal tissues, since the blood vessels and nervous system are poorly developed in the tumor. In fact, the beneficial heat effect is well known and used for a long time. Different heating techniques of heating of tumors were attempted, including heating with hot water, infrared waves, ultrasound, as well as microwaves. In the case of deep-seated tumors, these techniques are not effective and consequently ferromagnetic microspheres have to be used to generate hyperthermia [58].

Magnetic composite materials are often obtained by combining the useful properties of magnetic nanoparticles and different organic or inorganic components, the most used being polymers: collagen, chitosan, chitin, dextran, as well as inorganic oxides like ZnO, SiO_2, TiO_2, and titanates [56, 59].

Ferrimagnetic glass ceramic microspheres as well as magnetite microspheres were produced by different researchers and were reviewed by Kawashita et al. [58]. Magnetite microspheres of ~20-30 μm were already prepared by Kawashita et al. [58]. Also, glass-ceramics containing magnetite in a wolastonite and bioglass matrix was proved to be effective in cancer treatment. The cancer cells were transplanted in rabbit tibiae by inserting into the medullary canal as a glass ceramic pin. The hyperthermia is generated by placing it into an alternating magnetic field. Based on these data, it can be assumed that glass-ceramic microspheres (20-30 μm in diameter) could be easier applied because the cancer cells might be scattered around and consequently a larger area must be covered. Comparing magnetite and glass-ceramic microspheres it can be concluded that magnetite exhibits a higher heat generation capacity (41W/g) compared with the glass-ceramic-loaded magnetite microspheres (10W/g), which is consistent with the lower magnetite content. Under these conditions, the maximum coercive force corresponds to a crystallite size of ~40nm.

Muzquiz-Ramos et al. [55] have obtained biomimetic apatite coatings on magnetite particles for bone cancer treatment. For this purpose, firstly, they obtained magnetite nanoparticles of ~12nm by coprecipitation and, then, by immersing magnetite nanoparticles into simulated body fluid – SBF or 1.5 SBF (50% more concentrated SBF than human blood plasma – see concentrations in Table 2) – for certain period of time they deposited HA coating onto the magnetite nanoparticles. Hydroxyapatite formation is strongly dependent on the composition and immersion time in SBF. It was found that, the immersion in SBF does not alter the superparamagnetic behavior of the magnetite core and consequently it can be used as potential candidates for the treatment of solid bone tumors.

	Na^+	K^+	Ca^{2+}	Mg^{2+}	Cl^-	HCO_3^-	HPO_4^{2-}	SO_4^{2-}
Human blood plasma	142.00	5.00	2.50	1.50	148.80	4.20	1.00	0.50
SBF	213.00	7.50	3.75	2.25	223.20	6.30	1.50	0.75
1.5SBF	142.00	5.00	2.50	1.50	103.00	27.00	1.00	0.50

Table 2. Composition of human blood plasma, SBF, and 1.5SBF

In 2010, Andronescu et al. [13] proposed to slightly change the existent protocol of bone cancer treatment. In short, the protocol involves the combination of surgery and chemotherapy in the treatment of bone cancer. Depending on several facts, the chemotherapeutic drugs can precede and/or follow the surgery (Figure 1). During the surgical resection of the tumoral bony tissue, the surgeon can introduce into the newly resulted defect(s) multifunctional materials. Two main roles can be identified and have to be noted. First of all, the material can act as a scaffold contributing to a faster healing and, secondly, it can assure a supplementary, antitumoral activity based on the delivered components, interactions with the tumoral cells, or produced hyperthermia.

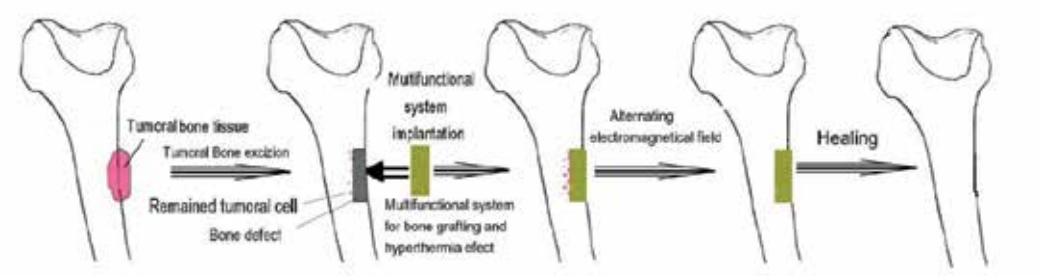

[With kind permission from Springer Science+Business Media: J Mater Sci—Mater M., Andronescu E, Ficai M, Voicu G, Ficai D, Maganu M, Ficai. A Synthesis and characterization of collagen/ hydroxyapatite: magnetite composite material for bone cancer treatment. 21, 2010, 2237–2242 [13]

Figure 1. Bone cancer treatment of osteosarcoma

3. Role of metal nanoparticles in cancer diagnostics and treatment

Metal nanoparticles (silver and gold) are widely used in cell imaging, DNA hybridization detection, proteins interaction, and photothermal therapy due to their extremely strong absorption and light scattering in the plasmon resonance [60]. In principle, the high attractiveness for using gold and silver nanoparticles in the cancer diagnosis and therapy is due to the unique optical properties, facile surface chemistry, and appropriate size scale. The tumor detection and treatment can be further improved by controlling size and shape or by conjugation of these nanoparticles with specific ligands/biomarkers [61]. The selective delivery of the metal nanoparticles is crucial for *in vivo* imaging and/or therapy. There are several

strategies for delivery of these nanoparticles into the tumor: topical application for the skin tumors; direct injection or intraoperative application for the accessible deep tumors, or intravascular injection for the inaccessible tumors. In the case of tumors localized in hard tissues, the low diffusion of the body fluids does not assure the necessary flow through these tissues and consequently through the tumoral tissue and therefore direct, intraoperative application is necessary.

PEGylated gold or silver nanoparticles can also act as carrier of anticancer chemotherapeutics. PEG coating assures high biocompatibility, lower agglomeration tendency, and masking against immune systems. When intravenously injected into the body, it exhibits high retention time especially in solid tumors. After retention in the tumor, NIR irradiation can be applied and selective ablation of the nanoparticles-enhanced tumor occurs [62-64]. Molecular specific imaging and therapy of cancer is easily achieved by the synthetic conjugation of the nanoparticles with antibodies targeted to receptors overexpressed on the cancer cells.

Silver-based nanostructured materials can be used as bioimaging labels for human lung cancer H1299 cells as proved by Guo et al.

Xu et al. [65] reported the synthesis of silver and gold spherical metal nanoparticles of various sizes for IR-sensitive antitumoral activity. Silver nanoparticles (AgNPs) of 10, 20, and 40nm as well as gold nanoparticles (AuNPs) of 20, 50, and 100nm were prepared and modified with Fetal Bovine Serum. Also, AgNPs with 12nm diameter were obtained and functionalized with meso-2,3-dimercaptosuccinic acid and silanes bearing various functional groups including amino group, short chain PEG and carboxylic group. The thus obtained nanoparticles were tested on three lines of C6 glioma cells (originated from mouse), U251, and SHG-44 cells (originated from human GBM). They found that the antitumoral ability of these nanoparticles is dependent on concentration, IR dose, and nanoparticle size. In short, the smaller nanoparticles have higher efficiency; the higher irradiation dose leads to higher killing ability; and the higher concentration leads to lower survival cells. The used capping agent is also important, even if, the mathematical quantification is more difficult. The tests highlighted that meso-2,3-dimercaptosuccinic acid and PEGylated silane modified nanoparticles do not affect the cell sensitivity to radiation but, carboxy- and amino-silane bearing nanoparticles drastically decrease the cell survival.

Gold nanocages were synthesized by galvanic replacement reaction between Ag template and $HAuCl_4$. In short, silver nanoparticles of 30–200nm nanocubes are transformed in Au nanoboxes and nanocages (nanoboxes with porous walls) with tunable optical properties from blue (400nm) to near-infrared (1200nm). In order to obtain deeper penetration, near-infrared light is necessary. At present, three strategies of shifting the surface plasmon resonance from visible to near-infrared are known:

- form agglomerates from spherical Au nanoparticles;
- by elongating the nanoparticles from spherical gold nanoparticles to nanorods/whiskers;
- by emptying the interiors of spherical nanoparticles to form hollow gold nanostructures.

Most of these structures can be designed by using adequate capping agents or changing synthesis route.

4. Silicate-based materials as vectors against tumor cells

Targeted action is many a time necessary for both diagnosis and therapy. Complex systems based on magnetic core, different shells, and tumoral receptors are of great importance. The locoregional drug delivery systems are well known to be beneficial because the systemic toxicity can be reduced compared with the other administration routes [4, 10, 14]. The targeted delivery is very useful especially when local administration is not possible. In most cancer treatment protocols, active components must be administrated that, due to their high toxicity, are desired to be delivered at a certain site without spreading to other tissues or organs. Silicates are interesting materials for industrial and medical field. Montmorillonite was largely exploited in biomedical field because it is pH-sensitive and can be loaded with large amount of drugs into its layered structure. The pH-sensitiveness is determined by the ability of this material to modify its characteristic interlayer spacing. In acid solutions, the interlayer spacing is minimal and increases in basic conditions. This property is exploited in medicine, montmorillonite being used, for instance, to deliver active components in neutral/basic media like colon or intestines. It is also important to mention that montmorillonite-based formulations can be used for oral administration of different active components that are unstable in stomach conditions because of the protective role of the silicate (proteic drugs, for instance, cannot be administrated orally; the stomach environment will destroy them). For this purpose, montmorillonite was tested for oral administration of cytostatics [66-68]. Schematically, the targeted delivery of cytostatics form silicates are presented and discussed in Figure 2.

In oral delivery, the contact of the DDS with the digestive tract is the most important factor which has to be considered when designing orally administrated DDS. It is important to mention that the contact of the DDS with gastric acid can destroy the active component(s). There are a lot of active components which, under the action of gastric acid, became inactive (inactivation due to the action of pepsin and/or hydrochloric acid), and amongst these active components there are also many cytostatics which can be inactivated by gastric acid. In these conditions, some drugs cannot be orally administrated or different protective measures must be taken. One of the most common protective way is the entrapping of the drug into organic or inorganic matrix, which, if correctly selected, can release the drug or its complexes at the intestine/colon level [66]. At this level, different scenarios are possible: free active component(s) acts locally fighting against colon cancer or, can be absorbed into the blood and enter the blood circulatory system. At this moment targeted or nontargeted delivery can occur. In the case of targeted delivery, the active component/complex is predominantly delivered at the desired tissue/organs due to the presence of recognizing agents linked on the complex or simply, due to the intratumoral microenvironment, as we presented in Figure 2.

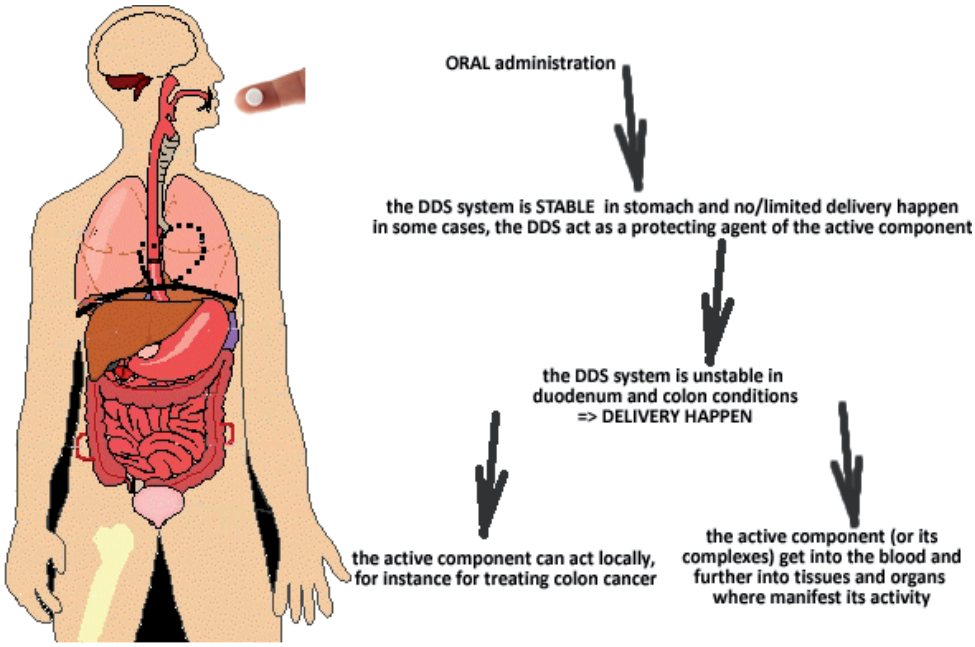

Figure 2. Schematic representation of cytostatics targeted delivery for oral administration

5. Conclusions

Metal and metal oxide nanoparticles are of great interest for medical and industrial applications. Magnetite is an important metal oxide with many potential applications in nanomedicine. Hyperthermia, targeted drug delivery system, and carrier and contrast agents are the most known medical applications with proved applicability in cancer diagnosis and treatment. The properties of magnetite nanoparticles are dependent on size and shape as well as composition and synthesis route. The bare magnetite is usually not recommended for biomedical applications because the host body recognizes it as a "foreign body" and consequently core–shell structures are usually obtained and tested for these applications.

Even if long-term toxicity of the nanoparticles is the subject of controversies, the use of gold and silver nanoparticles bring many advantages compared with other actual alternatives (like cytostatics). Further studies related to the influence of shape and size, capping agents, receptors immobilization onto the metal nanoparticles are still necessary. Surface plasmon resonance can be designed by size and shape and surface functionalization of both silver and gold nanoparticles. The surface plasmon resonance shift from blue to near-infrared is important because it allows a better/deeper penetration of the radiation into the body.

Mesoporous silicates are intensively studied for drug delivery and especially for cancer treatment, alone or in combination with other organic or inorganic polymers. Mesoporous silicates can be used for targeted delivery systems. These DDSs can be administrated orally, the delivery being intensified in neutral/basic conditions from intestines/colon.

Acknowledgements

The present work was possible due to the EU-funding grant POSCCE-A2-O2.2.1-2013-1/Axa prioritara 2, Project No. 638/12.03.2014, cod SMIS-CSNR 48652.

Author details

Denisa Ficai[1,2], Anton Ficai[1,3*] and Ecaterina Andronescu[1,3]

*Address all correspondence to: anton.ficai@upb.ro

1 University Politehnica of Bucharest, Faculty of Applied Chemistry and Materials Science; National Centre for Micro and Nanomaterials, Bucharest, Romania

2 University Politehnica of Bucharest, Faculty of Applied Chemistry and Materials Science; Department of Physical Chemistry, Inorganic Chemistry and Electrochemistry, Bucharest, Romania

3 University Politehnica of Bucharest, Faculty of Applied Chemistry and Materials Science; Department of Science and Engineering of Oxide Materials and Nanomaterials, Bucharest, Romania

References

[1] Ficai, D., Andronescu, E., Ficai, A., Voicu, G., Vasile, B., Ionita, V., Guran, C. Synthesis and characterization of mesoporous magnetite based nanoparticles. *Curr Nanosci*, 2012, 8: 875-879.

[2] Khandhar, A.P., Ferguson, R.M., Arami, H., Krishnan, K.M. Monodisperse magnetite nanoparticle tracers for in vivo magnetic particle imaging. *Biomaterials*, 2013, 34: 3837-3845. DOI 10.1016/j.biomaterials.2013.01.087

[3] Ficai, D., Ficai, A., Alexie, M., Maganu, M., Guran, C., Andronescu, E. Fe_3O_4/SiO_2/APTMS Nanoparticles with core-shell structure as potential materials for Copper removal. *Rev Chim* (Bucharest), 2011, 62: 622-625.

[4] Ficai, A., Ficai, D., Sonmez, M., Albu, M.G., Mihaiescu, D.E., Bleotu, C. Antitumoral materials with regenerative function obtained by Layer by Layer; Drug Des Dev Ther, 2015, 9:1269-1279.

[5] Bhatnagar, S., Venuganti, V.V.K. Cancer targeting: responsive polymers for stimuli-sensitive drug delivery. *J Nanosci Nanotechnol*, 2015, 15: 1925-1945. DOI 10.1166/jnn.2015.10325

[6] Peppas, L.B., Blanchette, J.O. Nanoparticle and targeted systems for cancer therapy. *Adv Drug Del Rev*, 2004, 56: 1649.

[7] Iyer, A.K., Khaled, G., Fang, J., Maeda, H. Exploiting the enhanced permeability and retention effect for tumor targeting. *Drug Disc Today*, 2006, 11: 812-818. DOI 10.1016/j.drudis.2006.07.005

[8] Nalwa, H.S., Webster, T. (Eds.), *Cancer Nanotechnology: Nanomaterials for Cancer Diagnosis and Therapy*, American Scientific Publishers; 2007. 500 p.

[9] Tong, R., Cheng, J.J. Anticancer polymeric nanomedicines. *Polymer Rev*, 2007, 47: 345-381. Doi 10.1080/15583720701455079

[10] Marques, C., Ferreira, J.M.F., Andronescu, E., Ficai, D., Sonmez, M., Ficai, A. Multifunctional materials for bone cancer treatment. *Int J Nanomed*, 2014, 9: 2713-2725. Doi 10.2147/Ijn.S55943

[11] Boissiere, M., Allouche, J., Brayner, R., Chaneac, C., Livage, J., Coradin, T. Design of iron oxide/silica/alginate hybrid magnetic carriers (HYMAC). *J Nanosci Nanotechnol*, 2007, 7: 4649-4654.

[12] van Driel, M., van Leeuwen, J.P.T.M. Cancer and bone: a complex complex. *Arch Biochem Biophys*, 2014, 561: 159-166. DOI 10.1016/j.abb.2014.07.013

[13] Andronescu, E., Ficai, M., Voicu, G., Ficai, D., Maganu, M., Ficai, A. Synthesis and characterization of collagen/hydroxyapatite: magnetite composite material for bone cancer treatment. *J Mat Sci-Mat Med*, 2010, 21: 2237-2242. DOI 10.1007/s10856-010-4076-7

[14] Andronescu, E., Ficai, A., Georgiana, M., Mitran, V., Sonmez, M., Ficai, D., Ion, R., Cimpean, A. Collagen-hydroxyapatite/Cisplatin drug delivery systems for locoregional treatment of bone cancer. *Technol Canc Res Treat*, 2013, 12: 275-284. DOI 10.7785/tcrt.2012.500331

[15] Sebastianelli, A., Sen, T., Bruce, I.J. Extraction of DNA from soil using nanoparticles by magnetic bioseparation. *Lett Appl Microbiol*, 2008, 46: 488-491. DOI 10.1111/j.1472-765X.2008.02343.x

[16] Ficai, A., Andronescu, A., Ghitulica, C.D., Ficai, D., Voicu, G., Albu, M.G., Process for preparing composite multi-purpose materials with possible applicability in the treatment of bone cancer, A61K-033/38; A61K-008/64 ed., 2012.

[17] Caraceni, A., Brunelli, C., Martini, C., Zecca, E., De Conno, F. Cancer pain assessment in clinical trials. A review of the literature (1999-2002). *J Pain Symp Manage*, 2005, 29: 507-519. DOI 10.1016/j.jpainsymman.2004.08.014

[18] Guise, T.A., Mundy, G.R. Cancer and bone. *Endocr Rev*, 1998, 19: 18-54.

[19] Ding, J.X., He, C.L., Xiao, C.S., Chen, J., Zhuang, X.L., Chen, X.S. pH-responsive drug delivery systems based on clickable poly(L-glutamic acid)-grafted comb copolymers. *Macromol Res*, 2012, 20: 292-301. DOI 10.1007/s13233-012-0051-0

[20] SCOPUS database, www.scopus.com, accessed on 28th January 2015.

[21] Thompson Reuters database, http://isiknowledge.com/, accessed on 28th January 2015.

[22] Rodgers, P., Chun, A., Cantrill, S., Thomas, J. Editorial, "Small is different." *Natur Nanotechnol*, 2006, 1, 1.

[23] Medeiros, S.F., Santos, A.M., Fessi, H., Elaissari, A. Stimuli-responsive magnetic particles for biomedical applications. *Int J Pharma*, 2011, 403: 139-161. DOI 10.1016/j.ijpharm.2010.10.011

[24] Ruiz, A., Salas, G., Calero, M., Hernandez, Y., Villanueva, A., Herranz, F., Veintemillas-Verdaguer, S., Martinez, E., Barber, D.F., Morales, M.P. Short-chain PEG molecules strongly bound to magnetic nanoparticle for MRI long circulating agents. *Acta Biomater*, 2013, 9: 6421-6430. DOI 10.1016/j.actbio.2012.12.032

[25] Shieh, D.B., Cheng, F.Y., Su, C.H., Yeh, C.S., Wu, M.T., Wu, Y.N., Tsai, C.Y., Wu, C.L., Chen, D.H., Chou, C.H. Aqueous dispersions of magnetite nanoparticles with NH3+ surfaces for magnetic manipulations of biomolecules and MRI contrast agents. *Biomaterials*, 2005, 26: 7183-7191. DOI 10.1016/j.biomaterials.2005.05.020

[26] Ito, A., Shinkai, M., Honda, H., Kobayashi, T. Medical application of functionalized magnetic nanoparticles. *J Biosci Bioengin*, 2005, 100: 1-11. Doi 10.1263/Jbb.100.1

[27] Taylor, J.I., Hurst, C.D., Davies, M.J., Sachsinger, N., Bruce, I.J. Application of magnetite and silica-magnetite composites to the isolation of genomic DNA. *J Chromat* A, 2000, 890: 159-166.

[28] Vlad, M., Andronescu, E., Grumezescu, A.M., Ficai, A., Voicu, G., Bleotu, C., Chifiriuc, M.C. Carboxymethyl-cellulose/Fe3O4 nanostructures for antimicrobial substances delivery. *Biomed Mat Engin*, 2014, 24: 1639-1646. 10.3233/Bme-140967

[29] Luo, B., Xu, S.A., Ma, W.F., Wang, W.R., Wang, S.L., Guo, J., Yang, W.L., Hu, J.H., Wang, C.C. Fabrication of magnetite hollow porous nanocrystal shells as a drug carrier for paclitaxel. *J Mat Chem*, 2010, 20: 7107-7113. Doi 10.1039/C0jm00726a

[30] Chowdhury, S.R., Yanful, E.K. Arsenic and chromium removal by mixed magnetite-maghemite nanoparticles and the effect of phosphate on removal. *J Environ Manage*, 2010, 91: 2238-2247.

[31] Zhao, X., Wang, J., Wu, F., Wang, T., Cai, Y., Shi, Y., Jiang, G. Removal of fluoride from aqueous media by Fe_3O_4@$Al(OH)_3$ magnetic nanoparticles. *J Hazard Mat*, 2010, 173: 102-109.

[32] Liu, J., Flores, G.A., Sheng, R.S. In-vitro investigation of blood embolization in cancer treatment using magnetorheological fluids. *J Magnet Magnet Mat*, 2001, 225: 209-217.

[33] Mornet, S., Vasseur, S., Grasset, F., Veverka, P., Goglio, G., Demourgues, A., Portier, J., Pollert, E., Duguet, E. Magnetic nanoparticle design for medical applications. *Prog Solid State Chem*, 2006, 34: 237-247. DOI 10.1016/j.progsolidstchem.2005.11.010

[34] Mornet, S., Vasseur, S., Grasset, F., Duguet, E. Magnetic nanoparticle design for medical diagnosis and therapy. *J Mat Chem*, 2004, 14: 2161-2175. Doi 10.1039/B402025a

[35] Kayal, S., Ramanujan, R.V. Doxorubicin loaded PVA coated iron oxide nanoparticles for targeted drug delivery. *Mat Sci Engin C-Mat Biol Appl*, 2010, 30: 484-490. DOI 10.1016/j.msec.2010.01.006

[36] Alexiou, C., Arnold, W., Klein, R.J., Parak, F.G., Hulin, P., Bergemann, C., Erhardt, W., Wagenpfeil, S., Lubbe, A.S. Locoregional cancer treatment with magnetic drug targeting. *Can Res*, 2000, 60: 6641-6648.

[37] Yi, D.D., Zeng, P.Y., Wiedmann, T.S. Magnetic activated release of umbelliferone from lipid matrices. *Int J Pharma*, 2010, 394: 143-146. DOI 10.1016/j.ijpharm.2010.04.040

[38] Duguet, E., Vasseur, S., Mornet, S., Devoisselle, J.M. Magnetic nanoparticles and their applications in medicine. *Nanomedicine*, 2006, 1: 157-168. Doi 10.2217/17435889.1.2.157

[39] Hafeli, U.O. Magnetically modulated therapeutic systems. *Int J Pharma*, 2004, 277: 19-24. DOI 10.1016/j.ijpharm.2003.03.002

[40] Liang, M., Yang, T.M., Chang, H.P., Wang, Y.M. Dual-responsive polymer-drug nanoparticles for drug delivery. *React Func Poly*, 2015, 86: 27-36. DOI 10.1016/j.reactfunctpolym.2014.11.006

[41] Barrera, C., Herrera, A.P., Rinaldi, C. Colloidal dispersions of monodisperse magnetite nanoparticles modified with poly(ethylene glycol). *J Coll Interface Sci*, 2009, 329: 107-113. DOI 10.1016/j.jcis.2008.09.071

[42] Kikkawa, S., Takagi, S., Tamura, H. Preparation of titanate coated magnetite powder for cisplatin delivery. *J Cer Soc Jap*, 2008, 116: 380-383.

[43] Hamidi, M., Azadi, A., Rafiei, P. Hydrogel nanoparticles in drug delivery. *Adv Drug Del Rev*, 2008, 60: 1638-1649. DOI 10.1016/j.addr.2008.08.002

[44] Zapata, E.V.E., Perez, C.A.M., Gonzalez, C.A.R., Carmona, J.S.C., Lopez, M.A.Q., Garcia-Casillas, P.E. Adherence of paclitaxel drug in magnetite chitosan nanoparticles. *J All Comp*, 2012, 536: S441-S444. DOI 10.1016/j.jallcom.2011.12.150

[45] Sahin, Y.M., Yetmez, M., Oktar, F.N., Gunduz, O., Agathopoulos, S., Andronescu, E., Ficai, D., Sonmez, M., Ficai, A. Nanostructured biomaterials with antimicrobial properties. *Curr Med Chem*, 2014, 21: 3391-3404.

[46] Zhu, A.P., Yuan, L.H., Jin, W.J., Dai, S., Wang, Q.Q., Xue, Z.F., Qin, A.J. Polysaccharide surface modified Fe3O4 nanoparticles for camptothecin loading and release. *Acta Biomater*, 2009, 5: 1489-1498. DOI 10.1016/j.actbio.2008.10.022

[47] Zhang, J., Misra, R.D.K. Magnetic drug-targeting carrier encapsulated with thermosensitive smart polymer: core-shell nanoparticle carrier and drug release response. *Acta Biomater*, 2007, 3: 838-850. DOI 10.1016/j.actbio.2007.05.011

[48] Chen, C.E., Geng, J., Pu, F., Yang, X.J., Ren, J.S., Qu, X.G. Polyvalent nucleic acid/mesoporous silica nanoparticle conjugates: dual stimuli-responsive vehicles for intracellular drug delivery. *Angewandte Chemie-Int Edit*, 2011, 50: 882-886. DOI 10.1002/anie.201005471

[49] Thomas, L., *Nanoparticle Synthesis for Magnetic Hyperthermia*, University College London, 2010 (Ph.D. thesis), 220 pages.

[50] Kikumori, T., Kobayashi, T., Sawaki, M., Imai, T. Anti-cancer effect of hyperthermia on breast cancer by magnetite nanoparticle-loaded anti-HER2 immunoliposomes. *Breast Can Res Treat*, 2009, 113: 435-441. DOI 10.1007/s10549-008-9948-x

[51] Kawai, N., Ito, A., Nakahara, Y., Futakuchi, M., Shirai, T., Honda, H., Kobayashi, T., Kohri, K. Anticancer effect of hyperthermia on prostate cancer mediated by magnetite cationic liposomes and immune-response induction in transplanted syngeneic rats. *Prostate*, 2005, 64: 373-381. Doi 10.1002/Pros.20253

[52] Okayama, T., Kokura, S., Ishikawa, T., Adachi, S., Hattori, T., Takagi, T., Handa, O., Naito, Y., Yoshikawa, T. Antitumor effect of pretreatment for colon cancer cells with hyperthermia plus geranylgeranylacetone in experimental metastasis models and a subcutaneous tumor model of colon cancer in mice. *Int J Hypertherm*, 2009, 25: 141-149. Doi 10.1080/02656730802631783

[53] Toraya-Brown, S., Fiering, S. Local tumour hyperthermia as immunotherapy for metastatic cancer. *Int J Hypertherm*, 2014, 30: 531-539. Doi 10.3109/02656736.2014.968640

[54] Oliveira, T.R., Stauffer, P.R., Lee, C.T., Landon, C.D., Etienne, W., Ashcraft, K.A., McNerny, K.L., Mashal, A., Nouls, J., Maccarini, P.F., Beyer, W.F., Inman, B., Dewhirst, M.W. Magnetic fluid hyperthermia for bladder cancer: a preclinical dosimetry study. *Int J Hypertherm*, 2013, 29: 835-844. Doi 10.3109/02656736.2013.834384

[55] Muzquiz-Ramos, E.M., Cortes-Hernandez, D.A., Escobedo-Bocardo, J. Biomimetic apatite coating on magnetite particles. *Mat Lett*, 2010, 64: 1117-1119. DOI 10.1016/j.matlet.2010.02.025

[56] Zhao, D.L., Wang, X.X., Zeng, X.W., Xia, Q.S., Tang, J.T. Preparation and inductive heating property of Fe(3)O(4)-chitosan composite nanoparticles in an AC magnetic field for localized hyperthermia. *J All Comp*, 2009, 477: 739-743. DOI 10.1016/j.jallcom.2008.10.104

[57] Hornback, N.B. Historical aspects of hyperthermia in cancer-therapy. *Radiol Clin N Am*, 1989, 27: 481-488.

[58] Kawashita, M., Tanaka, M., Kokubo, T., Inoue, Y., Yao, T., Hamada, S., Shinjo, T. Preparation of ferrimagnetic magnetite microspheres for in situ hyperthermic treatment of cancer. *Biomaterials*, 2005, 26: 2231-2238. DOI 10.1016/j.biomaterials.2004.07.014

[59] Zhang, L.Y., Gu, H.C., Wang, X.M. Magnetite ferrofluid with high specific absorption rate for application in hyperthermia. *J Magnet Magnet Mat*, 2007, 311: 228-233. DOI 10.1016/j.jmmm.2006.11.179

[60] Khlebtsov, N.G., Dykman, L.A. Optical properties and biomedical applications of plasmonic nanoparticles. *J Quant Spect Rad Trans*, 2010, 111: 1-35. DOI 10.1016/j.jqsrt.2009.07.012

[61] Jain, P.K., El-Sayed, I.H., El-Sayed, M.A. Au nanoparticles target cancer. *Nano Today*, 2007, 2: 18-29.

[62] Guo, S.R., Gong, J.Y., Jiang, P., Wu, M., Lu, Y., Yu, S.H. Biocompatible, luminescent silver@phenol formaldehyde resin core/shell nanospheres: large-scale synthesis and application for in vivo bioimaging. *Adv Func Mat*, 2008, 18: 872-879. DOI 10.1002/adfm.200701440

[63] Portney, N.G., Ozkan, M. Nano-oncology: drug delivery, imaging, and sensing. *Anal Bioanal Chem*, 2006, 384: 620-630. DOI 10.1007/s00216-005-0247-7

[64] O'Neal, D., Hirsch, L., Halas, N., et al. Photo-thermal tumor ablation in mice using near infrared-absorbing nanoparticles. *Can Lett*, 2004, 209: 171–176.

[65] Xu, R., Ma, J., Sun, X.C., Chen, Z.P., Jiang, X.L., Guo, Z.R., Huang, L., Li, Y., Wang, M., Wang, C.L., Liu, J.W., Fan, X., Gu, J.Y., Chen, X., Zhang, Y., Gu, N. Ag nanoparticles sensitize IR-induced killing of cancer cells. *Cell Res*, 2009, 19: 1031-1034. Doi 10.1038/Cr.2009.89

[66] Iliescu, R.I., Andronescu, E., Ghitulica, C.D., Berger, D., Ficai, A. Montmorillonite-alginate nanocomposite beads as drug carrier for oral administration of carboplatin-preparation and characterization. UPB *Sci Bull*, Series B: *Chem Mat Sci*, 2011, 73: 3-16.

[67] Iliescu, R.I., Andronescu, E., Ghitulica, C.D., Voicu, G., Ficai, A., Hoteteu, M. Montmorillonite-alginate nanocomposite as a drug delivery system incorporation and in vitro release of irinotecan. *Int J Pharma*, 2014, 463: 184-192. DOI 10.1016/j.ijpharm.2013.11.041

[68] Iliescu, R.I., Andronescu, E., Voicu, G., Ficai, A., Covaliu, C.I. Hybrid materials based on montmorillonite and citostatic drugs: preparation and characterization. Appl Clay Sci, 2011, 52: 62-68. DOI 10.1016/j.clay.2011.01.031

Chapter 2

Evaluation Strategies of Nanomaterials Toxicity

María González-Muñoz, Paula Díez,
María González-González, Rosa Mª Dégano,
Nieves Ibarrola, Alberto Orfao and Manuel Fuentes

Additional information is available at the end of the chapter

http://dx.doi.org/10.5772/60733

Abstract

The revolutionary development of nanoscience during the last years has increased the number of studies in the field to evaluate the toxicity and risk levels. The design of different nanomaterials together with biological components has implemented the advances in biomedicine. Specifically, nanoparticles seem to be a promising platform due to their features, including nanoscale dimensions and physical and chemical characteristics than can be modified in function of the final application. Herein, we review the main studies realized with nanoparticles in order to understand and characterize the cellular uptake mechanisms involved in biocompatibility, toxicity, and how they alter the biological processes to avoid disease progression.

Keywords: Nanoparticle, toxicity, nanomaterial, cellular uptake, immunogenicity

1. Introduction

The nanoscience revolution that sprouted throughout the 1990s is becoming part of our daily life in the form of cosmetics, food packaging, drug delivery systems, therapeutics, or biosensors, among others [1]. It has been estimated that the production of nanomaterials would increase in 2020 by 25 times what it is today.

This is due to the wide range of applications that they have in numerous fields, ranging from commercial products such as electronic components, cosmetics, household appliances, semiconductor devices, energy sources, food color additives, surface coatings, and medical

products such as biological sensors, drug carriers, biological probes, implants, and medical imaging. Despite this future dependence on nanomaterials, studies regarding their safe incorporation in our lives are very limited [2].

Recently, several studies suggested that nanoparticles (NPs) could easily enter into the human body [3]. This is mainly because their nanoscale dimensions are of a similar size to typical cellular components. Moreover, proteins–NPs may bypass natural mechanical barriers, possibly leading to adverse tissue reactions. As a result, the particles might be taken up into cells. Generally, NPs of different physical and chemical properties may enter the cells by different mechanisms, such as phagocytosis, macropinocytosis, endocytosis, or directly by "adhesive interactions" [4].

In order to understand the exact cellular influences of NPs, a thorough characterization of individual nanoparticles is necessary. Nanoparticles can get into the human body through various ways, such as skin penetration, inhalation, or injection, and due to their small size and diffusion abilities; they have the potential to interact with cells and organs. In addition to involuntary exposure to NPs by means of contacting nanomaterials-based products, there are cases where nanoparticles would interact with the human body for biomedical purposes.

In case of using nanoparticles for targeted-drug delivery, NPs are required to traverse the cell membranes and interact with specific components. Hence, the success rate of drug delivery is based on the biocompatibility of NPs. Research has shown that different physicochemical properties of NPs result in different cellular uptake. Currently, it has been described that several factors play a critical role in toxicity (Fig. 1); such as (i) size and surface, very important for liposomes, silicon microparticles, quantum dots, polymeric NPs, or gold NPs; (ii) concentration, crystallinity, and mechanical strength, toxicity is directly related to these parameters [2]; (iii) chemical attributes, the development of hydrophilic polymer functionalization (i.e. polyethylene glycol, polycarboxybetaine) at the surface of NPs enhances the systemic circulation; however, the response of the immune system is also related with this hydrophilic coating.

The discovery of Enhanced Permeation and Retention (EPR) effect and its combination with hydrophilic polymers is related to the accumulation of NP-based carrier systems in tumor tissues followed by the release of the drug either in the proximity to the tissue. However, EPR effect is commonly inconsistent due to the heterogeneity associated with the tumor tissue. For this reason, novel nanomedicines are being designed and developed in order to target only a particular cell, tissue, and organ by linking an affinity reagent to the NP, which is targeting a specific biomolecule differentially expressed at the tissue or cells of interest.

Although some concerns have been raised about poor systemic circulation, enhanced clearance by the mononuclear phagocyte system and limited tissue penetration has been shown to improve the cellular uptake and efficacy of their payload in comparison with passively targeted counterparts. This improvement in cellular uptake is a key point because mostly of the targets present intracellular location. Bearing this in mind, the characterization of endocytosis pathways plays a critical role in designing efficient intracellular trafficking, subcellular

http://dx.doi.org/10.5772/60733

targeting, and nanomedicines with ideal features (biocompatibility, low-toxicity, and low-immune response) [4].

Herein, we present a comprehensive review on recent developments and outline future strategies of nanotechnology-based medicines. Specifically, the trials *in vivo/in vitro*, requested by The National Cancer Institute, that evaluate NP toxicity for nanomedicines are detailed below. They can be sorted in two large groups: biocompatibility and immunological studies.

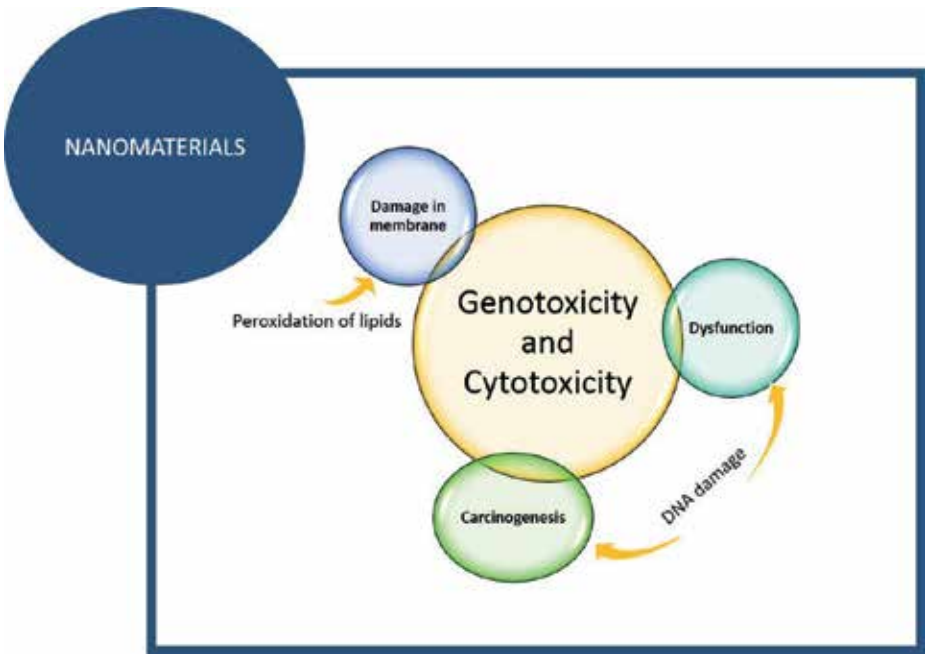

Figure 1. Effects of nanomaterials on cells.

2. Biocompatibility studies

Once the NPs are in biological environment, it is expected that their interaction with biomolecules, such as proteins, lipids, nucleic acids, and even metabolites, is to a large extent because of their high surface-to-mass ratio. Bearing in mind that proteins are one of the majority components in biological fluids, formation of a protein corona at the surface of NPs is expected. This protein corona may substantially influence the biological response [5].

2.1. Relation of biomolecular corona and nanoparticles toxicity

Herein, we briefly describe how this biomolecular corona influences mainly in cellular uptake, toxicity, and biodistribution and targeting ability to a lesser extent.

2.1.1. Effect of physicochemical properties

2.1.1.1. Size

The size of nanomaterials has a direct and significant impact on the physiological activity. In fact, the NP size may be expanded by the biomolecular corona. Then, the NP size plays a critical role in cellular uptake, efficiency of particle processing in the endocytic pathway, and physiological response of cells to NPs. Kim and collaborators [6] thoroughly studied the size-dependent cellular toxicity of Ag NPs using different characteristic sizes against several cell lines, including MC3T3-E1 and PC12. They demonstrated that NP toxicity was precisely size- and dose-dependent in terms of cell viability, intracellular reactive oxygen species generations, LDH release, and ultra-structural changes in the cell.

In general, biodegradable NPs are less cytotoxic than non-biodegradable ones [7]. Apart from the nature of NP coating, particle size can also affect the degradation of the polymer matrix. With the decrease of particle size, the surface area-to-volume ratio increases greatly, leading to an easier penetration and release of the polymer degradation products. Even though it can be assumed that the smaller the NP size, the more likely it can enter into cells and cause potential damages, the mechanisms of toxicity are very complicated, so the size factor cannot be viewed as the only influence parameters.

Yuan and collaborators studied the effect of size of hydroxyapatite NPs on the antitumor activity and apoptotic signaling proteins. They studied the effect of particle size on cell apoptosis, the Hep62 cells (incubated with and without hydroxyapaptite NPs), presented morphological changes related to apoptosis which were related to the size of the NPs [8].

2.1.1.2. Nanomaterial and shape

The structure and shape influence in the toxicity of nanomaterials (Fig. 2). Commonly, nanomaterials have different shapes and structures such as tubes, fibers, spheres, and planes. For instance, several studies compared cytotoxicity of multi-wall carbon nanotubes *vs.* single-wall carbon nanotubes or graphene [9, 10], obtaining results that suggest a strong influence of the shape and toxicity. Furthermore, other authors have evaluated the toxicity of nanocarbon materials *vs.* NPs [11].

2.1.1.3. Concentration of nanomaterial

In 2013, a research was carried out to inspect the cytotoxicity of a cisplatin derivative, known as PtU2. Minor toxicity was detected when this compound was conjugated with 20 nm gold NPs (Au-NPs). Cisplatin is one of the most used anticancer agents and its conjugation with Au-NPs gives it benefits thanks to Au characteristics: biocompatibility, inactivity, non-toxicity, and stability. In this way, the compound becomes a powerful tool for the treatment of solid tumors. In the present trial, osteosarcoma cell line (MG-63) was treated with different concentrations of AuNPs, PtU2 and a combination of both, PtU2-AuNPs. Firstly, one of the aims was the determination of the carrier activity. In order to achieve this, the metal content (gold and platinum) was measured in cells and supernatants separately. The results showed that metal

http://dx.doi.org/10.5772/60733

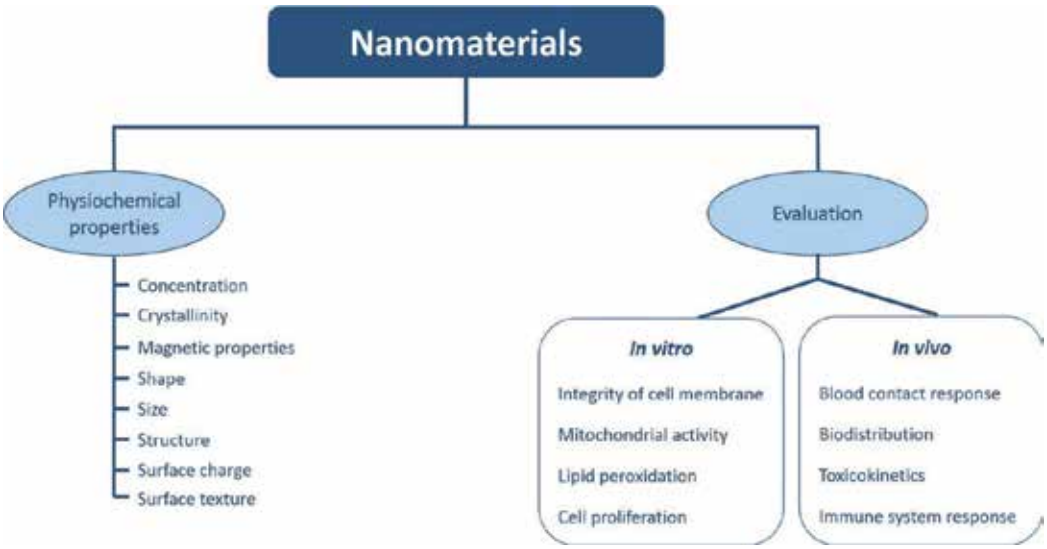

Figure 2. Characteristics and studies about the nanomaterials effect. Adapted from Li X. et al. [2].

uptake capacity from cells is the same for AuNPs or AuNPs conjugated with PtU2. Then, the cytotoxicity was evaluated by Annexin V-FITC assay by flow cytometry. As a result of MG-63 incubation with the two compounds, higher cytotoxicity was detectable after 48 hours of culture in cells treated with PtU2-AuNPs. To sum up, PtU2-AuNPs are more effective inciting cellular toxicity on the same culture conditions [12].

2.2. Relation of biomolecular corona and cellular uptake

Due to protein nature of the biomolecular corona, it is important to distinguish between specific and nonspecific cellular uptake. Specific uptake is regulated by membrane receptors that are internalized by interaction with specific ligands. In turn, nonspecific uptake is considered a random process without control by the cell [5].

Overall, nonspecific uptake seems to be decreased in the presence of a corona whereas specific uptake seems to be promoted by protein corona because a misfolding of corona proteins triggers NPs uptake by specific cells that otherwise would not have done so or because there is a protein in the corona able to target a specific receptor expressed in the cell line used. So far, all the performed studies suggest how important cell line specificity is for this protein corona effect. However, a more extensive revision of literatures is recommended because in many occasions some inconsistencies of cellular uptake of NPs have been found, particularly regarding incubation conditions or fluidic For example, several studies for cellular uptake of differential macrophage-like cell line (dTHP1) have different outcomes. In such a way, Yan and colleagues [13] did not observe any changes in effective association and internalization in the presence of serum. However, these cells present phagocytosis activity when unfolded BSA is presented in the protein corona; in this case, phagocytosis is mediated by Scavenger receptor subclass A.

2.3. Effect of protein corona on biodistribution

Despite the knowledge about the influence of NP PEGylation on biodistribution, the characterization and consequences of a biomolecular corona formed *in vivo* has not been investigated yet.

Hence, it has been described that, independently of the nature of the NPs, pre-coating with proteins, such as serum albumin, or apolipoprotein E, increases the blood circulation time and reduces the clearance speed. This effect is explained by a reduction in opsonization and phagocytosis; meanwhile, liver is the main organ for NP accumulation and the protein used for pre-coating seems to be distributed in other organs (i.e. albumin targeting and apolipoprotein E target lungs and brain, respectively) [14].

2.4. Different assays for evaluation of cytotoxicity/biocompatibility

In general, the mechanisms of toxicity are very complicated. Several studies have been developed for biological characterization of nanomaterials which are vital to guarantee the safety of the material that will be in contact with food or humans. Here, a brief description of the most conventional assays to evaluate cytotoxicity/biocompatibility is reported.

2.4.1. Cytotoxicity analysis

In order to determine the viability of cells exposed to NPs, toxicity tests *in vitro* are very useful to understand the toxic mechanisms [2]. Some of these tests are listed: Alamar Blue Assay, MTT, LDH leakage assay [2, 15], and quick cell [16]. First and second approaches constitute an index of intrinsic cytotoxicity.

On the one hand, 3-[4,5-dimethylthiazol-2-yl]-2,5-diphenyl tetrazolium bromide assay (mitochondrial toxicity, MTT, assay) is based on the transformation of tetrazolium salt by mithocondrial succinate dehydrogenases in metabolically active cells generating purple formazan crystals [17]. This oxidation–reduction reaction can be only produced in presence of dehydrogenase enzymes, so it is a good way to determine the activity of mitochondria [2]. Thus, the number of living cells is proportional to the amount of formazan produced.

Cells with culture medium and NPs are seeded in 96-well plates and then 20 μL/well of MTT, with a final concentration of 5 mg/mL added to each well. This compound must be incubated for 4 h at 37ºC and 5% CO_2. After the incubation, the solution is removed and the crystals that have been formed are dissolved by DMSO. Finally, the optical density is measured at 595 nm expressing the percent cell viability [3, 17]. This method also allows the measurement of cell survival and proliferation.

Although MTT is the most accepted assay method [2], there is another test to evaluate the nanotoxicity, the resazurin assay (Alamar Blue, AB, assay). This study is based on the reduction of blue, nonfluorescent resazurin to pink, fluorescent resorufin by living cells [18]. This reduction is mediated by mitochondrial enzymes located in the mitochondria, cytosol, and microsomal fractions [17, 18]. The decrease in the magnitude of resazurin reduction indicates loss of cell viability.

http://dx.doi.org/10.5772/60733

The AB assay is commonly used with a final concentration of 10% (w /v). Then, plates are exposed to an excitation wavelength of 530 nm and emission at 590 nm to determine if any of the dyes interact with the compound. Lastly, the fluorescence is read 5 hours later and the percent viability is calculated [17]. Moreover, AB assay has many advantages: it is a simple, rapid and versatile test and reveals a high correlation with other methods to evaluate nanotoxicity [18].

Sometimes, problems with interference between NPs and this type of assay arise [17], so care must be taken with the dyes used. The confidence degree of toxicity studies significantly depends on this interaction. Few researchers have found that carbon nanotubes can interact with dyes such as AB and neutral red [2].

According to the analysis carried out by Hamid R and collaborators, AB assay and MTT are advisable to identify the cytotoxic compound. However, the AB assay is homogenous and presents more sensitivity that can detect densities as low as 200 cells per well [17].

In turn, cell death is also determined by evaluating the activity of the enzyme lactate dehydrogenase (LDH). LDH is an enzyme generally located in the cytosol, but it is quickly released when cellular damage is produced. In this way, the LDH release assay allows the assessment of the membrane integrity of cells by measuring this enzyme in the extracellular medium. This method, like MTT, uses the measure of a color compound absorbance to determine the cell viability that can be affected by the uptake of NPs [19].

The Quick Cell Proliferation Colorimetric Assay Kit works in a similar way. This is based on the cleavage of the tetrazolium salt to formazan by mitochondrial dehydrogenases. An increase in the activity of these enzymes is connected with cellular proliferation. The formazan dye produced by viable cells can be quantified by a spectrophotometer by measuring the absorbance of the solution at 440 nm. Moreover, the Quick Cell Assay has several advantages in face of MTT because it is a new simple method, requiring no washing, no harvesting, and no solubilization steps, and it is more sensitive and faster too [20].

2.4.2. Assays for studying cell death by effects of nanomaterials

The cytotoxicity analysis can be complemented by other studies. Here, we present different methods to determine cell death or apoptosis, including trypan blue (TB) and propidium iodide (PI) protocols.

TB exclusion test marks which cells are viable. This is because live cells have intact cell membranes and certain dyes, such as TB or PI, cannot entry into them [21]. In dead cells, the membrane is ruptured and the dye is able to cross it and stain the cytoplasm of blue. In 2014, Mendes and colleagues [22] published a work where their aim was to investigate different diameters of iron oxide NPs. Four cell lines were incubated with NPs to assess the material toxicity and the possible size dependence. Cell viability was measured using the MTT and TB tests. For the dye exclusion assay, the cells were seeded in 6-well flat-bottom plates and incubated for 12 or 48 h with a NP suspension at 10 μg/mL concentration. Then, 20 μL of each suspension was mixed with 0.4% TB to count the number of living and dead cells. This method was used because with the MTT it was not clear if NPs caused cell death or whether they only

reduced the cellular metabolic activity. The results showed that cells incubated with the carbon-coated iron oxide NPs tend to decrease their mitochondrial activity (indicated by MTT test) rather than die (indicated by the dye exclusion test). In conclusion, cytotoxicity analysis showed no apparent difference between the diameters studied, whereas there are clear differences in particle uptake.

On the other hand, Alshatwi and collaborators [23] have published a work where the toxicity of platinum NPs is evaluated. The objective in this project is to investigate the effects of platinum NPs on cell viability, nuclear morphology, and cell cycle distribution on SiHa cells (a cervical cancer cell line). To study the nuclear morphology, SiHa cells were incubated with platinum NPs for 24 hours. Then, cell nucleus were stained by 1mg/mL PI and examined under a fluorescence inverted microscope. In treated cells, nuclear fragmentation, chromatin condensation, and nuclear swelling were observed. The nuclear fragmentation is a hallmark of late apoptosis.

In the same way, PI was also used to determine the cell cycle stage of treated cells by a flow cytometer. The results showed that these NPs induced a G2/M phase cell cycle arrest due to DNA damage. Briefly, this investigation suggests that platinum NPs inhibit cell proliferation because they induce cell death via apoptosis. Moreover, the NPs also have effect by reducing cell viability and causing DNA fragmentation and G2/M cell cycle arrest. That is why; they can be a potential therapy agent in the cervical cancer treatment.

Secondly, we describe two different ways to evaluate the cell death induced by apoptosis. Apoptosis or program cell death occurs in the normal physiology during development and aging to keep a balance between proliferation and cell death [24, 25]. It is also a defense mechanism and it is important for removing damaged cells and decreasing the damage on neighbor cells.

This process is carried out by loss of the mitochondrial transmembrane potential and activation of caspases (cysteine proteases). These proteins can be categorized into initiators (caspases 2, 8, 9, 10), effectors (caspases 3, 6, 7), and inflammatory caspases (caspases 1, 4, 5) [24].

Frequently, cell apoptosis is usually evaluated using a caspase-3 activation assay. For instance, Xun et al. put into effect a work where they tried to study the effect of silica NP size (7, 20, and 50 nm) on cytotoxicity. The cell line HepG2, a human hepatoma model, was selected for the study. HepG2 cells were treated with silica NPs of 20 nm (SNP20) at concentrations of 160 μg/mL and 320 μg/mL for 24 and 48 hours, respectively. Then, caspase-3 assay buffer and caspase-3 lysis buffer were added into the cell culture. After reaction, the fluorescence intensity was detected under a fluorescence plate reader. Caspase-3 is an essential molecule in the final phase of apoptosis induced by diverse stimulus. Results obtained in this analysis showed an increase of caspase-3 activity about 2–3 fold higher in cells treated with SNP20 than that of controls after 24 hours of incubation and about 3–5 fold after 48 hours. About this evidence, silica NPs could activate caspase-3 and downregulate procaspase-9, indicating an activation of caspase-9 in HepG2 cells. That is, these NPs can change apoptotic protein expression and greatly increase apoptosis in mitochondria-dependent pathways in hepatoma cells. In

addition, Annexin V-FITC/PI assay was used in this study to quantify cell apoptosis. This test allows distinguishing between normal, apoptotic, and necrotic cells.

HepG2 cells and normal L-02 hepatic cell lines exposed to SNP20, at the same two concentration used before, were stained using Annexin V-FITC and PI and analyzed by flow cytometry. Apoptotic cells undergo changes in the distribution of their membrane lipids. Phosphatidylserine is a phospholipid commonly presented inside the membrane, whereas during apoptosis, processes are expressed on the cellular surface.

In this way, Annexin V, which has a high affinity for phosphatidylserine, is used as a marker of early apoptosis. However, PI is used to distinguish necrotic cells from apoptotic cells. This is an agent which is intercalated in the DNA of dead cells when losing the membrane integrity. As a result, almost no apoptotic cells were detected in controls and treated L-02 cells and in control HepG2 cells. On the contrary, many apoptotic cells were found in HepG2 treated with SNP20, indicating that apoptosis induced by NPs is dose-dependent [25].

Annexin V is a method commonly used for assessing cellular apoptosis. For example, Ashokkumar and collaborators as well as Grudzinski et al. employed this procedure in their studies. In the first one, the aim was to evaluate whether gold NPs are able to induce apoptosis in cancer cells. HepG2 cell line was used for the investigation and these were treated for 24 hours with gold NPs. After that, cells were stained with Annexin V and the level of apoptosis was quantified as a percentage of Annexin V positive cells. Finally, the results showed that HepG2 treated with gold NPs undergo cell apoptosis whereas untreated cells did not show it [26]. In the second investigation, they tried to study the cytotoxicity of carbon-encapsulated iron nanoparticles (CEIN) in murine glioma cells (GL261). These cells were divided into two groups: one was treated at two different concentrations during 24 hours, whereas the other group was the control group (untreated cells). Then, both groups were stained with Annexin V and the analysis was performed by flow cytometer. The results indicated that the samples treated with the higher concentration of CEIN induced some pro-apoptotic and necrotic events in the glioma cell line. As a summary, this work have supposed a huge progress because it is the first report which clearly displays that CEINs with surface modifications with acidic groups cause murine glioma cell-specific cytotoxicity [27].

3. Immunological studies

Besides the fact that NPs play an important role in medicine area and their properties can be used to improve traditional treatments and diagnostic agents [28], there are many biocompatibility studies about size, shape, charge, solubility, and surface modification of NPs. However, the interphase related to interactions between NPs and immune system is still not well understood.

According to literature, NPs can activate and/or suppress immune response and the compatibility with this system is determined by its surface chemistry. Therefore, NPs can be designed to avoid immunotoxicity and reach desirable immunomodulation [29, 30].

Preclinical data shows that NPs are not more immunotoxic than conventional drugs, so NPs employed like drug carriers can provide advantages, such as the reduction of systemic immunotoxicity. For instance, NPs can release the drug in a specific tissue in order to not alter safe tissues and they may keep drugs away from blood cells. Moreover, NPs can also decrease drug immunotoxicity by raising their solubility. However, NPs are generally picked up by phagocytic cells of the immune system, such as macrophages. This incident can produce immunostimulation or immunosuppression, which may promote inflammatory or autoimmune disorders. For example, granuloma formation was observed in the lungs and skin of animals treated with carbon nanotubes [29].

Next, we briefly describe immunostimulation and immunosuppression linked to NPs uptake.

3.1. Immunosuppression

There are not many studies about this area for NPs because most of the researches focused on the inflammatory properties of NPs [29].

One of the studies about immunosuppression has revealed that inhalation of carbon nanotube (CNT) results in a reduction of immune system in mice. This is produced through a mechanism that involves the release of TFG-β1 from lungs. Then, TFG-β1 goes into circulation and increases the expression of two molecules whose function is to inhibit T-cell proliferation [31].

Other NPs that can produce immunosuppression are zinc oxide (ZnO) particles. They are able to induce immunosuppression *in vitro* and *in vivo* in function of the different size and charge. ZnO NPs suppress innate immunity such as natural killer cell activity. Moreover, the $CD4^+/CD8^+$ ratio, a marker for matured T-cells, serum levels of T helper-1 cytokines (interferon-γ and IL-12p70) and pro/anti-inflammatory were slightly reduced. In the opposite sense, no significant changes were detected in T- and B-cell proliferation [32].

3.2. Immunostimulation

Biological therapeutics, where NPs are included, are able to activate the immune system. In other words, nanomaterials are identified by this system and innate or adaptive immune responses are produced. We briefly describe several effects of NPs on cytokine secretion, immunogenicity and the mechanism through which nanoparticles are recognized by the immune system.

On the one hand, many immunostimulatory reactions, driven by NPs, are mediated by the release of inflammatory cytokines. Cytokines are signaling molecules inducted by different types of nanomaterials: gold, dendrimers, or lipid nanoparticles, among others. Moreover, NP size is an important factor for determining whether antigens loaded into NPs stimulate type I (interferon-γ) or II (IL-4) [29, 30]. For example, a study carried out from peripheral blood mononuclear cells of non-atopic women showed that palladium NPs improved the release of IFN-γ [33]. In other study about THP1-macrophages, the results showed that chitosan-DNA nanoparticles did not produce pro-inflammatory cytokines, whereas the secretion of metalloproteinase 9 and 2 was increased in cell supernatants [34].

This kind of analysis is often evaluated by enzyme-linked immunosorbent assay (ELISA). Antibodies and an enzyme-mediated color change are used to determine the presence and relative concentrations of particular cytokines present in the tissue or cell culture media. [35, 36]. ELISA is based on the concept of an antigen binding to its specific antibody, which allows identification of small quantities of molecules such as cytokines [36].

In turn, NPs induce antibody response (immunogenicity). NPs raise a special interest in this area because immunogenicity is improved by stimulating the production of antibodies [30]. Plasma B cells are responsible for making antibodies, specialized proteins, in response to an antigen [29].

A recent *in vivo* study about a novel dengue nanovaccine (DNV) has demonstrated that the vaccine can stimulate humoral and cell-mediated immune responses. This vaccine is composed by the dengue virus type 2 inactivated. Moreover, the adjuvant chitosan together with NPs including cell wall components from *Mycobacterium bovis* were used to improve the action of the DNV. Mice treated with this compound showed an increase of cytokine levels and a strong anti-dengue IgM and IgG antibody response. The release of IFN-γ produced by $CD4^+$ and $CD8^+$ T cell was also incremented. In conclusion, these results demonstrated that the DNV can be an important vaccine candidate for treatment of dengue disease [37].

Finally, we briefly mention the mechanism through which NPs are phagocyted into the cells. Macrophages are responsible for the first line of defense in the organism. They detect and uptake foreign molecules and synthesize mediators which warn the immune system about infection. Raw 264.7, a mouse leukemic monocyte macrophages cell line, is the model line used for the phagocytosis assays. For instance, Raw 264.7 was utilized in a new *in vitro* research about the effect of silica and gold NPs in macrophages. The results showed that silica and gold NPs decreased the ability of phagocytosis in 50%, while surface markers and cytokine secretion were not disturbed due to the particles [38]. To evaluate this analysis, different methods can be used depending on the composition of the nanomaterial. These procedures include confocal microscopy, optical and fluorescence microscopy, transmission electron microscopy (TEM), or scanning electron microscopy (SEM) [38, 39].

4. Conclusions and perspectives

Bearing in mind the importance and relevancy of the NPs in biomedical field, a better understanding of their effects on the human body is therefore required. According to the points described above, the physicochemical properties of nanomaterials play a critical role in toxicity. Thus, the alteration of these properties could be used to modify the toxicity and/or biocompatibility of these materials. On the other side, it is also necessary to obtain the maximum amount information about the interaction of biological interactions of NPs with cells, tissues, and proteins. In fact, this could be a critical parameter for the future application of nanomaterials in the biomedical area. In this review, special attention has been paid to the protein corona because it plays a critical role in toxicity and biocompatibility. Many studies have been performed; however, further studies are needed to know how to exploit the benefits

of the corona *in vivo*; mainly, because it seems quite complicated to predict the composition of proteins corona and its biological consequences.

Despite immense progress on the evaluation of toxicity and biocompatibility of nanomaterials, from this comprehensive review it is pointed out that further experimentation is still ongoing in this field to obtain a better and optimal understanding of the interaction between nanomaterials and the human body.

Acknowledgements

We gratefully acknowledge financial support from the Carlos III Health Institute of Spain (ISCIII, FIS PI14/0153), Fondos FEDER (EU). The Proteomics Unit belongs to ProteoRed, PRB2-ISCIII, supported by grant PT13/0001. P.D. is supported by a JCYL-EDU/346/2013 PhD scholarship.

Author details

María González-Muñoz[1], Paula Díez[1,2], María González-González[1,2], Rosa Mª Dégano[2], Nieves Ibarrola[2], Alberto Orfao[1] and Manuel Fuentes[1,2*]

*Address all correspondence to: mfuentes@usal.es

1 Department of Medicine and General Cytometry Service-Nucleus, Cancer Research Centre (IBMCC/CSIC/USAL/IBSAL), Salamanca, Spain

2 Proteomics Unit. Cancer Research Centre (IBMCC/CSIC/USAL/IBSAL), Salamanca, Spain

References

[1] W. Lu, D. Senapati, S. Wang, O. Tovmachenko, A. K. Singh, H. Yu, and P. C. Ray, "Effect of surface coating on the toxicity of silver nanomaterials on human skin keratinocytes," *Chem. Phys. Lett.*, vol. 487, pp. 92–96, 2010.

[2] X. Li, W. Liu, L. Sun, K. E. Aifantis, B. Yu, Y. Fan, Q. Feng, F. Cui, and F. Watari, "Effects of physicochemical properties of nanomaterials on their toxicity," *J. Biomed. Mater. Res. A*, 2014.

[3] M. Milic, G. Leitinger, I. Pavicic, M. Zebic Avdicevic, S. Dobrovic, W. Goessler, and I. Vinkovic Vrcek, "Cellular uptake and toxicity effects of silver nanoparticles in mammalian kidney cells," *J. Appl. Toxicol.*, Oct. 2014.

[4] B. Yameen, W. Il Choi, C. Vilos, A. Swami, J. Shi, and O. C. Farokhzad, "Insight into nanoparticle cellular uptake and intracellular targeting," *Journal of Controlled Release*, 2014.

[5] E. Brun and C. Sicard-Roselli, "Could nanoparticle corona characterization help for biological consequence prediction?," *Cancer Nanotechnol.*, vol. 5, no. 1, p. 7, 2014.

[6] T. H. Kim, M. Kim, H. S. Park, U. S. Shin, M. S. Gong, and H. W. Kim, "Size-dependent cellular toxicity of silver nanoparticles," *J. Biomed. Mater. Res. - Part A*, vol. 100 A, pp. 1033–1043, 2012.

[7] B. Semete, L. Booysen, Y. Lemmer, L. Kalombo, L. Katata, J. Verschoor, and H. S. Swai, "In vivo evaluation of the biodistribution and safety of PLGA nanoparticles as drug delivery systems," *Nanomedicine Nanotechnology, Biol. Med.*, vol. 6, pp. 662–671, 2010.

[8] Y. Yuan, C. Liu, J. Qian, J. Wang, and Y. Zhang, "Size-mediated cytotoxicity and apoptosis of hydroxyapatite nanoparticles in human hepatoma HepG2 cells," *Biomaterials*, vol. 31, pp. 730–740, 2010.

[9] C. Grabinski, S. Hussain, K. Lafdi, L. Braydich-Stolle, and J. Schlager, "Effect of particle dimension on biocompatibility of carbon nanomaterials," *Carbon N. Y.*, vol. 45, pp. 2828–2835, 2007.

[10] X. Zhang, S. Hu, M. Wang, J. Yu, Q. Khan, J. Shang, and L. Ba, "Continuous graphene and carbon nanotube based high flexible and transparent pressure sensor arrays," *Nanotechnology*, vol. 26, no. 11, p. 115501, Feb. 2015.

[11] J. R. Gurr, A. S. Wang, C. H. Chen, and K. Y. Jan, "Ultrafine titanium dioxide particles in the absence of photoactivation can induce oxidative damage to human bronchial epithelial cells," *Toxicology*, vol. 213, no. 1–2, pp. 66–73, Sep. 2005.

[12] S. Sánchez-Paradinas, M. Pérez-Andrés, M. J. Almendral-Parra, E. Rodríguez-Fernández, Á. Millán, F. Palacio, A. Orfao, J. J. Criado, and M. Fuentes, "Enhanced cytotoxic activity of bile acid cisplatin derivatives by conjugation with gold nanoparticles," *J. Inorg. Biochem.*, vol. 131, pp. 8–11, 2014.

[13] Y. Yan, K. T. Gause, M. M. Kamphuis, C. S. Ang, N. M. O'Brien-Simpson, J. C. Lenzo, E. C. Reynolds, E. C. Nice, and F. Caruso, "Differential roles of the protein corona in the cellular uptake of nanoporous polymer particles by monocyte and macrophage cell lines," *ACS Nano*, vol. 7, no. 12, pp. 10960–10970, 2013.

[14] M. Schäffler, F. Sousa, A. Wenk, L. Sitia, S. Hirn, C. Schleh, N. Haberl, M. Violatto, M. Canovi, P. Andreozzi, M. Salmona, P. Bigini, W. G. Kreyling, and S. Krol, "Blood protein coating of gold nanoparticles as potential tool for organ targeting," *Biomaterials*, vol. 35, pp. 3455–3466, 2014.

[15] T. Tsukahara and H. Haniu, "Cellular cytotoxic response induced by highly purified multi-wall carbon nanotube in human lung cells," *Mol. Cell. Biochem.*, vol. 352, pp. 57–63, 2011.

[16] Nanoimmunotech S.L. Available online: http://nanoimmunotech.eu (27th January 2015).

[17] R. Hamid, Y. Rotshteyn, L. Rabadi, R. Parikh, and P. Bullock, "Comparison of alamar blue and MTT assays for high through-put screening," *Toxicol. Vitr.*, vol. 18, pp. 703–710, 2004.

[18] D. Breznan, D. Das, C. MacKinnon-Roy, B. Simard, P. Kumarathasan, and R. Vincent, "Non-specific interaction of carbon nanotubes with the resazurin assay reagent: impact on in vitro assessment of nanoparticle cytotoxicity," *Toxicol. In Vitro*, vol. 29, no. 1, pp. 142–147, Feb. 2015.

[19] A. L. Holder, R. Goth-Goldstein, D. Lucas, and C. P. Koshland, "Particle-induced artifacts in the MTT and LDH viability assays," *Chem. Res. Toxicol.*, vol. 25, pp. 1885–1892, 2012.

[20] BioVision Incorporated. Available online: http://www.biovision.com (29th January 2015).

[21] W. Strober, "Trypan blue exclusion test of cell viability," *Curr. Protoc. Immunol.*, vol. 21, p. A.3B.1–A.3B.2, 2001.

[22] R. G. Mendes, B. Koch, A. Bachmatiuk, A. A. El-Gendy, Y. Krupskaya, A. Springer, R. Klingeler, O. Schmidt, B. Büchner, S. Sanchez, and M. H. Rümmeli, "Synthesis and toxicity characterization of carbon coated iron oxide nanoparticles with highly defined size distributions," *Biochim. Biophys. Acta*, 2013.

[23] A. A. Alshatwi, J. Athinarayanan, and P. Vaiyapuri Subbarayan, "Green synthesis of platinum nanoparticles that induce cell death and G2/M-phase cell cycle arrest in human cervical cancer cells," *J. Mater. Sci. Med.*, vol. 26, no. 1, pp. 5330–014–5330–1. Epub 2015 Jan 11, 2015.

[24] S. Elmore, "Apoptosis: a review of programmed cell death," *Toxicol. Pathol.*, vol. 35, pp. 495–516, 2007.

[25] X. Lu, J. Qian, H. Zhou, Q. Gan, W. Tang, J. Lu, Y. Yuan, and C. Liu, "In vitro cytotoxicity and induction of apoptosis by silica nanoparticles in human HepG2 hepatoma cells," *Int. J. Nanomedicine*, vol. 6, pp. 1889–1901, 2011.

[26] T. Ashokkumar, D. Prabhu, R. Geetha, K. Govindaraju, R. Manikandan, C. Arulvasu, and G. Singaravelu, "Apoptosis in liver cancer (HepG2) cells induced by functionalized gold nanoparticles," *Colloids and surfaces.B, Biointerfaces*, vol. 123, pp. 549–556, Nov. 2014.

[27] I. P. Grudzinski, M. Bystrzejewski, M. A. Cywinska, A. Kosmider, M. Poplawska, A. Cieszanowski, Z. Fijalek, and A. Ostrowska, "Comparative cytotoxicity studies of carbon-encapsulated iron nanoparticles in murine glioma cells," *Colloids Surfaces B Biointerfaces*, vol. 117, pp. 135–143, 2014.

[28] L. Zhang, F. X. Gu, J. M. Chan, A. Z. Wang, R. S. Langer, and O. C. Farokhzad, "Nanoparticles in medicine: therapeutic applications and developments," *Clin. Pharmacol. Ther.*, vol. 83, pp. 761–769, 2008.

[29] M. A. Dobrovolskaia and S. E. McNeil, "Immunological properties of engineered nanomaterials," *Nat. Nanotechnol.*, vol. 2, pp. 469–478, 2007.

[30] B. S. Zolnik, Á. González-Fernández, N. Sadrieh, and M. A. Dobrovolskaia, "Minireview: Nanoparticles and the immune system," *Endocrinology*, vol. 151. pp. 458–465, 2010.

[31] E. A. Thompson, B.C. Sayers, E. E. Glista-Baker, K. A. Shipkowski, A. J. Taylor and J. C. Bonner, "Innate immune responses to nanoparticle exposure in the lung," *J. of Environmental Immunology and Toxicology*, vol.1, pp. 150–156, 2013.

[32] C. S. Kim, H. D. Nguyen, R. M. Ignacio, J. H. Kim, H. C. Cho, E. H. Maeng, Y. R. Kim, M. K. Kim, B. K. Park, and S. K. Kim, "Immunotoxicity of zinc oxide nanoparticles with different size and electrostatic charge," *Int. J. Nanomedicine*, vol. 9 Suppl 2, pp. 195–205, 2014.

[33] P. Boscolo, V. Bellante, K. Leopold, M. Maier, L. Di Giampaolo, A. Antonucci, I. Iavicoli, L. Tobia, A. Paoletti, M. Montalti, C. Petrarca, N. Qiao, E. Sabbioni, and M. Di Gioacchino, "Effects of palladium nanoparticles on the cytokine release from peripheral blood mononuclear cells of non-atopic women," *J. Biol. Regul. Homeost. Agents*, vol. 24, pp. 207–214, 2010.

[34] F. Chellat, A. Grandjean-Laquerriere, R. Le Naour, J. Fernandes, L. H. Yahia, M. Guenounou, and D. Laurent-Maquin, "Metalloproteinase and cytokine production by THP-1 macrophages following exposure to chitosan-DNA nanoparticles," *Biomaterials*, vol. 26, pp. 961–970, 2005.

[35] E. I. Levy, J. E. Paino, P. S. Sarin, A. L. Goldstein, A. J. Caputy, D. C. Wright, and L. N. Sekhar, "Enzyme-linked immunosorbent assay quantification of cytokine concentrations in human meningiomas," *Neurosurgery*, vol. 39, pp. 823–828; discussion 828–829, 1996.

[36] S. D. Gan and K. R. Patel, "Enzyme immunoassay and enzyme-linked immunosorbent assay," *J. Invest. Dermatol.*, vol. 133, no. 9, p. e12, Sep. 2013.

[37] T. Hunsawong, P. Sunintaboon, S. Warit, B. Thaisomboonsuk, R. G. Jarman, I. K. Yoon, S. Ubol, and S. Fernandez, "A novel dengue virus serotype-2 nanovaccine induces robust humoral and cell-mediated immunity in mice," *Vaccine*, Feb. 2015.

[38] S. Bancos, D. L. Stevens, and K. M. Tyner, "Effect of silica and gold nanoparticles on macrophage proliferation, activation markers, cytokine production, and phagocytosis in vitro," *Int. J. Nanomedicine*, vol. 10, pp. 183–206, 2014.

[39] Nitbiosafe. Available online: http://www.nitbiosafe.com (22nd February 2015).

Chapter 3

Focussing on Neutrophils for Evaluating In vitro and In vivo Inflammatory Activities of Nanoparticles

Denis Girard

Additional information is available at the end of the chapter

http://dx.doi.org/10.5772/60703

Abstract

A tremendous interest to use nanomaterials for medical diagnosis and therapeutic purposes has increased in the past few years. Although a lot of investigations focus on the use of nanoparticles (NPs) for drug delivery in cancer therapies, there are several studies investigating the potential use of NPs as carriers to detect allergies or to alleviate inflammatory symptoms. However, although this represents a very interesting interest and a potential avenue to use nanodrug systems, there are some potential toxic risks. For example, cytotoxicity, oxidative stress, genotoxicity, and inflammation have been reported both in in vitro and in vivo models for testing NPs. In addition to medicine, a variety of other sectors, including electronics, cosmetics, aerospace, textile industries, and even in food, used NPs. Consequently, the probability of human exposure to NPs has risen, leading to the possibility that NPs may reach the blood circulation and interact with immune blood cells. Therefore, it is crucial to evaluate the risk that NPs represent to human health. In different studies using in vivo models of inflammation, especially those investigating airway NP exposure, an increased number of leukocytes, mainly neutrophils, in the lungs and bronchoalveolar lavages have been reported. In fact, neutrophil counts are used as biomarkers of inflammation. Despite this and knowing that neutrophils are key player cells in inflammation, it is intriguing that few nanotoxicology studies have focused on how NPs can directly alter the biology of these cells. However, an increasing amount of studies, including some from my laboratory, demonstrate that NPs can activate human neutrophils by different manners in vitro and can attract them or not in vivo. The focus of this review will be to cover this new area of research.

Keywords: Inflammation, neutrophils, nanotoxicology

1. Introduction

The use of nanoparticles (NPs) has increased in the past few years in various fields, including textile, sport, defense, aerospace, electronics, biology, medicine, etc. There is also a growing interest to use NPs in different applications, including diagnostic technology, bioimaging, and drug/gene delivery. Therefore, voluntary or nonvoluntary human exposure to NPs and nanomaterials is unavoidable and will certainly expand in the near future. This has led to a growing interest in nanotoxicology, the study of toxicity of nanomaterials. Especially, a number of studies reported the effects of NPs on pulmonary inflammation by investigating in vitro activation of pulmonary cells with NPs and in vivo in a variety of models in which neutrophils appear to be the predominant leukocyte cell type in the lungs and in bronchoalveolar lavages following inhalation or intratracheal instillation of NPs. It is reasonable that the first studies focussed on pulmonary effects of NPs since inhalation is one of the major routes of human exposure to NPs. However, even if several studies reported an increased number of neutrophils, the literature dealing with the direct effects of given NP with neutrophils is poorly documented and has been neglected until the last few years. In addition, since NPs are used in a variety of sectors and are already included in several consumable products, NPs could reach the blood stream and interact with immune cells. This review will summarize the current literature dealing on the direct interaction of NPs with human neutrophils as well as recent data indicating that the murine air pouch model of inflammation is suitable for evaluating the ability of NPs to attract neutrophils in vivo.

2. Neutrophils: A brief overview

Polymorphonuclear neutrophil cells (PMNs) are important cells of the immune system involved in host defense. In particular, they are primordial players of innate immunity and provide a very effective defense against bacterial and fungal infections. Other than erythrocytes and platelets, PMNs are the most abundant cell type in circulation, representing more than 65 % of total leukocytes. They are terminally mature nondividing cells which develop in the bone marrow from CD34+ stem cells, resulting from a series of cell divisions and stages as myeloblasts, promyelocytes, myelocytes, metamyelocytes, band neutrophils, and finally, mature neutrophils. The mechanism is still not well understood; however, this occurs under the influence of regulatory cytokines [1-3]. It takes about 14 days to obtain fully mature neutrophils from the CD34+ precursor cells. Of note, more than 50 % of the bone marrow is dedicated to the generation of PMNs. A huge number of neutrophils are released from the bone marrow. Indeed, this has been estimated at $\sim 5 \times 10^{10}$ cells on a daily basis in a normal adult. This represents one of the fastest cell turnovers in the human body [2, 3]. Therefore, cell turnover must be under strict control in order to prevent diseases. The number of PMNs remains relatively constant in healthy individuals, and this is due to the limited life span (half-life of ~12 h in circulation) of these cells. In addition, PMNs are known to undergo constitutive or spontaneous apoptosis, an important step for regulating cell number. Apoptosis renders PMNs unresponsive to extracellular stimuli and leads to expression of “eat-me” signals, some

http://dx.doi.org/10.5772/60703

molecules involved in the elimination of apoptotic PMNs by professional phagocyte, a process called efferocytosis, largely responsible for the resolution of inflammation [4-7]. Because of this, identification of proapoptotic or antiapoptotic agents is therefore of major importance. When the rate of PMN apoptosis is accelerated, this results in an increase in bacterial susceptibility. In contrast, when apoptosis is delayed or suppressed, this can aggravate inflammation and lead to autoimmune disorders [4, 7].

Although different biochemical hallmarks of apoptosis, including cell shrinkage, chromatin condensation and internucleosomal DNA degradation, appearance of pyknotic nuclei, caspase activation, flip–flop of phosphatidylserines to the extracellular (outer) surface of the cell, etc., are observable in neutrophils [4, 6, 8], these cells are different from several other cell types. In this respect, the common caspase substrates such as poly(ADP-ribose) polymerase, the catalytic subunit of DNA-dependent protein kinase, the small ribonucleoprotein U1-70 kDa, and the nuclear/mitotic apparatus proteins are not detected in PMNs [9, 10]. In addition, human neutrophils do not express caspase-2 as well as the antiapoptotic Bcl-2 (B-cell lymphoma 2) proteins [11]. In contrast, a predominant expression of the antiapoptotic protein myeloid cell leukemia-1 (Mcl-1) is observed in these cells. Also, it is important to mention that PMNs possess a very low number of mitochondria that may have a role restricted to apoptosis rather than for energy generation [12]. During apoptosis, mature neutrophils can release proteases from azurophilic granules, including cathepsin D, which may contribute to caspase-3 activation through processing of caspase-8 [13]. Finally, unusual roles for nuclear proteins have been reported in PMNs [14]. For example, unlike other cells, proliferating cell nuclear antigen (PCNA) is expressed in the cytoplasm of mature neutrophils where it could bind to procaspases, affecting their apoptotic rates.

Interestingly, both intrinsic and extrinsic pathways of cell apoptosis appear to be activated during spontaneous human neutrophil apoptosis as evidenced, for example, by caspase-9 (intrinsic) and caspase-8 (extrinsic) activation [15-17]. More recently, increasing evidences indicate that the endoplasmic reticulum (ER) stress-induced cell apoptotic pathway is also operational in human PMNs [18, 19]. These cells were found to express inositol-requiring protein-1 (IRE1), activating transcription factor-6 (ATF6), and protein kinase RNA (PKR)-like ER kinase (PERK), the three major sensors of protein folding status in the ER [20, 21].

During acute inflammation, PMNs are the first type of leukocytes to migrate to an inflammatory site, where they will produce several proinflammatory mediators including chemokines that first attract other PMNs and then other cell types like monocytes–macrophages and lymphocytes, corresponding to chronic inflammation. PMNs are phagocytes well recognized for their ability to eliminate invading pathogens via two important mechanisms: *i*) the respiratory burst, which is an oxygen-dependent process leading to the generation of reactive oxygen species (ROS), and *ii*) degranulation, an oxygen-independent mechanism by which PMNs release potent toxic degradative products stored in granules. In addition to reactive oxygen metabolites and granule enzymes, PMNs are known to be an important source of products implicated in tissue damage and inflammation such as leukotriene B_4, platelet-activating factor, and various cytokines (IL-1α, IL-8, IL-12, TNF-α, TGF-β, GRO-α), to name a few [1]. The importance of PMNs in inflammation is further supported by the observation that

various PMN priming and activating agents such as IL-1β, IL-8, IL-15, GM-CSF, TGF-β, C5a, C9, etc., are present, for example, in the synovial fluids of rheumatic patients [22-24]. PMNs are also known to adhere onto cell substratum (e.g., endothelial cells) [25] or onto extracellular matrix proteins, including fibronectin [26]. Finally, PMNs can move toward a chemotactic gradient (chemotaxis) and exert phagocytosis, two important functions involved in killing and eliminating pathogens. About ten years ago, an important new discovery was made concerning the biology of neutrophils; upon activation, these cells were found to release neutrophil extracellular traps (NETs) composed of decondensed chromatin DNA in association with histones, granular proteins, and a few cytoplasmic proteins [27]. NETosis, a sort of PMNs suicide-generating NETs, was identified as a novel antimicrobial mechanism able to kill extracellular bacteria, fungi, and parasites.

It is important to mention that the same arsenal and biological responses of PMNs discussed above that are involved in host defense can also be deleterious for an organism when deregulation occurs. This phenomenon is known as the neutrophil paradox. Because of this, and knowing the role of PMNs during inflammation (PMNs are seen as conductors of inflammation), it is very important to carefully understand the mode of action of PMN agonists as well as to identify new ones, including the new actors, NPs. Because how NPs interact with PMNs is an area of research that is still in infancy and that a lot of work needs to be done, it is important to determine how a given NP will alter or not several PMN functions in order to obtain a general picture rather than investigating only one or two functions. Also, even if an agent is not a direct PMN agonist by itself, it can be indirectly proinflammatory by attracting these cells in vivo, as is the case with the cytokine IL-21 [28]. This aspect needs also to be studied with NPs. For this reason, the following sections will describe how several PMN functions can be studied in vitro. Of note, several techniques and methods can be used to determine a given PMN function; but for clarity and simplicity, I will describe those that are used by several laboratories, especially the assays that are routinely used in mine. In addition to this in vitro aspect, I will described how we performed the murine air pouch model, a model recently proposed by a consortium of 18 researchers from six different countries, as a future standard assay for testing NPs in vivo [29].

3. Evaluating neutrophil functions In vitro

3.1. Neutrophil source

The first step for investigating neutrophil cell biology is to have access to a PMN source. Although some researchers, including ourselves, used immature human cell lines such as HL-60 and PLB-9895, these cells are not primary neutrophils and may respond differently [30]. Others used rodent PMNs for investigating the role of different agents on neutrophil biology. However, it is important to remember that unlike humans where more than 65–70 % of circulating leukocytes are neutrophils, this proportion do not exceed ~25 % in rodents [31]. In addition, although methods for human neutrophil isolation are now standardized, similar procedures for isolating PMNs from nonhuman species are not as well developed. Because

http://dx.doi.org/10.5772/60703

PMNs are very reactive cells, the method of isolation is extremely important to avoid cell activation during the isolation process. In respect with this, different techniques have been proposed [32] for isolating highly purified PMNs from large animals (bovine, equine, ovine), small animals (rodents, rabbit), and nonhuman primates (macaques). In my laboratory, we are using human blood as a source of neutrophils and we freshly isolate them in order to perform several studies, including the role of chemicals of environmental concern [30, 33-35], plant lectins and extracts [36, 37], cytokines [28, 38-46], myeloid-related proteins [47-49], different other compounds [19, 50-55], and, more recently, NPs [56-59]. Blood is obtained from healthy consenting individuals according to institutionally approved procedures, but it is also possible to isolate PMNs from blood of patients suffering from a given disease for comparison with age- and sex-matched healthy individuals.

3.2. Cell viability, necrosis, and purity

It is important to evaluate cell viability immediately after PMN cell isolation. We propose to determine this by the trypan blue exclusion assay since, during this method, it is also possible to simultaneously evaluate if cells are activated (irregular cell shape) or not (round or spherical shape) following the isolation procedure. In addition, it is mandatory to evaluate cell viability over time, especially after 24 h of incubation, since the rate of apoptotic PMNs is normally in the range of 30–50 % without addition of any exogenous agents. Moreover, apoptotic PMNs are known to exclude trypan blue and are thus considered "viable" and not necrotic. In parallel, we strongly suggest to evaluate neutrophil purity that could be verified by cytology from cytocentrifuged preparations colored with Hema-3 stain set, a procedure allowing a differential count. We never performed experiments with samples having ≥ 3 % eosinophils, the most contaminant cell type observed in our preparations. Other methods can also be used to evaluate cell viability, such as the determination of the release of lactate dehydrogenase (LDH) measured by a colorimetric assay and the dimethylthiazolyl-diphenyltetrazolium (MTT) reduction assay. Several commercially available kits exist; however, it is mandatory to first verify if a given NP could interfere with the assay to avoid false assessment of toxicity [60-62].

3.3. Cell shape changes

Naive non-activated neutrophils possess a round or spherical shape [41]. To study the effect of a given agent on neutrophil activation, cells have simply to be incubated in the presence of the molecule of interest, and morphological examination is monitored over time by optical microscopy [41, 58].

3.4. Actin polymerization

Actin is a cytoskeletal protein involved in several (if not all) PMN functions. It is possible to study its polymerization as a marker of neutrophil activation [63] where actin monomer (G-actin) will be reorganized to form, for example, filaments or F-actin. To do so, PMNs are incubated for short periods of time (normally from 0 to 30 min) at 37 °C with buffer (control) or with a molecule of interest in a final volume of 100 μL. Synthetic peptide N-formyl-

methionyl-leucyl-phenylalanine (fMet-Leu-Phe) is used as a positive control for the assay [36]. After incubation, digitonin and paraformaldehyde are used for permeabilization and cell fixation, respectively, and then PMNs are washed twice by centrifugation and incubated with phalloidin-FITC (binds to filamentous of actin) for 20 min at 4 °C (light protected) prior to FACS analysis.

3.5. Expression of tyrosine phosphorylated proteins

Another manner to determine rapid PMN activation by a given agent is to determine its potential induction of phosphorylation events, especially tyrosine phosphorylation [44, 48]. This consists of incubating PMNs with a given agent for several short periods of time (typically, 30–60 s and 5, 15, and 30 min), and then the reaction is stopped by adding Laemmli's sample buffer, as described previously [30, 48]. Aliquots corresponding to a desire number of cells (we are using normally 1 x 10^6 cells) are then loaded onto 10 % SDS–PAGE and transferred from gel to a nitrocellulose or polyvinylidene difluoride membrane and nonspecific sites are treated with a blocking solution [48]; the membrane is then washed and incubated with monoclonal anti-phosphotyrosine antibody. The membrane is washed and incubated with a horseradish peroxidase-conjugated anti-mouse IgG + IgM antibodies for about 1 h, and, after washing, phosphorylated bands are revealed with ECL Western blotting detection system. In our hands, protein loading is verified by probing the membrane (after stripping) with an anti-β-actin or anti-GAPDH antibody and/or by staining the membranes with Coomassie blue at the end of each experiment.

3.6. Neutrophil adherence assay

Adhesion of PMNs is an important biological response involved during inflammation. This response could be studied by several ways. In my laboratory, we determine the capacity of PMNs to adhere onto a cell substratum using the well-characterized human epithelial A549 cells [64]. Briefly, after obtaining the desired confluence of A549 cells grown onto coverslips, PMNs (pretreated or not with a given agent for a desire period of time) are stained for 30 min with calcein AM and incubated with A549 cells. The number of adherent PMNs are then calculated by counting the number of fluorescent cells from five randomly selected high-power fields, as previously published [43, 64].

3.7. Chemotaxis

Chemotaxis of human PMNs could be easily studied using a Boyden chamber assay. The bottom wells are loaded with buffer or agonists to be tested (typically in a final volume of 25 μl), the membrane is then placed over the wells, and the top layer of the chamber is added over the membrane. Cells (in 50 μl) are added to the top chamber wells, and the chamber is incubated at 37 °C for a given period of time (normally 0–60 min) in a humidified incubator in the presence of 5 % CO_2. After the incubation, the top of the chamber is removed and the upper side of the membrane is wiped carefully with the rubber scraper furnished by the manufacturer. Then, the membrane is fixed in methanol, colored with Hema-3 stain kit, mounted on a glass slide, and examined under oil immersion at 400 x. The details of the

http://dx.doi.org/10.5772/60703

procedure have been previously published [65, 66]. In this assay, the potent neutrophil chemokine CXCL8 (IL-8) is used as a positive control [67].

3.8. ROS generation

3.8.1. Superoxide production

Several assays can be used to evaluate ROS generation by human PMNs. Since the major source of ROS in PMNs occurred after NADPH oxidase activation leading to superoxide production (O_2^-), we routinely used the colorimetric assay based on reduction of cytochrome c, as previously published [48, 51]. Briefly, PMNs (1 x 10^6 cells/ml) are suspended in buffer supplemented with 1.6 mM $CaCl_2$ with or without 10 μg/ml superoxide dismutase (SOD) with 130 μM ferrocytochrome c for 5–90 min at 37 °C in the presence of various concentrations of the agonists to be tested or phorbol 12-myristate 13-acetate (PMA) at 10^{-7} M, used as a positive control. The reduction of cytochrome c is then monitored at 550 nm, and the concentration of O_2^- anions produced is calculated by the difference between corresponding wells with or without SOD using an extinction coefficient of 21.1.

3.8.2. Detection of intracellular ROS

Flow cytometry is frequently used to measure ROS production. Using different probes, we can evaluate the production of ROS mainly originating from the mitochondria or endoplasmic reticulum, depending on the probe used. We routinely used the CM-H2DCFDA probe and measured the fluorescence with a FACScan. ROS production is expressed as mean fluorescence intensity (MFI) [48].

3.9. Degranulation

Degranulation is one of the most important functions exerted by PMNs for the defense of an organism. Following activation, PMNs will rapidly release potent degradative enzymes and several receptors involved in the recognition and ingestion of pathogens. These products are localized in different kinds of granules: azurophil, specific/gelatinase, and secretory granules [68, 69].Because granules will fuse with the cytoplasmic membranes and release some products on the cell surface and then in the external milieu, it is possible to study in the laboratory the cell surface expression of markers of the different types of granules [70]. Therefore, we routinely determine the cell surface expression of CD35, CD63a, andCD66b by flow cytometry, since these molecules are specific markers of azurophil, specific/gelatinase, and secretory granules, respectively [47, 53, 56]. Excellent antibodies to these markers are commercially available.

Although the expression of the above markers could be increased (or not) at the PMN cell surface after stimulation, it is also important to determine if a protein known to be expressed in a given type of granule is released into the external milieu. To do so, we harvested the extracellular milieu after several periods of time following stimulation and performed Western blot experiments using antibodies specific for myeloperoxidase (azurophil), matrix metalloproteinase-9 or MMP-9 (specific/gelatinase), or albumin (secretory). The details of the protocol have been previously described [47, 53].

Even if a given granule product is released by activated PMNs into the external milieu, it is interesting to know also if an enzymatic activity could be preserved in the fluids. To test this, we performed zymography assay. After stimulation of human PMNs, cells are centrifuged at 13,000 rpm for 10 min at 4 °C and the pellets are discarded. The supernatants (10–50 µl, corresponding to 50,000 cells) are then mixed with a nonreducing buffer (40 % glycerol, Tris-HCl 1 M, pH 6.8, SDS 8 %) and separated on 10 % acrylamide gels containing 0.2 % gelatin. Gels are washed twice for 30 min with 2.5 % Triton X-100 and incubated overnight in digestion buffer (Tris-HCl 50 mM, pH 7.4, NaCl 150 mM, $CaCl_2$ 5 mM). The gels are stained with Coomassie blue 0.1 % and then destained. Densitometric analysis is performed to quantify the intensity of the white zones corresponding to gelatinase activity digesting gelatin incorporated into the gel [47, 53, 71].

3.10. Phagocytosis

Our preferred technique for evaluating PMN phagocytosis consists of the ingestion of opsonized sheep red blood cells (SRBCs). In this assay, PMNs are treated with a given agent or the corresponding buffer for a given period of time and cells are incubated with SRBCs pretreated with a final 1/200 dilution of commercially available rabbit IgG anti-SRBCs for 30–45 min at 37 °C in a 1:5 ratio. The samples are centrifuged 200 x g at 4 °C for 10 min. Supernatants are discarded and, to eliminate noningested SRBCs, the pellets are treated with 300 µl of H_2O for 20 s followed immediately by the addition of 4.5 ml ice-cold PBS [45, 48, 54, 72]. After washing, the final pellets are suspended to a final concentration of 10 x 10^6 cells/ml. Duplicate cytocentrifuged preparations are then stained with Hema-3 stain kit, and the phagocytosis rate is determined by counting the number of PMNs ingesting at least one opsonized SRBC.

3.11. Apoptosis

Apoptosis can be evaluated by several different methods. We routinely determine the apoptotic rate of human PMNs by two assays in parallel, by cytology and flow cytometry [37, 38, 40, 44, 51, 73]. For both assays, freshly isolated human PMNs are incubated (10 x 10^6 cells/ml in RPMI-1640 supplemented with 10 % autologous serum) at 37 °C in 5 % CO_2 in 96-well plates for 24 h with a given agonist and its corresponding buffer/vehicle. Cells are then harvested to perform the assays as follows.

3.11.1. Cytology

For cytology, cells are cytocentrifuged on microscope slides, stained with the Hema-3 staining kit and examined by light microscopy at 400x final magnification. Apoptotic neutrophils are defined as cells containing one or more characteristic darkly stained pyknotic nuclei. Results are expressed as the percentage of PMNs in apoptosis.

3.11.2. Flow cytometry

For the flow cytometric procedures, PMNs are stained with FITC annexin-v or an FITC antihuman CD16 antibody. During apoptosis, the flip–flop of phosphatidylserines occurred, leading to their expression at the cell surface. Since annexin-v possesses a very high affinity to bind to phosphatidylserines, apoptotic cells will be positive to FITC annexin-v. In this assay,

http://dx.doi.org/10.5772/60703

propidium iodide can also be used to measure cell necrosis in parallel. In contrast, cell surface expression of CD16 (that is very high in normal PMNs) is lost during PMN apoptosis resulting from CD16 shedding.

3.12. Cytokine production

PMNs are known to produce several cytokines [74]. There are several different approaches that can be used to measure the production of cytokine. We prefer to study production of cytokine at the protein level. We used an antibody array assay for screening purpose and then quantified a given cytokine by ELISA. For both assays, supernatants of activated PMNs are harvested and used for the detection of cytokines. When fluids are frozen, we normally use them within three weeks after the experiments to eliminate possible cytokine/chemokine degradation occurring over time.

3.12.1. Antibody array: Proteome profiler™ array

We used a commercially available human cytokine array panel for the screening purpose. All the steps for the detection of different analytes are performed following the manufacturer recommendation and as previously described [50, 75]. To detect the different analytes (cytokines/chemokines), we used pooled supernatants harvested from neutrophils (10 x 10^6 cells/ml in RPMI1640-HEPES p/s supplemented with 10 % autologous serum) treated for different periods of time with buffer (negative control) and LPS (positive control) or with the tested agents to probe the membranes. The chemiluminescent signal from the bound analytes present in the supernatants is then detected on Kodak X-OMAT-RA film. The signal intensity of each analyte (in duplicate) is normalized to the membrane's positive controls. Protein array membranes are scanned and densitometric analysis is performed using the AlphaEaseFC (FluorChem HD2) software.

3.12.2. ELISA

The measurement of a given cytokine/chemokine (such as IL-6/IL-8) is determined with commercially available specific enzyme-linked immunosorbent assay (ELISA) kits. Neutrophils are incubated as above in a 96-well plate, and the supernatants are harvested, centrifuged, and stored at -80 °C for no more than three weeks before performing ELISA. Unlike the antibody array assay described above, each supernatant (normally at least from five different blood donors) is used to quantify the amount of the tested analyte.

3.13. De novo protein synthesis

Cells (10 x 10^6 cells/ml in RPMI-1640 medium supplemented with 10 % autologous serum) are metabolically labeled with 4.625 MBq of the Redivue Pro-Mix L-[^{35}S] in vitro cell labeling mix in the presence or absence of a given agonist or with 1–10 μg/ml cyclohexymide (CHX), an inhibitor of protein synthesis, or a mixture of both the agonist and CHX for 24 h [38, 41, 51, 76]. Cells are then harvested, and cell lysate is prepared for SDS–PAGE as previously described. After electrophoresis, gels are stained with Coomassie blue (to verify

equivalent loading), dried, and exposed with Kodak X-OMAT-RA film at -80 °C for 1–3 days. Absence of new polypeptides is observed in the lanes where the cells were treated with CHX.

4. Evaluating PMN infiltration In vivo

Several animal models of inflammation have been developed over the years. Some are suitable for understanding the mechanisms involved in the development of inflammatory diseases. The collagen-induced arthritis model is a good example [77-79]. Other models focus on pulmonary inflammation, including mouse models of allergic asthma. Typically, in this latter model, animals are sensitized to a foreign antigen by intraperitoneal injection in the presence or absence of an adjuvant. After the sensitization period, mice are challenged with the antigen directly in the lungs or the nose, and airway inflammation is then elicited. Although PMNs are known to exert some pathological effects during arthritis and in some cases during asthma, the observed cells in these models are not necessarily PMNs, but rather mainly some lymphocytes and eosinophils in collagen-induced arthritis and asthma models, respectively. However, in several other inflammatory models where a given agent is administered by inhalation, intratracheally or directly into lungs, PMNs will be easily observed in the bronchoalveolar lavages or lungs. However, these models are time consuming, are not the cheapest, and, in addition, necessitate a certain degree of technical skills. The rodent air pouch model of acute inflammation is probably the best, simple, not time-consuming, and cheapest model for monitoring leukocyte influx, including PMNs. This model has been used for investigating the inflammatory activity of a large number of compounds, including cytokines [28, 43, 80], plant extracts and lectins [81-83], different drugs [84-86], etc.

4.1. Murine air pouch

Several kinds of mice can be used to perform this model. For screening purpose, we recommended to use outbred CD-1 mice since they are less expensive than other inbred mice. Normally, we use female mice (6−8 weeks of age). A period of acclimation of about one week is allowed to animals prior to initiation of the experiments. On days zero and three, mice are anesthetized with isoflurane, and 3 cc of sterile air was injected subcutaneously, in the back, with a 26-gauge needle to form an air pouch as published previously. On day six, 1 mL of buffer control (HBSS or PBS) or an increasing concentration of a given compound is injected directly into the air pouch. Mice are then killed by CO_2 asphyxiation 3, 9, 12, or 24 h after the treatment, and the pouches are washed once with 1 ml and then twice with 2 ml of buffer containing 10 mM EDTA. Exudates are centrifuged at 100 X g for 10 min at room temperature, and supernatants are collected and stored at -80 °C for further analysis. Cells are resuspended at 0.5 x 10^6 cells/ml, spread onto microscope slides, and stained with Hema-3 stain kit for identification/quantification of leukocyte cell

http://dx.doi.org/10.5772/60703

subpopulations. The details of the model have been previously discussed [28, 35, 50, 87, 88]. Interestingly, several kinetics could be done with this model as well as several different experiments using the exudates such as the determination and quantification of different soluble factors including cytokines and chemokines. Moreover, the exudates could be used to perform zymography experiments to determine, for example, gelatinase activity. After centrifugation of the collected exudates, cells can also be incubated in vitro for studying the different PMN functions, especially in an experimental condition such as LPS-induced murine air pouches, where more than 85 % of cells are PMNs. It is also possible to purify a given type of leukocyte before performing in vitro assays. In brief, this model allows a panoply of different experiments. For example, we have used this model to demonstrate that an intraperitoneal administration of curcumin, prior to LPS-induced air pouch, was able to inhibit the proinflammatory effect induced by LPS [50].

5. Nanotoxicology and PMNs

While NPs have great potential for human needs, there are increasing concerns that the same features that make them so attractive and interesting also represent potential risks to human health [89]. Consequently, a new branch of toxicology, nanotoxicology, has recently emerged. Nanotoxicology could be defined simply as a discipline evaluating the role and safety of NPs on health. Exposure to NPs has increased dramatically in the past few years due to anthropogenic sources given that NPs can be formed via a wide variety of processes/methods. These sources are numerous and include internal combustion engines, power plants, and many other sources of thermodegradation [90]. Furthermore, intense research and development by the industry and academia multiply the number of individuals potentially exposed to NPs. Nanotoxicology is, therefore, a very complex discipline, and the diversity and complexity of NPs makes chemical characterization not only more important but also more difficult [91].

One of the most adverse effects of NPs reported in the literature is certainly inflammation. A variety of NPs were found to possess proinflammatory activities, principally based on their ability to increase the production of different proinflammatory cytokines [92-95] and on the observations that NPs can exacerbate airway inflammation in vivo [96-99]. However, as previously mentioned, inflammation is a normal biological response of the body to various assaults, including microorganisms, injuries, dusts, drugs, and other chemicals. Under normal circumstances, inflammation will subside and resolve itself in a healthy individual through a series of tightly regulated responses. However, when deregulation occurs, inflammation can lead to inflammatory disorders and diseases including asthma and several pulmonary lung diseases, dermatitis, arthritis, inflammatory bowel diseases, etc. [1, 100]. Curiously, despite the importance of PMNs in inflammation and since several studies reported an increased number of PMNs in NP-induced pulmonary inflammation, there are few studies investigating the direct effects of NPs and

their mode of action in PMNs. The following sections will cover different studies that have been done regarding the effects of some NPs on PMN cell physiology.

6. Interaction between nanoparticles and human PMNs

6.1. Interaction between nanoparticles and human PMNs: Not so novel finally

Probably the first study reporting a direct effect of NPs with human neutrophils was done more than 25 years ago where Hedenborg published in 1988 that titanium dioxide (TiO_2) dust induced the production of ROS by human neutrophils as measured by a chemiluminescence assay [101]. Different dust particles (ranging in size from 345 to 1,000 nm) were tested, and none of them were cytotoxic, as assessed by lysozyme release or trypan blue exclusion [101]. It was concluded that TiO_2 stimulated the chemiluminescence activity of PMNs in a concentration-dependent manner and that particle size and surface structure of the dust were important for determining the intensity of the response. Although the nanomaterial used for this study was not-typical NPs based on the definition that the three dimensions need to be smaller than 100 nM, the size was still in the nanometer range. In fact, the definition of an NP is complex, and according to the 2011 Commission of the European Union, the definition of an NP is: *"a natural, incidental or manufactured material containing particles, in an unbound state or as an aggregate or as an agglomerate and where, for 50% or more of the particles in the number size distribution, one or more external dimensions is in the size range 1-100 nm."* Therefore, according to such a definition, a "nano" object needs only one of its dimensions, <100 nm, to be classified as an NP, even if its other dimensions are not in that range. Strictly based on the nanometer terminology, one can define any objects in the nm range as a nanoparticle or at least as a "nano" object as was the case with this study investigating the effect of TiO_2 dust.

6.2. Studies from different laboratories

The next section will cover studies investigating the direct interaction between NPs and human neutrophils. Before describing works performed by others, I would like to mention that if some studies have been forgotten, this is completely unintentional on my part. Also, it is important to specify that few studies reported the effects of NPs on nonhuman neutrophils, including fish [102, 103] and rat [104] PMNs that are not part of this present review. Nevertheless, in brief, the results indicate that TiO_2 NPs stimulated oxidative burst and NET release in fathead minnow PMNs [102], whereas fullerenes were found to inhibit oxidative burst and suppressed the release of NETs and degranulation of primary granules [103]. In rats, poly(lactide acid) or PLA nanoparticles were reported to be more efficiently phagocytosed than PLA/poly(ethylene glycol) or PEG blends [104].

In one study, human PMNs incubated with increasing concentrations of polymethylmethacrylate (PMMA) NPs (50–60 nm) in vitro were found to release lactate dehydrogenase, lysosome, and beta-glucuronidase in a dose-dependent fashion [105]. In contrast, PMMA NPs diminished migration of PMNs in a dose-dependent manner, as assessed by measuring the

http://dx.doi.org/10.5772/60703

distance attained by the leading front of cells in Boyden chambers. Interestingly, polystyrene beads (50 nm in diameter) were employed as a physical control throughout the study, and they were also found to affect the same PMN functions as compared with cells incubated with the buffer alone, but the intensity of the response was inferior to that of PMMA NPs.

In 1996, using solid lipid NPs (SLN) produced by high-pressure homogenization of melted lipids (glycerolbehenate, cetylpalmitate), Müller and colleagues modified the surface of these NPs with hydrophilic poloxamine 908 and poloxamer 407 block copolymers and found slightly different results regarding the phagocytic uptake and cell viability of human PMNs [106]. Interestingly, cell viability was ≥ 80 % for all studied NPs with a diameter ranging from 123 to 246 nm, as assessed by the colorimetric MTT assay. Modification of the solid lipid NPs with poloxamine 908 and poloxamer 407 reduced phagocytic uptake to 8–15 % of hydrophobic polystyrene particles. The same team also reported, in another study, the in vitro cytotoxicity of SLN as a function of lipid matrix and stabilizing surfactant not only in mature PMNs but also in human promyelocyte HL-60 cells. These latter cells, which can be differentiated in laboratory toward neutrophil-like cells with dimethyl sulfoxide, were used for comparison with fully mature PMNs isolated from the blood of healthy volunteers. The aim was to use this cell line to replace the daily PMN isolation that is costly and time consuming. They reported that the nature of the lipid had no effect on PMN and HL-60 cell viability. However, some distinct differences were found for the surfactants. For example, binding of poloxamer 184 to the SLN surface reduced the cytotoxicity of the surfactant by a factor of ~65. They concluded that HL-60 cells represented a potentially good model for replacement of primary PMNs. In addition to HL-60, PLB-985 cells can also be driven by chemical treatment into "neutrophil-like cells but, as we previously documented, both cell lines can respond differently than PMNs [30, 107]. Therefore, I believe that results obtained from "real" human mature PMNs are more easily interpretable for the evaluation of human risk.

The cytotoxicity of injectable cyclodextrin nanoparticles/nanocapsules (specifically, β-CDC6) in mouse L929 fibroblasts and human PMNs has been determined in one study [108]. The cytotoxicity was evaluated in the presence or absence of PF68, the most commonly used surfactant in NP formulations and designed to be potentially utilized as an injectable nanosized drug carrier. Depending on the formulation, the particle size distribution was between ~110 and 350 nm. Using MTT assay, it was concluded that β-CDC6 NPs do not exert a significant cytotoxicity against both types of cells. Of note, although the experimental conditions were appropriate for fibroblasts (three days before performing the assay), this is not necessarily the same for human PMNs known to spontaneously undergo apoptosis when incubated in vitro; about 50 % of PMNs are already in apoptosis after only 24 h [4, 37]. In 2006, the effects of cholesteryl butyrate (chol-but) solid lipid NPs and PMNs were investigated [109]. In vitro incubation of PMNs with 10^{-8}-10^{-4} M cholesteryl butyrate solid lipid nanoparticles (chol-but SLNs, mean diameter of 130–160 nm) for 10–240 min did not lead to cytotoxic effects as determined by the trypan blue exclusion assay [109]. Chol-but SLNs were found to inhibit adhesion of PMNs onto fetal calf serum-coated plastic wells as well as onto human umbilical vein endothelial cells. Also, in this study, the ability of FMLP-induced O_2^- production and FLMP-induced MPO release by PMNs was inhibited by chol-but SLN. More recently, the

capacity of human immune cells to internalize rod-shaped and spherical gold NPs (AuNPs), with diameters of 15–50 nm and a variety of surface chemistries, has been determined. Interestingly, in contrast to monocytes–macrophages that were found to ingest AuNPs [110], PMNs rather "trap" them in NETs [111]. The cell-gold networks, already observed after 15 min of treatment of immune cells with the AuNPs, were predominantly observed in PMNs and, to a lesser extent, in monocytes and macrophages. This indicates that NETs act as a physical barrier for NPs. In addition, in this study, the authors demonstrated that the particle shape is not very important for particle trapping, whereas the positive charges significantly enhance this phenomenon [111]. Influence of AuNPs on activation of human PMNs was also investigated in another study where AuNPs with a size of 60 nm were found to induce generation of free radicals as assessed by a chemiluminescence assay [112]. The authors proposed that the influence of AuNPs on the membrane surface potential of PMNs was most likely the mechanism involved.

Interaction between silver nanoparticles-polyvinyl-alcohol (AgNPs-PVA) and human PMNs was recently investigated. In this study, PMNs were incubated in the presence of 10 μM of AgNPs-PVA, and the increased ROS production was determined by flow cytometry using the DCFH-DA probe [113]. Curiously, in this study, the authors determined necrosis and apoptosis by flow cytometry after staining with PI and annexin-v in human hepatocellular carcinoma (HepG2) and in peripheral blood mononuclear cells (PBMCs), but not in PMNs. Both cell necrosis and apoptosis were significantly increased after treatment with the NPs. Further, they investigated cellular uptake in HepG2 and PBMCs based on increased SSC fluorescence intensity recorded by flow cytometry, but, again, not in human PMNs.

Several PMN functions, including viability, chemotaxis, phagocytosis, oxidative burst, and cytokine production (IL-1β, IL-6, and IL-8), were investigated in response to an immunosuppressive agent sirolimus (SRL) alone, SRL-loaded poly(d,l-lactide) nanoparticles (SRL-PLA-NPs), and plain PLA-NPs [114]. While phagocytic activity was markedly reduced, but recovered within 3 h, the other tested PMN functions were not affected.

In their study, Haase et al. (2014) compared the effects of AgNPs and ionic silver (Ag+) on cells of the innate immune system, in particular on PMNs and macrophages [115]. They generated five kinds of AgNPs (diameters ranging from 2 to 35 nm) and did not observe any impact on phagocytosis, oxidative burst, as well as activation of the TNF-α promoter. In contrast, AgNPs and Ag+ were found to induce NET release and to inhibit the formation of nitric monoxide. Also, both AgNPs and Ag+ were found to increase intracellular ROS levels as well as the second messenger Zn2+. Therefore, based on these data, the effect of AgNPs on human PMNs is not specific to the particles since they are also observed with Ag+.

6.3. Our involvement in studying interaction with NPs and human PMNs

Our laboratory has been interested in investigating the role of NPs on the biology of human PMN because one of the most reported adverse effects of NPs after administration in animals or when incubated in vitro in different type of cells is inflammation, our main expertise. Of note, we voluntary use unloaded, naked, or plain engineered NPs in our present studies based on the fact that several kinds of NPs are commercially available and since we believe that it is

http://dx.doi.org/10.5772/60703

important to first establish how human PMNs will react with a given NP before trying to use this latter as potential carrier for drug delivery, for example. In addition, since these NPs are relatively easy to obtain and that several of them are probably already used by workers in different kinds of industries, it is warranted to understand their mode of action as they are handled and/or used by individuals. The first study was published in 2010, indicating that our involvement in this area of research is recent [57]. We investigated how human PMNs respond to TiO_2 NPs since these NPs were (and are still) the most studied NPs reported in the literature. We used a commercially available preparation of TiO_2 NPs (anatase crystals) of 1–10 nm in size, as determined by transmission electronic microscopy (mentioned in the technical data sheet and also confirmed by us). We first incubated freshly isolated human PMNs with increasing concentrations of TiO_2 NPs (0–800 μg/ml) over time and determined their potential cytotoxicity. As assessed by trypan blue exclusion assay, the NPs did not decrease cell viability and only a small portion ≤ 3 % of cells were in necrosis after 24 h of incubation at the highest concentration tested. We next determined if TiO_2 NPs could induce morphological cell shape changes in PMNs, an indicator of cell activation. After 24 h, the optimal concentration inducing cell shape changes was 100 μg/ml, a concentration used by others with human lymphocytes [116]. Others reported the use of TiO_2 NPs up to 4,000 μg/ml for in vitro studies, but in U937 human monoblastoid cell line [117]. Interestingly, we demonstrated that TiO_2 NPs were able to induce rapid tyrosine phosphorylation events in PMNs as quickly as 15 s, with a maximal effect at 1 min of treatment. More specifically, we identified Erk-1/2 and p38 MAP kinases, the two major enzymes involved in different PMNs functions, as targets of TiO_2 NPs [57]. Concordant with our data indicating TiO_2 NPs were not cytotoxic, we reported and demonstrated that they significantly inhibited PMN apoptosis. Using an antibody array assay allowing the simultaneous detection of different cytokines/chemokines, TiO_2 NPs were found to increase the production of 13 analytes, including IL-8 and Gro-α, two potent neutrophil activators. They exhibited the greatest increase (~16 times and ~4 times more vs control cells, respectively). Because antibody assay is a semiquantitative assay, we next confirmed that TiO_2 NPs increased IL-8 production by quantitative ELISA. Taken together, these results clearly indicate that TiO_2 NPs are neutrophil activators.

In another study, we focused our attention on the human PMN degranulation process not only in response to TiO_2 NPs but also after treatment with two other metal oxide NPs, zinc oxide (ZnO) and cerium dioxide (CeO_2) [56]. This was probably the first study investigating the effect of NPs on degranulation. Because TiO_2 was previously found to activate PMNs, we first determine whether or not ZnO and CeO_2 NPs could be neutrophil modulators. We found that all NPs (having the size of 1–10 nm) were able to activate PMNs, based on induction of actin polymerization. As assessed by flow cytometry, the three types of NPs slightly downregulated cell surface expression of the granule marker CD35 but increased CD66b and CD63 expression. In addition, the protein expression of myeloperoxidase, MMP-9 and albumin stored in azurophil, specific/gelatinase, and secretory granules, respectively, was significantly increased in the supernatants of NP-induced PMNs vs supernatant from untreated cells. Also, both TiO_2 and CeO_2 were found to markedly increase the enzymatic activity of MMP-9 released into the supernatants, as determined by gelatin zymography. ZnO NPs were found to only exert a modest effect in these experiments. Therefore, the three NPs can differentially affect all steps

involved during neutrophil degranulation, namely, cell surface expression of granule markers, liberation of proteins in the supernatants, and enzymatic activity [56].

We next examined the role of AgNPs with a starting size of 20 nm ($AgNP_{20}$) on human PMN apoptosis. Treatment of PMNs with $AgNP_{20}$ results in increased cell size, and TEM experiments revealed that $AgNP_{20}$ can rapidly interact with the cell membrane, penetrate inside neutrophils, localize in vacuole-like structures, and be randomly distributed in the cytosol after 24 h [59]. Treatment with 100 μg/ml $AgNP_{20}$ for 24 h (but not 10 μg/ml) increased the PMN apoptotic rate as determined by cytology and by flow cytometry after staining with FITC annexin-v. Also, $AgNP_{20}$ was found to inhibit de novo protein synthesis as demonstrated by gel electrophoresis of metabolically [^{35}S]-labeled cells as strong as the potent protein inhibitor cycloheximide. Therefore, $AgNP_{20}$ was identified as potent PMN proapoptotic agents. Preliminary experiments indicate that $AgNP_{70}$ (70 nm), in contrast to $AgNP_{20}$, delays human PMN apoptosis (*our unpublished data*) in agreement with the fact that an NP with a different size (here 20 vs 70 nm) can act completely different.

Based on these results, we were interested in investigating more in depth how ZnO NPs can alter human PMN biology. We demonstrated that ZnO increased the cell size, induced cell shape changes, activated phosphorylation events, and enhanced cell spreading onto glass, but did not induce the generation ROS [58]. In contrast to $AgNP_{20}$, treatment of PMNs with ZnO markedly and significantly inhibited apoptosis and increased de novo protein synthesis. Utilization of cycloheximide reversed not only the ability to increase de novo protein synthesis but also the antiapoptotic effect of ZnO NPs. It was concluded that ZnO NPs are activators of several human PMN functions and that they inhibit apoptosis by a de novo protein synthesis-dependent and ROS-independent mechanism. In the future, it will be of interest to identify the nature of proteins that are neo-synthesized in response to ZnO NPs.

7. In vivo infiltration of PMNS induced by NPs using the murine air pouch model

The effect of different sets of nanoparticles were tested by Vandooren et al. [29] using the murine air pouch model. The tested NPs were CANs maghemite, type I PEI-CAN-maghemite, type II PEI-CAN-maghemite, PDMAEMA-SCPNs, PMAAc-SCPNs, PLGA-COOH, PLGA-b-PEG-COOH, Magh@PNPs, LNP LII, and CAN CIII. All details regarding their characterization (size, zeta potential, PDI, etc.) are described in their study. When compared with the negative control (phosphate-buffered saline or PBS), the number of attracted leukocytes were increased with all NPs, but PMAAc-SCPNs and CAN CIII. The highest count they observed was ~2.8 x 10^6 cells/pouch, after treatment with type II PEI-CAN-maghemite NPs vs ~0.8 x 10^6 cells/pouch. Interestingly, for almost all tested NPs, the majority of leukocytes recruited into air pouch were PMNs (sometime up to ~90 %). From this study, it was proposed to use the air pouch leukocytosis model as a future standard assay for an in vivo test for nanoparticles. Although I am in favor, it is important to mention that the leukocyte infiltration was only determined after 24 h of treatment, a time point that is probably not the optimal one. As

http://dx.doi.org/10.5772/60703

previously proposed [118], it is better to perform kinetic experiments with the murine air pouch model, especially between 3 and 12 h, as we previously documented for determining the effect of different kinds of agents on inflammation [28, 35, 43, 50, 87, 88, 119]. This is particularly true for NPs, since their mode of action is still not fully understood. Moreover, time points after 24 h should also be investigated because of lack of knowledge with proinflammatory activity of NPs in such a model.

The potential proinflammatory activity of iron oxide-containing magnetic nanoparticles (MNPs) was investigated using the murine air pouch model. Administration of 1,000-MNPs and 2,000-MNPs (1,000 and 2,000 referring to 1,000 μg or 2,000 μg of iron in terms of CAN maghemite particles) in C57BL/6 mice induced a prominent influx of leukocytes, mainly PMNs as determined by differential count and by flow cytometry using anti-CD11b + anti-/Gr-1 antibodies. The neutrophilia was similar to the effect obtained with the positive control chlorite-oxidized oxyamylose [120]. Since several authors of this study were also authors in the original work describing the use of the murine air pouch as a standard assay for in vivo testing of NPs, they did not evaluate the effects of the NPs before the 24 h time point.

Although we have been using the murine air pouch model in our laboratory for ~13 years for testing potential effects of different agents on inflammation, it is only recently in 2011 that we used it to demonstrate for the first time that a given NP, namely, titanium dioxide (TiO_2), was proinflammatory. Indeed, administration of a single dose of TiO_2 NPs into the air pouch attracted leukocytes after 3–9 h, where more than 80 % of cells were PMNs [75]. In addition, in this study, we reported that TiO_2 NPs induced the production of several chemokines locally present in the air pouch exudates. This model is a simple model that allows investigation of an acute inflammatory response, the first step leading to chronic inflammation when deregulation occurs, such as the many studies reporting an increased number of PMNs in the lung/BALS [98, 99, 121-125]. On the other hand, the fact that an NP possesses some proinflammatory properties could be of help for the design of drug delivery by NPs for clinical purposes. In this regard, one can imagine attracting leukocytes such as PMNs into an inflammatory site by a NP delivering (or coated with) a neutrophil proapoptotic molecule. Although this is speculative at the moment, this remains an interesting avenue of research that needs to be explored in the future.

Kinetic and dose-dependent experiments performed with the murine air pouch model of acute inflammation revealed that, unlike TiO_2 used as a positive control in this model, C_{60}(OH)n (fullerenols) NPs were not proinflammatory in CD-1 mice [126]. To further confirm this negative result and since, yet, no genetic susceptibility has been reported regarding the biological activity of NPs, we performed other sets of experiments using C57BL/6 and BALB/c mice. Again, no significant leukocyte attraction was observed into air pouch. However, after 3 h of treatment, C_{60}(OH)n NPs were found to amplify the effect of lipopolysaccharides (LPS) causing a rapid leukocyte influx in which the major cells observed were PMNs. Using an antibody array assay to detect different analytes present in the exudate led us to conclude that the amplification effect is explained, at least partially, by an increased local production of several cytokines/chemokines in the exudates, including the proinflammatory cytokines IL-1β and IL-6. In fact, the profile of analytes was different in response to LPS alone, C_{60}(OH)n alone, and the mixture of both.

Using an ELISA to quantify the amount of IL-6, we demonstrated that C_{60}(OH)n increases the LPS-induced local production of this cytokine. Therefore, although C_{60}(OH)n NPs alone do not exert proinflammatory activity under certain conditions, they can act in concert with other agents to cause inflammation, a situation that is likely to occur in vivo. These results further reinforce that the murine air pouch model is to be performed at different periods of time (kinetic experiments) as discussed above.

8. Conclusion

Most of the in vitro studies discussed above evaluated the cytotoxicity and/or only one or few PMN response(s). Yet, no study other than our own has determined the effects of NPs on the PMN apoptotic rate, a very important process for regulating the number of PMNs. However, more recent reports have investigated the interaction between NPs and PMNs by studying different functions/responses, an approach that we encourage. The fact that TiO_2 NPs induced the production of several analytes, including two potent chemokines (IL-8 and Gro-α) is a good example demonstrating that NPs can indeed target PMNs that, in turn, could attract/activate other cells [57]. It is highly probable that, in the forthcoming years, several aspects regarding the effects of different NPs on the biology of human PMNs will be studied. Although there is a growing interest in developing in vitro assays in nanotoxicology [127], it is also strongly encouraged to use primary human cells as a source of in vitro cells for testing NPs, since cancerous cell lines of different origins will complicate data interpretation for the evaluation of human risk. In addition, determining how a given NP alters inflammation in vivo in other models than those exclusively targeting the lungs, such as the murine air pouch model, will help us to better evaluate the potential toxic mechanisms of NPs, especially how they alter the inflammatory process.

Acknowledgements

This study was supported by the Institut de recherche Robert-Sauvé en santé et en sécurité du travail (IRSST).

Author details

Denis Girard*

Address all correspondence to: denis.girard@iaf.inrs.ca

Laboratoire de recherche en inflammation et physiologie des granulocytes, Université du Québec, INRS-Institut Armand-Frappier, Laval, Qc, Canada

http://dx.doi.org/10.5772/60703

References

[1] Edwards, S. W. and Hallett, M. B. (1997) Seeing the wood for the trees: the forgotten role of neutrophils in rheumatoid arthritis. Immunol Today 18, 320-4.

[2] Edwards, S. W. and Watson, F. (1995) The cell biology of phagocytes. Immunol Today 16, 508-10.

[3] Ward, C., Dransfield, I., Chilvers, E. R., Haslett, C., Rossi, A. G. (1999) Pharmacological manipulation of granulocyte apoptosis: potential therapeutic targets. Trends Pharmacol Sci 20, 503-9.

[4] Duffin, R., Leitch, A. E., Fox, S., Haslett, C., Rossi, A. G. (2010) Targeting granulocyte apoptosis: mechanisms, models, and therapies. Immunol Rev 236, 28-40.

[5] Silva, M. T. (2010) Secondary necrosis: the natural outcome of the complete apoptotic program. FEBS Lett 584, 4491-9.

[6] Akgul, C., Moulding, D. A., Edwards, S. W. (2001) Molecular control of neutrophil apoptosis. FEBS Lett 487, 318-22.

[7] Savill, J. (1997) Apoptosis in resolution of inflammation. J Leukoc Biol 61, 375-80.

[8] Fox, S., Leitch, A. E., Duffin, R., Haslett, C., Rossi, A. G. (2010) Neutrophil apoptosis: relevance to the innate immune response and inflammatory disease. J Innate Immun 2, 216-27.

[9] Sanghavi, D. M., Thelen, M., Thornberry, N. A., Casciola-Rosen, L., Rosen, A. (1998) Caspase-mediated proteolysis during apoptosis: insights from apoptotic neutrophils. FEBS Lett 422, 179-84.

[10] Bhatia, M., Kirkland, J. B., Meckling-Gill, K. A. (1995) Modulation of poly(ADP-ribose) polymerase during neutrophilic and monocytic differentiation of promyelocytic (NB4) and myelocytic (HL-60) leukaemia cells. Biochem J 308 (Pt 1), 131-7.

[11] Santos-Beneit, A. M. and Mollinedo, F. (2000) Expression of genes involved in initiation, regulation, and execution of apoptosis in human neutrophils and during neutrophil differentiation of HL-60 cells. J Leukoc Biol 67, 712-24.

[12] Maianski, N. A., Geissler, J., Srinivasula, S. M., Alnemri, E. S., Roos, D., Kuijpers, T. W. (2004) Functional characterization of mitochondria in neutrophils: a role restricted to apoptosis. Cell Death Differ 11, 143-53.

[13] Conus, S., Perozzo, R., Reinheckel, T., Peters, C., Scapozza, L., Yousefi, S., Simon, H. U. (2008) Caspase-8 is activated by cathepsin D initiating neutrophil apoptosis during the resolution of inflammation. J Exp Med 205, 685-98.

[14] Witko-Sarsat, V., Mocek, J., Bouayad, D., Tamassia, N., Ribeil, J. A., Candalh, C., Davezac, N., Reuter, N., Mouthon, L., Hermine, O., Pederzoli-Ribeil, M., Cassatella, M.

A. (2010) Proliferating cell nuclear antigen acts as a cytoplasmic platform controlling human neutrophil survival. J Exp Med 207, 2631-45.

[15] Ge, Y. and Rikihisa, Y. (2006) Anaplasma phagocytophilum delays spontaneous human neutrophil apoptosis by modulation of multiple apoptotic pathways. Cell Microbiol 8, 1406-16.

[16] Bruno, A., Conus, S., Schmid, I., Simon, H. U. (2005) Apoptotic pathways are inhibited by leptin receptor activation in neutrophils. J Immunol 174, 8090-6.

[17] Cross, A., Moots, R. J., Edwards, S. W. (2008) The dual effects of TNFalpha on neutrophil apoptosis are mediated via differential effects on expression of Mcl-1 and Bfl-1. Blood 111, 878-84.

[18] Binet, F., Chiasson, S., Girard, D. (2010) Evidence that endoplasmic reticulum (ER) stress and caspase-4 activation occur in human neutrophils. Biochem Biophys Res Commun 391, 18-23.

[19] Binet, F., Chiasson, S., Girard, D. (2010) Arsenic trioxide induces endoplasmic reticulum stress-related events in neutrophils. Int Immunopharmacol 10, 508-12.

[20] Ron, D. and Walter, P. (2007) Signal integration in the endoplasmic reticulum unfolded protein response. Nat Rev Mol Cell Biol 8, 519-29.

[21] Todd, D. J., Lee, A. H., Glimcher, L. H. (2008) The endoplasmic reticulum stress response in immunity and autoimmunity. Nat Rev Immunol 8, 663-674.

[22] Ottonello, L., Frumento, G., Arduino, N., Bertolotto, M., Mancini, M., Sottofattori, E., Dallegri, F., Cutolo, M. (2002) Delayed neutrophil apoptosis induced by synovial fluid in rheumatoid arthritis: role of cytokines, estrogens, and adenosine. Ann N Y Acad Sci 966, 226-31.

[23] Cordero, O. J., Salgado, F. J., Mera-Varela, A., Nogueira, M. (2001) Serum interleukin-12, interleukin-15, soluble CD26, and adenosine deaminase in patients with rheumatoid arthritis. Rheumatol Int 21, 69-74.

[24] Steiner, G., Tohidast-Akrad, M., Witzmann, G., Vesely, M., Studnicka-Benke, A., Gal, A., Kunaver, M., Zenz, P., Smolen, J. S. (1999) Cytokine production by synovial T cells in rheumatoid arthritis. Rheumatology (Oxford) 38, 202-13.

[25] Kasper, B., Brandt, E., Ernst, M., Petersen, F. (2006) Neutrophil adhesion to endothelial cells induced by platelet factor 4 requires sequential activation of Ras, Syk, and JNK MAP kinases. Blood 107, 1768-75.

[26] Anceriz, N., Vandal, K., Tessier, P. A. (2007) S100A9 mediates neutrophil adhesion to fibronectin through activation of beta2 integrins. Biochem Biophys Res Commun 354, 84-9.

[27] Brinkmann, V., Reichard, U., Goosmann, C., Fauler, B., Uhlemann, Y., Weiss, D. S., Weinrauch, Y., Zychlinsky, A. (2004) Neutrophil extracellular traps kill bacteria. Science 303, 1532-5.

[28] Pelletier, M., Bouchard, A., Girard, D. (2004) In vivo and in vitro roles of IL-21 in inflammation. J Immunol 173, 7521-30.

[29] Vandooren, J., Berghmans, N., Dillen, C., Van Aelst, I., Ronsse, I., Israel, L. L., Rosenberger, I., Kreuter, J., Lellouche, J. P., Michaeli, S., Locatelli, E., Franchini, M. C., Aiertza, M. K., Sanchez-Abella, L., Loinaz, I., Edwards, D. R., Shenkman, L., Opdenakker, G. (2013) Intradermal air pouch leukocytosis as an in vivo test for nanoparticles. Int J Nanomedicine 8, 4745-56.

[30] Pelletier, M., Savoie, A., Girard, D. (2000) Activation of human neutrophils by the air pollutant sodium sulfite (Na(2)SO(3)): comparison with immature promyelocytic HL-60 and DMSO-differentiated HL-60 cells reveals that Na(2)SO(3) is a neutrophil but not a HL-60 cell agonist. Clin Immunol 96, 131-9.

[31] Mestas, J. and Hughes, C. C. (2004) Of mice and not men: differences between mouse and human immunology. J Immunol 172, 2731-8.

[32] Siemsen, D. W., Malachowa, N., Schepetkin, I. A., Whitney, A. R., Kirpotina, L. N., Lei, B., Deleo, F. R., Quinn, M. T. (2014) Neutrophil isolation from nonhuman species. Methods Mol Biol, 845-4_3.

[33] Gauthier, M., Roberge, C. J., Pelletier, M., Tessier, P. A., Girard, D. (2001) Activation of human neutrophils by technical toxaphene. Clin Immunol 98, 46-53.

[34] Lavastre, V. and Girard, D. (2002) Tributyltin induces human neutrophil apoptosis and selective degradation of cytoskeletal proteins by caspases. J Toxicol Environ Health A 65, 1013-24.

[35] Pelletier, M., Roberge, C. J., Gauthier, M., Vandal, K., Tessier, P. A., Girard, D. (2001) Activation of human neutrophils in vitro and dieldrin-induced neutrophilic inflammation in vivo. J Leukoc Biol 70, 367-73.

[36] De Liz, R., Horst, H., Pizzolatti, M. G., Frode, T. S., Girard, D. (2012) Activation of human neutrophils by the anti-inflammatory mediator Esenbeckia leiocarpa leads to atypical apoptosis. Mediators Inflamm 198382, 8.

[37] Lavastre, V., Pelletier, M., Saller, R., Hostanska, K., Girard, D. (2002) Mechanisms involved in spontaneous and Viscum album agglutinin-I-induced human neutrophil apoptosis: Viscum album agglutinin-I accelerates the loss of antiapoptotic Mcl-1 expression and the degradation of cytoskeletal paxillin and vimentin proteins via caspases. J Immunol 168, 1419-27.

[38] Bouchard, A., Ratthe, C., Girard, D. (2004) Interleukin-15 delays human neutrophil apoptosis by intracellular events and not via extracellular factors: role of Mcl-1 and decreased activity of caspase-3 and caspase-8. J Leukoc Biol 75, 893-900.

[39] Ennaciri, J. and Girard, D. (2009) IL-4R(alpha), a new member that associates with Syk kinase: implication in IL-4-induced human neutrophil functions. J Immunol 183, 5261-9.

[40] Girard, D., Paquet, M. E., Paquin, R., Beaulieu, A. D. (1996) Differential effects of interleukin-15 (IL-15) and IL-2 on human neutrophils: modulation of phagocytosis, cytoskeleton rearrangement, gene expression, and apoptosis by IL-15. Blood 88, 3176-84.

[41] Girard, D., Paquin, R., Beaulieu, A. D. (1997) Responsiveness of human neutrophils to interleukin-4: induction of cytoskeletal rearrangements, de novo protein synthesis and delay of apoptosis. Biochem J 325 (Pt 1), 147-53.

[42] Girard, D., Paquin, R., Naccache, P. H., Beaulieu, A. D. (1996) Effects of interleukin-13 on human neutrophil functions. J Leukoc Biol 59, 412-9.

[43] Pelletier, M. and Girard, D. (2005) Interleukin-15 increases neutrophil adhesion onto human respiratory epithelial A549 cells and attracts neutrophils in vivo. Clin Exp Immunol 141, 315-25.

[44] Pelletier, M., Ratthe, C., Girard, D. (2002) Mechanisms involved in interleukin-15-induced suppression of human neutrophil apoptosis: role of the anti-apoptotic Mcl-1 protein and several kinases including Janus kinase-2, p38 mitogen-activated protein kinase and extracellular signal-regulated kinases-1/2. FEBS Lett 532, 164-70.

[45] Ratthe, C. and Girard, D. (2004) Interleukin-15 enhances human neutrophil phagocytosis by a Syk-dependent mechanism: importance of the IL-15Ralpha chain. J Leukoc Biol 76, 162-8.

[46] Ratthe, C., Pelletier, M., Chiasson, S., Girard, D. (2007) Molecular mechanisms involved in interleukin-4 (IL-4)-induced human neutrophils: expression and regulation of suppressor of cytokine signaling (SOCS). J Leukoc Biol.

[47] Simard, J. C., Girard, D., Tessier, P. A. (2010) Induction of neutrophil degranulation by S100A9 via a MAPK-dependent mechanism. J Leukoc Biol 87, 905-14.

[48] Simard, J. C., Simon, M. M., Tessier, P. A., Girard, D. (2011) Damage-associated molecular pattern S100A9 increases bactericidal activity of human neutrophils by enhancing phagocytosis. J Immunol 186, 3622-31.

[49] Simard, J. C., Noel, C., Tessier, P. A., Girard, D. (2014) Human S100A9 potentiates IL-8 production in response to GM-CSF or fMLP via activation of a different set of transcription factors in neutrophils. FEBS Lett 588, 2141-6.

[50] Antoine, F., Simard, J. C., Girard, D. (2013) Curcumin inhibits agent-induced human neutrophil functions in vitro and lipopolysaccharide-induced neutrophilic infiltration in vivo. Int Immunopharmacol 17, 1101-7.

[51] Binet, F., Cavalli, H., Moisan, E., Girard, D. (2006) Arsenic trioxide (AT) is a novel human neutrophil pro-apoptotic agent: effects of catalase on AT-induced apoptosis,

degradation of cytoskeletal proteins and de novo protein synthesis. Br J Haematol 132, 349-58.

[52] Binet, F., Chiasson, S., Girard, D. (2008) Arsenic trioxide induces de novo protein synthesis of annexin-1 in neutrophils: association with a heat shock-like response and not apoptosis. Br J Haematol 140, 454-63.

[53] Binet, F. and Girard, D. (2008) Novel human neutrophil agonistic properties of arsenic trioxide: involvement of p38 mitogen-activated protein kinase and/or c-jun NH2-terminal MAPK but not extracellular signal-regulated kinases-1/2. J Leukoc Biol.

[54] Antoine, F., Ennaciri, J., Girard, D. (2010) Syk is a novel target of arsenic trioxide (ATO) and is involved in the toxic effect of ATO in human neutrophils. Toxicol In Vitro 24, 936-41.

[55] Beaulieu, J., Girard, D., Dupont, C., Lemieux, P. (2009) Inhibition of neutrophil infiltration by a malleable protein matrix of lactic acid bacteria-fermented whey proteins in vivo. Inflammation Research : Official Journal of the European Histamine Research Society [et al.] 58, 133-8.

[56] Babin, K., Antoine, F., Goncalves, D. M., Girard, D. (2013) TiO2, CeO2 and ZnO nanoparticles and modulation of the degranulation process in human neutrophils. Toxicol Lett 221, 57-63.

[57] Goncalves, D. M., Chiasson, S., Girard, D. (2010) Activation of human neutrophils by titanium dioxide (TiO2) nanoparticles. Toxicol In Vitro 24, 1002-8.

[58] Goncalves, D. M. and Girard, D. (2014) Zinc oxide nanoparticles delay human neutrophil apoptosis by a de novo protein synthesis-dependent and reactive oxygen species-independent mechanism. Toxicol In Vitro 28, 926-31.

[59] Poirier, M., Simard, J. C., Antoine, F., Girard, D. (2014) Interaction between silver nanoparticles of 20 nm (AgNP20) and human neutrophils: induction of apoptosis and inhibition of de novo protein synthesis by AgNP20 aggregates. J Appl Toxicol 34, 404-12.

[60] Oh, S. J., Kim, H., Liu, Y., Han, H. K., Kwon, K., Chang, K. H., Park, K., Kim, Y., Shim, K., An, S. S., Lee, M. Y. (2014) Incompatibility of silver nanoparticles with lactate dehydrogenase leakage assay for cellular viability test is attributed to protein binding and reactive oxygen species generation. Toxicol Lett 225, 422-32.

[61] Holder, A. L., Goth-Goldstein, R., Lucas, D., Koshland, C. P. (2012) Particle-induced artifacts in the MTT and LDH viability assays. Chem Res Toxicol 25, 1885-92.

[62] Kroll, A., Pillukat, M. H., Hahn, D., Schnekenburger, J. (2012) Interference of engineered nanoparticles with in vitro toxicity assays. Arch Toxicol 86, 1123-36.

[63] Carulli, G. (1996) Applications of flow cytometry in the study of human neutrophil biology and pathology. Hematopathol Mol Hematol 10, 39-61.

[64] Pelletier, M., Lavastre, V., Girard, D. (2002) Activation of human epithelial lung a549 cells by the pollutant sodium sulfite: enhancement of neutrophil adhesion. Toxicol Sci 69, 210-6.

[65] Lavastre, V., Roberge, C. J., Pelletier, M., Gauthier, M., Girard, D. (2002) Toxaphene, but not beryllium, induces human neutrophil chemotaxis and apoptosis via reactive oxygen species (ROS): involvement of caspases and ROS in the degradation of cytoskeletal proteins. Clin Immunol 104, 40-8.

[66] Ratthe, C., Pelletier, M., Roberge, C. J., Girard, D. (2002) Activation of human neutrophils by the pollutant sodium sulfite: effect on cytokine production, chemotaxis, and cell surface expression of cell adhesion molecules. Clin Immunol 105, 169-75.

[67] Bignold, L. P., Harkin, D. G., Rogers, S. D. (1992) Interleukin-8 and neutrophil leucocytes: adhesion, spreading, polarisation, random motility, chemotaxis and deactivation in assays using 'sparse-pore' polycarbonate (nuclepore) membranes in the Boyden chamber. Int Arch Allergy Immunol 97, 350-7.

[68] Borregaard, N. and Cowland, J. B. (1997) Granules of the human neutrophilic polymorphonuclear leukocyte. Blood 89, 3503-21.

[69] Borregaard, N., Theilgaard-Monch, K., Sorensen, O. E., Cowland, J. B. (2001) Regulation of human neutrophil granule protein expression. Curr Opin Hematol 8, 23-7.

[70] Jog, N. R., Rane, M. J., Lominadze, G., Luerman, G. C., Ward, R. A., McLeish, K. R. (2007) The actin cytoskeleton regulates exocytosis of all neutrophil granule subsets. Am J Physiol Cell Physiol 292, C1690-700.

[71] Antoine, F. and Girard, D. (2014) Curcumin increases gelatinase activity in human neutrophils by a p38 mitogen-activated protein kinase (MAPK)-independent mechanism. J Immunotoxicol 13, 1-6.

[72] Vallieres, F. and Girard, D. (2013) IL-21 enhances phagocytosis in mononuclear phagocyte cells: identification of spleen tyrosine kinase as a novel molecular target of IL-21. J Immunol 190, 2904-12.

[73] Moisan, E. and Girard, D. (2006) Cell surface expression of intermediate filament proteins vimentin and lamin B1 in human neutrophil spontaneous apoptosis. J Leukoc Biol 79, 489-98.

[74] Cassatella, M. A. (1995) The production of cytokines by polymorphonuclear neutrophils. Immunol Today 16, 21-6.

[75] Goncalves, D. M. and Girard, D. (2011) Titanium dioxide (TiO(2)) nanoparticles induce neutrophil influx and local production of several pro-inflammatory mediators in vivo. Int Immunopharmacol 21, 21.

[76] Savoie, A., Lavastre, V., Pelletier, M., Hajto, T., Hostanska, K., Girard, D. (2000) Activation of human neutrophils by the plant lectin Viscum album agglutinin-I: modula-

tion of de novo protein synthesis and evidence that caspases are involved in induction of apoptosis. J Leukoc Biol 68, 845-53.

[77] Moon, D. O., Kim, M. O., Choi, Y. H., Park, Y. M., Kim, G. Y. (2010) Curcumin attenuates inflammatory response in IL-1beta-induced human synovial fibroblasts and collagen-induced arthritis in mouse model. Int Immunopharmacol 10, 605-10.

[78] Young, D. A., Hegen, M., Ma, H. L., Whitters, M. J., Albert, L. M., Lowe, L., Senices, M., Wu, P. W., Sibley, B., Leathurby, Y., Brown, T. P., Nickerson-Nutter, C., Keith, J. C., Jr., Collins, M. (2007) Blockade of the interleukin-21/interleukin-21 receptor pathway ameliorates disease in animal models of rheumatoid arthritis. Arthritis Rheum 56, 1152-63.

[79] Hu, Y., Cheng, W., Cai, W., Yue, Y., Li, J., Zhang, P. (2013) Advances in research on animal models of rheumatoid arthritis. Clinical rheumatology 32, 161-5.

[80] Tessier, P. A., Naccache, P. H., Clark-Lewis, I., Gladue, R. P., Neote, K. S., McColl, S. R. (1997) Chemokine networks in vivo: involvement of C-X-C and C-C chemokines in neutrophil extravasation in vivo in response to TNF-alpha. J Immunol 159, 3595-602.

[81] Liz, R., Pereira, D. F., Horst, H., Dalmarco, E. M., Dalmarco, J. B., Simionatto, E. L., Pizzolatti, M. G., Girard, D., Frode, T. S. (2011) Protected effect of Esenbeckia leiocarpa upon the inflammatory response induced by carrageenan in a murine air pouch model. Int Immunopharmacol 1, 1.

[82] Freire, M. G., Desouza, I. A., Silva, A. C., Macedo, M. L., Lima, M. S., Tamashiro, W. M., Antunes, E., Marangoni, S. (2003) Inflammatory responses induced in mice by lectin from Talisia esculenta seeds. Toxicon : Official Journal of the International Society on Toxinology 42, 275-80.

[83] Neves, S. A., Dias-Baruff, M., Freitas, A. L., Roque-Barreira, M. C. (2001) Neutrophil migration induced in vivo and in vitro by marine algal lectins. Inflammation Research : Official Journal of the European Histamine Research Society [et al.] 50, 486-90.

[84] Lee, J. H., Choi, J. K., Noh, M. S., Hwang, B. Y., Hong, Y. S., Lee, J. J. (2004) Anti-inflammatory effect of kamebakaurin in in vivo animal models. Planta Med 70, 526-30.

[85] Dalmarco, E. M., Astolfi, G., De Liz, R., De Cordova, C. M., Frode, T. S. (2012) Modulatory effect of mycophenolate mofetil on carrageenan-induced inflammation in the mouse air pouch model. Int Immunopharmacol 13, 476-82.

[86] Cho, Y. S., Song, J. S., Huh, J. Y., Kim, C. H., Gong, Y. D., Cheon, H. G. (2011) Discovery of (2-fluoro-benzyl)-(2-methyl-2-phenethyl-2H-chromen-6-yl)-amine (KRH-102140) as an orally active 5-lipoxygenase inhibitor with activity in murine inflammation models. Pharmacology 87, 49-55.

[87] Lavastre, V., Cavalli, H., Ratthe, C., Girard, D. (2004) Anti-inflammatory effect of Viscum album agglutinin-I (VAA-I): induction of apoptosis in activated neutrophils and

inhibition of lipopolysaccharide-induced neutrophilic inflammation in vivo. Clin Exp Immunol 137, 272-8.

[88] Moisan, E., Chiasson, S., Girard, D. (2007) The intriguing normal acute inflammatory response in mice lacking vimentin. Clin Exp Immunol 150, 158-68.

[89] Maynard, A. D. (2007) Nanotechnology: the next big thing, or much ado about nothing? Ann Occup Hyg 51, 1-12.

[90] Oberdorster, G., Oberdorster, E., Oberdorster, J. (2005) Nanotoxicology: an emerging discipline evolving from studies of ultrafine particles. Environ Health Perspect 113, 823-39.

[91] EPA-Nanotechnology-White-Paper (2007) Nanotechnology White Paper. (U. S. E. P. A. (EPA), ed), Washington 120p.

[92] Wu, W., Samet, J. M., Peden, D. B., Bromberg, P. A. (2010) Phosphorylation of p65 is required for zinc oxide nanoparticle-induced interleukin 8 expression in human bronchial epithelial cells. Environ Health Perspect 118, 982-7.

[93] Skuland, T., Ovrevik, J., Lag, M., Schwarze, P., Refsnes, M. (2014) Silica nanoparticles induce cytokine responses in lung epithelial cells through activation of a p38/TACE/TGF-alpha/EGFR-pathway and NF-kappaBeta signalling. Toxicol Appl Pharmacol 279, 76-86.

[94] Nagakura, C., Negishi, Y., Tsukimoto, M., Itou, S., Kondo, T., Takeda, K., Kojima, S. (2014) Involvement of P2Y11 receptor in silica nanoparticles 30-induced IL-6 production by human keratinocytes. Toxicology 322, 61-8.

[95] Elsabahy, M. and Wooley, K. L. (2013) Cytokines as biomarkers of nanoparticle immunotoxicity. Chem Soc Rev 42, 5552-76.

[96] Brandenberger, C., Rowley, N. L., Jackson-Humbles, D. N., Zhang, Q., Bramble, L. A., Lewandowski, R. P., Wagner, J. G., Chen, W., Kaplan, B. L., Kaminski, N. E., Baker, G. L., Worden, R. M., Harkema, J. R. (2013) Engineered silica nanoparticles act as adjuvants to enhance allergic airway disease in mice. Part Fibre Toxicol 10, 26.

[97] Chen, H. W., Su, S. F., Chien, C. T., Lin, W. H., Yu, S. L., Chou, C. C., Chen, J. J., Yang, P. C. (2006) Titanium dioxide nanoparticles induce emphysema-like lung injury in mice. Faseb J 20, 2393-5.

[98] Hussain, S., Vanoirbeek, J. A., Luyts, K., De Vooght, V., Verbeken, E., Thomassen, L. C., Martens, J. A., Dinsdale, D., Boland, S., Marano, F., Nemery, B., Hoet, P. H. (2011) Lung exposure to nanoparticles modulates an asthmatic response in a mouse model. Eur Respir J 37, 299-309.

[99] Srinivas, A., Rao, P. J., Selvam, G., Murthy, P. B., Reddy, P. N. (2011) Acute inhalation toxicity of cerium oxide nanoparticles in rats. Toxicol Lett 23, 23.

[100] Watt, A. P., Schock, B. C., Ennis, M. (2005) Neutrophils and eosinophils: clinical implications of their appearance, presence and disappearance in asthma and COPD. Curr Drug Targets Inflamm Allergy 4, 415-23.

[101] Hedenborg, M. (1988) Titanium dioxide induced chemiluminescence of human polymorphonuclear leukocytes. Int Arch Occup Environ Health 61, 1-6.

[102] Jovanovic, B., Anastasova, L., Rowe, E. W., Zhang, Y., Clapp, A. R., Palic, D. (2011) Effects of nanosized titanium dioxide on innate immune system of fathead minnow (Pimephales promelas Rafinesque, 1820). Ecotoxicol Environ Saf 74, 675-83.

[103] Jovanovic, B., Anastasova, L., Rowe, E. W., Palic, D. (2011) Hydroxylated fullerenes inhibit neutrophil function in fathead minnow (Pimephales promelas Rafinesque, 1820). Aquat Toxicol 101, 474-82.

[104] Mainardes, R. M., Gremiao, M. P., Brunetti, I. L., Da Fonseca, L. M., Khalil, N. M. (2009) Zidovudine-loaded PLA and PLA-PEG blend nanoparticles: influence of polymer type on phagocytic uptake by polymorphonuclear cells. J Pharm Sci 98, 257-67.

[105] Papatheofanis, F. J. and Barmada, R. (1991) Polymorphonuclear leukocyte degranulation with exposure to polymethylmethacrylate nanoparticles. J Biomed Mater Res 25, 761-71.

[106] Muller, R. H., Maassen, S., Weyhers, H., Mehnert, W. (1996) Phagocytic uptake and cytotoxicity of solid lipid nanoparticles (SLN) sterically stabilized with poloxamine 908 and poloxamer 407. J Drug Target 4, 161-70.

[107] Ratthe, C. and Girard, D. (2008) Investigation of the interleukin (IL)-4/IL-4 receptor system in promyelocytic leukaemia PLB-985 cells during differentiation toward neutrophil-like phenotype: mechanism involved in IL-4-induced SOCS3 protein expression. Br J Haematol 140, 59-70.

[108] Memisoglu-Bilensoy, E., Dogan, A. L., Hincal, A. A. (2006) Cytotoxic evaluation of injectable cyclodextrin nanoparticles. J Pharm Pharmacol 58, 585-9.

[109] Dianzani, C., Cavalli, R., Zara, G. P., Gallicchio, M., Lombardi, G., Gasco, M. R., Panzanelli, P., Fantozzi, R. (2006) Cholesteryl butyrate solid lipid nanoparticles inhibit adhesion of human neutrophils to endothelial cells. Br J Pharmacol 148, 648-56.

[110] Bartneck, M., Keul, H. A., Singh, S., Czaja, K., Bornemann, J., Bockstaller, M., Moeller, M., Zwadlo-Klarwasser, G., Groll, J. (2010) Rapid uptake of gold nanorods by primary human blood phagocytes and immunomodulatory effects of surface chemistry. ACS Nano 4, 3073-86.

[111] Bartneck, M., Keul, H. A., Zwadlo-Klarwasser, G., Groll, J. (2010) Phagocytosis independent extracellular nanoparticle clearance by human immune cells. Nano Lett 10, 59-63.

[112] Chekanov, A. V., Baranova, O. A., Levin, A. D., Solov'eva, E., Fedin, A. I., Kazarinov, K. D. (2013) [Study of the influence of gold nanoparticles on activation of human blood neutrophils]. Biofizika 58, 495-500.

[113] Paino, I. M. and Zucolotto, V. (2014) Poly(vinyl alcohol)-coated silver nanoparticles: Activation of neutrophils and nanotoxicology effects in human hepatocarcinoma and mononuclear cells. Environmental toxicology and pharmacology 39, 614-21.

[114] Moeller, S., Kegler, R., Sternberg, K., Mundkowski, R. G. (2012) Influence of sirolimus-loaded nanoparticles on physiological functions of native human polymorphonuclear neutrophils. Nanomedicine 8, 1293-300.

[115] Haase, H., Fahmi, A., Mahltig, B. (2014) Impact of silver nanoparticles and silver ions on innate immune cells. J Biomed Nanotechnol 10, 1146-56.

[116] Kang, S. J., Kim, B. M., Lee, Y. J., Hong, S. H., Chung, H. W. (2009) Titanium dioxide nanoparticles induce apoptosis through the JNK/p38-caspase-8-Bid pathway in phytohemagglutinin-stimulated human lymphocytes. Biochem Biophys Res Commun 386, 682-7.

[117] Vamanu, C. I., Cimpan, M. R., Hol, P. J., Sornes, S., Lie, S. A., Gjerdet, N. R. (2008) Induction of cell death by TiO2 nanoparticles: studies on a human monoblastoid cell line. Toxicol In Vitro 22, 1689-96.

[118] Girard, D. (2014) Using the air pouch model for assessing in vivo inflammatory activity of nanoparticles. Int J Nanomedicine 9, 1105-7.

[119] Ratthe, C., Ennaciri, J., Garces Goncalves, D. M., Chiasson, S., Girard, D. (2009) Interleukin (IL)-4 induces leukocyte infiltration in vivo by an indirect mechanism. Mediators Inflamm 193970, 10.

[120] Rosenberger, I., Schmithals, C., Vandooren, J., Bianchessi, S., Milani, P., Locatelli, E., Israel, L. L., Hubner, F., Matteoli, M., Lellouche, J. P., Franchini, M. C., Passoni, L., Scanziani, E., Opdenakker, G., Piiper, A., Kreuter, J. (2014) Physico-chemical and toxicological characterization of iron-containing albumin nanoparticles as platforms for medical imaging. Journal of Controlled Release : Official Journal of the Controlled Release Society 194, 130-7.

[121] Sayes, C. M., Reed, K. L., Warheit, D. B. (2011) Nanoparticle toxicology: measurements of pulmonary hazard effects following exposures to nanoparticles. Methods Mol Biol 726, 313-24.

[122] Roursgaard, M., Poulsen, S. S., Poulsen, L. K., Hammer, M., Jensen, K. A., Utsunomiya, S., Ewing, R. C., Balic-Zunic, T., Nielsen, G. D., Larsen, S. T. (2010) Time-response relationship of nano and micro particle induced lung inflammation. Quartz as reference compound. Hum Exp Toxicol 29, 915-33.

[123] Rossi, E. M., Pylkkanen, L., Koivisto, A. J., Vippola, M., Jensen, K. A., Miettinen, M., Sirola, K., Nykasenoja, H., Karisola, P., Stjernvall, T., Vanhala, E., Kiilunen, M., Pasa-

nen, P., Makinen, M., Hameri, K., Joutsensaari, J., Tuomi, T., Jokiniemi, J., Wolff, H., Savolainen, K., Matikainen, S., Alenius, H. (2010) Airway exposure to silica-coated TiO2 nanoparticles induces pulmonary neutrophilia in mice. Toxicol Sci 113, 422-33.

[124] Larsen, S. T., Roursgaard, M., Jensen, K. A., Nielsen, G. D. (2010) Nano titanium dioxide particles promote allergic sensitization and lung inflammation in mice. Basic Clin Pharmacol Toxicol 106, 114-7.

[125] Jacobsen, N. R., Moller, P., Jensen, K. A., Vogel, U., Ladefoged, O., Loft, S., Wallin, H. (2009) Lung inflammation and genotoxicity following pulmonary exposure to nanoparticles in ApoE-/- mice. Part Fibre Toxicol 6, 2.

[126] Goncalves, D. M. and Girard, D. (2013) Evidence that polyhydroxylated C60 fullerenes (fullerenols) amplify the effect of lipopolysaccharides to induce rapid leukocyte infiltration in vivo. Chem Res Toxicol 26, 1884-92.

[127] Arora, S., Rajwade, J. M., Paknikar, K. M. (2012) Nanotoxicology and in vitro studies: the need of the hour. Toxicol Appl Pharmacol 258, 151-65.

Chapter 4

In Vitro Assessment of Chronic Nanoparticle Effects on Respiratory Cells

Eleonore Fröhlich and Claudia Meindl

Additional information is available at the end of the chapter

http://dx.doi.org/10.5772/60701

Abstract

Nanoparticles (NPs) are included in a variety of consumer products including cosmetics, food, and food packaging. They are also used in medical products for dermal and oral application and for inhalation. The thinness of the air–blood barrier, the large absorption area of the lung, and the relatively low inactivation by enzymes provide fast entry to the systemic blood circulation at high drug concentrations. In addition to intended uptake, exposure to airborne particles from the environment and to NPs released during the manufacturing process may occur. Cytotoxicity is routinely studied for 4–48 h of exposure, but NPs may accumulate in cells and can cause cellular effects after longer times. Both extent and consequences of cellular NP accumulation are currently largely unknown.

In vitro studies could help estimating the extent and the consequences of cellular accumulation and classify NPs according to their potential to cause adverse effects upon chronic exposure. Furthermore, such information could help to decrease the amount of labor- and cost-intensive and ethically problematic animal studies. Important parameters for representative chronic cytotoxicity testing in vitro include choice of the appropriate cells and of physiological relevant culture and exposure conditions, verification of uptake, and identification of cell damage.

Calu-3 bronchial epithelial cells are a suggested cell line for physiologically relevant testing when cultured on membranes, which allows supplying the cells with nutrients only from the basal side (culture at an air–liquid interface). This culturing also enables the exposure to NPs by aerosol. Cytotoxicity can be identified by changes in cell number, membrane integrity, amount of DNA or protein, and metabolic activity.

When cells are cultured on membranes and not in plates, measurements of the transepithelial electrical resistance are a useful indicator for cell damage.

By slight modification of the culture conditions on the membranes, we could maintain constant transepithelial electrical resistance values of Calu-3 monolayers for 28 days. Every seven days, cells were exposed to two different doses of fluorescently labeled 20 nm carboxyl-functionalized polystyrene particles either suspended in a small volume of liquid or by MicroSprayer® IA-1C aerosolizer. It was found that cells accumulated particles in a linear way over the entire observation time without apparent cell damage.

The presented system appears suitable for chronic cytotoxicity testing of inhaled NPs in a physiologically relevant manner.

Keywords: Nanoparticles, Chronic effects, Particle uptake, Particle accumulation, Cytotoxicity, Respiratory system

1. Introduction

Exposure of humans to nanoparticles (NPs) can occur accidentally by environmental particles (e.g., air pollution) and intentionally because a variety of consumer products, cosmetics, and medical products contain NPs. Release of NPs during the manufacturing process may result in exposure of workers by the dermal, oral, and inhalation route.

Exposure to air pollution, such as ultrafine particles, is known to cause inflammatory airway diseases and cardiovascular problems in humans [1]. Pope et al. [2] concluded that even low levels of ambient particle exposure have a significant effect on mortality. The log-linear dose–response relationship between particles and mortality, which was found in their study, highlighted the risk upon exposure to relatively low ambient levels.

Less information is available on health risk of inhaled NPs at the workplace. Reported exposure levels in manufactories for printed electronics, nanoscale metal oxides, and ceramics were low and below the allowed limits [3-6]. On the other hand, exposure to metal NPs in precious metal refinery was higher than recommended limits, and mitigating measures were suggested [7]. Adverse effects of respiratory exposure to occupational NPs included allergic symptoms of the respiratory tract and accumulation in the lung and peritoneum [8-10].

The lung is also one of the suggested routes for noninvasive medication because, compared to dermal and oral exposure, inhalation provides higher bioavailability of active pharmaceutical ingredients. The thinness of the air–blood barrier allowing fast entry to the systemic blood circulation combined with the large absorption area of the lung and the low degree of inactivation through enzymatic degradation by enterocyte and liver enzymes are the main reasons for high systemic levels of inhaled drugs. Several NP-based products, such as nano-salbutamol and nano-fluticasone [11, 12] for chronic obstructive pulmonary disease and

http://dx.doi.org/10.5772/60701

asthma and nano-atropine sulfate against organophosphorus poisoning [13], successfully finished testing in healthy volunteers. Furthermore, the safety of heavy chains of Fab fragments of antibodies produced by Nanobody® technology for respiratory syncytial virus infections has been demonstrated in a recent phase I trial [14]. Technosphere® (bis-3,6(4-fumarylamino-butyl)-2,5-diketopiperazine that adsorbs active pharmaceutical ingredients) insulin has passed clinical phase II and III trials [15] and is currently being reviewed by the FDA as inhaled mealtime insulin for managing hyperglycemia in patients with type 1 and type 2 diabetes mellitus. All applications are intended for longer time periods and raise the issue of potential adverse effects on the respiratory epithelium upon chronic exposure.

2. Epithelial barriers of the lung

Airborne particles pass the conducting airways (trachea and large bronchi) and the small bronchi and bronchioli and finally reach the alveoli, where gas exchange takes place. The surface area of the lung is estimated to be 80–140 m^2 large [16]. This large surface is covered by a small amount of lining fluid, approximately 10–20 ml in total, and separates the environment from the systemic blood circulation by only a thin air–blood barrier (0.1–0.2 μm thick).

2.1. Airway lining fluid

The mucus layer covering the trachea and main bronchi is much thinner than the mucus layer in the oro-gastrointestinal tract. Indications of mucus thickness vary according to the different techniques that were used for the measurement (Fig. 1). The layer appears to possess a minimum thickness of 5–10 μm in the large airways, while a thickness of 6.9 μm has been measured for segmental bronchi [17, 18]. Other data report a constant thickness of 7 μm of the periciliary layer of all large airways that possess cilia covered by a mucus gel layer with maximum thickness of 5 μm in the trachea and to 0.5 μm in the bronchi [19]. There is a gradual decrease in thickness of this layer, and 1.8 μm of lining fluid has been measured for human bronchioles. It is likely that the mucus gel layer is not continuous and exposure to particles might differ between cells [20]. Mucus and surfactant have different compositions; mucus contains up to 95 % of water, followed by 2–3 % glycoproteins, 0.1–0.5 % proteoglycans, and 0.3–0.5 % lipids. Surfactant, on the other hand, consists of up to 90 % of lipids and 10 % of proteins and therefore resembles more the composition of the human plasma membranes, which on average contain 50 % lipid and 50 % protein [21]. The surfactant is not only reducing the surface tension of the alveoli and preventing their collapse but presents also an effective barrier against dehydration and invasion of pathogens.

2.2. Airway epithelium

The epithelium of the airways representing the main barrier for molecules and particles in aerosols becomes thinner from the conducting (large) airways toward the alveoli, where gas exchange takes place. In the large airways, the epithelium consists of columnar bronchial epithelial cells with microvilli at their apical surface and goblet cells (Fig. 1). Smaller bronchi,

bronchioles, have a cubic epithelium and secretory Clara cells, while alveoli are coated with a squamous epithelium consisting of alveolar epithelial cell types I and II. Alveolar macrophages migrate on the surface of this epithelium.

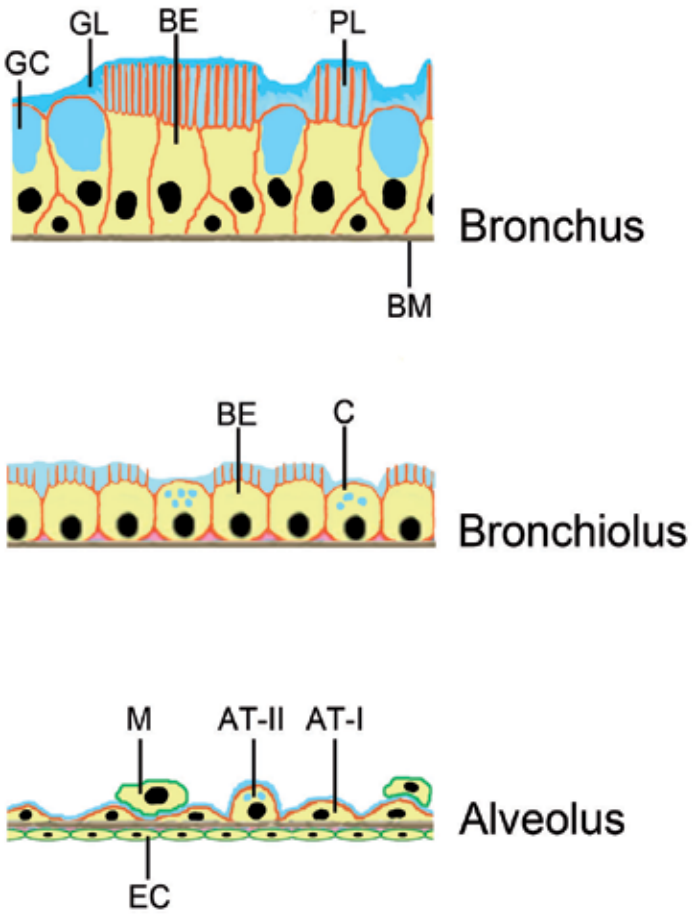

Figure 1. Barriers for particle uptake by the respiratory system. The mucus layer of the large bronchi can be divided in the periciliary (PL) surrounding the cilia of the bronchial epithelial cells and the gel layer (GL). The epithelial layer of the large (conducting) airways consists of columnar bronchial epithelial cells with cilia (BE) and mucus-producing goblet cells (GC). In the bronchioli, cuboidal bronchial epithelial cells (BE) and mucus-producing Clara cells (C) are found. All epithelial cells reside on a basement membrane (BM). The air–blood barrier at the alveolus consists of alveolar epithelial cell type I (AT-I) and surfactant-producing AT-II cells. Alveolar macrophages (M) migrate on top of the alveolar epithelial cell layer. On the other side of the basement membrane, endothelial cells (EC) of capillaries are located.

Cytotoxicity testing is one of the first steps in the evaluation of toxicants and preclinical testing of drugs. Cytotoxicity of conventional compounds is routinely studied after 4–48 h of exposure because conventional toxicants either acutely damage cells or are degraded by the cell. In

http://dx.doi.org/10.5772/60701

contrast to many conventional compounds, NPs have the ability to accumulate in cells and can cause cellular effects also after longer times, for instance, by interference with organelle function. Both extent and effect of cellular accumulation of NPs are currently largely unknown. Most likely these effects are both particle dependent (e.g., content of metal ions, solubility/biodegradability) and cell dependent (expression of uptake routes, proliferation rate, intracellular location). The thickness of the mucus layer on top of intestinal cells can reach up to 900 μm, while respiratory cells are covered only by a mucus layer of 12 μm. Permeability of the epidermis is low due to the formation of the stratum corneum. In addition to the lack of a protective acellular layer, the turnover time of lung cells is slow. Cells of colon crypts are completely renewed after 3–4 days, and cells of the epidermis need 39 days. In contrast to that, after one year, only 7 % of alveolar cells are renewed [22-24]. This combination results in a higher accumulation and a lower regenerative capacity. Accumulation of NPs upon chronic inhalation has been shown, for instance, for titanium dioxide NPs applied to rats over 28 days and three months [25].

In vitro studies could help to estimate the extent and the consequences of cellular accumulation and classify NPs according to their potential for chronic effects. Such information could decrease the amount of labor- and cost-intensive and ethically problematic animal studies. As some defense mechanisms, particularly mucociliary clearance and clearance by the systemic circulation, are lacking in cellular models, such studies might be a tool to identify NPs with a low potential of accumulation and cytotoxicity and probably a lower need for chronic in vivo testing.

3. Components of a representative chronic cytotoxicity model

In order to assess the effects of NP accumulation in a relevant way, the in vitro model has to fulfill several requirements. The important biological parameters are 1) selection of the appropriate cells, 2) physiologically relevant culture system, 3) appropriate NP exposure, 4) demonstration of cellular uptake and accumulation, and 5) information on cell damage/cytotoxicity (Fig. 2). For interpretation of the findings, changes in physicochemical properties of particles have to be taken into account.

3.1. Selection of the appropriate cells

Cellular studies are performed with primary cells or with cell lines. Primary cells have to be isolated from fresh tissues prior to the experiments. They retain many of the cell-specific properties but have a limited life span in culture. Due to the reduced availability of fresh human tissue, mainly rat or murine primary cells are used. In addition to potential inter-species differences, quality (cell viability) and purity (contamination with other cells) of the preparation may vary leading to low reproducibility of the experiments. In contrast to primary cells, immortalized cells, cell lines, provide more reproducible results. Cell lines show a much slower senescence rate and are termed "immortal." Cell lines have different origins; they may arise during transformation of tumors, due to the presence of a viral gene that partially deregulates

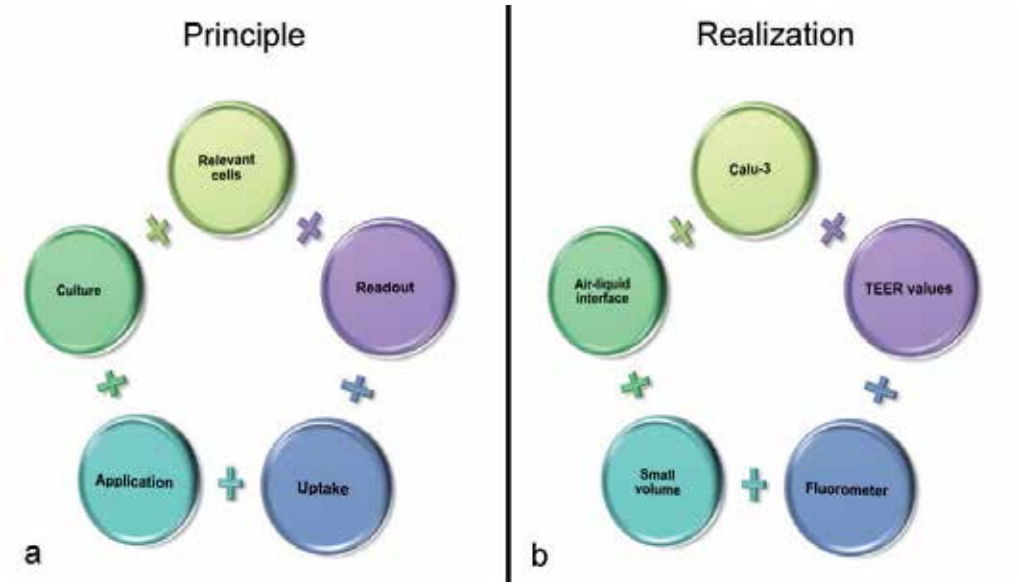

Figure 2. Key parameters for physiologically relevant testing of chronic exposure of airway cells. One potential realization of the principle (a) is presented (b).

the cell cycle, by introduction of telomerase and by fusion with cancer (myeloma) cells. The negative side of immortalization is that cells lose several cell-specific functions. Telomerase immortalized cells are currently believed to be the best way of immortalization because relatively many cell-specific functions are still present but only few TERT-immortalized bronchial epithelial cell lines are available by commercial suppliers, mainly by the American Type Culture Collection (ATCC). As a general rule, the selection of one or the other types of cell is based on the scientific question that should be addressed. Studies on cell-specific functions are performed better in primary cells. Basic cellular processes, such as proliferation, necrosis, and apoptosis, are generally studied in cell lines. Several cell lines have been described as representative models for respiratory cells [26]. They differ in their ability to form a tight intercellular barrier, expression of specific transporters, and secretion products typical for the respective cells. A549 cells and NCI-H441 cells are derived from alveolar epithelial cells. Although they do not form a monolayer with sufficient tightness, A549 cells show surfactant production and have been used in numerous toxicity studies [27, 28]. NCI-H441 cells are the preferred line for transport studies since they form polarized tight monolayers and express organic cation transporters and P-glycoprotein. Cell lines derived from bronchial epithelium comprise BEAS-2B, NuLi-1, 16HBE14o-, and Calu-3 cells. BEAS-2B cells lack tight junctions and mucus production but express organic cation transporters. NuLi-1 cells have been characterized to a lower extent and are rarely used although they form a tight monolayer. 16HBE14o- cells have the ability to form tight junctions and express a variety of transporters. Their main disadvantage is that they do not show the desired phenotype when cultured at an the air–liquid interface, the most physiologically relevant type of culture for cells of the respiratory system.

http://dx.doi.org/10.5772/60701

Calu-3 cells have been described as the suitable model for pulmonary permeability studies [29] with good correlation of permeability values with drug absorption from the rat lung in vivo [30]. Calu-3 cells are derived from bronchial submucosal glands, which explains their ability to produce airway surface liquid, mucins, and other immunological active substances [31]. When cultured on membranes at an air–liquid interface, they form cellular monolayers with tightness and expression of membrane transporters similar to the situation in vivo. Calu-3 cells show mucin-containing granules at the apical pole of the cell (e.g., [32]), but a mucus layer covering the cells cannot be discerned. This problem is linked to the high solubility of mucus in water. After fixation of the tissue and staining either with anti-mucin antibodies or with alcian blue, no mucus layer can be discerned neither in native bronchial tissue nor in Calu-3 cells [33].

3.2. Culture conditions for respiratory cells

Culture at an air–liquid interface is required to provide the most physiologically relevant exposure conditions. This culture method is characterized by supply of the cells with nutrients only from the basal side. This is usually obtained by culturing the cells on membranes in polystyrene housings. These inserts vary in membrane material and pore size and provide the cells with enough support and nutrient supply to form a stable monolayer. Air–liquid interface culture, where the apical part of the cell is exposed to air and not to medium, compared to conventional culture is illustrated in Fig. 3. Respiratory cells cultured at an air–liquid interface show increased differentiation resulting in production of mucus in Calu-3 cells and surfactant in A549 cells [34, 35].

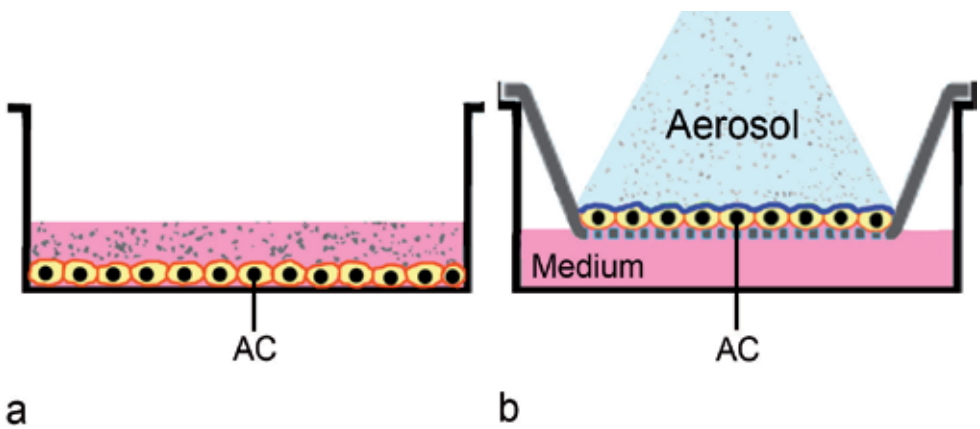

Figure 3. Different ways of culture: Cell grown at the bottom of well and exposed to NPs suspended in medium (a). In culture at an air–liquid interface, cells are grown on membranes and supplied with nutrients from the basal side. In this culture, respiratory cells secrete pulmonary surfactant (blue line). Cells are exposed to NPs applied as aerosols (b). AC: alveolar cell.

For the testing of particle effects after prolonged exposure, a constant cell population is desired. Routine cell culture systems are less ideal because cells on plastic surfaces proliferate faster

than cells in the human body, and intracellularly located NPs are diluted to a greater extent than in vivo. In addition, the high proliferation rate makes compensation of minimal damage possible. Fast proliferation in the culture system has another disadvantage in the evaluation by physiology-based assays used for cytotoxicity testing. All results are normalized to the data of the untreated control cells. This normalization poses the problem that if the untreated cells show physiological growth inhibition due to high cell densities, cell damage by NP could be overlooked.

In order to prevent nonphysiologically high proliferation rates, physiologically relevant culture systems have been developed. Culture in a polar environment, such as growth on microspheres and on membranes, slows down proliferation. Three-dimensional systems such as hanging drops and seeding in hydrogels, on microspheres, and on other scaffolds have been developed. These systems are suitable for several types of cells but do not provide adequate conditions for respiratory cells because cells are cultured submerged. An adaptation of the hanging drop method, however, has been developed and validated for evaluation of gaseous toxicants up to 20 days [36]. Cell culture on membrane inserts, which has been developed to study active and passive transport mechanisms of compounds across cell monolayers, appears suitable. A microfluidic system has been adapted in a way that culture on transwells at an air–liquid interface is possible and A549 cells cultured that way maintained differentiation and viability for 14 days [37]. It is, however, not clear whether under these culture conditions a stable monolayer of cells is obtained since some research groups report multilayer formation of A549 cells in air–liquid interface culture already after three days, while other studies observed A549 monolayers for up to four weeks of air–liquid interface culture [38]. Also 16HBE14o- cells start the formation of multilayers after 17 days in this culture. One hypothesis for the formation of multilayers was absence of cell removal from the apical side by medium changes. Calu-3 bronchial epithelial cells in air-liquid interface culture appear to be suitable because transepithelial electrical resistance (TEER) values remain constant for 17 days [39], while the most often used Caco-2 cells maintain constant values for a maximum of seven days.

3.3. Exposure with particles

Several methods have been used to expose cells to aerosols either as dry powders or by nebulization of solutions. Deposition by aerosols results in a heterogeneous distribution pattern (e.g., [40]) not unlike the in vivo situation where also different densities of particle deposition have been measured [41]. Several groups assessed the effects of environmental NPs (diesel exhaust, smoke) in vitro using either diffusion chambers or more advanced devices in static or dynamic exposure. Setups usually used exposures over 15–60 min, where the aerosol is generated and cells are exposed in a humid atmosphere at physiological temperature (37 °C). Particle deposition in most of the systems is driven by sedimentation and diffusion. Only few established systems, including electrostatic aerosol in vitro exposure system (EAVES) and CULTEX® radial flow system, employ electrostatic precipitation. The Voisin chamber [42, 43], Minucell system [44, 45], Nano Aerosol Chamber In Vitro Toxicity [46, 47], biological aerosol trigger [48], air–liquid interface cell exposure (ALICE) system [49-51], and electrostatic

http://dx.doi.org/10.5772/60701

aerosol in vitro exposure system [52, 53] were developed by specific researcher groups. Other systems, such as CULTEX® [54, 55], CULTEX® RFS, and VITROCELL® [56], are commercially available. CULTEX® and VITROCELL® systems have been used in the testing of volatile organic compounds, copper NPs, carbon NPs, zinc oxide NPs, gold NPs, polystyrene NPs, cerium oxide NPs, and laser printer emission particles [44, 57-60]. ALICE system [49-51] and VITROCELL/PARI BOY [61] have been used for aerosolization of NP-containing liquid aerosols. The deposition rates by these devices showed considerable variations related to the aerosolization technique. Related to the total aerosolized amount in nebulizers particle deposition ranged between 0.037 % for aerosolized polystyrene particles/well in the VITROCELL/PARI BOY system, 0.157 % in the ALICE system [51], and 2.8 % in the optimized ALICE CLOUD system [62]. These systems may also lead to particle-dependent differences in deposition [61].

To avoid differences in delivery due to material properties, the use of manual devices, like the ones developed for animal exposures, might be advantageous. Delivery by these devices is easy to perform, less expensive, and technically less demanding and results in a higher relative deposition (amount of particles on cells related to total amount aerosolized) than by the more physiological setups mentioned before. Frequently used syringe-based devices are available from Penn Century Ltd and deliver aerosols generated from dry powder or from suspensions. MicroSprayer® IA-1C aerosolizer for liquid aerosols and DP-4 Dry Powder Insufflator™ for powder aerosols have been used for intratracheal delivery of nanoparticles and occupational and environmental toxicants to mice and rats [63-66]. Both devices have also been used in cellular studies [35, 61, 67-74]. Particle sizes produced by DP-4 Dry Powder Insufflator™ were linked to the respective sizes of the formulated or of the not-formulated powders [75] and are roughly similar before and after aerosolization [76]. The high amount of material that has to be applied is problematic for in vitro studies. The minimal amount is linked to the accuracy of the analytical balance and can be 1 mg as the minimum. An additional problem represents the potential cell damage due to application. When using different distances between tip of the device and cell surface, an optimum distance, when no cell damage occurred, can be identified. With aerosolization devices from suspensions, such as the MicroSprayer® IA-1C aerosolizer, also small amounts of NPs can be applied and the system, therefore, is less dependent from the material. These systems show less electrostatic interaction between particles and devices, aggregation of particles, and hygroscopy that decrease reproducibility of the experiments. The main disadvantage of the MicroSprayer® IA-1C aerosolizer is the generation of droplet in sizes of 20 μm that under normal conditions cannot reach the deep lung.

4. Readout parameters

In order to correlate cytotoxicity and accumulation, particle parameters and cellular uptake of the NPs have also to be determined.

4.1. Particle stability

Stability of particles, including chemical stability as well as colloidal stability may change over the incubation time. Chemical stability is changed by degradation and dissolution of the particles, while colloidal stability is influenced by pH, ions, and macromolecules in the biological fluid. Biodegradability is given for therapeutic aerosols, not for NP inhaled as air pollution and at the workplace. Detection of degradation products is particle specific and usually detected by mass spectrometry. Particle characterization includes changes in bulk composition, in size and structure, and in surface composition, surface charge, electrophoretic properties, surface hydrophobicity, and aggregation [77]. Changes in bulk composition are measured by energy dispersive X-ray spectroscopy (EDS), inductively coupled plasma mass spectrometry (ICP-MS), and combustion analysis (CA) but are less likely to show incubation-dependent changes in biological systems. Particle imaging by transmission electron microscopy, scanning electron microscopy, and atomic force microscopy can identify changes in size and structure. X-ray photoelectron spectroscopy (XPS), Brunauer–Emmett–Teller (BET) method, atomic force microscopy (AFM), and laser-Doppler velocimetry (LDV) are common techniques to characterize surface properties of NPs. Agglomeration can be followed by static light scattering (SLS), photon correlation spectroscopy (PCS)/dynamic light scattering (DLS), small-angle neutron scattering (SANS), and nanoparticle tracking analysis (NTS) [78].

The most important parameter that has to be monitored during prolonged incubation is colloidal stability. Colloidal stability of electrostatically stabilized particles is relatively low because the surface charges are neutralized by ions in the solution and particles prone to agglomeration. Binding of macromolecules may cause complex changes in surface charge, composition, and hydrophobicity and often results in particle agglomeration. Coating of the NPs with hydrophilic bulky molecules, such as polyethylene glycol (PEG), prevents binding of proteins and sterically hinders agglomeration. For instance, gold NPs with PEG coating are stable in physiological solution for 2–15 days [79]. Capping with biocompatible bulky organic molecules, such as serum albumin and starch, also stabilized silver NPs better than electrostatic repulsion by citrate [80]. This coating is absent for unintentionally inhaled NPs from the workplace and environment, which therefore shows lower colloidal stability. Depending on the particle properties with longer incubation in cell culture medium, either the average size of the agglomerates or the fraction of large aggregates increased [81].

4.2. Cellular uptake/accumulation

Colorimetric reading might lack sensitivity but in principle is useful for quantification. Prussian blue staining, for instance, is an established technique for demonstration of cellular uptake of iron oxide particles [82]. Uptake can either be performed on the single-cell level or in the entire population of exposed cells with fluorometric reading and flow cytometry. Also inductively coupled plasma mass spectrometry (ICP-MS) is used for this purpose [83]. Microscopy-based techniques, such as laser scan microscopy and transmission electron microscopy, may be suitable to confirm intracellular localization but are too laborious for quantification. Software programs, e.g., provided as ImageJ macro, could be used to analyze data from more cells [84]. Systems based on transmission electron microscopy scanning, rapid

scanning X-ray fluorescence microscopy, and NMR relaxometric techniques are more specialized techniques for quantification of intracellular NPs [85-87].

4.3. Cytotoxicity

The assessment of cytotoxicity commonly uses changes in physiology such as cell number, membrane integrity, amount of DNA or protein, and metabolic activity as readout and indicated as changes in viability. Signals that are obtained after treatment with samples are referred to untreated or solvent-treated cells. Screening assays are usually followed by other tests because decrease of viability can be the result of a variety of influences: depletion of nutrients, interference with organelle function, changes in pH, disruption of membrane integrity, induction of apoptosis, inhibition of proliferation, etc. When cells are cultured on membranes and not in plates, also measurements of TEER values can be used to indicate cell damage. A breakdown in TEER values can be caused by disruption of intercellular junctions or by induction of cell death. Since no indicators are used in these measurements, TEER measurements belong to the label-free detection techniques. A variety of other label-free assays are used for cytotoxicity testing of NPs. They have the advantage that no dye can interfere with cell metabolism or with the particles. NPs have been reported to interfere with conventional cell-based assays in various ways and cause false-positive and false-negative results [88, 89]. Interference of NPs with colorimetric, fluorometric, and luminescent readout is usually identified by inclusion of additional controls and performance of more than one assay. The majority of the aforementioned methods in acute cytotoxicity screening can also be used for the assessment of long-term exposure.

5. Own exposure system

In order to fulfill the requirements for organ-typical testing of NP accumulation, an exposure system based on Calu-3 cells has been developed, which is described in the following.

5.1. Particles accumulation in Calu-3

5.1.1. Methodology

Calu-3 cells were cultured on polyethylene terephthalate membranes with pore size of 3 μm at an air–liquid interface and showed constant TEER values from the 10th day until the end of the observation period, which was chosen at the 28th day (Fig. 4a). During the establishment of the model, cultures with different amounts of liquid in the basal compartment were characterized. When 1,500 μl was applied to the basal compartment, a pseudostratified columnar but not completely stable epithelium was formed. It appeared that the cells did not form a continuous monolayer but that at some locations also multilayers were formed. The epithelium was not stable because, as has been already hypothesized by Lehmann et al., removal of the medium detached cells of the upper layer [38]. When only 500 μl was applied to the basal chamber, the Calu-3 cells formed a stable simple columnar epithelium. The

different morphology appears to be caused by different volumes that reached the apical compartment resulting from hydrodynamic pressure of the fluid in the basal chamber. When 1,500 µl was applied to the basal compartment, the apical chamber contained about 250 µl of fluid. At volumes of 500 µl in the basal chamber, only 50 µl liquid was collected from the apical compartment.

Accumulation of 1.8 µg/cm^2 and 9 µg/cm^2 fluorescently labeled 20 nm carboxyl-functionalized polystyrene particles was studied. Addition as suspension in 10 µl cell culture medium was preferred to application as aerosol by MicroSprayer® IA-1C aerosolizer because data from pilot experiments did not show differences between these application forms. Furthermore, data were more reproducible upon application in small volume than with MicroSprayer® IA-1C aerosolizer. Particles in cell culture medium measured 42 nm with zeta potential of -41 mV. Cells were incubated with the particles for seven days with medium changes in the basal compartment every other day. After seven days, supernatants of cells were collected, cells were rinsed in cell culture medium, TEER measured, and cells incubated with the same amount of NPs for another seven days. This procedure was repeated up to a whole observation time of 28 days. Membranes with cells at each time point (7, 14, 21, 28 days) were subjected to quantification and visualization of uptake. For quantification of cellular uptake, cells were removed from the membrane by trypsin treatment and counted by electrochemical sensing and cellular uptake determined by fluorescence plate reader. Cellular uptake was determined using a standard curve produced from particle solutions diluted with cell culture medium containing cells. This dilution medium was chosen to correct for interference like quenching or autofluorescence by cells. Confocal images obtained by laser scan microscopy allowed visualization of stratification of the Calu-3 cell layer as well as verification of intracellular uptake. In addition, immunocytochemical detection of mucin 5AC was used to identify mucus production of the cells.

5.1.2. Results

During the entire exposure time, no decrease in TEER values was noted, suggesting absence of cell damage (Fig. 4a). Uptake of particles showed intercellular and regional differences (Fig. 4b). Over the entire observation time, Calu-3 cells formed a continuous monolayer, but not all cells showed obvious staining with anti-mucin 5AC antibody as indication for mucus production. This situation resembles the in-vivo condition, where also a non continuous mucus layer in the bronchi has been reported [20]. Cellular uptake of NPs was higher in cells with no mucus production (Fig. 4c). For both concentrations of polystyrene particles, linear cellular accumulation was noted (Fig. 4d).

5.2. Discussion of the presented model

Calu-3 cells were cultured on polyethylene terephthalate membranes with pore size of 3 µm. These pores should allow the passage of the particles, but pilot experiments using naked membranes showed that only a fraction of the carboxyl-functionalized polystyrene particles (52 %) was detected on the other side of the membrane. Permeation of polystyrene particles across 3 µm polycarbonate membranes has been reported differently; while one study

http://dx.doi.org/10.5772/60701

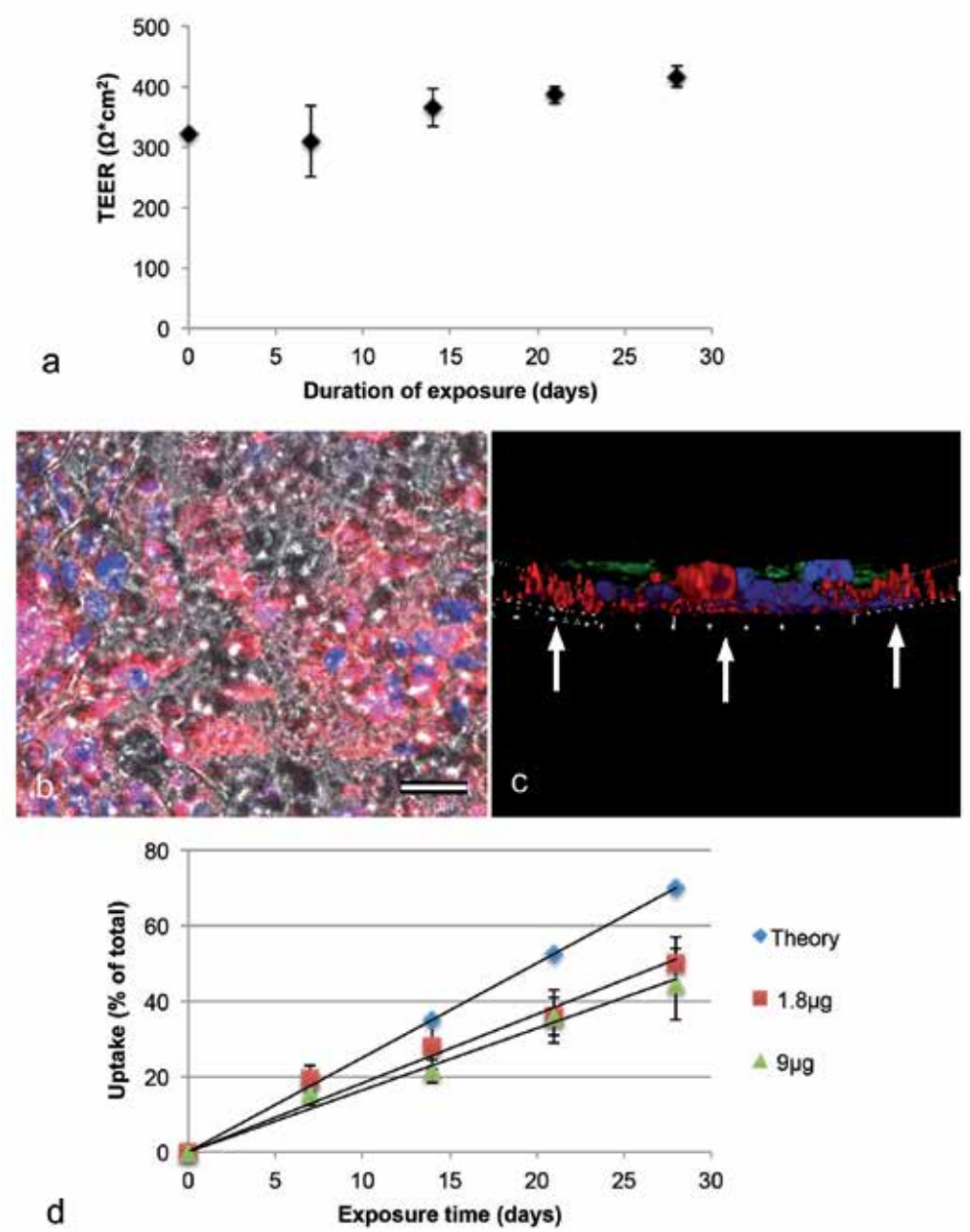

Figure 4. Accumulation of 20 nm fluorescently labeled carboxyl-functionalized polystyrene particles (red) in Calu-3 cells over 28 days. TEER values remained constant over the entire exposure time (a). Differences in accumulation of NPs between cells are seen (b). In the volume-rendered 3-D reconstruction performed on the z-series of images at d28, accumulation of NPs mainly in cells showing no prominent anti-mucus production (anti-mucin 5AC staining; green) is seen. Arrow indicates the membrane on which the Calu-3 cell monolayers were grown (c). Quantification of cellular uptake by fluorometric reading shows a linear accumulation of the particles over time (d). Doses of 1.8 μg/cm^2 and 9 μg/cm^2 were applied and theoretical uptake (Theory) is extrapolated based on the uptake after seven days. Scale bar: 20 μm.

recovered almost 100 % of 50 nm carboxyl-functionalized and plain polystyrene particles after 6 h [90], another group reported passage of about 25 % of 37 nm carboxyl-functionalized polystyrene particles [91]. Low translocation rates after 24 h of incubation across the same membranes are also reported for 50 nm silica NPs; more than 90 % of the applied particles were trapped in the membranes [92]. These studies suggest that particle transport across cellular monolayers may give erroneous data on cellular transport of polystyrene particles.

Growth of Calu-3 cells in air–liquid interface culture with different volume of medium in the basal chamber could help in identifying differences between monolayered and multilayered epithelium. However, the multilayers that were obtained when using a greater volume in the basal chamber were less stable, and morphological variations and less constant TEER values were obtained.

The currently used system is based on fluorescence labeling of the particles. This labeling may cause changes in surface properties or size. For polystyrene particles, changes in surface properties by fluorescence labeling can be excluded because the particles are synthesized and subsequently swollen in organic fluid containing the dye. This is followed by gradient evaporation of the solvent and repeated washing of the particles to remove dye from the surface [93]. Any fluorescent labeling mode, however, bears also the problem of stability because loss of the label may reduce the measured accumulation values when freshly prepared solutions are used for preparation of the standard curve. The advantage of the polystyrene particles that were used in this study is that they showed stable fluorescence over the entire incubation time of 28 days. Preparation of the standard curves using stock solutions, which are kept under the same conditions as for the cellular exposures, may be more appropriate. It is, however, not excluded that the dilution influences stability since fluorescently labeled particles are more stable in concentrated than in diluted solution (https://www.bdbiosciences.com/documents/BD_Accuri_SPHERO_RainbowCalibration_Particles_ProdInfoSheet.pdf). In addition, stability may be different for intracellular- and extracellular-located particles. Degradation of the label by intracellular enzymes might be expected to reduce the stability of the fluorescence of intracellularly located particles.

The estimate of NP uptake in this study was based on particle uptake after seven days; this uptake could be the result of an inhibited uptake already at that time. Sequential exposure to different NPs and measurement at shorter time points than seven days could be used to answer the question whether the presence of intracellular particles affects the uptake of new particles.

The type of intracellular localization/accumulation may influence cellular effects. Most NPs are taken up by endocytotic mechanisms that deliver their content to lysosomes. Studies on correlation of intralysosomal and extralysosomal accumulation to cell damage may provide further information.

In the concentration range tested, no obvious inhibition of particle uptake was seen, suggesting that cells can handle these particle concentrations without obvious damage. For the identification of potential threshold values and mechanistic studies, exposure to higher concentrations of NPs has to be performed. In addition to that, studies on other particle sizes may provide further insight into cellular effect of inhaled NPs.

http://dx.doi.org/10.5772/60701

In addition to cytotoxicity, exposure to NPs may induce inflammation and including cytokine release as readout parameter may identify this effect. Secretion of the cytokines interleukin-6 and interleukin-8 has been used as an indication for inflammatory response in Calu-3 cells [94].

Co-culture of alveolar epithelial cells with macrophages could provide more insight into the interplay of different cell types at the alveolar barrier. It is questionable that both cell types can be observed over longer periods because of the different medium requirements and proliferation rates.

6. Conclusion

Chronic cytotoxicity testing of respiratory cells is linked to specific problems. Only few cells tolerate air–liquid interface culture for a prolonged time and without change in morphology. Exposure to aerosol may present particle-dependent delivery rates. The presented exposure system fulfilled all requirements for physiologically relevant testing of prolonged contact to NPs by respiratory exposure. Doses that were applied in the model are in the same order of magnitude as therapeutic aerosols [95]. The data showed relatively low inhibition of particle uptake by intracellularly accumulated NPs. Study of particle transport is limited by the fact that insert membrane do not allow unimpeded passage of the particles.

Author details

Eleonore Fröhlich* and Claudia Meindl

*Address all correspondence to: eleonore.froehlich@medunigraz.at

Center for Medical Research, Medical University of Graz, Graz, Austria

References

[1] Van Hee VC, Kaufman JD, Budinger GR, Mutlu GM. Update in environmental and occupational medicine 2009. American Journal of Respiratory and Critical Care Medicine 2010; 181(11) 1174-80.

[2] Pope CA, 3rd, Burnett RT, Krewski D, Jerrett M, Shi Y, Calle EE, Thun MJ. Cardiovascular mortality and exposure to airborne fine particulate matter and cigarette smoke: shape of the exposure-response relationship. Circulation 2009; 120(11) 941-8.

[3] Plitzko S. Workplace exposure to engineered nanoparticles. Inhalation Toxicology 2009; 21 (Suppl 1) 25-9.

[4] Lee JH, Sohn EK, Ahn JS, Ahn K, Kim KS, Lee JH, Lee TM, Yu IJ. Exposure assessment of workers in printed electronics workplace. Inhalation Toxicology 2013; 25(8) 426-34.

[5] Lee JH, Kwon M, Ji JH, Kang CS, Ahn KH, Han JH, Yu IJ. Exposure assessment of workplaces manufacturing nanosized TiO2 and silver. Inhalation Toxicology 2011; 23(4) 226-36.

[6] Curwin B, Bertke S. Exposure characterization of metal oxide nanoparticles in the workplace. Journal of Occupational and Environmental Hygiene 2011; 8(10) 580-7.

[7] Miller A, Drake PL, Hintz P, Habjan M. Characterizing exposures to airborne metals and nanoparticle emissions in a refinery. The Annals of Occupational Hygiene 2010; 54(5) 504-13.

[8] Lee JH, Mun J, Park JD, Yu IJ. A health surveillance case study on workers who manufacture silver nanomaterials. Nanotoxicology 2012; 6(6) 667-9.

[9] Journeay W, Goldman R. Occupational handling of nickel nanoparticles: A case report. American Journal of Industrial Medicine 2014; 57(9) 1073-6.

[10] Theegarten D, Boukercha S, Philippou S, Anhenn O. Submesothelial deposition of carbon nanoparticles after toner exposition: case report. Diagnostic Pathology 2010; 5 77.

[11] Bhavna, Ahmad FJ, Mittal G, Jain GK, Malhotra G, Khar RK, Bhatnagar A. Nano-salbutamol dry powder inhalation: a new approach for treating broncho-constrictive conditions. European Journal of Pharmaceutics and Biopharmaceutics 2009; 71(2) 282-91.

[12] Ali R, Mittal G, Ali R, Kumar M, Kishan Khar R, Ahmad FJ, Bhatnagar A. Development, characterisation and pharmacoscintigraphic evaluation of nano-fluticasone propionate dry powder inhalation as potential antidote against inhaled toxic gases. Journal of Microencapsulation 2013; 30(6) 546-58.

[13] Ali R, Jain GK, Iqbal Z, Talegaonkar S, Pandit P, Sule S, Malhotra G, Khar RK, Bhatnagar A, Ahmad FJ. Development and clinical trial of nano-atropine sulfate dry powder inhaler as a novel organophosphorous poisoning antidote. Nanomedicine 2009; 5(1) 55-63.

[14] Vanlandschoot P, Stortelers C, Beirnaert E, Ibanez LI, Schepens B, Depla E, Saelens X. Nanobodies(R): new ammunition to battle viruses. Antiviral Research 2011; 92(3) 389-407.

[15] Rosenstock J, Bergenstal R, Defronzo RA, Hirsch IB, Klonoff D, Boss AH, Kramer D, Petrucci R, Yu W, Levy B, Study G. Efficacy and safety of Technosphere inhaled insulin compared with Technosphere powder placebo in insulin-naive type 2 diabetes suboptimally controlled with oral agents. Diabetes Care 2008; 31(11) 2177-82.

[16] Weibel E, Morphometry of the Human Lung. Berlin: Springer; 1963.

[17] Beachey W, The Airways and Alveoli. in: W. Beachey, (ed). Respiratory Care Anatomy and Physiology: Foundations for Clinical Practice. St Louis: Elsevier Mosby; 2013. p. 2-23.

[18] Widdicombe JG. Airway liquid: a barrier to drug diffusion? European Respiratory Journal 1997; 10(10) 2194-7.

[19] Fahy JV, Dickey BF. Airway mucus function and dysfunction. New England Journal of Medicine 2010; 363(23) 2233-47.

[20] Overton J, Miller F, Dosimetry Modeling of Inhaled Toxic Reactive Gases. in: A. Watson, R. Bates, D. Kennedy, (eds). Air Pollution, the Automobile, and Public Health. Washington: National Academy Press; 1988. p. 367-85.

[21] Waldmann C, Soni N, Rhodes A, Respiratory drugs. in: C. Waldmann, N. Soni, A. Rhodes, (eds). Oxford Desk Reference: Critical Care. Oxford: Oxford University Press; 2008. p. 153-164.

[22] Weinstein GD, McCullough JL, Ross P. Cell proliferation in normal epidermis. Journal of Investigative Dermatology 1984; 82(6) 623-8.

[23] Lipkin M, Bell B, Sherlock P. Cell proliferation kinetics in the gastrointestinal tract of man. I. cell renewal in colon and rectum. Journal of Clinical Investigation 1963; 42(6) 767-76.

[24] Desai TJ, Brownfield DG, Krasnow MA. Alveolar progenitor and stem cells in lung development, renewal and cancer. Nature 2014; 507(7491) 190-4.

[25] Shi H, Magaye R, Castranova V, Zhao J. Titanium dioxide nanoparticles: a review of current toxicological data. Particle and Fibre Toxicology 2013; 10 15.

[26] Haghi M, Ong HX, Traini D, Young P. Across the pulmonary epithelial barrier: Integration of physicochemical properties and human cell models to study pulmonary drug formulations. Pharmacology and Therapeutics 2014.

[27] Akhtar MJ, Ahamed M, Khan MA, Alrokayan SA, Ahmad I, Kumar S. Cytotoxicity and apoptosis induction by nanoscale talc particles from two different geographical regions in human lung epithelial cells. Environmental toxicology 2012.

[28] Stoehr LC, Gonzalez E, Stampfl A, Casals E, Duschl A, Puntes V, Oostingh GJ. Shape matters: effects of silver nanospheres and wires on human alveolar epithelial cells. Particle and Fibre Toxicology 2011; 8 36.

[29] Foster KA, Avery ML, Yazdanian M, Audus KL. Characterization of the Calu-3 cell line as a tool to screen pulmonary drug delivery. International Journal of Pharmaceutics 2000; 208(1-2) 1-11.

[30] Mathias NR, Timoszyk J, Stetsko PI, Megill JR, Smith RL, Wall DA. Permeability characteristics of calu-3 human bronchial epithelial cells: in vitro-in vivo correlation to predict lung absorption in rats. Journal of Drug Targeting 2002; 10(1) 31-40.

[31] Zhang Y, Reenstra WW, Chidekel A. Antibacterial activity of apical surface fluid from the human airway cell line Calu-3: pharmacologic alteration by corticosteroids and beta(2)-agonists. American Journal of Respiratory Cell and Molecular Biology 2001; 25(2) 196-202.

[32] Kreda SM, Okada SF, Van Heusden CA, O'Neal W, Gabriel S, Abdullah L, Davis CW, Boucher RC, Lazarowski ER. Coordinated release of nucleotides and mucin from human airway epithelial Calu-3 cells. Journal of Physiology 2007; 584(Pt 1) 245-59.

[33] Fuchs S, Gumbleton M, Schäfer U, Lehr CM, Bronchial Epithelial Cell Culture. in: C.M. Lehr, (ed). Cell Culture Models of Biological Barriers: In vitro Test Systems for Drug Absorption and Delivery. London: Taylor & Francis; 2002. p. 211-27.

[34] Grainger CI, Greenwell LL, Lockley DJ, Martin GP, Forbes B. Culture of Calu-3 cells at the air interface provides a representative model of the airway epithelial barrier. Pharmaceutical Research 2006; 23(7) 1482-90.

[35] Blank F, Rothen-Rutishauser BM, Schurch S, Gehr P. An optimized in vitro model of the respiratory tract wall to study particle cell interactions. Journal of Aerosol Medicine 2006; 19(3) 392-405.

[36] Liu FF, Peng C, Escher BI, Fantino E, Giles C, Were S, Duffy L, Ng JC. Hanging drop: an in vitro air toxic exposure model using human lung cells in 2D and 3D structures. Journal of Hazardous Materials 2013; 261 701-10.

[37] Nalayanda DD, Wang Q, Fulton WB, Wang TH, Abdullah F. Engineering an artificial alveolar-capillary membrane: a novel continuously perfused model within microchannels. Journal of Pediatric Surgery 2010; 45(1) 45-51.

[38] Lehmann A, Brandenberger C, Blank F, Gehr P, Rothen-Rutishauser B, A 3D Model of the Human Epithelial Airway Barrier. in: T. Maguire, E. Novik, (eds). Methods in Bioengineering: Alternatives to Animal Testing: Artech House; 2010. p. 239-260.

[39] Haghi M, Young PM, Traini D, Jaiswal R, Gong J, Bebawy M. Time- and passage-dependent characteristics of a Calu-3 respiratory epithelial cell model. Drug Development and Industrial Pharmacy 2010; 36(10) 1207-14.

[40] Panas A, Comouth A, Saathoff H, Leisner T, Al-Rawi M, Simon M, Seemann G, Dossel O, Mulhopt S, Paur HR, Fritsch-Decker S, Weiss C, Diabate S. Silica nanoparticles are less toxic to human lung cells when deposited at the air-liquid interface compared to conventional submerged exposure. Beilstein Journal of Nanotechnology 2014; 5 1590-602.

[41] Tena A, Clara P. Deposition of inhaled particles in the lungs. Arch Bronconeumol. 2012; 48(7) 240-6.

[42] Voisin C, Aerts C, Jakubczk E, Tonnel AB. [La culture cellulaire en phase gazeuse. Un nouveau modele experimental d'etude in vitro des activites des macrophages alveolaires]. Bulletin Europeen de Physiopathologie Respiratoire 1977; 13(1) 69-82.

[43] Voisin C, Wallaert B. [Occupational dust exposure and chronic obstructive bronchopulmonary disease. Etiopathogenic approach to the problem of compensation in the mining environment]. Bulletin de l'Academie Nationale de Medecine 1992; 176(2) 243-50; discussion 250-2.

[44] Bitterle E, Karg E, Schroeppel A, Kreyling WG, Tippe A, Ferron GA, Schmid O, Heyder J, Maier KL, Hofer T. Dose-controlled exposure of A549 epithelial cells at the air-liquid interface to airborne ultrafine carbonaceous particles. Chemosphere 2006; 65(10) 1784-90.

[45] Tippe A, Heinzmann U, Roth C. Deposition of fine and ultrafine aerosol particles during exposure at the air/cell interface. Journal of Aerosol Science 2002; 33(2) 207-218.

[46] Gaschen A, Lang D, Kalberer M, Savi M, Geiser T, Gazdhar A, Lehr CM, Bur M, Dommen J, Baltensperger U, Geiser M. Cellular responses after exposure of lung cell cultures to secondary organic aerosol particles. Environmental Science & Technology 2010; 44(4) 1424-30.

[47] Savi M, Kalberer M, Lang D, Ryser M, Fierz M, Gaschen A, Ricka J, Geiser M. A novel exposure system for the efficient and controlled deposition of aerosol particles onto cell cultures. Environmental Science & Technology 2008; 42(15) 5667-74.

[48] Phillips J, Kluss B, Richter A, Massey E. Exposure of bronchial epithelial cells to whole cigarette smoke: assessment of cellular responses. Alternatives to Laboratory Animals 2005; 33(3) 239-48.

[49] Brandenberger C, Muhlfeld C, Ali Z, Lenz AG, Schmid O, Parak WJ, Gehr P, Rothen-Rutishauser B. Quantitative evaluation of cellular uptake and trafficking of plain and polyethylene glycol-coated gold nanoparticles. Small 2010; 6(15) 1669-78.

[50] Brandenberger C, Rothen-Rutishauser B, Muhlfeld C, Schmid O, Ferron GA, Maier KL, Gehr P, Lenz AG. Effects and uptake of gold nanoparticles deposited at the air-liquid interface of a human epithelial airway model. Toxicology and Applied Pharmacology 2010; 242(1) 56-65.

[51] Lenz AG, Karg E, Lentner B, Dittrich V, Brandenberger C, Rothen-Rutishauser B, Schulz H, Ferron GA, Schmid O. A dose-controlled system for air-liquid interface cell exposure and application to zinc oxide nanoparticles. Particle and Fibre Toxicology 2009; 6 32.

[52] De Bruijne K, Ebersviller S, Sexton KG, Lake S, Leith D, Goodman R, Jetters J, Walters GW, Doyle-Eisele M, Woodside R, Jeffries HE, Jaspers I. Design and testing of

Electrostatic Aerosol in Vitro Exposure System (EAVES): an alternative exposure system for particles. Inhalation Toxicology 2009; 21(2) 91-101.

[53] Volckens J, Dailey L, Walters G, Devlin RB. Direct particle-to-cell deposition of coarse ambient particulate matter increases the production of inflammatory mediators from cultured human airway epithelial cells. Environmental Science & Technology 2009; 43(12) 4595-9.

[54] Aufderheide M, Mohr U. CULTEX--an alternative technique for cultivation and exposure of cells of the respiratory tract to airborne pollutants at the air/liquid interface. Experimental and Toxicologic Pathology 2000; 52(3) 265-70.

[55] Ritter D, Knebel JW, Aufderheide M. Exposure of human lung cells to inhalable substances: a novel test strategy involving clean air exposure periods using whole diluted cigarette mainstream smoke. Inhalation Toxicology 2003; 15(1) 67-84.

[56] Aufderheide M, Mohr U. A modified CULTEX system for the direct exposure of bacteria to inhalable substances. Experimental and Toxicologic Pathology 2004; 55(6) 451-4.

[57] Bakand S, Winder C, Khalil C, Hayes A. A novel in vitro exposure technique for toxicity testing of selected volatile organic compounds. Journal of Environmental Monitoring 2006; 8(1) 100-5.

[58] Gasser M, Riediker M, Mueller L, Perrenoud A, Blank F, Gehr P, Rothen-Rutishauser B. Toxic effects of brake wear particles on epithelial lung cells in vitro. Particle and Fibre Toxicology 2009; 6 30.

[59] Paur HR, Mülhopt S, Weiss C, Diabaté S. In Vitro exposure systems and bioassays for the assessment of toxicity of nanoparticles to the human lung. Journal für Verbraucherschutz und Lebensmittelsicherheit 2008; 3 3.

[60] Rothen-Rutishauser B, Grass RN, Blank F, Limbach LK, Muhlfeld C, Brandenberger C, Raemy DO, Gehr P, Stark WJ. Direct combination of nanoparticle fabrication and exposure to lung cell cultures in a closed setup as a method to simulate accidental nanoparticle exposure of humans. Environmental Science & Technology 2009; 43(7) 2634-40.

[61] Fröhlich E, Bonstingl G, Hofler A, Meindl C, Leitinger G, Pieber TR, Roblegg E. Comparison of two in vitro systems to assess cellular effects of nanoparticles-containing aerosols. Toxicology In Vitro 2013; 27(1) 409-17.

[62] Lenz AG, Stoeger T, Cei D, Schmidmeir M, Semren N, Burgstaller G, Lentner B, Eickelberg O, Meiners S, Schmid O. Efficient bioactive delivery of aerosolized drugs to human pulmonary epithelial cells cultured in air-liquid interface conditions. American Journal of Respiratory Cell and Molecular Biology 2014; 51(4) 526-35.

[63] Mantecca P, Sancini G, Moschini E, Farina F, Gualtieri M, Rohr A, Miserocchi G, Palestini P, Camatini M. Lung toxicity induced by intratracheal instillation of size-fractionated tire particles. Toxicology Letters 2009; 189(3) 206-14.

[64] Imanishi M, Dote T, Tsuji H, Tanida E, Yamadori E, Kono K. Time-dependent changes of blood parameters and fluoride kinetics in rats after acute exposure to subtoxic hydrofluoric acid. Journal of Occupational Health 2009; 51(4) 287-93.

[65] Gervelas C, Serandour AL, Geiger S, Grillon G, Fritsch P, Taulelle C, Le Gall B, Benech H, Deverre JR, Fattal E, Tsapis N. Direct lung delivery of a dry powder formulation of DTPA with improved aerosolization properties: effect on lung and systemic decorporation of plutonium. Journal of Controlled Release 2007; 118(1) 78-86.

[66] Niwa Y, Hiura Y, Murayama T, Yokode M, Iwai N. Nano-sized carbon black exposure exacerbates atherosclerosis in LDL-receptor knockout mice. Circulation Journal 2007; 71(7) 1157-61.

[67] Witzenrath M, Gutbier B, Schmeck B, Tenor H, Seybold J, Kuelzer R, Grentzmann G, Hatzelmann A, Van Laak V, Tschernig T, Mitchell TJ, Schudt C, Rosseau S, Suttorp N, Schutte H. Phosphodiesterase 2 inhibition diminished acute lung injury in murine pneumococcal pneumonia. Critical Care Medicine 2009; 37(2) 584-90.

[68] Steiner S, Mueller L, Popovicheva OB, Raemy DO, Czerwinski J, Comte P, Mayer A, Gehr P, Rothen-Rutishauser B, Clift MJ. Cerium dioxide nanoparticles can interfere with the associated cellular mechanistic response to diesel exhaust exposure. Toxicology Letters 2012; 214(2) 218-25.

[69] Sloane PA, Shastry S, Wilhelm A, Courville C, Tang LP, Backer K, Levin E, Raju SV, Li Y, Mazur M, Byan-Parker S, Grizzle W, Sorscher EJ, Dransfield MT, Rowe SM. A pharmacologic approach to acquired cystic fibrosis transmembrane conductance regulator dysfunction in smoking related lung disease. PLoS One 2012; 7(6) e39809.

[70] Kardia E, Yusoff NM, Zakaria Z, Yahaya B. Aerosol-based delivery of fibroblast cells for treatment of lung diseases. Journal of Aerosol Medicine and Pulmonary Drug Delivery 2014; 27(1) 30-4.

[71] Heuking S, Rothen-Rutishauser B, Raemy DO, Gehr P, Borchard G. Fate of TLR-1/TLR-2 agonist functionalised pDNA nanoparticles upon deposition at the human bronchial epithelium in vitro. Journal of Nanobiotechnology 2013; 11 29.

[72] Kim JS, Klosener J, Flor S, Peters TM, Ludewig G, Thorne PS, Robertson LW, Luthe G. Toxicity assessment of air-delivered particle-bound polybrominated diphenyl ethers. Toxicology 2014; 317 31-9.

[73] Bur M, Huwer H, Muys L, Lehr CM. Drug transport across pulmonary epithelial cell monolayers: effects of particle size, apical liquid volume, and deposition technique. Journal of Aerosol Medicine and Pulmonary Drug Delivery 2010; 23(3) 119-27.

[74] Diab R, Brillault J, Bardy A, Gontijo AV, Olivier JC. Formulation and in vitro characterization of inhalable polyvinyl alcohol-free rifampicin-loaded PLGA microspheres

prepared with sucrose palmitate as stabilizer: efficiency for ex vivo alveolar macrophage targeting. International Journal of Pharmaceutics 2012; 436(1-2) 833-9.

[75] Hoppentocht M, Hoste C, Hagedoorn P, Frijlink HW, De Boer AH. In vitro evaluation of the DP-4M PennCentury insufflator. European Journal of Pharmaceutics and Biopharmaceutics 2014; 88(1) 153-9.

[76] Duret C, Wauthoz N, Merlos R, Goole J, Maris C, Roland I, Sebti T, Vanderbist F, Amighi K. In vitro and in vivo evaluation of a dry powder endotracheal insufflator device for use in dose-dependent preclinical studies in mice. European Journal of Pharmaceutics and Biopharmaceutics 2012; 81(3) 627-34.

[77] Chen K, Smith B, Ball W, Fairbrother D. Assessing the colloidal properties of engineered nanoparticles in water: case studies from fullerene C60 nanoparticles and carbon nanotubes. Environmental Chemistry 2010; 7 10-27.

[78] Hasselöv M, Kaegi R, Analysis and Characterization of Manufactured Nanoparticles in Aquatic Environments. in: J. Lead, E. Smith, (eds). Environmental and Human Health Impacts of Nanotechnology. Chichester: John Wiley & Sons; 2009.

[79] Fang C, Bhattarai N, Sun C, Zhang M. Functionalized nanoparticles with long-term stability in biological media. Small 2009; 5(14) 1637-41.

[80] MacCuspie R. Colloidal stability of silver nanoparticles in biologically relevant conditions. Journal of Nanoparticle Research 2011; 13 2893-908.

[81] Mrakovcic M, Meindl C, Roblegg E, Fröhlich E. Reaction of monocytes to polystyrene and silica nanoparticles in short-term and long-term exposures. Toxicology Research 2014; 3 86-97.

[82] Zhu XM, Wang YX, Leung KC, Lee SF, Zhao F, Wang DW, Lai JM, Wan C, Cheng CH, Ahuja AT. Enhanced cellular uptake of aminosilane-coated superparamagnetic iron oxide nanoparticles in mammalian cell lines. International Journal of Nanomedicine 2012; 7 953-64.

[83] Bohme S, Stark HJ, Meissner T, Springer A, Reemtsma T, Kuhnel D, Busch W. Quantification of AlO nanoparticles in human cell lines applying inductively coupled plasma mass spectrometry (neb-ICP-MS, LA-ICP-MS) and flow cytometry-based methods. Journal of Nanoparticle Research 2014; 16(9) 2592.

[84] Torrano AA, Blechinger J, Osseforth C, Argyo C, Reller A, Bein T, Michaelis J, Brauchle C. A fast analysis method to quantify nanoparticle uptake on a single cell level. Nanomedicine (Lond) 2013; 8(11) 1815-28.

[85] Dadashzadeh ER, Hobson M, Henry Bryant L, Jr., Dean DD, Frank JA. Rapid spectrophotometric technique for quantifying iron in cells labeled with superparamagnetic iron oxide nanoparticles: potential translation to the clinic. Contrast Media & Molecular Imaging 2013; 8(1) 50-6.

[86] James SA, Feltis BN, De Jonge MD, Sridhar M, Kimpton JA, Altissimo M, Mayo S, Zheng C, Hastings A, Howard DL, Paterson DJ, Wright PF, Moorhead GF, Turney TW, Fu J. Quantification of ZnO nanoparticle uptake, distribution, and dissolution within individual human macrophages. ACS Nano 2013; 7(12) 10621-35.

[87] Brown A, Brydson R, Hondow N. Measuring in vitro cellular uptake of nanoparticles by transmission electron microscopy. Journal of Physics: Conference Series 2014; 522 012058.

[88] Fröhlich E. Cellular targets and mechanisms in the cytotoxic action of non-biodegradable engineered nanoparticles. Current drug metabolism 2013; 14(9) 976-88.

[89] Meindl C, Absenger M, Roblegg E, Fröhlich E. Suitability of cell-based label-free detection for cytotoxicity screening of carbon nanotubes. BioMed Research International 2013; 2013 564804.

[90] Schulze C, Schäfer U, Voetz M, Wohlleben W, Venzago C, Lehr C. Transport of metal oxide nanoparticles across Calu-3 monolayers modelling the air-blood barrier. EURO-NanoTox-Letters 2011; 1 0001-0011.

[91] Cartwright L, Poulsen MS, Nielsen HM, Pojana G, Knudsen LE, Saunders M, Rytting E. In vitro placental model optimization for nanoparticle transport studies. International Journal of Nanomedicine 2012; 7 497-510.

[92] George I, Vranic S, Boland S, Borot MC, Marano F, Baeza-Squiban A. Translocation of SiO2-NPs across in vitro human bronchial epithelial monolayer. Journal of Physics: Conference Series 2013; 429 012022.

[93] Zhang Q, Han Y, Wang W, Zhang L, Chang J. Preparation of fluorescent polystyrene microspheres by gradual solvent evaporation method. European Polymer Journal 2009; 45 550-6.

[94] Zhu Y, Chidekel A, Shaffer TH. Cultured human airway epithelial cells (calu-3): a model of human respiratory function, structure, and inflammatory responses. Critical Care Research and Practice 2010; 2010.

[95] Angelo R, Rousseau K, Grant M, Leone-Bay A, Richardson P. Technosphere® Insulin: Defining the Role of Technosphere Particles at the Cellular Level. Journal of Diabetes Science and Technology 3, 545- 54.

Chapter 5

In vivo Assessment of Nanomaterials Toxicity

Simona Clichici and Adriana Filip

Additional information is available at the end of the chapter

http://dx.doi.org/10.5772/60707

Abstract

The concern regarding the safety of nanomaterials for the human body is constantly raising. On one hand, there is an increase in the production of nanomaterials for technological applications, which raises the risk of accidental exposure of the workers during the technological manipulation. On the other hand, nanomaterials can be designed for medical applications and their faith in the human body, along with their interactions with different tissues, becomes of vital importance.

The mechanisms involved in nanomaterials toxicity are discussed, including oxidative stress and inflammation. *In vivo* toxicity evaluation includes different routes of administration or interaction between the nanomaterial and the organism, as well as a short-term or a long-term exposure or evaluation. Also, the characteristics of nanomaterials, including size, shape, impurities, function, surface coating in relation to their toxicity, were discussed. A particular attention has been given to the evaluation of the toxicity of dendrimers, silver nanoparticles, gold nanoparticles and carbon nanotubes.

Keywords: toxicity, oxidative stress, nanoparticles, carbon nanotubes

1. Introduction

Research in the field of nanomaterials and nanotechnology has seen exponential growth in recent years due to multiple applications in different areas such as molecular imaging, drug delivery, engineering technology, and development of materials and medical devices for diagnosis and treatment. Generally, the biological effects of nanomaterials depend on their

electronic, magnetic, optical, and mechanical properties and also on their size, composition, and shape.

However, the impact of these nanomaterials on human and environmental health is still limited. Most studies have investigated only the effects of unintended exposure (inhalation, medical procedures or accidental ingestion) and evaluated especially local effects, at the access site [1, 2]. Nevertheless, due to the development of various biomedical procedures using nanomaterials it is necessary to understand their potential toxic effects at systemic level.

An increasing number of studies published in the last decade have tried to decipher the complexity of interactions between different types of nanomaterials and cells. Nanomaterials usually get into the body either by inhalation and ingestion or transcutaneous [3, 4], most often accidentally in the process of synthesis, through their usage, after wearing gold and silver jewelry or by eating food containing gold. Nevertheless, the behavior of nanoparticles inside the cells is still an enigma, and not all the metabolic and immunological responses induced by these particles are completely understood. In addition, the conclusions obtained have been variable and contradictory according to the type of nanomaterials used, their size, shape, and surface chemistry. Based on the multitude of uses in pharmaceutical and medical applications, a thorough understanding of associated systemic and local toxicity is critically necessary.

2. Nanomaterial design considerations

Generally, the nanomaterials toxicity has been thought to originate in size and surface area, composition, and shape. Size influences the cellular uptake and response to nanomaterials, their distribution and elimination from the body. It has been shown that nanomaterials with small size have an exponential increase in surface area relative to volume, making the surface more reactive in itself and to biological components from surrounding environment. Several *in vitro* studies have shown that the latex nanospheres uptake into the nonphagocytic cells is higher at small sizes (50 - 100 nm) and decrease with the increase of the diameter (over 200 nm) [5]. Usually, nanomaterials with small sizes accumulate mainly in certain tissues (spleen, liver, lung, and kidneys) where they interfere with their biological functions [6, 7].

Chemical composition at the surface influences the chemical interactions of nanomaterials with biomolecules. Most nanomaterials are functionalized on the surface in order to increase blood circulation and to be more biocompatible for use in targeted therapy. Therefore, different functional groups were added to the outside to allow a better interaction with biological components and to aid the passage of nanomaterials in certain cells.

The phytochemical synthesis of nanoparticles using polyphenols from plants or fruits plays an important role in the field of nanomedicine as it offers a safe alternative therapeutic option. David et al. [8] synthesized silver nanoparticles using European black elderberry fruits extract (*Sambucus nigra - SN*, Adoxaceae family). The new materials were tested *in vitro* on spontaneously immortalized, human keratinocytes (HaCaT) exposed to UVB radiation, *in vivo* on acute inflammation model, and in humans on psoriasis lesions. The

http://dx.doi.org/10.5772/60707

results obtained demonstrated the anti-inflammatory effects of functionalized silver nanoparticles both *in vitro* as well as *in vivo*. Thus, the bionanocomposites reduced cytokine production induced by UVB irradiation and diminished the edema and cytokines levels in the paw tissues, early after the induction of inflammation and presented long-term protective effect. Silver nanoparticles functionalized with natural extracts applied on psoriasis lesions exhibited anti-inflammatory effect [8]. Materials based on gold nanoparticles and natural compounds extracted from native plants of the *Adoxaceae* family (European cranberrybush – *Viburnum opulus L.* and European black elderberry – *Sambucus nigra L.)* possessed anti-inflammatory activity, both in vitro as well as on psoriasis lesions, mainly due to their high content of anthocyanins and other polyphenols [9].

The degradability of the material is also an important factor for acute and long-term toxicity. Thus, the nondegradable nanomaterials can accumulate in cells, where they can cause detrimental effects similar to those of lysosomal storage diseases. By contrast, the biodegradable nanomaterials can undergo changes in cells and may lead to unpredicted toxicity due to unexpected toxic degradation products. They can release toxic products in the biological milieu leading to free radical formation and consequently to cellular damage. Recently, Champion et al. have shown that phagocytosis of nanomaterials depends on the contact with materials and consequently on their shape [10]. Thus, nanorods particles are less internalized in cells compared to spherical materials [11]. Wang et al. suggested that the difference between cellular uptake and cytotoxicity of spherical particles and nanorods depends on chemical compounds used to stabilize the nanomaterials [12]. For example, cetyltrimethylammonium bromide (CTAB), a cationic surfactant used to stabilize gold nanorods, can induce intracellular aggregation and explain nanorods cytotoxicity compared to spherical particles [12, 13]. In order to reduce nanorods toxicity other substances may be used: PEG, citric acid, and transferrin [11].

3. Mechanisms of nanomaterials toxicity

The most important mechanism of *in vitro* and *in vivo* nanotoxicity is related to the induction of oxidative stress by free radical formation, directly into the acidic environment of lysosomes [14]. Free radicals are released from phagocytic cells as a response to foreign material, insufficient amounts of anti-oxidants, presence of transition metals, or environmental factors [15]. The most exposed organs to nanomaterials are the liver and the spleen, especially due to the prevalence of phagocytic cells in their reticulo-endothelial system. In addition, the organs with high blood flow such as kidneys and lungs can be affected.

Hydrogen peroxide generated *in vivo* can react with silver nanoparticles and lead to releasing of Ag^+ ions [16]. In excess, free radicals cause the damage of cellular macromolecules through the oxidation of lipids, proteins, and DNA. Injury of cell membranes results in leakage of cytoplasmic contents and necrosis, whereas rupture of lysosomal membranes can induce apoptosis. In addition, the reactive oxygen species (ROS) can stimulate the inflammation through up-regulation of redox-sensitive transcription factors (nuclear factor kB – NF-kB, activator protein-1 – AP-1), and mitogen-activated protein kinases (MAPK) [15].

Intracellular, nanomaterials may interact with different components, especially with mitochondria and nucleus, considered as main sources of their toxicity. Nanomaterials such as metal nanoparticles, fullerenes, and carbon nanotubes are located in mitochondria and induce apoptosis and ROS formation [15]. The effect on nuclear DNA leads to nuclear damage, cell-cycle arrest, mutagenesis, and apoptosis. The action is due to the diffusion of nanomaterials into the nucleus and formation of ROS, which directly trigger DNA damage and induce chromosomal abnormalities [3]. Silver nanomaterials significantly up-regulate the gene encoding thiore-doxin-interacting protein (Txnip) and determine mitochondria-dependent apoptosis [17]. On the other hand, the oral silver administration did not induce micronucleus formation in rats following 28 days of treatment [18], suggesting lack of short-term toxicity.

It was demonstrated that silver nanoparticles were able to bind to thiol (-SH) groups within proteins and promoted their denaturation [19] including antioxidant enzymes such as superoxide dismutase and glutathione peroxidase. In blood, silver binds to albumin and decreases its ability to transport [20]. Gold nanoparticles can induce genotoxicity and block the transcription due to their ability to bind to DNA [21]. Some nanomaterials can stimulate the up-regulation of nicotinamide adenine dinucleotide phosphate-oxidase (NADPH) and xanthine oxidase in macrophages and neutrophils and generate free radicals. After absorption into the systemic circulation, the nanomaterials interact either with blood components and can lead to hemolysis and thrombosis or with the immune system and produce immunotoxicity.

Cho et al. [22] have shown that PEG-coated gold nanoparticles caused a transient inflammation and induced acute liver influx of neutrophils in parallel with increase of adhesion molecule levels (ICAM-1, E-selectin, and VCAM-1), chemokines, and inflammatory cytokines (IL-1β, IL-6, IL-10, IL-12β, and TNF-α) in liver up to 24 hours. Moreover, Lanone et al. suggested that intermediate metabolites of nanomaterials generated in the liver can contribute to hepatotoxicity [6]. Abdelhalim and Jarrar have shown that gold nanoparticles (10, 20, and 50 nm) administered for 3 or 7 days induced alterations in the hepatocytes, portal triads, and sinusoids. The changes were size-dependent and related with time exposure of nanoparticles and were explained by interaction with proteins, hepatic enzymes, and local antioxidant defense system [23].

4. Assessment of nanomaterials toxicity

As current studies show conflicting results on safety and the biocompatibility of nanomaterials, it is recognized that the validation of analytical methods used to determine toxicity is of major importance. A complete evaluation of nanoparticles for therapeutic use includes thorough physicochemical property characterization, biodistribution, and toxicity evaluation, both *in vitro* and *in vivo* [24]. Transmission electron microscopy (TEM) and dynamic light scattering (DLS) are commonly used techniques to measure the size and shape of nanomaterials in biological systems and to evaluate their aggregation into cells [24, 25]. *In vitro* toxicity will follow the cellular viability, apoptosis and oxidative stress markers, and genotoxicity.

http://dx.doi.org/10.5772/60707

In order to evaluate the acute *in vivo* toxicity of nanomaterials, the Organization for Economic Cooperation and Development (OECD) guidelines recommend oral toxicity test, eye irritation, corrosion and dermal toxicity, and lethal Dose 50 (LD50).

For acute oral toxicity test, the mice receive orally colloidal nanomaterials at the limited dose of 5000 mg/kg body weight (LD_{50}). The animals are observed for toxic symptoms for the first 3 hours and after 24 hours the number of survivors is noted. The animals are maintained and observed daily over 14 days for skin symptoms (edema, erythema, ulcers, bloody scabs, discoloration, and scars) and toxic signs (weight loss, water and food consumption, behavior). At 1, 7, and 10 days after exposure, skin biopsies are performed for histopathological evaluations and blood is taken for biochemical (triglyceride, cholesterol, glucose, glutamic oxaloacetic transaminase (GOT) and glutamic pyruvic transaminase (GPT)) and hematological investigations. All animals are sacrificed after 14 days and skin and liver are collected for routine histopathological examination.

For acute eye irritation and corrosion test the animals are treated with 1.50 ppm and 2.5000 ppm colloidal nanoparticles, respectively [26]. Briefly, 0.1 ml of colloidal suspension was placed in the conjunctival sac of one eye/animal and the other eye serves as a control and is treated with the same volume of distilled water. The animals are observed for toxic symptoms at 1, 12, 24, 48, and 72 hours after administration. The eye reactions of conjunctivae respectively cornea and chemosis are graded as recommended the grading system of OECD 405 guidelines. The animals are maintained and observed daily over 14 days for toxic symptoms.

For acute dermal toxicity test the animals are randomly divided in three groups (n=3) as follows: group 1 receives vehicle (distilled water) and groups 2 and 3, receive 50 and 100.000 ppm of colloidal suspension, respectively. All treated groups received the preceding chemicals at 300µl/cm^2. All animal experiments were performed according to the Organization for Economic Cooperation and Development (OECD) 434 guidelines (acute dermal toxicity-fixed dose procedure) [27]. Briefly, colloidal suspensions are applied to a shaved area of skin, an approximately 4 x 3 cm rectangle, then the area is covered with a dressing and non-irritating tape for 24 hours. After 24 hours of exposure, the dressing is removed and the treated area is gently washed with physiological saline and the number of survivors is noted. The animals are maintained and observed daily over 14 days for skin symptoms (edema, erythema, ulcers, bloody scabs, discoloration, and scars) and toxic signs (weight loss, water and food consumption, behavior). At 1, 3, and 7 days after exposure, skin biopsies are performed for histopathological investigations. All animals were sacrificed after a 14 days observation period and skin is collected for routine histopathological examination.

Maneewatttanapinyo et al. observed in an acute toxicity study of colloidal silver nanoparticles that the oral administration of particles at a limited dose of 5.000 mg/kg produced neither mortality nor acute toxic signs during 14 days. All the hematological and biochemical analysis and the histopathological investigations did not show any differences between the groups examined. The instillation of silver nanoparticles at 5.000 ppm determined a transient eye irritation for 24 hours. The skin application of tested substances did not induce toxicity at the macroscopical and microscopical level [28]. Another study showed that gold nanoparticles functionalized with natural compounds extracted from native plants of the Adoxaceae family

(European cranberrybush – *Viburnum opulus L.* and European black elderberry – *Sambucus nigra L.)* had no toxic effects at the dermal toxicity test [9]. All the parameters evaluated showed no significant changes in hematological, biochemical, and histopathological analyzes.

In addition, it is crucial to appreciate the biodistribution of nanomaterials. For this purpose, the materials are conjugated with a label or organic dye that can be tracked in blood and tissue at different time points. The methods have the disadvantage that the dye can be degraded in time and limits its detection in long-term toxicity studies. In addition, it may interfere with the metabolism of nanomaterials and transformation in intermediate compounds.

Moreover, the analysis of biomarkers of inflammation and oxidative stress would enhance mechanistic studies into nanomaterial toxicity. For the evaluation of chronic toxicity and carcinogenic potential of nanomaterials, the OECD guidelines recommend the administration of substances for 12 and 24 months, respectively. After this period, the survival rate, the clinical toxicity signs, animal behavior, tumor incidences, and histopathological findings in the liver, spleen, kidneys, brain, ovary, and testis will be assessed.

5. *In vivo* toxicity of nanomaterials

5.1. Dendrimers

Dendrimers or cascade polymers represent a heterogenic class of compounds consisting of linear or random-coil polymers such as polyethylene glycol, polylactic acid, polyglycolic acid, dextrin, hyaluronic acid, chitosans, polyglutamic acid, etc. [29]. They have different chain length and molecular weight, different chemical structures, and consequently different *in vivo* behavior (biodistribution, pharmacokinetics, stability, and toxicity). Dendrimers offer many advantages including spherical size, low viscosity, narrow polydispersity, and high density, qualities for which they were used as good vehicles for drug or gene delivery. However, their toxicity has not been systematically investigated.

In systemic circulation, positively charged dendrimers and cationic macromolecules can interact with blood components leading to hemolysis [30], which may induce nephrotoxicity and hepatotoxicity [31]. In fact, dendrimer toxicity is dose and generation dependent and is related to the surface charge, the cationic dendrimers being more toxic than anionic compounds. The toxicity of dendrimers is influenced by the nature of the terminal groups, and the addition of inert polyethylene glycol (PEG) or fatty acids can reduce their toxicity and improve biocompatibility [15].

5.2. Silver nanoparticles

Nanoparticles are defined as particles sized between 1 and 100 nanometers (10^{-7}m) [32]. Silver has been widely used in biomedical applications such as preservatives in cosmetics, textiles, water purification systems, coatings in catheters and wound dressings. In the Woodrow Wilson database of nanotechnology-based products, the most common nanomaterial described is silver [33], thus suggesting an increased risk of its exposure [34].

http://dx.doi.org/10.5772/60707

The properties of silver nanoparticles such as size, shape, surface charge and coating, agglomeration, and dissolution rate are particularly important for their biological interactions. Smaller particles have a larger surface area and, therefore, have a greater toxic potential [34]. The rate of particle dissolution depends on its chemical and surface properties as well as on its size and is further affected by the surrounding media [35]. This process leads to surface oxidation and releasing of cytotoxic silver ions.

Experimental data assigned silver nanostructures remarkably antimicrobial [36, 37], antiviral properties [17] and also antitumor effect [38]. The antimicrobian activity led over the years to the development of silver nanoparticles-based products, including textiles, food storage containers, antiseptic sprays, catheters, and bandages. Therefore, it is necessary to evaluate the adverse reactions associated with multiple ways of exposure to silver nanostructures. Recent *in vivo* studies have shown a reproductive toxicity of silver structures on *Caenorhabditis elegans* and thus draw attention to the toxicity of these compounds [17, 39]. In mice treated orally with different sizes of silver nanoparticles 1 mg/kg body weight for 14 days, small particles in brain, lung, liver, kidneys, and testis were found while large particles were not identified in these tissues [40]. In parallel, the transforming growth factor beta (TGF-β) levels were significantly increased in serum in the same groups. In serum of mice treated repeatedly for 28 days, with different doses of silver nanoparticles, increased levels of IL-1, IL-6, IL-4, IL-10, IL-12, and TGF-β in a dose-dependent manner were found, suggesting that frequent administration may cause organ toxicity and inflammation in mice [40].

Several studies have revealed that silver nanoparticles might induce cytotoxicity in phagocytic cells, macrophages, and monocytic cells, a process mediated by the generation of free radicals and induction of apoptosis. These effects are mediated by the release of silver ions, the liver being the major target organ, followed by the spleen, lungs, and kidneys [17]. In addition, silver nanoparticles can alter the mitochondrial membrane and reduce mitochondrial potential, determine glutathione (GSH) depletion, bind to DNA, and thus cause DNA strand breaks and consequently affect DNA replication [41].

Also, silver nanoparticles induced cytotoxicity and apoptosis on HeLa cells [42], determined cytotoxicty on Raw 264.7 cells [43], HepG2 (human hepatoma cells) [44], and human lung cell line [45]. Cytotoxicity and harmful effects on fish cell lines, embryos, and adult fishes were also induced [46]. On microorganisms as *S. typhimurium* and *E. coli* and cultured mammalian cells (CHO-k1) silver nanoparticles exerted cytotoxic effect without to induce genotoxicity [47].

The effects of silver materials on inflammation have not been fully understood and are rather contradictory. Some studies report an anti-inflammatory effect by suppressing cytokine production while others notice the induction of pro-inflammatory cytokines in different biological systems [48]. Several studies attested that exposure to silver induced the release of proinflammatory markers such as TNF-α, macrophage inflammatory protein*s* (MIPs) and G-CSF from macrophages [48, 49]. The persistence of cytokine production and signaling as response to nanoparticles may lead to inflammatory diseases. Park et al. [40] suggested that silver nanomaterials upon phagocytosis and internalization of silver in lysosomes released silver cytotoxic ions.

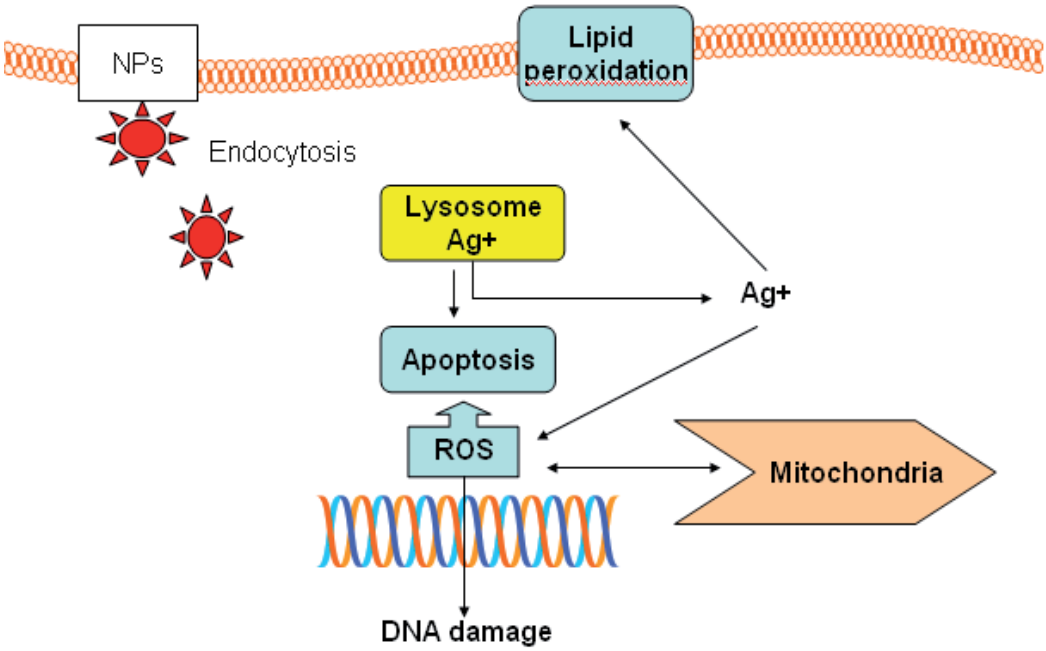

Abbreviations: NPs - nanoparticles; ROS – reactive oxygen species; Ag^{+} - silver ions

Figure 1. Mechanism of silver nanoparticles toxicity

The increased generation and utilization of silver nanoparticles in clinical practice facilitates the human exposure via inhalation and consequently lung toxicity. Takenaka et al. [50] have studied the biodistribution of different concentrations of inhaled silver particles. The particles were identified in the alveolar macrophages and alveolar walls, in the nasal cavity and regional lymph nodes even 7 days after their administration. Low concentrations of silver ions can be measured in the liver, kidneys, spleen, brain, and heart, suggesting translocation from the lung to other tissues. The authors concluded that nanoparticles were rapidly cleared from the lungs as a consequence of their solubilization, especially less agglomerated forms, those with small size.

Hyun et al. [41] have shown that chronic, repeated exposure to small size silver particles increased the mucins production in nasal respiratory mucosa suggesting the importance of mucus in defense against air pollutants. The respiratory exposure for 90 days to silver particles [52] induced an inflammatory response in alveoli and alteration in lung function, independently of the dose used. Sung et al. suggested that nanoparticles were transferred into the blood from the lung and then to the liver, olfactory bulb, brain, and kidneys. However, the data are contradictory because similar studies have not identified toxicities in tissues after exposure to silver nanostructures. Moreover, they could not specify if the silver was identified in tissues as ions or particles. Another study showed that silver nanomaterials had negligible impact on the nasal cavity and lungs [53]. The different results obtained can be explained by the variability of the synthesis methods, their various sizes, concentrations, and time exposures, the

http://dx.doi.org/10.5772/60707

presence or absence of capping agents, and type of experimental design used. Hence, their risks should be assessed on a case-by-case basis and require more extensive investigations.

Extensive use of silver nanoparticles in textiles and wound dressings allows the particle to come into direct contact with the skin and can alter the structure and function of the skin. Most research on dermal exposure to silver were focused on the study of clinical effects and less on systemic toxicity. Therefore, the real consequences of silver nanostructure penetration in skin need to be assessed. Tian et al. [54] have demonstrated, within an experimental model *in vivo*, a better wound-healing ability of silver nanoparticles compared to silver sulfadiazine, standard burn treatment, and compared the combination between amoxicillin and metronidazole. The effects were superior, both from the cosmetic and functionality point of view. In addition, the results suggested that silver nanoparticles exhibited more potent antibacterial activity than other treatments.

According to some studies, silver nanomaterials can induce apoptosis and reduce the level of matrix metalloproteinase in wounds [55], inhibit angiogenesis [56] and vascular permeability through vascular endothelial growth factor (VEGF) and also interleukin (IL)-1β [38].

In patients with burns, treated with Acticoat wound dressings impregnated with silver nanoparticles, biochemical and hematological changes related to silver absorption were not found and so the authors considered these dressings safe to use in clinical practice [57]. Probably, the permeability of silver nanoparticles within normal skin may be influenced by the quality of the skin barrier. Thus, the nanosilver particles get faster deep into the dermis through hair follicles and sweat ducts if the skin barrier is altered [58].

Rahman et al. [59] studied the effect of nanoparticles on gene expression in mouse brain after intraperitoneal injection. They noticed that high doses of silver nanoparticles exerted neurotoxicity in the caudate nucleus, frontal cortex, and hippocampus by inducing oxidative stress and apoptosis. The mechanism involved was related to silver ions released into the brain or indirectly by neural and humoral mediators.

Silver nanomaterials administered orally are converted into their ionic form due to the low pH of the stomach and induce inflammation evidenced by lymphocyte influx and changes in expression of proinflammatory genes. It is not known whether toxicity is due to the accumulation of particles or it is mediated by humoral or neural mediators [60]. After oral ingestion silver was identified in glial cells and neurons, in brain regions such as the hippocampus and pons. The localization in some regions can be explained by local differences in the permeability of the blood-brain barrier and special turnover in brain cells [61].

In conclusion, the successful translation of silver nanotechnology to the clinic requires the development of safe and eco-friendly synthesis of nanomaterials and understanding the mechanisms of their toxicity and safety control.

5.3. Gold nanoparticles

Gold has long been considered a noble metal, bio-inert, stable with some therapeutic values, being used as anti-inflammatory and anti-rheumatic agent in rheumatoid arthritis treatment.

These qualities were observed particularly in the bulk gold. When the size decreases to nanoscale, the material exhibits different properties due to its surface plasmon resonance excitation characteristics [15, 62, 63]. Besides, the gold nanomaterials can become toxic due to the oxidation of elemental gold or solubilization by cyanidation.

There is a great variety of sizes and shapes of synthesized gold nanoparticles: rods, spheres, tubes, wires, ribbons, plate, cubic, hexagonal, triangular, tetrapods, etc. [64, 65]. Generally, gold nanoparticles are synthesized by the chemical reduction of chloroauric acid (HAuCl4) using various reducing agents [66, 67]: citrate ions, hydroquinone, sodium boron tetrahydride (NaBH4), hydroxyl and sugar pyrolysis radicals, microbial enzymes, plant phytochemicals, or microorganisms such as bacteria and yeast cells [68, 69]. It seems that, on one hand, the biological synthesis of gold nanomaterials is more environmentally friendly than chemical synthesis [70, 71]. On the other hand, the green synthesis of nanomaterials has many disadvantages compared to chemical synthesis: poor mono-dispersity, aggregation, and non-uniform shape. These limits can be overcome through diversification and optimization of the synthesis methods. Thus, there are a lot of natural reducing agents and organic ligands such as peptides, proteins, fungus [72] or polymers (PEG) [73], poly-L- lysine (PLL), poly- D- L-lactic-co- glycolic acid (PLGA), and their co- polymers [74] used to prepare nanomaterials in order to stabilize them.

PEG has gained popularity due to amphiphilic and solubility properties [75]. Polysaccharides, such as glycosaminoglycans (GAGs) began to be incorporated onto nanomaterials. Thus, some researchers synthesized hybrid nanospheres using low molecular weight chitosan as reducing and stabilizing agents [76], chitosan and heparin [77], or hyaluronan [78].

However, the results from literature about gold toxicity are quite contradictory and insufficiently documented. Investigation of toxicity mechanisms is important because in the last years gold nanoparticles were extensively used in various medical applications including drug and protein delivery, gene therapy, *in vivo* delivery and targeting, etc.

Generally, the exposure to gold nanomaterials can occur during synthesis and applications by injection or ingestion [79, 80], inhalation, absorption through skin contact, and release from implants [81]. Another source of exposure is their accumulation in the soil or in organisms such as algae and fish consumed by animals and humans [17].

A very much discussed issue is the relationship between the size of nanoparticles and their toxicity. Small size particles are widely used in medical applications because they have the ability to penetrate into cells and transport various drugs without cell injury. These findings were confirmed by Conner et al.'s studies [82] which found that gold nanoparticles of 18 mm in diameter did not induce damage after penetration into the cell. Moreover, Tsoli et al. [83] demonstrated that very small particles (1 mm diameter) could penetrate into nucleus the without inducing DNA injury. Particles with a large ratio between surface area and volume are not able to be internalized within cells and therefore they cannot be used in biomedical applications. These statements are consistent with the results obtained *in vitro* on four cellular lines (fibroblasts, epithelial cells (HeLa), macrophages (J774A1), and melanoma cells (SK-Mel-28) [21] treated with triphenylphosphine stabilized gold nanoparticles. The cellular

http://dx.doi.org/10.5772/60707

response is size-dependent, suggesting that the "larger" particles are non-toxic *in vitro*. Goodman et al. demonstrated the ability of gold nanoparticles to inhibit RNA polymerase activity and block DNA transcription [84].

The influence of gold nanomaterials toxicity is related to their shape. Thus, the rod shape has been reported to be more toxic than its spherical counterparts, both on human keratinocyte cells (HaCaT) [11] as well as human breast adenocarcinoma cell line (MCF-7). The cells treated with nanorods lose the mitochondrial integrity [85], generate free radicals, and stimulate up-regulation of antioxidants, stress response genes, and protein expression [86].

Several reports have noticed that gold nanoparticles caused nephrotoxicity, hemolysis, cytotoxicity and genotoxicity, and size-dependent effects, the smaller size being less toxic than the larger size. Moreover, it has been shown that small particles (10 - 50 nm) dispersed in almost all tissues, mainly in the liver, lungs, spleen, and kidneys, 24 hours post i.v. administration compared to large particles. It has been shown that smaller gold nanoparticles can selectively and irreversibly bind to DNA and cause genotoxicity compared to larger particles [15]. This property can be exploited in cancer therapy because their interaction with DNA tumor cells may lead to cellular death. Thus, Pan et al. have demonstrated that nanoclusters of 0.8, 1.2, and 1.8 nm were four-to six-fold less toxic than nanoclusters of 1.4 nm while larger sizes were not toxic even at high concentrations [21]. Biodistribution of small particles was noticed in almost all tissues 24 hours post i.v. injection compared to larger nanomaterials.

It is possible that gold nanostructures are genotoxic without being cytotoxic and cause alteration of transcription without phenotypic changes [86, 87]. Some reports have revealed that gold nanoparticles with a diameter between 2 and 40 nm are non-toxic on fetal lung fibroblast-like (MRC)-cells while the particles >10 ppm can induce apoptosis and up-regulate the expression of proinflammatory cytokines [88]. Another toxicity mechanism involves oxidative attack on DNA and down-regulation of DNA repair [87]. Inductively coupled plasma mass spectrometry (ICP-MS) studies have shown that lungs, olfactory bulb, spleen, esophagus, tongue, kidney, aorta, heart, septum, and blood are the main tissues that accumulate the gold materials between 30 and 110 nm [89]. The mechanisms of biodistribution are via endocytotic-exocytotic activity and paracellular transport [90]. According to some authors a single nanoparticle has a greater health effect than the agglomerates particles [91]. However this statement was not confirmed in other experiments. The small size facilitates the crossing of the blood-brain barrier and accumulation of gold nanostructures in the brain, placenta, and fetus [92].

Overall, the cellular uptake and toxicity of gold nanoparticles depends not only on the size but also on the surface, functional attachments, and shape [85]. Cationic gold particles were moderately toxic and anionic particles were nontoxic, suggesting the electrostatic binding of the particles to the negatively charged cell membrane and interaction with membrane components as a probable mechanism of toxicity. Kim et al. examined the toxicity of gold nanoparticles (1.3 nm) functionalized with a monolayer of the cationic ligand, N,N,N-trimethylammoniumethanethiol on zebrafish embryos and noticed the occurrence of morphological abnormalities and embryo lethality [93]. The cause of these abnormalities was apoptosis of eye cells and aberrant expression of transcript factors that regulate eye pigmen-

tation development. Other studies showed that 1.4 nm gold nanoparticles capped with triphenylphosphine monosulfonate cause necrosis via the oxidative stress and mitochondrial damage [21], while PEG used to functionalize the 3.7 nm nanoparticles were non toxic on human cervical cancer (HeLa) [92]. The chitosan conjugated gold nanoparticles can transverse the cell membrane of Chinese hamster ovary cells by endocytosis without inducing cell death. Moreover, the authors revealed that >85% of the cells were viable after a long period of exposure [93] suggesting that these nanostructures can be used in cellular imaging and photothermal therapy.

To prevent this problem, researchers have conjugated these nanoparticles with various biomolecules and ligands. Thus, gold nanorods conjugated with PEG or citric acid ligands were less toxic than spherical particles. Surface charges measured by zeta potential determine the properties and functions of nanoparticles. Thus, the gold nanoparticles can promote protein refolding through electrostatic interactions, a mechanism used to refold proteins in a chemical denatured state [94]. In contrast to the silver nanoparticles, silver - gold nanoparticles induced the activation of cells due to the release of ions in the medium [95]. However, more studies are critically needed to establish exactly the potential toxicity of gold nanoparticles to fully evaluate gold nanoparticles for *in vivo* use.

5.4. Carbon nanotubes

5.4.1. The importance of studying carbon nanotube toxicity

An important class of nanomaterials is represented by carbon nanotubes (CNTs). They are cylindrical structures composed of a variable number of layers, each layer being formed of carbon atoms. Their diameter and length are variable, but, according to the number of layers, CNTs can be classified as single-walled (SWCNTs) and multi-walled (MWCNTs). SWCNTs have unique properties, including electrical, mechanical, and thermal particularities, which recommend them for particular applications in the field of electronics, as well as in the biomedical industries. In the meantime, MWCNTs, with a larger diameter, have a great potential to be used as targeted carriers for different substances into cells in medical applications. However, the concern regarding the safety of CNTs for the human body is constantly rising, because of at least two reasons. First of all, there is an increase in the production of CNTs for technological applications, which raises the risk of accidental exposure of the workers during the technological manipulation of the nanomaterial. CNT-based products are already being used in textiles, sport products, microelectronics, and energy storage [98]. On the other hand, for the medical applications, the administration of CNTs is required, and their faith in the human body, along with their interactions with different tissues, become of vital importance, for example, CNTs conjugated to siRNA for cancer therapy or CNTs for the imaging of colorectal cancer that may enter clinical trials in the next years [98].

Also, the environmental risk of CNTs, including even their interactions with some classical contaminants, such as pesticides, must be taken into consideration. There are studies indicating that CNTs could act as pesticide carriers, enhancing pesticide ecotoxicity, and affecting fish behavior, metabolism, and survival [99].

http://dx.doi.org/10.5772/60707

In the meantime, CNTs released into the aquatic medium, in high concentration, exert developmental toxicity, with increased mortality and malformation. The exposure to functionalized SWCNTs in the early stages of the life of rare minnow (*Gobiocypris rarus*) altered the activities of antioxidant enzymes, such as superoxide dismutase (SOD), catalase (CAT), and glutathione S-transferase and determined reactive oxygen species (ROS) generation and DNA damage [100].

5.4.2. Mechanisms of CNTs' toxicity

Until today, the environmental effects and the toxicity of nanomaterials to organisms are not entirely understood. In order to evaluate these effects, the methods should be cost-effective, rapid toxicity assays should be available, and the tests should be performed with minimal amounts of materials. Drosophila could be such an efficient and cost-effective model organism, which allows tissue-specific nanomaterial assessment through direct microtransfer into target tissues. SWCNTs and MWCNTs were evaluated for their toxicity using this new method of assessment [101].

To date, the studies performed *in vitro* and *in vivo* in order to evaluate the toxicological effects of CNTs have pointed out oxidative stress and inflammation as major mechanisms involved in their toxicity. These two mechanisms influence each other [102]. ROS generation produces lipid peroxidation, protein alteration, and intracellular GSH depletion [103]. Oxidized proteins gain chemically reactive groups and become new agents that can prolong the initial effects of ROS [104]. The next step is NF-kB activation, which in return, will regulate the expression of pro-inflammatory cytokines, such as TNF-α and IL-1β [103]. Also, NF-kB up-regulates the activation of superoxide dismutase [105].

MWCNTs can activate NADPH oxidase, as demonstrated in human macrophages [106] and in the spleen [107]. In the meantime, it was proven that carboxylated MWCNTs can bind to Cu/Zn SOD and the microenvironment of the amino acid residues in the enzyme was slightly changed [108]. MWCNTs inhibit the activity of catalase (CAT). They contribute both to the conformational changes of CAT and to enzyme dysfunction. Also, both in animals and cell cultures, a single-dose exposure to CNTs determines elevated levels of DNA damage [109].

In the past years, a few steps were made in order to understand the deep mechanisms involved in CNT toxicity. For example, for the biological functions, the protein-protein interactions or the protein-protein recognition are essential. It was proven that a graphene sheet can interrupt the hydrophobic interaction between two functional proteins and can disrupt the metabolism of the cell, leading to cell death [110].

For a typical type of CNT, the carbon nanohorns (CNHs), it was proven that they can accumulate in the lysosomes and can induce lysosomal membrane permeabilization. The consequence was the release of lysosomal enzymes, such as cathepsins, with the subsequent mitochondrial dysfunction and generation of ROS in the mitochondria. In return, ROS amplified the mitochondrial dysfunction and led to the activation of caspases followed by cell apoptosis [111].

Unmodified SWCNT aggregates are capable of suppressing the antigen-induced signaling pathways and pro-inflammatory degranulation responses in mast cells. The capacity of SWCNTs to suppress mast cells pro-inflammatory function is explained by remodeling the plasma membrane, with the disaggregation of the cortical actin cytoskeleton and the relocalization of clathrin [112].

In the meantime, embedded SWCNTs nanoparticles in plasma membrane induce cellular calcium outflow alteration [113].

The toxicity of MWCNTs has been evaluated lately at gene level. MWCNTs have microRNA (miRNA) targets, as shown in an *in vivo* Caenorhabditis elegans assay system [114].

CNTs can also determine the perturbation of immune functions in animal models. Different studies had contradictory results, showing that CNTs have, by themselves, either pro-inflammatory or immunosuppressive functions, locally and systematically. When exposed to CNTs, the immortalized airway epithelial cells showed reduced viability, impaired proliferation, and elevated ROS generation and lack of internalization of targets in macrophage cell lines [115].

CNTs can produce anomalies in multicellular behavior, due to ROS generation. In fact this effect is produced by the loss of multicellular chirality, including a decreased migration rate and loss of directional alignment on micropatterned surfaces. The cell chirality is in fact a cellular property important for embriogenic morphogenesis [116].

5.4.3. The impact of different parameters upon CNT cytotoxicity

CNT toxicity is influenced by a variety of parameters, depending both on the physicochemical properties of the material itself and on the environmental variables. The shape, length, diameter, number of layers, surface coating and functionalization, impurities content, the dose, route of administration, and type of dispersion media are just a few of these variables.

CNTs diameter and length influence cell aggregation, ROS generation, and injury extent, the effects depending on the cell type too [117]. For example, long and thick rather than short and thin MWCNTs can induce inflammatory effects [118] as well as those with a larger diameter [119]. When comparing the effects of long and rigid versus shorter and agglomerated MWCNTs at pulmonary level, the long MWCNTs induced a more pronounced pro-fibrotic, inflammatory, and apoptotic response [120].

When comparing the type of functionalization, MWCNTs functionalized with carboxylation and raw MWCNTs can induce oxidative stress and inflammation in macrophages, with the activation of MAPK and NF-kB signaling pathways, up-regulation of IL-1β, IL-6, TNF-α, and iNOs and subsequent cell death. MWCNTs functionalized with polyethylene glycol did not exert the same toxic effects [121].

When testing pristine MWCNTs and MWCNTs functionalized by hydroxylation-oxygenation, amination or carboxylation on human bronchial epithelial cells or on the nematode Caenorhabditis elegans, the results showed that carboxylated MWCNTs were the most cytotoxic and

genotoxic, but with no differences in survival following exposure, proving that surface functionalization can influence the bioactivity of MWCNTs [122].

The exposure of human monocyte-derived macrophages to long rigid MWCNTs elicited a response similar to the exposure to asbestos, in contrast to long-tangled MWCNTs, which induced a weaker protein secretion. The exposure determined lysosomal damage, but only long rigid MWCNTs determined apoptosis [123].

There are results sustaining that the contaminating metals for CNTs are responsible for their toxicity. However, long needle-like MWCNTs without metal impurities are capable of inducing the production of major proinflammatory cytokine IL-1β via the Nod-like receptor pyrin domain containing 3 (NLRP3) flammasome-mediated mechanisms [124].

Also, the dispersion medium can influence the ability of CNTs to bind to proteins and to exert specific biologic effects. For example, SWCNTs and double-walled nanotubes were dispersed in phosphate-buffered saline (PBS) or in bovine serum albumin (BSA). In BSA, CNTs were more stable, the aggregation was reduced, and the levels of IL-6 were increased, while the TNF-α production was decreased, as compared to the same samples, but without BSA [125].

In the meantime, the biotransformation of CNTs in organism is important when evaluating their toxicity. It seems that manganese peroxidase is capable of transforming the SWCNTs, but not oxidized SWCNTs, making the biodegradation of these compounds difficult [126].

5.4.4. Animal models for toxicity evaluation

CNTs from the environment can be a challenge for the respiratory and gastrointestinal mucosa as well as for the dermal system. For medical applications, the systemic administration of CNTs, s.c., i.p., or i.v., is important. Taking these possibilities into consideration, different models for the assessment of CNT toxicity *in vivo* were used. In the meantime, a short-term or a long-term exposure to CNTs can be evaluated.

5.4.4.1. Short-term evaluation

Pharyngeal aspiration of purified SWCNTs in mice determined, in a dose-dependent manner, inflammation, fibrosis, granulomatous pneumonia, and decrease in pulmonary function. The inhalation of nonpurified SWCNTs for 4 days also determined inflammatory response, oxidative stress, collagen deposition, and mutations of k-ras gene locus in the lung of mice [127].

Twenty-four hours after the intratracheal administration of pristine SWCNTs, acute inflammation was present in the lungs of mice, along with apoptosis through mitochondrial dysfunction and ROS generation [128]. When comparing the effects of MWCNTs on male Sprague-Dawley rats after intratracheal instillation or inhalation administered in different doses, for different periods of time and with different physicochemical characteristics, including functionalization, the results showed that MWCNTs produce inflammation in the lung, but transitory, despite the persistence of CNTs in the lung. The functionalization and the suspension media influenced the pulmonary response after MWCNTs administration [129].

When female mice were exposed to MWCNTs by pharyngeal aspiration technique 4 weeks after the previous exposure to cigarette smoke, it was proven that MWCNTs induced pulmonary toxicity, with a minor role in cigarette smoke exposure [130].

For a follow-up of 6 days after a single dose i.p. administration, transient oxidative stress and inflammation in blood and liver were obtained both for SWCNTs and MWCNTs functionalized with single-stranded DNA [102, 131]. Also, after i.p. administration, MWCNTs translocate in the spleen and determine oxidative stress, inflammation, lymphoid hyperplasia, and increase in the number of cells that undergo apoptosis [132].

5.4.4.2. Long-term evaluation

MWCNTs with different length and iron content were administered by intratracheal instillation to spontaneously hypertensive rats. Seven days and 30 days post exposure, lung inflammation was found, along with increased blood pressure, lesions in abdominal arteries,and accumulation of CNTs in liver, kidneys, and spleen [133].

SWCNTs administered through single intratracheal instillation in rats determined up-regulation of the genes involved in the inflammatory response, with a pattern that is time-dependent, until 180 days, 365 days, and 754 days post-exposure [134].

MWCNTs administered through transtracheal intrapulmonary spraying for 24 weeks translocated into the pleural cavity and induced inflammatory reactions, fibrosis and parietal mesothelial proliferation lesions, the effects being more important for the larger-sized MWCNTs, than for the smaller-sized [135].

Thirteen weeks exposure of rats to MWCNTs by whole-body inhalation, in different doses, determined increased expression of inflammatory cytokines in splenic macrophages, including IL-1β, IL-6, and IL-10. The expression of IL-2 in T lymphocytes was decreased, being a possible cause of reduction in the rats' anti-tumor responses [136]. In the meantime, in a similar experimental model, 0.2 mg MWCNTs/m^3 was established as the lowest dose for the occurrence of lung adverse effects, including inflammation and granulomatous changes [137]. Inhalation exposure of rats to MWCNTs for 28 days determined lung deposits even 90 days post-exposure, especially for short-length MWCNTs, emphasizing their potential to induce genotoxicity [138].

Ma Hock et al. (2009) proved that long-term (13 weeks) exposure of rats to SWCNTs or MWCNTs by inhalation did not produce systemic organ toxicity, for a follow-up period of 90 days post-exposure, even though local pulmonary effects were present. Fibrosis changes were absent [139].

5.4.5. Means to reduce toxicity

A few ways to reduce CNT toxicity are represented by the functionalization, surface coating, and stimulation of the autophagic flux. For example, the amino functionalization can reduce the CNT toxicity to the cells [140], as well as albumin coating for SWCNTs [141]. Also, the

toxicity of carboxylated MWCNTs can be reduced by the stimulation of the autophagic flux, with the extracellular release of the nanomaterial in autophagic microvesicles [142].

6. Perspectives

The extent of use of nanomaterials is currently growing and thus efficient screening methods for toxicity are needed to lower the expenses of testing and to reduce the cost of using. Nanomaterial size, shape, surface chemistry, and degree of aggregation are key factors that influence the toxicity. Generally, the *in vivo* toxicity studies can provide sufficient data in order to understand the absorption, distribution, metabolism, and excretion of nanomaterials. In order to fully evaluate their toxicity, acute and long-term toxicity studies are needed along with the examination of chronic exposure. *In vitro* studies may contribute in addition to explain the mechanisms involved in their toxic effects. However, not all the aspects involved in the use of nanomaterials are fully understood. Therefore, finding the appropriate methods for analysis and carefully designed experiments will contribute to the better understanding of the mechanisms of toxicity, so that nanomaterials could be safely used in biology and medicine.

Acknowledgements

This work was supported by the Ministry of Education, Research, Youth and Sports, Romania as part of research project no. 147/2012 PN-II-PT-PCCA-2011-3-1-0914.

Author details

Simona Clichici* and Adriana Filip

*Address all correspondence to: simonaclichici@yahoo.com

Department of Physiology, "Iuliu Haţieganu" University of Medicine and Pharmacy, Cluj-Napoca, Romania

References

[1] De Jong WH, Borm PJA: Drug delivery and nanoparticles: applications and hazards. Int. J. Nanomedicine 2008;3:133–149.

[2] Papp T, Schiffmann D, Weiss D, Castranova V, Vallyathan V, Rahman Q: Human health implications of nanomaterial exposure. Nanotoxicology 2008;2:9–27.

[3] AshaRani PV, Mun GLK, Hande MP, Valiyaveetti S: Cytotoxicity and genotoxicity of silver nanoparticles in human cells. ACS Nano 2009; 3: 279–290.

[4] Stern ST, McNeil SE: Nanotechnology safety concerns revisited. Toxicol Sci 2008; 101:4–21.

[5] Rejman J, Oberle V, Zuhorn IS, Hoekstra D: Size-dependent internalization of particles via the pathways of clarthrin- and caveolae-mediated endocytosis. Biochem. J 2004; 377:159–169.

[6] Lanone S, Boczkowski J: Biomedical applications and potential health risks of nanomaterials: molecular mechanisms. Curr. Mol. Med 2006; 6: 651–663.

[7] Nel A, Xia T, Mädler L, Li N: Toxic potential of materials at the nanolevel. Science 2006; 311:622–627.

[8] David L, Moldovan B, Vulcu A, Olenic L, Perde-Schrepler M, Fischer-Fodor E, Florea A, Crisan M, Chiorean I, Clichici S, Filip A: Green synthesis, characterization and anti-inflammatory activity ofsilver nanoparticles using European black elderberry fruits extract. Colloids Surf B Biointerfaces 2014; 122: 767-77.

[9] Crisan M, David L, Moldovan B, Vulcu A, Dreve S, Perde-Schrepler M, Tatomir C, Filip A, Bolfa P, Achim M, Ciorean I, Kacso I, Berghian Grosan C, Olenic L: New nanomaterials for the improvement of psoriatic lesions. J. Mater. Chem, B 2013; 1: 3152-3158.

[10] Champion JA, Mitragotri S: Shape induced inhibition of phagocytosis of polymer particles. Pharm Res 2009; 26:244–249.

[11] Chithrani BD, Ghazani AA, Chan WCW: Determining the size and shape dependence of gold nanoparticle uptake into mammalian cells. Nano Lett 2006; 6:662–668.

[12] Wang S, Lu W, Tovmachenko O, Rai US, Yu H, Ray PC: Challenge in understanding size and shape dependent toxicity of gold nanomaterials in human skin keratinocytes. Chem. Phys. Lett 2008; 463:145–149.

[13] Niidome T, Yamagata M, Okamoto Y, Akiyama Y, Takahashi H, Kawano T, Katayama Y, Niidome Y: PEG-modified gold nanorods with a stealth character in in vivo applications. J. Control. Release 2006; 114:343–347.

[14] Chang YN, Zhang M, Xia L, Zhang J, Xing G: The toxic effects and mechanisms of CuO and ZnO nanoparticles. Materials 2012; 5: 2850–2871.

[15] Aillon KL, Xie Y, El-Gendy N, Berkland CJ, Forrest ML: Effects of nanomaterial physicochemical properties on *in vivo* toxicity. Adv Drug Deliv Rev 2009; 61(6): 457–466. doi:10.1016/j.addr.2009.03.010

[16] Singh RP and Ramarao P: Cellular uptake, intracellular trafficking and cytotoxicity of silver nanoparticles. Toxicol. Lett. 2012; 213: 249–259.

[17] Wei L, Lu J, Xu H, Patel A, Chen ZS, Chen G: Silver nanoparticles: synthesis, properties, and therapeutic applications Drug Discovery Today 2015; http://dx.doi.org/10.1016/.drudis.2014.11.014

[18] Kim YS, Kim JS, Cho HS, Rga DS, Kim JM, Park JD, Choi BS, Lim R, Chang HK, Chung YH, Kwon H, Jeong J, Han BS, Yu J: Twenty-eight-day oral toxicity, genotoxicity, and gender-related tissue distribution of silver nanoparticles in Sprague–Dawley rats. Inhalation Toxicol 2008; 20: 75–583.

[19] Chen X and Schluesener HJ: Nano-silver: A nanoproduct in medical application. Toxicol Lett 2008; 176: 1-12.

[20] Wadhera A and Fung M: Systemic argyria associated with ingestion of colloidal silver. Dermatol Online J 2005; 11: 12. Available at http://dermatology. cdlib.org.

[21] Pan Y, Neuss S, Leifert A, Fischler M, Wen F, Simon U, Schmid G, Brandau W, Jahnen-Dechent W: Size dependent cytotoxicity of gold nanoparticles. Small 2007; 3: 1941.

[22] Cho WS, Cho M, Jeong J, Choi M, Cho HY, Kim BSH, Kim HO, Lim YT, Jeong BHC: Acute toxicity and pharmacokinetics of 13 nm-sized PEG-coated gold nanoparticles, *Toxicol and* Appl Pharmacol 2009; 236: 16–24.

[23] Abdelhalim MAK and Jarrar BM: Gold nanoparticles administration induced prominent inflammatory, central vein intima disruption, fatty change and Kupffer cells hyperplasia. Lipids in Health and Disease 2011; 10, 133. doi:10.1186/1476-511X-10-133.

[24] Hall JB, Dobrovolskaia MA, Patri AK, McNeil SE: Characterization of nanoparticles for therapeutics. Nanomedicine 2007; 2:789–803.

[25] Powers KW, Palazuelos M, Moudgil BM, Roberts SM: Characterization of the size, shape, and state of dispersion of nanoparticles for toxicological studies. Nanotoxicology 2007; 1:42–51.

[26] OECD 2002. Test guideline 405. Acute eye irritation and corrosion. In: OECD guidelines for the testing of chemicals Paris. France: Organization for Economic Cooperation and Development. Organization for Economic Cooperation and Development (OECD).

[27] OECD 2004. Test guideline 434. Acute dermal toxicity-fixed dose procedure. *In:* OECD guidelines for the testing of chemicals, Paris, France: Organization for Economic Cooperation and Development (OECD).

[28] Maneewatttanapinyo P, Banlunara W, Thammacharoen C, Ekgasit S, Kaewamatawong T: An evaluation of acute toxicity of colloidal silver nanoparticles. J. Vet. Med. Sci 2011; 73(11): 1417-1423.

[29] Duncan R and Izzo L: Dendrimer biocompatibility and toxicity. Adv. Drug Deliv. Rev 2005; 57:2215–2237.

[30] Malik N, Wiwattanapatapee R, Klopsch R, Lorenz K, Frey H, Weener JW, Meijer EW, Paulus W, Duncan R: Dendrimers: Relationship between structure and biocompatibility in vitro, and preliminary studies on the biodistribution of I-125-labelled polyamidoamine dendrimers in vivo. J. Control. Release 2000; 65:133–148.

[31] Neerman MF, Zhang W, Parrish AR, Simanek EE: In vitro and in vivo evaluation of a melamine dendrimer as a vehicle for drug delivery. Int. J. Pharm 2004; 281:129–132.

[32] Granqvist CG, Buhrman RA, Wyns J, Sievers AJ: Far-infrared absorption in ultrafine Al particles. Phys Rev Lett 1976, 37(10):625–629.

[33] http://www.nanotechproject.org/ inventories/consumer/analysis and draft/

[34] Johnston HJ, Hutchison G, Christensen FM, Peters S, Hankin S, Stone V: A review of the in vivo and in vitro toxicity of silver and gold particulates: particle attributes and biological mechanisms responsible for the observed toxicity. Crit. Rev. Toxicol 2010; 40: 328–346.

[35] Misra SK, Dybowska A, Berhanu D, Luoma SN, Valsami-Jones E: The complexity of nanoparticle dissolution and its importance in nanotoxicological studies. Sci. Total Environ 2012; 38: 225–232.

[36] Shahverdi AR, Fakhimi A, Shahverdi HR, Minaian S: Synthesis and effect of silver nanoparticles on the antibacterial activity of different antibiotics against Staphylococcus aureus and Escherichia coli. Nanomedicine 2009; 3: 168-171.

[37] Kim JS, Kuk E, Yu KN, Kim, JH, Park SJ, Lee HJ, Kim SH, Park YK, Park YH, Hwang CY, et al.: Antimicrobial effects of silver nanoparticles. Nanomedicine 2007; 3: 95–101.

[38] Rutberg FG, Dubina MV, Kolikov VA Moiseenko FV, Ignat'eva EV, Volkov NM, Snetov VN, Stogov Y: Effect of silver oxide nanoparticles on tumor growth in vivo. Dokl. Biochem. Biophys 2008; 421: 191-193.

[39] Roh JY, Sim SJ, Yi J, Park K, Chung KH, Ryu DY, Choi J: Ecotoxicity of silver nanoparticles on the soil nematode Caenorhabditis elegans using functional ecotoxicogenomics. Environ Sci Technol 2009; 15; 43(10):3933-40.

[40] Park EJ, Bae E, Yi J, Kim Y, Choi K, Lee SH, Yoon J, Lee BC, Park K: Repeated dose toxicity and inflammatory responses in mice by oral administration of silver nanoparticles. Environ. Toxicol. And Pharmacol 2010; 10: 162-168.

[41] Guo D, Zhu L, Huang Z, et al.: Anti-leukemia activity of PVP-coated silver nanoparticles via generation of reactive oxygen species and release of silver ions. Biomaterials 2013; 34: 7884–7894.

[42] Miura N and Shinohara Y: Cytotoxic effect and apoptosis induction by silver nanoparticles in HeLa cells. Biochem. Biophys. Res. Common 2009; 390 (3): 733-737.

[43] Park EJ, Yi J, Kim Y, Choi K, Park K: Silver nanoparticles induce cytotoxicity by a Trojan horse mechanism. Toxicol. In Vitro 2010; 24 (3): 872-878.

[44] Kawata K, Osawa M, Okabe S: In vitro toxicity of silver nanoparticles at noncytotoxic doses to HepG2 human hepatoma cells. Environ Sci Technol 2009; 43: 6046–6051.

[45] Foldbjerg R, Dang DA, Autrup H: Cytotoxicity and genotoxicity of silver nanoparticles in the human lung cancer cell line, A549. Archives Toxicol 2010; 85:743–750.

[46] Wise JPSr, Goodale BC, Wise SS, Craig GA, Pongan AF, et al.: Silver nanospheres are cytotoxic and genotoxic to fish cells. Aquatic Toxicol 2010; 97: 34–41.

[47] Kim JS, Song KS, Sung JH, Ryu HR, Choi BG, Cho HS, Lee JK, Yu IJ: Genotoxicity, acute oral and dermal toxicity, eye, and dermal irritation and corrosion and skin sensitization evaluation of silver nanoparticles. Nanotoxicology Early online, 2010; 1-8.

[48] Park MVDZ, Neigh AM, Jolanda PV, Fonteyne DL, Verharen HW, Briede JJ, Loveren HV, Jong WH: The effect of particle size on the cytotoxicity, inflammation, developmental toxicity and genotoxicity of silver nanoparticles. Biomaterials 2011; 32: 9810-9817.

[49] Nishanth RP, Jyotsna RG, Schlager JJ, Hussain SM, Reddanna R: Inflammatory responses of RAW 264.7 macrophages upon exposure to nanoparticles: role of ROS-NF-kB signaling pathway. Nanotoxicology 2011; 5(4):502-16.

[50] Takenaka S, Karg E, Roth C, Schulz H, Ziesenis A, Heinzmann U, Schramel P, Heyder J: Pulmonary and systemic distribution of inhaled ultrafine silver particles in rats. Environ Health Perspect 2001; 109:547–551.

[51] Hyun JS, Lee BS, Ryu HY, Sung JH, Chung KH, Yu IJ: Effects of repeated silver nanoparticles exposure on the histological structure and mucins of nasal respiratory mucosa in rats. Toxicol Lett 2008; 182:24–28.

[52] Sung JH, Ji JH, Park JD, Yoon JU, Kim DS, Jeon KS, Song MY, Jeong J, Han BS, Han JH, Chung YH, Chang HK, Lee JH, Cho MH, Kelman BJ, Yu IJ: Subchronic inhalation toxicity of silver nanoparticles. Toxicol Sci 2009; 108:452–461.

[53] Lee HY, Choi YJ, Jung EJ, Yin HQ, Kwon JT, Kim JE, et al.: Genomics-based screening of differentially expressed genes in the brains of mice exposed to silver nanoparticles via inhalation. J. Nanopart. Res 2009; 12: 1567–1578.

[54] Tian J, Wong KK, Ho CM, Lok CN, Yu WY, Che CM, Chiu JF, Tam PK: Topical delivery of silver nanoparticles promotes wound healing. Chem Med Chem 2007; 2:129–136.

[55] Warriner R, Burrell B: Infection and the chronic wound: a focus on silver, Adv. Skin. Wound Care 2005; 18(1): 2-12.

[56] Kalishwaralal K, Barathmanikanth S, Pandian SRK, Deepak V, Gurunathan S: Silver nano - a trove for retinal therapies. J. Control Release 2010; 145(2): 76-90.

[57] Vlachou E, Chipp E, Shale E, Wilson YT, Papini R, Moiemen NS: The safety of nanocrystalline silver dressings on burns: A study of systemic silver absorption. Burns 2007; 33:979–985.

[58] Hoet PHM, Bruske-Hohlfeld I, Salata OV: Nanoparticles—Known and unknown health effects. J Nanobiotechnol 2004; 2:12.

[59] Rahman MF, Wang J, Patterson TA, Saini UT, Robinson BL, Newport GD, Murdock R. C, Schlager JJ, Hussain SM, Ali SF: Expression of genes related to oxidative stress in the mouse brain after exposure to silver-25 nanoparticles. Toxicol Lett 2009; 187:15–21.

[60] Cha K, Hong HW, Choi YG, Lee MJ, Park JH, Chae HK, Ryu G, Myung H: Comparison of acute responses of mice livers to short-term exposure to nano-sized or micro-sized silver particles. Biotechnol Lett 2008; 30:1893–1899.

[61] Rungby J and Danscher G: Localization of exogenous silver in brain and spinal cord of silver exposed rats. Acta Europathol 1983; 60: 92–98.

[62] Marsich E, Travan A, Donati I, Luca AD, Benincasa M, Crosera M, Paoletti: Biological response of hydrogels embedding gold nanoparticles. Colloids and SurfaceB: Biointerfaces 2011; 83: 331-339.

[63] Jenkins JT, Halaney DL, Sokolov KV, Ma LL, Shipley HJ, Mahajan S, Louden CL, Asmis R, Milner TE, Johnsons KP, Feldman MD: Excretion and toxicity of gold–iron nanoparticles. Materials Science and Engineering C 2013; 33(1): 550–556.

[64] Wu HY, Liu M, and Huang MH: Direct synthesis of branched gold nanocrystals and their transformation into spherical nanoparticles. J. Phys. Chem. B 2006; 110: 19291-19294.

[65] Ghosh P, Han G, De M, Kim CK, Rotello VM: Gold nanoparticles in delivery applications. Advanced Drug Delivery Reviews 2008; 60: 1307–1315.

[66] Krause RWM, Mamba BB, Malefetse TJ, Bambo FM, Malefetse TJ: Cyclodectrins: Chemistry and Physics. ISBN: Chapter 9 cyclodextri polymers: Synthesis and application in water treatment. Editor. JIe Hu: Transworld Research Network, Kerala. India. 2010; 185-209.

[67] Lu X, Tuan HY, Korgelc BA, and Xia Y: Facile synthesis of gold Nanoparticles with narrow size distribution by using AuCl or AuBr as the precursor. Chemistry 2008; 14(5): 1584–1591.

[68] Prathna TC, Mathew L, Chandrasekaran N, Raichur AM, Mukherjee A: Biomimetic Synthesis of Nanoparticles: Science, Technology & Applicability.School of Bio Sciences & Technology, VIT University, Department of Materials Eng., Indian Institute of Science. India.www.intechopen.com, 2013.

[69] Chauhan A, Zubair S, Tufail S, Sherwani A, Sajid M, Raman SC, Azam A, Owais M: Fungusmediated biological synthesis of gold nanoparticles: potential in detection of liver cancer. Int J Nanomedicine 2011; 6: 2305 – 2319.

[70] Srivastava SK, Yamada R, i Ogino C, Kondo A: Biogenic synthesis and characterization of gold nanoparticles by Escherichia coli K12 and its heterogeneous catalysis in degradation of 4-nitrophenol. Nanoscale Research Letters 2013; 8:70.

[71] Narayanan KB, Sakthivel N: Biological synthesis of metal nanoparticles by microbes. Adv Colloid Interface Sci.2010; 156:1–13.

[72] Mukherjee P, Ahmad A, Mandal D, Senapati S, Sainkar SR, Khan MI, Ramani R, Parischa R, Ajayakumar PV, Alam M, Sastry M, Kumar R: Bioreduction of AuCl4- ions by the fungus *Verticillum* species and surface trapping of gold nqanoparticles formed. Angew. Chem. Int. Ed 2001; 40:3585–3588.

[73] Pillay J, Ozoemena KI, Tshikhudo RT, Moutloali RM: Monolayer-Protected Clusters of Gold Nanoparticles: Impacts of Stabilizing Ligands on the Heterogeneous Electron Transfer Dynamics and Voltammetric Detection. Langmuir 2010; 26(11): 9061–9068.

[74] Zhang XD, Wu HY, Wu D, Wang YY, Chang JH, Zhai ZB, Meng AM, Liu PX, Zhang LA, Fan FY: Toxicologic effects of gold nanoparticles in vivo by different administration routes. Int. J. of Nanomed 2010; 5: 771–781.

[75] Pissuwan D, Niidome T, Cortie MB : The forthcoming applications of gold nanoparticles in drug and gene delivery systems. Journal of Controlled Release 2011; 149(1): 65-71.

[76] Guo, R. Zhang, L. Zhu, Z. Jiang X: Direct facile approach to the fabrication of chitosan-gold hybrid nanospheres. Langmuir 2008; 24(7): 3459-3464.

[77] Huang H and Yang X: Synthesis of polysaccharide-stabilized gold and silver nanoparticles: A green method. Carbohydr Res 2004; 339: 2627-2631.

[78] Kemp M, Kumar A, Mousa S, Park TJ, Ajayan P, Kubotera N, Mousa SA, Linhardt R.J: Synthesis of gold and silver nanoparticles stabilized with glycosaminoglycans having distinctive biological activities. Biomacromolecules 2009; 10 (3): 589-595.

[79] Lewinski N, Colvin V, Drezek R: Cytotoxicity of nanoparticles. Small 2008; 4(1): 26-49.

[80] Yah CS, Iyuke SE, Simate GS: Nanoparticles toxicity and their routes of exposures. PJPS 2012; 25(2): 477-491.

[81] Byrne HJ, Lynch I, De Jong WH, Kreyling WG, Loft S, Park MVDZ, Riediker M, Warheit D: Protocols for assessment of biological hazards of engineered nanomaterials. The European Network on the Health and Environmental Impact of Nanomaterials 2010;1-30.

[82] Connor EE, Mwamuka J, Gole A, Murphy CJ, Wyatt MD: Gold nanoparticlesv are taken up by human cells but do not cause acute cytotoxicity. Small 2005;1: 325–327.

[83] Tsoli M, Kuhn H, Brandau W, Esche H, Schmid G: Cellular Uptake and Toxicity of Au55 Clusters. Small 2005; 1(8-9): 841–844.

[84] Goodman CM, Chari NS, Han G, Hong R, Ghosh P, Rotello, VM: DNA binding by functionalized gold anoparticles: mechanism and structural requirements. Chem Biol Drug Des 2006; 67: 297–304.

[85] Qiu Y, Liu Y, Wang L, Xu L, Ba R, Ji Y, Wu X, Zhao Y, Chen C: Surface chemistry and aspect ratio mediated cellular uptake of Au nanorods. Biomaterials 2010; 31(30): 7606–7619.

[86] Li JJ, Hartono D, Ong CN, Bay BH, Yung LYL: Autophagy and oxidative stress associated with gold nanoparticles. Biomaterials 2010; 31: 5996-6003.

[87] Coradeghini R, Gioria S, García CP, Nativo P, Franchini F, Gilliland D, Ponti J, Rossi F: Size dependent toxicity and cell interaction mechanisms of gold nanoparticles on mouse fibroblasts. Toxicology Letters 2013; 217(3): 205–216.

[88] Yen HJ, Hsu SH, Tsai CL: Cytotoxicity and immunological response of gold and silver nanoparticles of different sizes. Small 2009; 5(13):1553-61.

[89] Yu LE, Yung LYL, Ong CN, Tan YL, Balasubramaniam KS Hartono D, Shu G, Wenk MR, Ong WY: Translocation and effects of gold nanoparticles after inhalation exposure in rats. Nanotoxicology 2007; 1(3), 235 – 242.

[90] Sadauskas E, Jacobsen NR, Danscher G, Stoltenberg M, Vogel U, Larsen A, Kreyling W, Wallin H: Biodistribution of gold nanoparticles in mouse lung following intratracheal instillation. Chemistry Central Journal 2009; 3:16.

[91] Gosens I, Post JA, de la Fonteyne LJJ, Jansen EHJM, Geus JW, Cassee FR, De Jong WH: Impact of agglomeration state of nano- and submicron sized gold particles on pulmonary inflammation. Particle and Fibre Toxicology 2010; 7:37.

[92] Lasagna-Reeves C, Gonzalez-Romero D, Barria MA, Olmedo I, Clos A, Ramanujam VMS, Urayama A, Vergara L, Kogan MJ, Soto C: Bioaccumulation and toxicity of gold nanoparticles after repeated administration in mice. Biochem Biophys Res Commun 2010; 393:649–655.

[93] Kim KT, Zaikova T, Hutchison JE, Tanguay RL: Gold nanoparticles disrupt zebrafish eye development and pigmentation. Toxicol Sci 2013, 133(2):275–288.

[94] Goodman CM, Mccusker CD, Yilmaz T, Rotello VM: Toxicity of gold Nanoparticles functionalized with cationic and anionic side chains. Bioconjugate Chem 2004; 15: 897-900.

[95] Shukla R, Bansal V, Chaudhary M, Basu A, Bhonde RR, Sastry M: Biocompatibility of gold nanoparticles and their endocytotic fate inside the cellular compartment: a microscopic overview. Langmuir 2005; 21: 10644.

[96] Hirn S, Behnke MS, Schleh C, Wenk A, Lipka J, Schäffler M, Takenaka S, Möller W, Schmidn G, Simon U, Kreyling WG: Particle size-dependent and surface charge-dependent biodistribution of gold nanoparticles after intravenous administration. Eur J of Pharm Biopharm 2011; 77(3):407-16.

[97] Mahl D, Diendorf J, Ristig S, Greulich C, Li ZA, Farle M, Kuller M, Epple M: Silver, gold and alloyed silver-gold nanoparticles: characterization and comparative cell-biologic action. J. Nanopart. Res 2012; 14, 1153. DOI 10.1007/s1151-012-1153-5.

[98] Amenta V, Aschberger K.: Carbon nanotubes: potential medical applications and safety concerns, Wiley Interdiscip Rev Nanomed Nanobiotechnol, 2014; 27. doi: 10.1002/wnan.1317. [Epub ahead of print]

[99] Campos-Garcia J, Martinez DS, Alves OL, Leonardo AF, Barbieri E:. Ecotoxicological effects of carbofuran and oxidised multiwalled carbon nanotubes on the freshwater fish Nile tilapia: Nanotubes enhance pesticide ecotoxicity. Ecotoxicol Environ Saf. 2015 Jan; 111: 131-137. doi: 10.1016/j.ecoenv.2014.10.005.

[100] Zhu B, Liu GL, Ling F, Song LS, Wang GX.: Development toxicity of functionalized single-walled carbon nanotubes on rare minnow embryos and larvae. Nanotoxicology, 2014 Sep 11: 1-12 [Epub ahead of print]

[101] Vega-Alvarez S, Herrera A, Rinaldi C, Carrero-Martinez FA.: Tissue-specific direct microtransfer of nanomaterials into Drosophila embryos as a versatile in vivo test bed for nanomaterial toxicity assessment. Int J Nanomedicine. 2014; 9: 2031-2041. doi: 10.2147/IJN.S56459. eCollection 2014.

[102] Clichici S, Biris AR, Tabaran F, Filip A.: Transient oxidative stress and inflammation after intraperitoneal administration of multiwalled carbon nanotubes functionalized with single strand DNA in rats. Toxicol Appl Pharmacol. 2012. 259(3): 281-292. doi: 10.1016/j.taap.2012.01.004.

[103] Rahman I, MacNee W.: Oxidative stress and regulation of glutathione in lung inflammation. Eur. Respir. J. 2000; 16: 534–554.

[104] Berlett BS, Stadtman ER.: Protein oxidation in aging, disease and oxidative stress. J. Biol. Chem. 1997; 272 (33): 20313–20316.

[105] Tasaka S, Amaya F, Hashimoto S, Ishizaka A.: Roles of oxidants and redox signaling in the pathogenesis of acute respiratory distress syndrome. Antioxid. Redox Signal. 2008; 10(4): 739–753.

[106] Ye S, Wang Y, Jiao F, Zhang H, Lin C, Wu Y, Zhang Q.: The role of NADPH oxidase in multi-walled carbon nanotubes-induced oxidative stress and cytotoxicity in human macrophages. J. Nanosci. Nanotechnol. 2011; 11(5): 3773–3781.

[107] Mitchell LA, Gao J, Wal RV, Gigliotti A, Burchiel SW, McDonald JD.: Pulmonary and systemic immune response to inhaled multiwalled carbon nanotubes. Toxicol. Sci. 2007; 100 (1): 203–214.

[108] Guan J, Liu G, Cai K, Gao C, Liu R.: Probing the interactions between carboxylated multi-walled carbon nanotubes and copper-zinc superoxide dismutase at a molecular level. Luminiscence. 2014 Oct 29. doi: 10.1002/bio.2807. [Epub ahead of print]

[109] Møller P, Hemmingsen JG, Jensen DM, Danielsen PH, Karottki DG, Jantzen K, Roursgaard M, Cao Y, Kermanizadeh A, Klingberg H, Christophersen DV, Hersoug LG, Loft S.: Applications of the comet assay in particle toxicology: air pollution and engineered nanomaterials exposure. Mutagenesis. 2015; 30(1): 67-83.

[110] Luan B, Huynh T, Zhao L, Zhou R.: Potential toxicity of graphene to cell functions via disrupting protein-protein interactions, ACS Nano, 2014 Dec 17[Epub ahead of print]

[111] Yang M, Zhang M, Tahara Y, Chechetka S, Miyako E, Iijima S, Yudasaka M.: Lysosomal membrane permeabilization: carbon nanohorn-induced reactive oxygen species generation and toxicity by this neglected mechanism. Toxicol Appl Pharmacol. 2014; 280(1): 117-126. doi: 10.1016/j.taap.2014.07.022.

[112] Umemoto EY, Speck M, Shimoda LM, Kahue K, Sung C, Stokes AJ, Turner H.: Single-walled carbon nanotube exposure induces membrane rearrangement and suppression of receptor-mediated signalling pathways in model mast cells. Toxicol Lett. 2014; 229(1): 198-209. doi: 10.1016/j.toxlet.2014.06.009.

[113] Wang J, Liu R, Su Y, Li W.: Embedded carbon nanotubes nanoparticles in plasma membrane induce cellular calcium outflow imbalancing. J Nanosci Nanotechnol. 2014; 14(6): 4058-4065.

[114] Zhao Y, Wu Q, Li Y, Nouara A, Jia R, Wang D.: In vivo translocation and toxicity of multi-walled carbon nanotubes are regulated by microRNAs. Nanoscale 2014; 6(8): 4275-4284. doi: 10.1039/c3nr06784j

[115] Walling BE, Lau GW.: Perturbation of pulmonary immune functions by carbon nanotubes and susceptibility to microbial infection. J Microbiol. 2014; 52(3): 227-234.

[116] Singh AV, Mehta KK, Worley K, Dordick JS, Kane RS, Wan LQ.: Carbon nanotube-induced loss of multicellular chirality on micropatterned substrate is mediated by oxidative stress. ACS Nano 2014; 8(3): 2196-2205.

[117] Haniu H, Saito N, Matsuda Y, Tsukahara T, Usui Y, Maruyama K, Takanashi S, Aoki K, Kobayashi S, Nomura H, Tanaka M, Okamoto M, Kato H.: Biological responses according to the shape and size of carbon nanotubes in BEAS-2B and MESO-1 cells. Int J Nanomedicine 2014; 9: 1979-1990, doi: 10.2147/IJN.S58661. eCollection 2014.

[118] Yamashita K, Yoshioka Y, Higashisaka K, Morishita Y, Yoshida T, Fujimura M, Kayamuro H, Nabeshi H, Yamashita T, Nagano K, Abe Y, Kamada H, Kawai Y, Majumi T,

Yoshikawa T, Itoh N, Tsunoda S, Tsutsumi Y.: Carbon nanotubes elicit DNA damage and inflammatory response relative to their size and shape. Inflammation 2010; 33(4): 276–280.

[119] Wang X, Jia G, Wang H, Nie H, Yan L, Deng XY, Wang S.: Diameter effects on cytotoxicity of multi-walled carbon nanotubes. J. Nanosci. Nanotechnol. 2009; 9(5): 3025–3033.

[120] van Berlo D, Wilhelmi V, Boots AW, Hullmann M, Kuhlbusch TA, Bast A, Schins RP, Albrecht C.: Apoptotic, inflammatory, and fibrogenic effects of two different types of multi-walled carbon nanotubes in mouse lung. Arch Toxicol, 2014 Sep; 88(9): 1725-1737. doi: 10.1007/s00204-014-1220-z.

[121] Zhang T, Tang M, Kong L, Li H, Zhang T, Xue Y, Pu Y.: Surface modification of multiwall carbon nanotubes determines the pro-inflammatory outcome in macrophage. J Hazard Mater, 2015 Mar 2; 284:73-82. doi: 10.1016/j.jhazmat.2014.11.013.

[122] Chatterjee N, Yang J, Kim HM, Jo E, Kim PJ, Choi K, Choi J.: Potential toxicity of differential functionalized multiwalled carbon nanotubes (MWCNT) in human cell line (BEAS2B) and Caenorhabditis elegans. J Environ health A. 2014; 77(22-24): 1399-1408. doi: 10.1080/15287394.2014.951756

[123] Palomaki J, Sund J, Vippola M, Kinaret P, Greco D, Savolainen K, Puustinen A, Alenius H.: A secretomics analysis reveals major differences in the macrophage responses towards different types of carbon nanotubes. Nanotoxicology 2014 Oct 17:1-10. [Epub ahead of print]

[124] Cui H, Wu W, Okuhira K, Miyazawa K, Hattori T, Sai K, Naito M,Suzuki K, Nishimura T, Sakamoto Y, Ogata A, Maeno T, Inomata A, Nakae D, Hirose A, Nishimaki-Mogami T.: High-temperature calcined fullerene nanowhiskers as well as long needle-like multi-wall carbon nanotubes have abilities to induce NLRP3-mediated IL-1β secretion. Biochem Biophys Res Commun. 2014 Sep 26; 452(3): 593-599. doi: 10.1016/j.bbrc.2014.08.118.

[125] Liu WT, Bien MY, Chuang KJ, Chamg TY, Jones T, BeruBe K, Laley G, Tsai DH, Chuang HC, Cheng TJ.: Taiwan Cardio Pulmonary Research (T-CPR) Group. Physicochemical and biological characterization of single-walled and double-walled carbon nanotubes in biological media. J Hazard Mater. 2014 Sep 15; 280: 216-225. doi: 10.1016/j.jhazmat.2014.07.069.

[126] Zhang C, Chen W, Alvarez PJ.: Manganese peroxidase degrades pristine but not surface-oxidized (carboxylated) single-walled carbon nanotubes. Environ Sci Technol. 2014 Jul 15; 48(14):7918-7923. doi: 10.1021/es5011175.

[127] Shvedova AA, Kisin E, Murray AR, Johnson VJ, Gorelik O, Arepalli S, Hubbs AF, Mercer RR, Keohavong P, Sussman N, Jin J, Yin J, Stone S, Chen BT, Deye G, Maynard A, Castranova V, Baron PA, Kagan VE.: Inhalation vs. aspiration of single-walled carbon nanotubes in C57BL/6 mice: inflammation, fibrosis, oxidative stress, and

mutagenesis. Am J Physiol Lung Cell Mol Physiol. 2008 Oct; 295(4): L552–L565. doi: 10.1152/ajplung.90287.2008.

[128] Park EJ, Zahari NE, Kang MS, Lee Sj, Lee K, Lee BS, Yoon C, Cho MH, Kim Y, Kim JH.:Toxic response of HIPCO single-walled carbon nanotubes in mice and RAW264.7 macrophage cells. Toxizol Lee. 2014 Aug 17; 229(1): 167-177 doi: 10.1016/j.toxlet. 2014.06.015.

[129] Silva RM, Doudrick K, Franzi LM, TeeSy C, Anderson DS, Wu Z, Mitra S, Vu V, Dutrow G, Evans JE, Westerhoff P, Van Winkle LS, Raabe OG, Pinkerton KE.: Instillation versus inhalation of multiwalled carbon nanotubes: exposure-related health effects, clearance, and the role of particle characteristics. ACS Nano 2014 Sep 23; 8(9): 8911-8931. doi: 10.1021/nn503887r

[130] Han SG.: Pulmonary response of mice to a sequential exposure of side-stream cigarette smoke and multi-walled carbon nanotubes. Inhal Toxicol 2014 May; 26(6): 327-332. doi: 10.3109/08958378.2014.890683.

[131] Clichici S, Mocan T, Filip A, Biris A, Simon S, Daicoviciu D, Decea N, Parvu A, Moldovan R, Muresan A.: Blood oxidative stress generation after intraperitoneal administration of functionalized single-walled carbon nanotunes in rats. Acta Physiol Hung. 2011 Jun; 98(2): 231-241. doi: 10.1556/APhysiol.98.2011.2.15.

[132] Clichici S, Biris AR, Catoi C, Filip A, Tabaran F.: Short-term splenic impact of single-strand DNA functionalized multi-walled carbon nanotubes intraperitoneally injected in rats. J Appl Toxicol. 2014 Apr; 34(4): 332-344. doi: 10.1002/jat.2883.

[133] Chen R, Zhang L, Ge C, Tseng M, Bai R, Qu Y, Beer C, Autrup H, Chen C.: Subchronic toxicity and cardiovascular responses in spontaneously hypertensive rats after exposure to multiwall carbon nanotubes by Iintratracheal instillation. Chem Res Toxicol 2015 Jan 12 [Epub ahead of print]

[134] Fujita K, Fukuda M, Fukui H, Horie M, Endoh S, Uchida K, Shichiri M, Morimoto Y, Ogami A, Iwahashi H.: Intratracheal instillation of single-wall carbon nanotubes in the rat lung induces time-dependent changes in gene expression. Nanotoxicology 2014 Jun 9: 1-12. [Epub ahead of print]

[135] Xu J, Alexander DB, Futakuchi M, Numano T, Fukamachi K, Suzui M, Omori T, Kanno J, Hirose A, Tsuda H: Size- and shape-dependent pleural translocation, deposition, fibrogenesis, and mesothelial proliferation by multiwalled carbon nanotubes. Cancer Sci. 2014 Jul; 105(7): 763-769. doi: 10.1111/cas.12437.

[136] Kido T, Tsunoda M, Kasai T, Sasaki T, Umeda Y, Senoh H, Yanagisawa H, Asakura M, Aizawa Y, Fukushima S.: The increases in relative mRNA expressions of inflammatory cytokines and chemokines in splenic macrophages from rats exposed to multi-walled carbon nanotubes by whole-body inhalation for 13 weeks. Inhal Toxicol. 2014 Oct; 26(12): 750-758. doi: 10.3109/08958378.2014.953275.

[137] Kasai T, Umeda Y, Ohnishi M, Kondo H, Takeuchi T, Aiso S, Nishizawa T, Matsumoto M, Fukushima S.: Thirteen-week study of toxicity of fiber-like multi-walled carbon nanotubes with whole-body inhalation exposure in rats. Nanotoxicology. 2014; 17: 1-10.

[138] Kim JS, Sung JH, Choi BG, Ryu HY, Song KS, Shin JH, Lee JS, Hwang JH, Lee JH, Lee GH, Jeon K, Ahn KH, Yu IJ:.In vivo genotoxicity evaluation of lung cells from Fischer 344 rats following 28 days of inhalation exposure to MWCNTs, plus 28 days and 90 days post-exposure. Inhal Toxicol. 2014 Mar; 26(4): 222-234. doi: 10.3109/08958378.2013.878006.

[139] Warheit DB.: Long-term inhalation toxicity studies with multiwalled carbon nanotubes: closing the gaps or initiating the debate?Toxicol Sci. 2009; 112(2): 273-275. doi: 10.1093/toxsci/kpf237

[140] Chen W, Xiong Q, Ren Q, Guo Y, Li G.: Can amino-functionalized carbon nanotubes carry functional nerve growth factor? Neural Regen Res., 2014; 9(3): 285-292. doi: 10.4103/1673-5374.128225.

[141] Liu Y, Ren L, Yan D, Zhong W.: Mechanistic Study on the Reduction of SWCNT-induced Cytotoxicity by Albumin Coating. Part Part Syst Charact, 2014; 31(12): 1244-1251.

[142] Orecna M, De Paoli SH, Janouskova O, Tegegn TZ, Filipova M, Bonevich JE, Holada K, Simak J.: Toxicity of carboxylated carbon nanotubes in endothelial cells is attenuated by stimulation of the autophagic flux with the release of nanomaterial in autophagic vesicles. Nanomedicine 2014 Jul; 10(5): 939-948. doi: 10.1016/j.nano. 2014.02.001.

Chapter 6

Single-Walled Carbon Nanohorn (SWNH) Aggregates Inhibited Proliferation of Human Liver Cell Lines and Promoted Apoptosis, Especially for Hepatoma Cell Lines

Guoan Xiang, Jinqian Zhang and Rui Huang

Additional information is available at the end of the chapter

http://dx.doi.org/10.5772/61109

Abstract

Research focus: SWNHs (single-walled carbon nanohorns) may be utilized to treat cancer as drug carriers based on their particular structure. But, the effect mechanism of the material itself on liver cells has not been investigated. **Research methods used**: To answer those questions, the roles of rude SWNHs on the biology functions of human liver normal and cancer cells were studied. **Results/findings of the research**: The results indicated that SWNHs suppressed growth, proliferation, and mitotic entry of human liver normal and cancer cells, and also pushed cell apoptosis, especially in cancer cells. We had found SWNHs in the lysosomes of L02 cells and in the nuclei of HepG2 cells. It indicated that individual spherical SWNH particles could enter into liver cells. **Main conclusions and recommendations**: Our results identified that it had different mechanisms between SWNHs and hepatoma cell lines or human normal cell lines. Advanced research about application and mechanisms in the treatment of HCC (hepatocellular carcinoma) by SWNHs should be carried out.

Keywords: SWNHs (single-walled carbon nanohorns), hepatocellular carcinoma, apoptosis, proliferation

1. Introduction

SWNHs (single-walled carbon nanohorns) were first synthesized by Iijima et al. [1] in 1999. On the basis of their special surface structures and large surface areas, SWNHs may be used

in pharmacy and biomedicine. [2, 8] Some investigators [4] have applied oxidized SWNHs (SWNHox) as drug carriers with cisplatin for treatment of cancer. They found that SWNHs could slowly release cisplatin and inhibit effectively the proliferation of human lung cancer cells NCI-H460.

The results from their research also demonstrated that SWNHox itself could not suppress or promote the proliferation of human cancer cells as carrier material. In addition, up to now, the functions of unembellished SWNHs on cells were not very apparent. [9] Many researchers have studied the biological functions of graphene, fullerene, and carbon nanotubes (CNTs). [10, 32] They found that nanoparticles of carbon could enter into cells, even subcellular organelles such as lysosomes or nuclei. [17, 21, 23, 24] Carbon nanoparticles can induce apoptosis related to oxidative stress. [33, 36]

How SWNHs influence the functions of L02 (human normal liver cell lines) and HepG2 (human hepatoma cell lines) was unknown. Moreover, the differences role mechanisms between the material and normal liver cells or cancer liver cells had not been studied. To answer these questions, the direct effects of SWNHs on human hepatoma cell line HepG2 and human liver normal cell line L02 were investigated. We performed internalization in liver cell lines with SWNH particles. The extraordinarily different role induced by SWNHs on hepatoma cell lines and liver normal cell lines, will be useful for the treatment of HCC (hepatocellular carcinoma). To understand how studies on nanomaterial toxicology might relate to nanomedicine safety, it is important to consider the current regulatory framework (legally binding requirements and guidelines) in place for all medicine evaluations.

2. Characterization of material

By arc-discharge method, SWNHs was synthesized in air. It's characterized by high-resolution transmission electron microscopy (HRTEM), Raman spectra, and thermogravimetry, as previously reported [37]. SWNHs are dahlia-like structures and spherical aggregates; the diameters of SWNHs ranged from 60–100 nm. We determined other elemental contents of SWNHs with S4 Explorer X-ray fluorescence spectrometer. We detected the elemental contents of SWNHs with rapid N tube.

2.1. Preparation of dishes coated with SWNHs

SWNHs were suspended in ultrapure dialysis water from Milli-Q Integral Water 5 Purification System. SWNHs solution (10 μg/mL) were placed on PS (polystyrene) dishes and dried at 80°C in air for 4 h. Then these dishes were treated with ultraviolet irradiation for 1 h. The abbreviations SWNHs10, SWNHs20, SWNHs30, and SWNHs40 correspond to 0.21 μg/cm^2, 0.42 μg/cm^2, 0.64 μg/cm^2, and 0.85μg/cm^2 in each dish (60 mm), respectively. [24] Dataphysics OCA 40 Contact Angle Measuring System was used to determine the contact angles of 2 μl volume water droplets on the noncoated PS surfaces and the SWNHs40-coated surfaces at 20°C.

http://dx.doi.org/10.5772/61109

2.2. Cell culture

HepG2 and L02 cells were seeded onto noncoated PS dishes and dishes were coated with SWNHs10, SWNHs20, SWNHs30, SWNHs40, and then cultured with DMEM (Dulbecco's Modified Eagle's Medium supplemented), 1% penicillin-streptomycin solution, and 10% fetal bovine serum at 37°C in 5% CO_2. [24]

2.3. Growth curve and morphology of liver cells cultured with SWNHs

HepG2 (3×10^5) and L02 (3×10^5) cells were seeded onto dishes, respectively. After being cultured for 48 h, these cells were subsequently visualized with optical microscope, based on the general protocol. These cells were observed and photos were acquired with a camera. At 48 h, cells were numbered with cell counter plate. The polynomial fitting about relationship between quantities (μg) of SWNHs (NH) and number of cells (CN) was carried out with using Origin 8 software.

2.4. Measurement of mitotic entry

These cells were synchronized with thymidine and cultured on dishes coated with SWNHs for 16 h. Then the cells were released into cell cycle with fresh medium. In the end, these cells were gathered or treated at different time points for subsequent specific analyses. DNA synthesis was measured with bromodeoxyuridine (BrdU) labeling in these cells. The BrdU-positive and the total number of cells were counted. Mitotic cells were evaluated by time-lapse videomicroscopy with Openlab software. [38]

2.5. Assessment of SWNHs

Elemental composition of SWNHs included 0.25% total metal content and 95.3% carbon, each metal less than 0.1%. [39, 41] Our results indicated that the surface area of BET was 631.55m^2/g. [42] The results with regard to adsorptive isotherm plot of SWNHs showed that the surface of SWNHs particles was hydrophobic.

At the relative pressure 0.994 (P/P_o), the diameter of SWNHs material was less than 308.7 nm. Moreover, the pore volume of SWNHs was 1.57 cm^3/g. The average pore diameter of SWNHs was 9.97 nm. The particle density was 1.0077 g/cm^3. The pore size distribution by Barrett-Joyner-Halenda (BJH) indicated that diameters of most mesopores were 2–8 nm in the SWNHs material. These results showed that SWNHs had many closed pores. The dimension range of suspended SWNHs particle was 295–615 nm in aqueous solution.

2.6. Characterization of dishes coated with SWNHs

Single particles of SWNHs on the surface of dishes were showed in images from scanning electron microscope (SEM); their diameters were 60–100 nm (Figure 1). The aggregates of secondary SWNH were dispersed and exhibited on individual particles on the surface of PS dishes. On surface of PS dishes, the contact angle of water droplet was 44.9°, less than the dried

SWNHs-coated surface at 74.5°. The hydrophobicity of uncoated PS surface was lower than that of SWNHs40/PS surface.

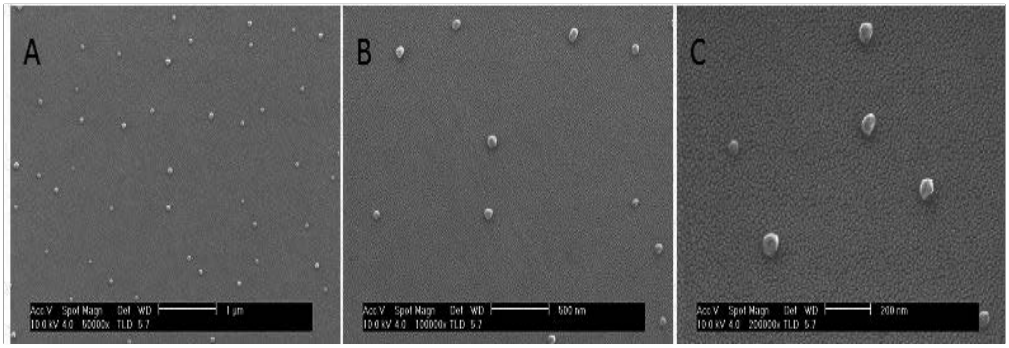

Figure 1. The films of SWNHs40/PS observed by SEM. SWNHs40-coated PS (0.85 μg/cm^2) dishes with a bottom area of about 1 cm^2 were prepared for SEM measurements. After pretreated by spraying gold on films of samples, SEM measurements were carried out using a SIRION field emission scanning electronic microscope (FEI Corporation Ltd) with accelerating voltage of 10.0kV. The SEM of films showed that SWNHs40 on PS surface (0.85 μg/cm^2) were individual spherical particles with diameters of 60-100nm. (A) 50,000×, scale bar represents 1μm. (B) 100,000×, scale bar represents 500 nm. (C) 200,000×, scale bar represents 200nm.

2.7. Morphology of cells

The morphology of cells cultured for 48 h in SWNH-coated and uncoated dishes was observed by optical microscope. The images showed that the number of L02 (Figure 2 A–C) and HepG2 (Figure 2 D–F) decreased in a concentration-dependent manner. More spherical cells could be observed, which became smaller in size. That was remarkable in HepG2 cells. SWNHs had a much larger effect on liver cancer cells than normal as proliferation inhibitor factor.

2.8. SWNHs inhibit mitotic entry, proliferation, and growth of liver cells

With increased quantities of SWNHs, the growth curves of HepG2 and L02 cells are shown at 48 h; both the amounts of L02 (Figure 2G, lower curve) and HepG2 (Figure 2H, upper curve) decreased noticeably in a concentration-dependent manner (P<0.01). In addition, polynomial fitting with regard to relationships between NH and CN was carried out. The proliferate rate of HepG2 was faster than L02 cells, but follow with the increase of NH, proliferation of HepG2 was remarkably shut down and gradually approached to L02 cells. The polynomial fitting formula of L02 (lower dotted curve, Figure 2G) was as follows:

$$\left[CN\right] = -26.2\left[NH\right]^4 + 1.23\times10^3\left[NH\right]^3 - 1.29\times10^4\left[NH\right]^2 - 1.20\times105\left[NH\right] + 1.96\times10^6,\ R2=1. \quad (1)$$

The polynomial fitting formula of HepG2 (upper dotted curve, Figure 2G) was as follows:

$$\left[CN\right] = -1.46\times10^2\left[NH\right]^4 + 7.42\times10^3\left[NH\right]^3 - 1.19\times10^5\left[NH\right]^2 + 4.56\times10^5\left[NH\right] + 4.33\times10^6,\ R2=1. \quad (2)$$

http://dx.doi.org/10.5772/61109

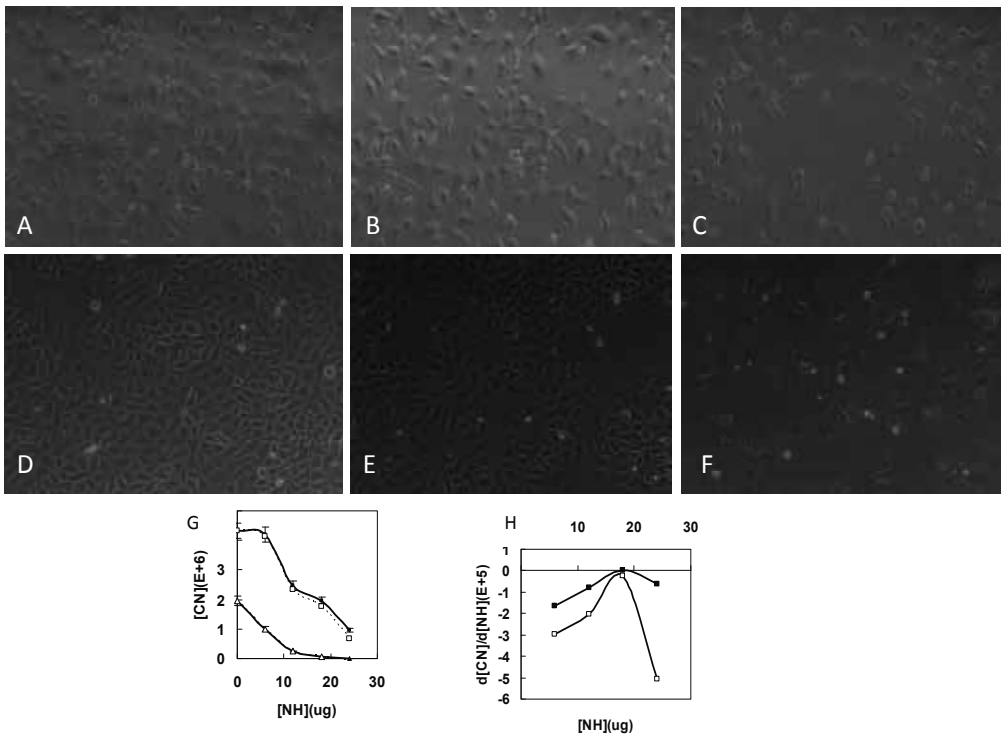

Figure 2. Morphology observed by optical microscope and growth curves of L02 and HepG2 cells cultured onto non- and SWNHs-coated dishes. L02 (3×10^5) and HepG2 (3×10^5) cells were seeded onto 60-mm non- and SWNHs-coated dishes and cultured for 48 h, and then images of the cells were observed according to the general protocol by optical microscope and total numbers of L02 and HepG2 cells [CN] were counted, respectively. The cells were visualized and digital images were acquired using Nikon camera (Nikon, Japan). Fig. 2G are cell growth curves of L02 (Fig. 2G Lower curve) and HepG2 (Fig. 2G Upper curve) ($P<0.01$). All data are represented as mean ±SEM. The polynomial fitting formulas for the relationship between cell number [CN] and quantity of SWNHs (μg) [NH] was performed by Origin 8 (Fig. 2G Dotted curves). Fig. 2H are the first-order derivates *d [CN]/d [NH]* deduced from the two polynomial fitting formulas (A) Control, L02 untreated with SWNHs; (B) L02 treated with SWNHs20 (0.42ìg/cm^2); (C) L02 treated with SWNHs40 (0.85ìg/cm^2) (400×); (D) Control, HepG2 untreated with SWNHs; (E) HepG2 treated with SWNHs20 (0.42ìg/cm^2); (F) HepG2 treated with SWNHs40 (0.85ìg/cm^2) (400×); (G) Lower curve: —▲—L02 determined, ---△--polynomial fitting L02 Upper curve: —■—HepG2 determined, ---□-- polynomial fitting HepG2 (H) Lower curve: —□— The first-order derivate d [CN]/d [NH] of HepG2 Upper curve: ---■--The first-order derivate d [CN]/d [NH] of L02

Both the relationships between the number of L02 or HepG2 cells and the quantities of SWNHs are quartic polynomial.

The first-order derivates of the above two formulas (d [CN]/d [NH]) were also deduced. The first-order derivate of L02 (upper curve, Figure 2H) was as follows:

$$d\left[CN\right]/d\left[NH\right] = -1.048\times10^2\left[NH\right]^3 + 3.69\times10^3\left[NH\right]^2 - 2.58\times10^4\left[NH\right] - 1.20\times10^5 \quad (3)$$

The first-order derivate of HepG2 (lower curve, Figure 2H) was as follows:

$$d\left[CN\right]/d\left[NH\right] = -5.84\times10^{2}\left[NH\right]^{3} + 2.23\times10^{4}\left[NH\right]^{2} - 2.38\times10^{5}\left[NH\right] + 4.56\times10^{5} \quad (4)$$

First-order derivative denoted that the changed rate of cell numbers followed with the increasing concentration of SWNHs. The formula of the changed rate was negative value, which suggested that SWNHs suppressed proliferation of liver cells. Moreover, the low changed rate of HepG2 cells compared to L02 cells revealed the more obvious inhibitory effect of SWNHs on cancer cells than normal (Figure 2H).

Cells were mixed with BrdU to investigate the effect of SWNHs on mitosis entry. Our results indicated that mitotic entry of both cells was delayed noticeably by SWNHs (Figure 3A and B) and that proliferation of cells was suppressed (Figure 3C,D) in a concentration- and time-dependent manner (P<0.01). The role was more significant in HepG2 than in L02.

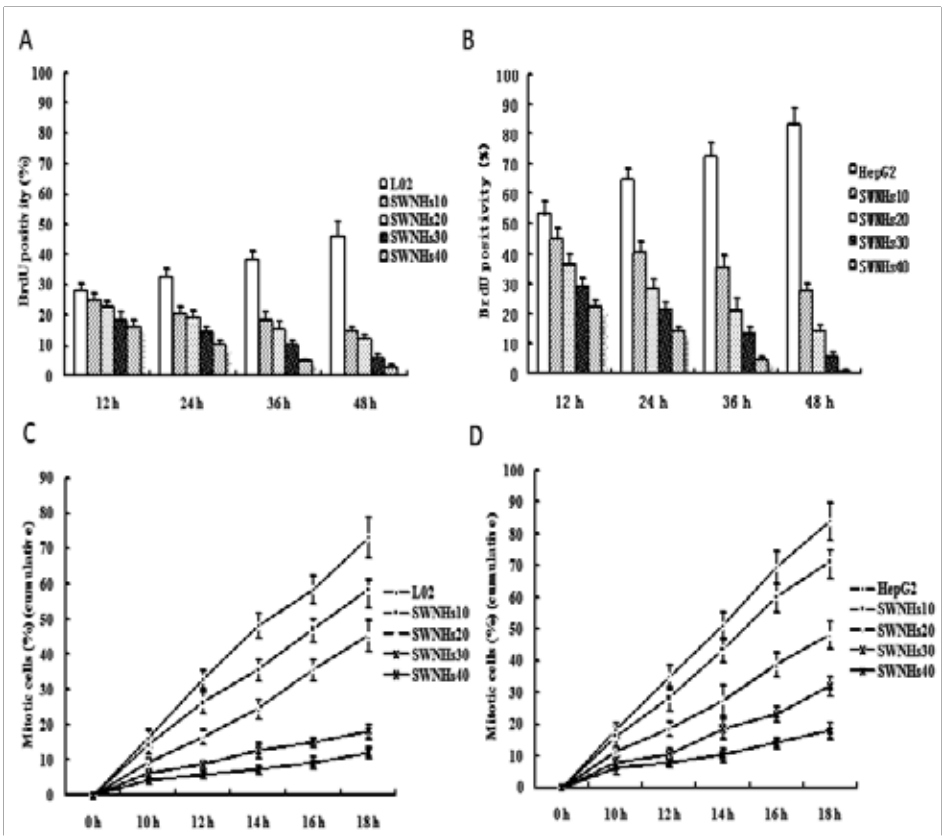

Figure 3. SWNHs inhibited mitotic entry of liver cells. L02 (3×10^5) and HepG2 (3×10^5) cells were seeded onto 60-mm Non- and SWNHs-coated dishes, and cultured for 48 h. To assure how the SWNHs affect cellular mitosis, we incorporated BrdU into the control, and found that accumulations of both mitotic L02 (A) and HepG2 (B) cells were significantly delayed and their mitotic entry (C,D) was inhibited by SWNHs at every time point followed with the increasing quantities of SWNHs (P<0.01). All data are represented as mean ±SEM.

http://dx.doi.org/10.5772/61109

The results of XTT assay suggested that HepG2 and L02 cells (Figure 4) all were noticeably inhibited in a concentration- and time-dependent manner (P<0.001). The cell viability was valued by the CCK-8 assay, and these results demonstrated that cell proliferation of HepG2 and L02 cells (Figure 4) was inhibited by SWNHs in a concentration- and time-dependent manner (P<0.001).

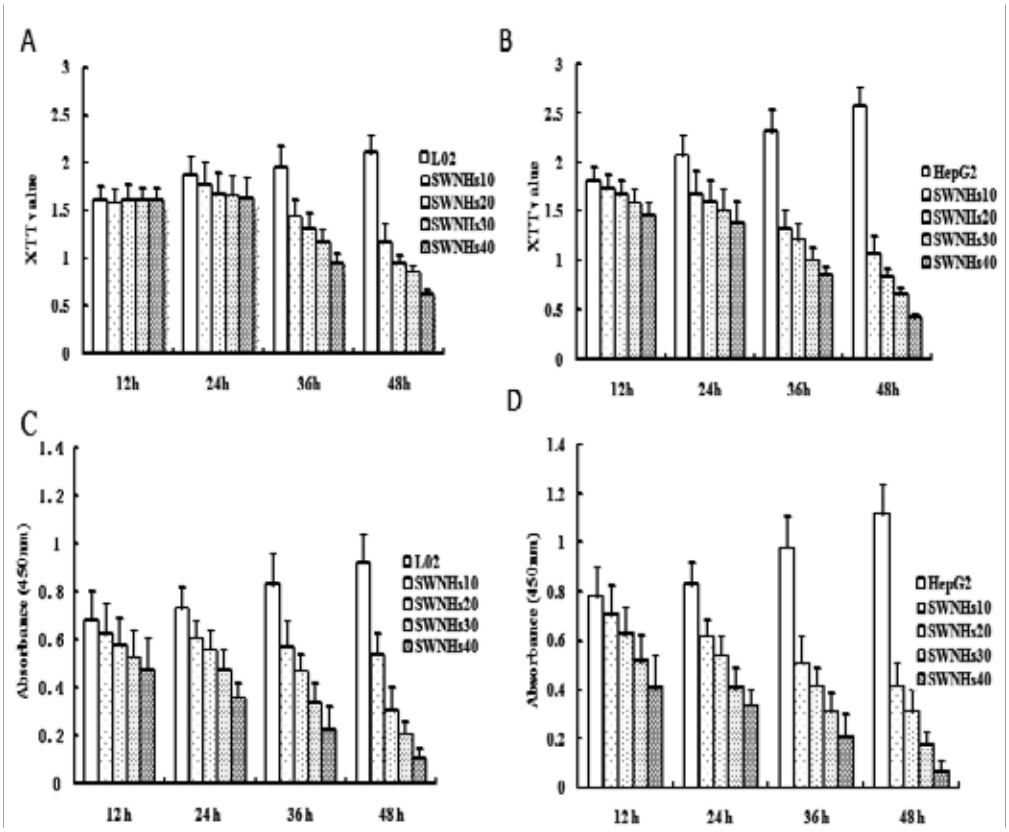

Figure 4. SWNHs inhibited growth and proliferation of liver cells. L02 (3×10^5) and HepG2 (3×10^5) cells were seeded onto 60-mm non- and SWNHs-coated dishes, and cultured for 48 h. Then the effects of SWNHs on L02 (Fig. 4A) and HepG2 (Fig. 4B) cells growth were investigated by XTT assays (P<0.001). L02 (Fig. 4C, 3×10^3) and HepG2 (Fig. 4D, 3×10^3) cells were cultured in 96- plate (6-mm) treated with or without SWNHs, then the cell viabilities were evaluated by CCK-8 assay. All data are represented as mean ±SEM.

2.9. Cell cycle affected by SWNHs

Cell cycle affected by SWNHS was detected with flow cytometry. Our results identified that cell cycles of L02 and HepG2 were affected by SWNHs (Figure 5), and in a concentration-dependent manner. The S phase of liver cells noticeably decreased, and the G1 phase increased obviously in a concentration-dependent manner (L02, P<0.05 and HepG2 P<0.01). Furthermore, G2 phase decreased in both cells, but only increased noticeably in HepG2 treated with

SWNHs40 (P<0.05). SWNHs induced different grades of G1 phase delay in HepG2 and L02 cells, which identified different cytotoxic effects on the two cell lines. It led to much stronger suppression of DNA replication in HepG2. The cell cycle was blocked in G2 phase, the gap from DNA synthesis to mitosis was delayed by SWNHs40 in HepG2, which induced apoptosis of HepG2 cells. [27]

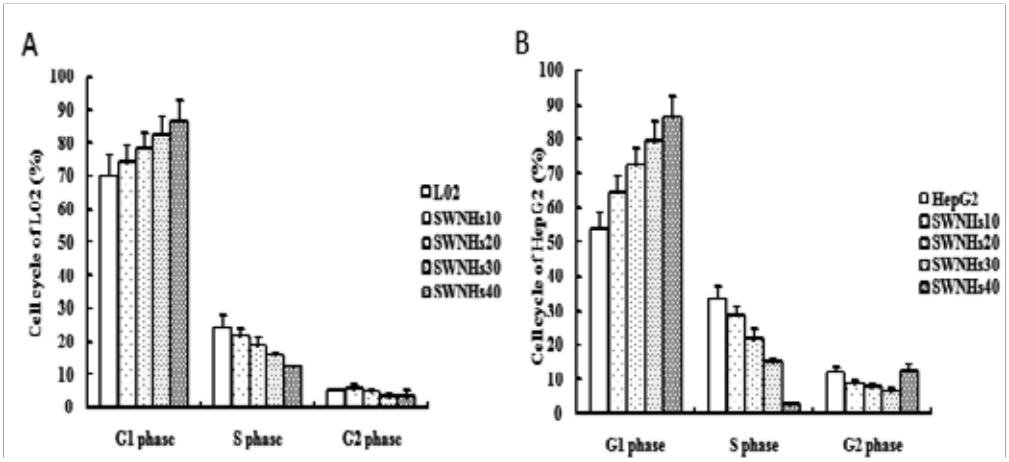

Figure 5. SWNHs affected cell cycle of liver cells. L02 (3×10^5) and HepG2 (3×10^5) cells were seeded onto non- and SWNHs-coated 60mm-dishes, and cultured for 48 h, respectively. Then the roles of SWNHs on L02 (A) and HepG2 (B) cell cycles were measured by cytometry. All data are represented as mean ±S.E.M.

2.10. SWNHs induced apoptosis

The apoptotic cells were determined by 7-AAD and Annexin-V. Our results indicated that apoptosis of HepG2 and L02 (Figure 6) were caused by SWNHs in a concentration-dependent manner, especially in HepG2 (P<0.001).

Biochemical events of apoptosis induce characteristic changes and death of cells. These changes include chromosomal DNA fragmentation, chromatin condensation, nuclear fragmentation, cell shrinkage and blebbing. Apoptosis in mammalian animal cells is regulated by SIRT1 and p53. Caspases are a group of cysteine proteases, and the key factors in cell apoptosis, such as caspase-3 and caspase-7. Our results identified that the expression of p53, caspase-7, and caspase-3 increased in L02 and HepG2 (Figure 6) in a concentration-dependent manner. Moreover, activation cleavage SIRT1 expression decreased in a dose-dependent manner. It confirmed that apoptosis of liver cells was promoted by SWNHs.

2.11. Cellular morphology observed by confocal microscope

The confocal images showed the morphology of L02; cell shapes of their nuclei were similar to control (Figure 7A), and number of cells decreased in a concentration-dependent manner.

http://dx.doi.org/10.5772/61109

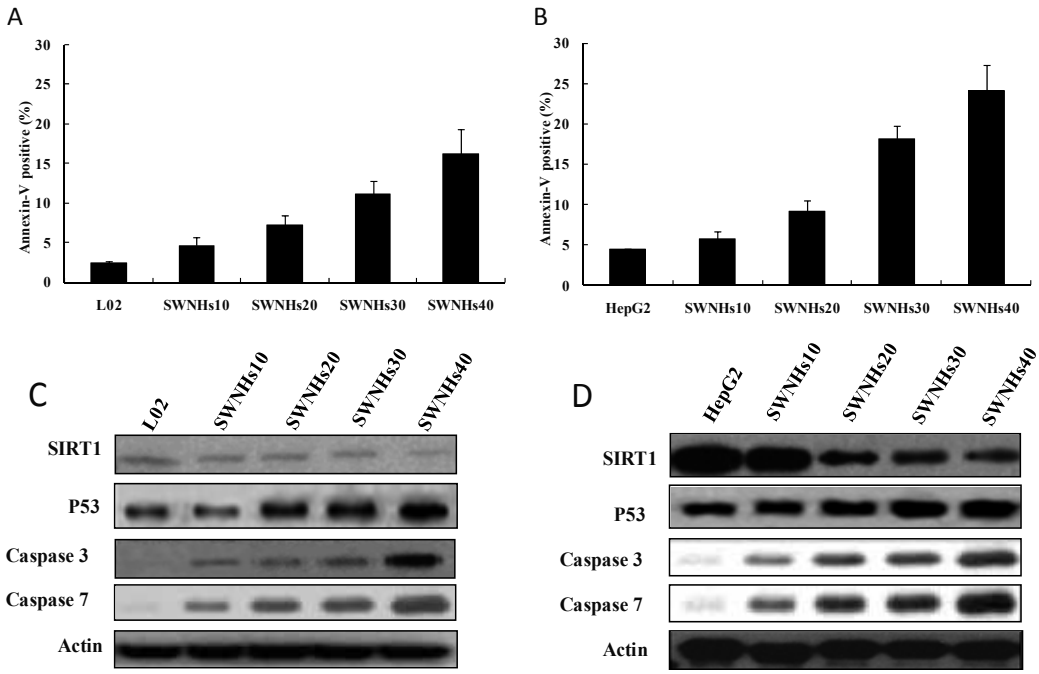

Figure 6. SWNHs promoted cell apoptosis of liver cells and apoptosis involves key factors in vivo. L02 (3×10^5) and HepG2 (3×10^5) Cells were seeded onto 60-mm non- and SWNHs-coated PS dishes, and cultured for 48 h, respectively. Then the effect of SWNHs on L02 (A) and HepG2 (B) cell apoptosis distribution was determined by flow cytometry (P=0.001). The expression levels of SIRT1 and those of activation cleavage of P53, caspase-3 and caspase-7 L02 (C) and HepG2 (D) were determined by western blotting. All data are represented as mean ±S.E.M.

In L02 treated with SWNHs, the size of nuclei was slightly larger than control (Figure 7B,C); the nuclei swelled following the increasing of SWNHs concentration.

The number of viable HepG2 decreased remarkably and apoptotic HepG2 increased in a concentration-dependent manner. Apoptotic HepG2 cells could be found in Figure 7F (showed as arrow), but could not be observed in controls (Figure 7D).

The images of HepG2 treated with SWNHs40 indicated that the size of nuclei was much smaller than control. As reported by Romero et al., [23] karyopyknosis was induced by SWNHs (Figure 7 F, showed as arrows). The karyopyknosis and larger nuclei caused by SWNHs were benefit of increased protein content of earlier apoptosis and decreased content of late apoptosis in nuclei. It may elucidate the suddenly increased G2 phase in HepG2 cells deal with SWNHs 40 (Figure5B). HepG2 cells deal with SWNHs 40 was nearly all apoptotic, meanwhile the ratio of S phase decreased remarkably and cells were obstructed at the G2/M phase. But, few L02 cells were apoptosis effects induced by SWNHs. HepG2 deal with SWNHs40 illustrated classic apoptotic morphology, but there were not so obvious apoptotic L02 cells. The apoptotic cells showed typical features, such as cell shrinkage, chromatin condensation, membrane blebbing, scant cytoplasm, and apoptotic body, [43, 45] especially in HepG2 cells.

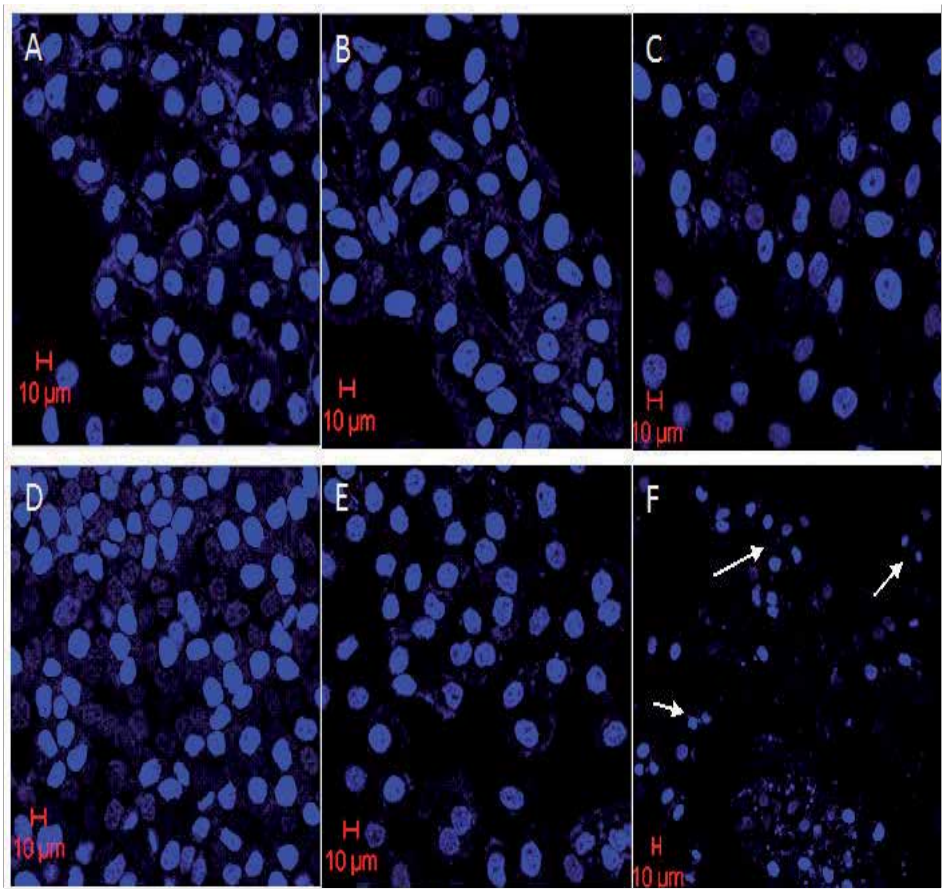

Figure 7. Morphology of L02 and HepG2 cells cultured onto SWNHs-coated dishes observed by confocalmicroscope. L02 (1×10^4) and HepG2 (1×10^4) cells were seeded onto 10-mm non- and SWNHs-coated dishes, and cultured in DMEM with FBS and PSN at 37 °C in humidified 5% CO_2/95% air for 48 h, respectively. Then L02 and HepG2 cells were treated with PFA and DAPI, and confocal images were acquired by Zeiss 510 META confocal microscope. (A) Control, L02 untreated with SWNHs; (B) L02 treated with SWNHs20 (0.42ìg/cm^2); (C) L02 treated with SWNHs40 (0.85ìg/cm^2) (D) Control, HepG2 untreated with SWNHs; (E) HepG2 treated with SWNHs20 (0.42ìg/cm^2). (F) HepG2 treated with SWNHs40 (0.85ìg/cm^2). Scale bars represent 10 ìm.

2.12. TEM

Cells deal with SWNHs40 (0.85 μg/cm^2) were collected for Transmission Electron Microscopy (TEM) measurement. By TEM, SWNHs can be found in cells. In L02, SWNHs aggregate localized at lysosomes and was smaller than 100 nm (Figure 8B and C). Moreover, it localized at nuclei in HepG2 cells (Figure 8E and F). The individual particles of SWNHs were easily dispersed from their neighbor molecules based on SWNHs possess high electronic densities on the surface than other molecules in organelles. The TEM images of organelles showed that both lysosomes and mitochondria in L02 (Figure8G) and HepG2 (Figure8H) deal with SWNHs were larger than control, respectively. And it was more remarkable in HepG2. Outside L02

http://dx.doi.org/10.5772/61109

(Figure8G) and HepG2 cells (Figure8H) deal with SWNHs, there were a lot of secretory vesicles, but not seen outside control cells. The secretory vesicles outside HepG2 (Figure8H) deal with SWNHs were larger than those outside L02 (Figure8G). SWNHs were heterogeneous materials, so cells secreted ingested SWNHs as normal response. HepG2 may have ingested much more SWNHs than L02. And the more cells ingested SWNHs, the more there were secretory vesicles.

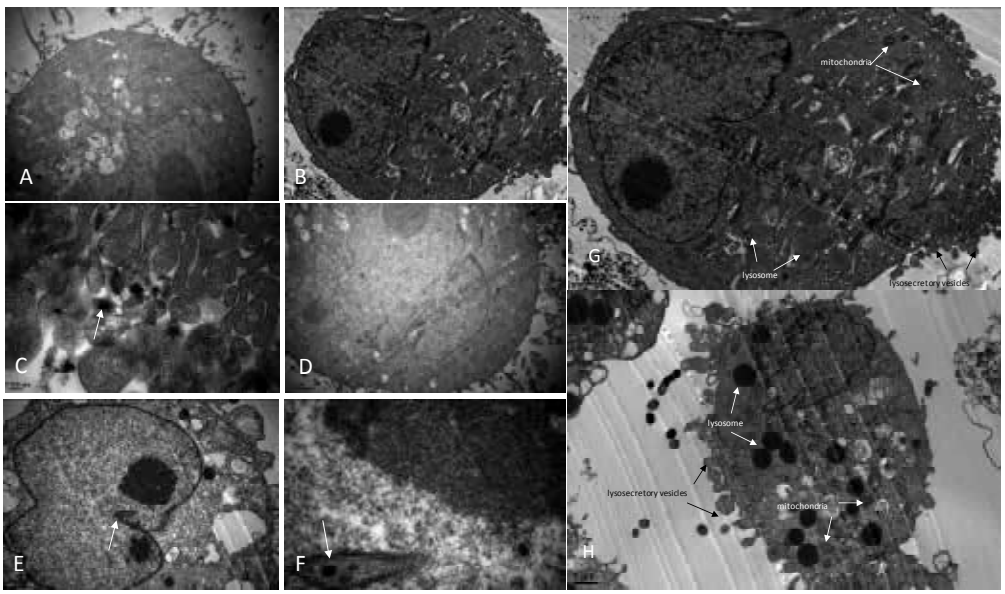

Figure 8. TEM images of liver cells. L02 (3×10^5) and HepG2 (3×10^5) Cells were seeded onto 60-mm non- and SWNHs40-coated (0.85 ìg/cm^2) dishes, and cultured for 48 h, respectively. The cells were collected and fixed with 3% glutaraldehyde. For TEM, ultrathin cells slices of 100 nm thickness were cut using an ultramicrotome and mounted on grids. The slices were contrasted with aqueous solution of uranyl acetate and lead citrate, and examined on JEM-1400 Transmission Electron Microscope (JEOL Ltd, Japan) with accelerating voltage of 80 kV. (A) L02 untreated with SWNHs as control (15,000×). Scale bar represents 1 ìm. (B) L02 cultured onto SWNHs40-coated dishes (0.85 ìg/cm^2) for 48 h (15,000×). Scale bar represents 1 ìm. (C) L02 cultured onto SWNHs40-coated dishes (0.85 ìg/cm^2) for 48 h (80,000×). Scale bar represents 100 nm. The arrow in Fig. 8B and Fig. 8C showed that there were individual spherical SWNHs particles with diameter less than 100 nm inside lysosomes of L02 cells. (D) HepG2 untreated with SWNHs as control (15,000×). Scale bar represents 1 ìm. (E) HepG2 cultured onto SWNHs40-coated dishes (0.85 ìg/cm^2) for 48 h (15,000×). Scale bar represents 1 ìm. (F) HepG2 cultured onto SWNHs40-coated dishes (0.85 ìg/cm^2) for 48 h (80,000×). Scale bar represents 100 nm. The arrow in Fig. 8E and Fig. 8F showed that there were individual spherical SWNHs particles with diameters less than 100 nm inside nuclei of HepG2 cells. (G) L02 cultured onto SWNHs40-coated dishes (0.85 ìg/cm^2) for 48 h (15,000×). Scale bar represents 1 ìm. (H) HepG2 cells cultured onto SWNHs40-coated dishes (0.85 ìg/cm^2) for 48 h (15,000×). Scale bar represents 1 ìm.

3. Discussion

The aforementioned studies have illustrated that some carbon nanomaterials suppressed growth and proliferation of L02 or HepG2. Fullerene C60 inhibited proliferation of HepG2 at

a low dosage of 0.46 μg/mL. [30]Liu et al. [29]suggested that unmodified MWNTs (multiwalled nanotubes), MWNTs modified with carboxyl, and MWNTs modified with hydroxyl at dosages of 12.5–200.0 μg/mL inhibited viability of L02 cells in a dose-dependent manner. Romero et al. [23] illustrated that poly [sulfopropyl methacrylate] (PSPM), or oxidized, lipid, poly [allylamine hydrochloride] (PAH)-modified MWNTs at higher dosage (100 μg/mL) suppressed growth and proliferation of HepG2. It was well known that SWCNTs (single-walled carbon nanotubes) had great potential to benefit biomedicine, for example, photothermal ablation therapy for tumor bond with near-infrared irradiation. Hashida et al. [46] reported the photothermal activity of a novel SWCNT bond with (KFKA) 7 peptide [H-(-Lys-Phe-Lys-Ala-)7-OH] with repeated structure, which could be used to treat tumor. The SWCNTs–(KFKA) 7 compounds could be used to ablate tumor in photothermal cancer therapy with its high aqueous dispersibility. [46] Our results were similar in HepG2 and L02 cells deal with SWNHs at low dose (1.5–6.0 μg/mL). Ajima et al. [4] reported that SWNHox (oxidized SWNHs) did not suppress or promote proliferation of lung cancer cells at dose of 0–20 μg/mL. But *in vivo*, their results indicated that SWNHox itself could be used to treat cancer, contrary to results from *in vitro* experiments. [7] Fan et al. [8] identified that there was no significant decrease in cell viability in Hela cells treated with SWNHs modified with gum Arabic (10–1000 μg/mL). These results illustrated that these nanoparticles were nontoxic to the cells. Tahara et al. [9] found recently that oxidized SWNHs coated with 1, 2-distearoyl-Sn-glycero-3-phosphoethanolamine-N- [amino (polyethylene, glycol) 2000] could suppress the growth and proliferation of murine macrophage RAW 264.7 cells in a concentration-dependent manner. The different modification styles for carbon nonmaterial based on different chemical compounds may induce change of various biological functions in different cells. [43]

After exposure to a chemical toxicant, the most easily and first visualized change and effect in cells could be observed come from cell morphology. So, morphological changes were benefit for toxicity biomarker. TEM could be used to identify the location of nanoparticles in organelles of cells based on its powerful denote to observing micron and nanometer structures. Oxidized SWNTs or modified and unmodified MWNTs could be found in endosomes, cytoplasm, or lysosomes of human macrophage cells by TEM. [19, 20] Porter et al. [18] found that dispersed SWNTs in tetrahydrofuran localized in nuclei and lysosomes of human macrophages. And fullerene C_{60} could be found in nuclei and cytoplasm of human macrophages. [47] Besides in endosomes, cytoplasm, or lysosomes, in human embryonic kidney 293 cells, MWNT-NH2 was first found in nuclei. [21] In HepG2 cells, the PSPM, lipid, or oxidized-modified MWNTs could be discovered in cytoplasm. However, there were no references involved in carbon nanoparticles locating in the nuclei of cells. Although, in nuclei of HepG2 cells, changes of protein and DNA had been obtained based on confocal Raman microscope induced by modified MWNTs. [23] Combining the results from TEM and confocal microscope, we identified the different interactive mechanisms between SWNHs and L02 or HepG2 cells, respectively. SWNHs could directly enter into nuclei of HepG2 and could induce cell apoptosis, while SWNHs could induce apoptosis of L02 cells associated with activation of lysosomal function.

Changes in growth of cells also could be determined as a toxic effect. The chemical toxicities could be assessed by an assay called plating efficiency. This evaluated the ability of cells to form colonies after 15 days of culture in the presence of a substance, signaling cell survival and ability to reproduce. Another assay that evaluated the capability of cells to replicate and

http://dx.doi.org/10.5772/61109

determined the concentration of the substance at which 50% of the cells do not multiply is named the median inhibitory dose (ID50). Romero et al. [23] illustrated the effects of inhibiting role on cell proliferation caused by apoptosis, which as toxicity of carbon nanotubes (CNTs) for HepG2 *in vitro*. Moreover, cytotoxicity for cancer cells may have potential therapeutic value. Our results indicated that SWNHs had larger toxicity in HepG2 cells than in L02. In different cells, this major difference may be based on SWNHs surface structure selective affinity to subcellular structures. Based on these differences, new drug carriers or drugs with special structures of SWNHs may be planned for clinical pharmaceutical therapy, especially cancer photothermal therapy. [48, 50] According to the affinity to nuclei in HepG2, the scene of designing cell-targeted drugs might be considered to SWNHs.

In fact, SWNHs themselves suppressed growth and proliferation of HepG2 cells; meanwhile induced their apoptosis. It revealed that SWNHs material could be used as a drug carrier for anti-HCC, and carried anticancer drugs such as cisplatin based on its cooperative therapeutic role.

Nanoparticle almost all located in lysosome and was degradated and sequestrated. The mitochondrial apoptosis and lysosomal dysfunctions could induce toxicological consequences. [51, 52] Based on oxidative stress pathway related to apoptosis caused by nanoparticle, [33] localization of nanoparticles may induce activation of lysosome, which with high content of digestive enzyme, triggering mitochondrial apoptosis. [34] Mitochondria was the main basis of redox and ROS (reactive oxygen species) machinery in cells, and could activate inflammatory cytokines. [32] Oxidative stress toke place in HepG2 cells deal with oxidized or unmodified MWNTs and SWNTs, [25, 28] and in L02 cells deal with hydroxyl-modified, carboxyl-modified or unmodified MWNTs, [29] and in rat hepatocytes deal with fullerenes $C_{60}(OH)_{24}$, $C_{60}(OH)_{12}$, and C_{60}. [31] Gao et al. [19] found that modified MWNTs internalized into human macrophages cells THP-1 and located in lysosomes, induced ROG generation and low mitochondrial membrane potential. Tahara et al. [9] identified that high concentration of SWNHs caused destabilization of lysosomal membrane and ROS generation in murine macrophage RAW 264.7. The results of us demonstrated individual SWNH particles located at mitochondria of L02 and HepG2, or lysosomes of L02 cells. It suggested that mitochondrial apoptosis and lysosomal dysfunctions in liver cells play key role on physiological process related to SWNHs exposure.

The model of transmembrane pathways divided MWNTs into two classes types, singles and clusters. The clusters of CNT were collected in cells associated with energy-dependent endocytosis process; meanwhile extremely dispersed single CNTs directly penetrated cellular membranes entried into cells. [2, 1] We will assure the transmembrane pathway of SWNHs. Because one spherical SWNH aggregate were assembled by about 2000 nanohorns, the aggregates showed clusters of SWNHs. [9] Nevertheless, the aggregate more like one single nanoparticle, and not easy to separate into individual nanohorns. Porter et al. [1, 8] identified the internalization of SWNTs with smaller diameters of SWNTs (0.6–3.5 nm) in cells through nuclear pore complex and other pores. [18] A single SWNHs aggregate has larger diameter (60–100 nm) than fullerene C_{60} (0.7 nm) and single SWNTs (0.6–3.5 nm). It is very interesting how aggregates of individual spherical SWNH composed with 2000 nanohorns internalize in cells and localize at lysosomes in L02 cells, and even entry into the nuclei of HepG2 cells.

Because it was suggested that only nanoparticles less than 40 nm in diameter could enter into nuclei of cells. [53] The low negative charge density on surfaces of SWNHs and the bovine serum proteins used in cell culture may be benefit for SWNH dispersion in culture media, or induce SWNHs recognized with cellular membranes by receptors on the surface of cells. [54]

Researches in this area remain many questions. How SWNHs enter into different cells and locate at different destinations (such as nuclei, liposome, or mitochondria) in different cells? How SWNHs induce the apoptosis in different cells? However, toxicity is a complex event showing several effects, even cell death until metabolic aberrations. Neuro-, liver, and/or kidney toxicity are examples of functional changes not necessarily events linked to cell death. Due to these evidences, the *in vitro* cytotoxicity assays need to exploit different parameters in the cell biochemistry. The assays are important tools to amplify the knowledge about the cytotoxic effects triggered by chemical substances and to predict the toxicity in humans.

Nanotoxicology examines the bioeffects of nanomaterials concerning the toxic activities and depends on the *in vitro* system investigated. Then, validation of *in vitro* assays will be valuable for safety or hazard investigation in an analysis against standard nanostructures. The cell-based toxicity assays can be used to assess potential safety use in the investigation of new potential drugs and to study the correlation between structure, toxicity, and biological activity, permitting changes in the structure chemical or in the formulation with the aim to improve drug-like properties.

The cell culture assays have as advantages the fast results in the research, reduced cost, and a few quantities of substance to be used. Besides that, those models can predict toxicity in animals including humans to get more precise results to establish multitiered *in vitro* screening models.

In this way, the primary goal of *in vitro* models in the toxicity evaluation could be to predict the toxicity *in vivo*, especially human toxicity. The screening permits investigation of the metabolism and biochemical reactions of different substances in order to obtain knowledge about the pharmacokinetics and bioavailability of the drugs. Studies about bioavailability, chemical and metabolic stability, and permeability are necessary *in vitro* screening models that help predicting the human toxicity.

Author details

Guoan Xiang[1*], Jinqian Zhang[2] and Rui Huang[1]

*Address all correspondence to: guoan_66@163.com

1 Department of General Surgery, The Second People's Hospital of Guangdong Province, Southern Medical University, Guangzhou, People's Republic of China

2 Research Center, The Second People's Hospital of Guangdong Province, Southern Medical University, Beijing, People's Republic of China

http://dx.doi.org/10.5772/61109

References

[1] Iijima S, Yudasaka M, Yamada R, et al. Nano aggregates of single-walled graphitic carbon nano-horns. *Chem Phys Lett*. 1999;309(3):165–170.

[2] Murakami T, Tsuchida K. Recent advances in inorganic nanoparticle-based drug delivery systems. *Mini Rev Med Chem*. 2008;8(2):175–183.

[3] Xu JX, Yudasaka M, Kouraba S, Sekido M, Yamamoto Y, Iijima S. Single-wall carbon nanohorn as a drug carrier for controlled release. *Chem Phys Lett*. 2008;461(4–6):189–192.

[4] Ajima K, Yudasaka M, Murakami T, Maigné A, Shiba K, Iijima S. Carbon nanohorns as anticancer drug carriers. *Mol Pharm*. 2005;2(6): 475–480.

[5] Matsumura S, Ajima K, Yudasaka M, Iijima S, Shiba K. Dispersion of cisplatin-loaded carbon nanohorns with a conjugate comprised of an artificial peptide aptamer and polyethylene glycol. *Mol Pharm*. 2007;4(5): 723–729.

[6] Murakami T, Sawada H, Tamura G, Yudasaka M, Iijima S, Tsuchida K. Water-dispersed single-wall carbon nanohorns as drug carriers for local cancer chemotherapy. *Nanomedicine (Lond)*. 2008;3(4):453–463.

[7] Ajima K, Murakami T, Mizoguchi Y, et al. Enhancement of in vivo anticancer effects of cisplatin by incorporation inside single-wall carbon nanohorns. *ACS Nano*. 2008;2(10):2057–2064.

[8] Fan XB, Tan J, Zhang GL, Zhang FB. Isolation of carbon nanohorn assemblies and their potential for intracellular delivery. *Nanotechnology*. 2007;18(19):195103–195108.

[9] Tahara Y, Nakamura M, Yang M, Zhang M, Iijima S, Yudasaka M. Lysosomal membrane destabilization induced by high accumulation of single-walled carbon nanohorns in murine macrophage RAW 264.7. *Biomaterials*. 2012;33(9):2762–2769.

[10] Akasaka T, Yokoyama A, Matsuoka M, Hashimoto T, Watari F. Thin films of single-walled carbon nanotubes promote human osteoblastic cells (Saos-2) proliferation in low serum concentrations. *Mater Sci Eng C*. 2010;30(3):391–399.

[11] Nayak TR, Jian L, Phua LC, Ho HK, Ren Y, Pastorin G. Thin films of functionalized multiwalled carbon nanotubes as suitablescaffold materials for stem cells proliferation and bone formation. *ACS Nano*. 2010;4(12):7717–7725.

[12] Namgung S, Baik KY, Park J, Hong S. Controlling the growth and differentiation of human mesenchymal stem cells by the arrangement of individual carbon nanotubes. *ACS Nano*. 2011;5(9):7383–7390.

[13] Davoren M, Herzog E, Casey A, et al. In vitro toxicity evaluation of single walled carbon nanotubes on human A549 lung cells. *Toxicol In Vitro*. 2007;21(3):438–448.

[14] Albini A, Mussi V, Parodi A, et al. Interactions of single-wall carbon nanotubes with endothelial cells. *Nanomedicine*. 2010;6(2):277–288.

[15] Cheng C, Porter AE, Muller K, et al. Imaging carbon nanoparticles and related cytotoxicity. *J Phys Conf Ser*. 2009;151(1):012030.

[16] Neves V, Gerondopoulos A, Heister E, et al. Cellular localization, accumulation and trafficking of double-walled carbon nanotubes in human prostate cancer cells. *Nano Res*. 2012;5(4):223–234.

[17] Di Giorgio ML, Di Bucchianico S, Ragnelli AM, Aimola P, Santucci S, Poma A. Effects of single and multi walled carbon nanotubes on macrophages: cyto and genotoxicity and electron microscopy. *Mutat Res*. 2011;722(1):20–31.

[18] Porter AE, Gass M, Muller K, Skepper JN, Midgley PA, Welland M. Direct imaging of single-walled carbon nanotubes in cells. *Nat Nanotechnol*. 2007;2(11):713–717.

[19] Gao N, Zhang Q, Mu Q, et al. Steering carbon nanotubes to scavenger receptor recognition by nanotube surface chemistry modification partially alleviates NFκB activation and reduces its immunotoxicity. *ACS Nano*. 2011;5(6):4581–4591.

[20] Porter AE, Gass M, Bendall JS, et al. Uptake of noncytotoxic acid treated single-walled carbon nanotubes into the cytoplasm of human macrophage cells. *ACS Nano*. 2009;3(6):1485–1492.

[21] Mu Q, Broughton DL, Yan B. Endosomal leakage and nuclear translocation of multiwalled carbon nanotubes: developing a model for cell uptake. *Nano Lett*. 2009;9(12): 4370–4375.

[22] Zhou F, Xing D, Wu B, Wu S, Ou Z, Chen WR. New insights of transmembranal mechanism and subcellular localization of noncovalently modified single-walled carbon nanotubes. *Nano Lett*. 2010;10(5): 1677–1681.

[23] Romero G, Estrela-Lopis I, Castro-Hartmann P, et al. Stepwise surface tailoring of carbon nanotubes with polyelectrolyte brushes and lipid layers to control their intracellular distribution and 'in vitro' toxicity. *Soft Matter*. 2011;7(15):6883–6890.

[24] Li L, Zhang J, Yang Y, et al. Single-wall carbon nanohorns inhibited activation of microglia induced by lipopolysaccharide through blocking of Sirt3. *Nanoscale Res Lett*. 2013;8(1):100.

[25] Piret JP, Vankoningsloo S, Noël F, et al. Inflammation response at the transcriptional level of HepG2 cells induced by multi-walled carbon nanotubes. *J Phys Conf Ser*. 2011;304(1):012040.

[26] Yuan J, Gao H, Sui J, Chen WN, Ching CB. Cytotoxicity of singlewalled carbon nanotubes on human hepatoma HepG2 cells: an iTRAQcoupled 2D LC-MS/MS proteome analysis. *Toxicol In Vitro*. 2011; 25(8):1820–1827.

[27] Yuan J, Gao H, Sui J, Duan H, Chen WN, Ching CB. Cytotoxicity evaluation of oxidized single-walled carbon nanotubes and graphene oxide on human hepatoma

HepG2 cells: an iTRAQ-coupled 2D LC-MS/MS proteome analysis. *Toxicol Sci*. 2012;126(1):149–161.

[28] Yuan J, Gao H, Ching CB. Comparative protein profile of human hepatoma HepG2 cells treated with graphene and single-walled carbon nanotubes: an iTRAQ-coupled 2D LC-MS/MS proteome analysis. *Toxicol Lett*. 2011;207(3):213–221.

[29] Liu ZB, Zhou B, Wang HY, et al. Effect of functionalized multi-walled carbon nanotubes on L02 cells. *Acta Academiae Medicinae Sinicae*. (Chinese) 2010;32(4):449–455.

[30] Matsuda S, Matsui S, Shimizu Y, Matsuda T. Genotoxicity of colloidal fullerene C60. *Environ Sci Technol*. 2011;45(9):4133–4138.

[31] Nakagawa Y, Suzuki T, Ishii H, Nakae D, Ogata A. Cytotoxic effects of hydroxylated fullerenes on isolated rat hepatocytes via mitochondrial dysfunction. *Arch Toxicol*. 2011;85(11):1429–1440.

[32] Wang X, Xia T, Duch MC, et al. Pluronic F108 coating decreases the lung fibrosis potential of multiwall carbon nanotubes by reducing lysosomal injury. *Nano Lett*. 2012;12(6):3050–3061.

[33] Shvedova AA, Pietroiusti A, Fadeel B, Kagan VE. Mechanisms of carbon nanotube-induced toxicity: focus on oxidative stress. *Toxicol Appl Pharmacol*. 2012;261(2):121–133.

[34] Andón FT, Fadeel B. Programmed cell death: molecular mechanisms and implications for safety assessment of nanomaterials. *Acc Chem Res*. 2013;46(3):733–742.

[35] Wei L, Lu N, Dai Q, et al. Different apoptotic effects of wogonin via induction of H(2)O(2) generation and Ca(2+) overload in malignant hepatoma and normal hepatic cells. *J Cell Biochem*. 2010;111(6): 1629–1641.

[36] Das SK, Hashimoto T, Kanazawa K. Growth inhibition of human hepatic carcinoma HepG2 cells by fucoxanthin is associated with down-regulation of cyclin D. *Biochim Biophys Acta*. 2008;1780(4):743–749.

[37] Li N, Wang Z, Zhao K, Shi Z, Gu Z, Xu S. Synthesis of single-wall carbon nanohorns by arc-discharge in air and their formation mechanism. *Carbon*. 2010;48(5):1580–1585.

[38] Jiang H, Wu J, He C, Yang W, Li H. Tumor suppressor protein C53 antagonizes checkpoint kinases to promote cyclin-dependent kinase 1 activation. *Cell Res*. 2009;19(4):458–468.

[39] Ford J, Jiang M, Milner J. Cancer-specific functions of SIRT1 enable human epithelial cancer cell growth and survival. *Cancer Res*. 2005; 65(22):10457–10463.

[40] Hamamoto R, Furukawa Y, Morita M, et al. SMYD3 encodes a histone methyltransferase involved in the proliferation of cancer cells. *Nat Cell Biol*. 2004;6(8):731–740.

[41] Li H, Bergeron L, Cryns V, et al. Activation of caspase-2 in apoptosis. *J Biol Chem*. 1997;272(34):21010–21017.

[42] Murata K, Kaneko K, Kokai F, Takahashi K, Yudasaka M, Iijima S. Pore structure of single-wall carbon nanohorn aggregates. *Chem Phys Lett*. 2000;331(1):14–20.

[43] Sohaebuddin SK, Thevenot PT, Baker D, Eaton JW, Tang L. Nanomaterial cytotoxicity is composition, size, and cell type dependent. *Part Fibre Toxicol*. 2010;7:22.

[44] Stewart MS, Davis RL, Walsh LP, Pence BC. Induction of differentiation and apoptosis by sodium selenite in human colonic carcinoma cells (HT29). *Cancer Lett*. 1997;117(1):35–40.

[45] Edinger AL, Thompson CB. Death by design: apoptosis, necrosis and autophagy. *Curr Opin Cell Biol*. 2004;16(6):663–669.

[46] Hashida Y, Tanaka H, Zhou S, et al. Photothermal ablation of tumor cells using a single-walled carbon nanotube-peptide composite. *J Control Release*. 2013;173C:59–66.

[47] Porter AE, Gass M, Muller K, Skepper JN, Midgley P, Welland M. Visualizing the uptake of C60 to the cytoplasm and nucleus of human monocyte-derived macrophage cells using energy-filtered transmission electron microscopy and electron tomography. *Environ Sci Technol*. 2007;41(8):3012–3017.

[48] Iancu C, Mocan L, Bele C, et al. Enhanced laser thermal ablation for the in vitro treatment of liver cancer by specific delivery of multiwalled carbon nanotubes functionalized with human serum albumin. *Int J Nanomedicine*. 2011;6:129–141.

[49] Lei HY, Peng CA, Tang MJ, Reindhart K, Szu HH. Con_A-carbone nanotube conjugate with short wave near-infrared laser ablation for tumor therapy. *Proc SPIE*. 2009;7343:73430Q.

[50] Zhou F, Xing D, Chen WR. Direct imaging the subcellular localization of single-walled carbon nanotubes. *Proc SPIE*. 2011;7900:79000E.

[51] Stern ST, Adiseshaiah PP, Crist RM. Autophagy and lysosomal dysfunction as emerging mechanisms of nanomaterial toxicity. *Part Fibre Toxicol*. 2012;9:20.

[52] Teodoro JS, Simões AM, Duarte FV, et al. Assessment of the toxicity of silver nanoparticles in vitro: a mitochondrial perspective. *Toxicol In Vitro*. 2011;25(3):664–670.

[53] Dawson KA, Salvati A, Lynch I. Nanotoxicology: nanoparticles reconstruct lipids. *Nat Nanotechnol*. 2009;4(2):84–85.

[54] Fleischer CC, Payne CK. Nanoparticle surface charge mediates the cellular receptors used by protein-nanoparticle complexes. J Phys Chem B. 2012;116(30):8901–8907.

Chapter 7

Progress in Genotoxicity Evaluation of Engineered Nanomaterials

Xiaoqing Guo and Tao Chen

Additional information is available at the end of the chapter

http://dx.doi.org/10.5772/61013

Abstract

Engineered nanomaterials (ENMs) are being produced at an increasing rate. Because of their unique physicochemical properties, ENMs have been used in a wide variety of commercial products. The specific properties of ENMs, such as their relatively larger surface area, however, could also cause adverse biological effects different from their bulk counterparts. Nanomaterials can be genotoxic while their bulk counterparts are not, or vice versa, due to these specific characteristics. Also, the differences between nanomaterials and bulk materials can generate uncertainty when measuring the genotoxic potential of ENMs using current genotoxicity assays that were developed for conventional chemicals or bulk materials. In this chapter, we summarize current progress in evaluating the genotoxicity of ENMs with a focus on results from the standard genotoxicity assays, possible mechanisms underlying the genotoxicity of ENMs, the suitability of current genotoxicity assays for evaluation of ENMs, and application of ENM genotoxicity data for risk assessment. Future perspectives for the evaluation of ENM genotoxicity are also addressed.

Keywords: Engineered nanomaterial, genotoxicity, Ames test, Comet assay, Micronucleus assay, reactive oxygen species, risk assessment

1. Introduction

Nanomaterials (NMs) are generally defined as materials having at least one dimension ranging from 1 to 100 nm in size. They may exist in nature, or be purposely engineered from various materials, such as carbon or minerals. Materials engineered to nanoscale size are referred to

as engineered nanomaterials (ENMs). Recently, the European Commission Delegated Regulation redefined ENMs as "any intentionally manufactured material, containing particles, in an unbound state or as an aggregate or as an agglomerate and where, for 50 % or more of the particles in the number size distribution, one or more external dimensions is in the size range 1 nm to 100 nm" [1]. ENMs can be categorized into four classes: carbon-based NMs such as carbon nanotubes and graphene, metal-based NMs such as quantum dots and metal or metal-oxide NMs, dendrimers such as nanosized polymers, and composite NMs [2].

Novel ENMs are now designed and produced at an increasing rate, and having unique physicochemical features such as small size, particular shapes, large surface areas, and surface activity. These features provide ENMs specific characteristics of high thermal and energy conductivity, durability, strength, and/or reactivity [3], which facilitate their applications in a whole host of areas ranging from aerospace, engineering, and nanoelectronics to medical healthcare. According to a Wilson Center study, more than 1,600 manufacturer-identified nanotechnology-based consumer products have been introduced to the market, and more than half were in the Health and Fitness subcategory [4]. A wide range of human-application-related ENM products have emerged in textiles, the food industry, cosmetics, sunscreens, and the biomedical field including gene/drug delivery platforms, biosensors, cell and tumor imaging, and cancer photothermal therapy [5, 6]. With their widespread human exposure, the potential health risks stemming from ENMs have drawn increasing attention since the first report highlighting the immediate need for evaluating possible adverse health, safety, and environmental impacts of ENMs published by the Royal Society and Royal Academy of Engineering in 2004 [7]. In the same year, a new scientific field named "Nanotoxicology" emerged to investigate the toxic effects of ENMs. The genotoxicity evaluation of ENMs has attracted much attention due to its importance for nanotechnology regulation and risk assessment [8].

Genotoxicity is the ability of substances to damage DNA, the genetic information, within organisms. Thus, genotoxic agents can give rise to mutations. Because mutations can lead to cancer, genotoxicity evaluation has been utilized widely to evaluate the carcinogenic potential of chemical and physical exposures. International organizations and regulatory agencies, such as the Organization for Economic Co-operation and Development (OECD) and the International Conference on Harmonization (ICH), have published consensus guidance documents that describe a battery of test assays for genotoxicity assessment to support regulatory decision-making. These *in vitro* and *in vivo* assays measure different genotoxicity endpoints such as DNA breaks, gene mutations, and chromosomal alterations [9, 10]. The most widely used genotoxicity battery includes the bacterial *Salmonella* mutagenicity test (the Ames test); *in vitro* mammalian cell assays, such as the Comet assay, the mouse lymphoma gene mutation assay (MLA), and the micronucleus (MN) assay; and *in vivo* assays, including the *in vivo* MN and Comet assays. Although designed for conventional chemicals and bulk materials, these assays have commonly been adopted for measuring the genotoxicity of ENMs. In this chapter, we summarize test results from the genotoxicity evaluation of ENMs, focusing on those using standard genotoxicity assays, possible mechanisms underlying the genotoxicity of ENMs, the suitability of current genotoxicity assays for the genotoxicity evaluation of ENMs, and the use of genotoxicity data for the risk assessment of ENMs.

http://dx.doi.org/10.5772/61013

2. Genotoxicity of ENMs

In comparison to the fast-growing ENM market, studies evaluating ENM genotoxicity are still limited [11]. A literature search performed by Magdolenova et al. [12] found that from 2000 to 2012 only 2.6% of articles on ENM toxicity describe genotoxicity studies. Although both positive and negative results have been reported on the genotoxicity of ENMs in various cell and animal test models, the existing data indicate that many ENMs are genotoxic [2, 11, 13, 14]. In order to provide a holistic picture of the current situation on genotoxicity testing of ENMs, we performed a literature search in PubMed using "nanoparticles" or "nanomaterial" and "Comet," "micronuclei," "Ames," "*Hprt*," or "mouse lymphoma assay" as key words. A total of 274 publications were identified; the distribution of year of publication is shown in Figure 1. There was a clear increase in the number of publications/year for both the *in vitro* and *in vivo* ENM genotoxicity studies, up to 2012, where a plateau may have been reached. Among the different assays used for evaluation of ENM genotoxicity in the publications, the Comet assay was the most frequently employed assay, followed by the MN assay, both *in vitro* (Figure 2A) and *in vivo* (Figure 2B). This observation is consistent with a previous report that summarized 112 ENM genotoxicity studies (94 *in vitro*, 22 *in vivo*) from years 2000 to 2012 [12].

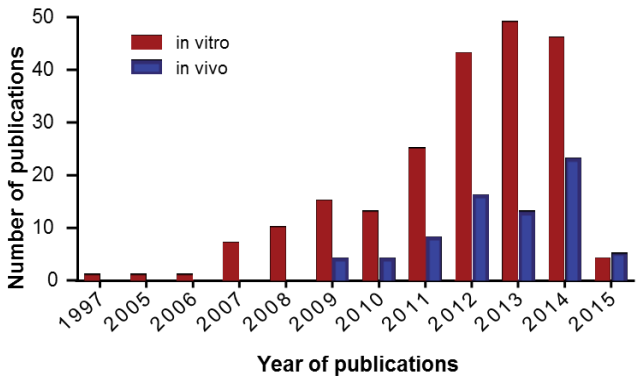

Figure 1. Literature review results of the publications per year on genotoxicity of engineered nanomaterials. Red bars indicate *in vitro* studies and blue bars indicate *in vivo* studies.

2.1. *In vitro* studies

A total of 215 publications were found that investigated the *in vitro* genotoxicity of ENMs. The Ames test is usually the initial step used for quickly screening potential mutagens and for identifying potential human carcinogens. This assay detects base substitution and frameshift mutations depending on the strain of the bacteria *Salmonella typhimurium* used [15]. Although this assay has been widely used for testing bulk materials, the Ames test was used less frequently for ENMs as compared to other genotoxicity assays [16]. Based on our literature search, among the most tested ENMs are nanoparticles (NPs) of silver (Ag), titanium dioxide (TiO_2), aluminium oxide (Al_2O_3), Zinc oxide, iron oxide, iron-platinum (FePt), single-wall

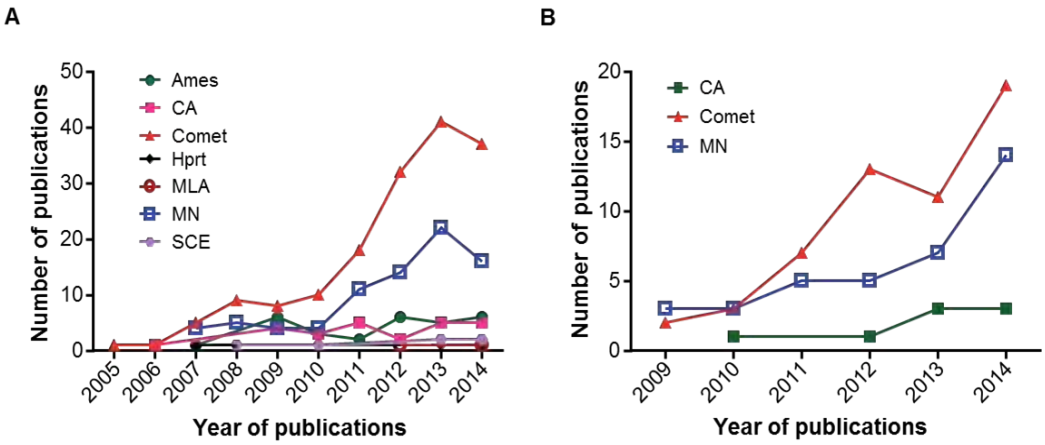

Figure 2. The trend in genotoxicity endpoint studies on engineered nanomaterials. (A) *in vitro* genotoxicity assays; (B) *in vivo* genotoxicity assays.

carbon nanotubes (SWCNTs), multiwalled carbon nanotubes (MWCNTs), and fullerenes [17-32]. Most of the Ames tests were negative both in the presence and the absence of metabolic activation. As shown in Table 1, only 27% of ENMs were positive in one or more tester strains in the Ames test. Most of the positive responses were weak or resulted from water-soluble NPs [16, 20, 24, 28, 30, 31]. Among possible explanations for the negative responses are the inability of the ENMs to penetrate the bacterial cell wall and the insensitivity of most of the tester strains to oxidative DNA damage, the primary mechanism for ENM genotoxicity [17]. In addition, the antimicrobial properties of some ENMs, such as Ag NPs, may limit the test concentrations due to cytotoxicity, thus reducing the sensitivity of the test [17]. In a study using 5 tester strains (TA98, TA100, TA1535, TA1537, and TA102) of *Salmonella typhimurium*, due to antimicrobial properties, the highest testable concentrations of 5 nm Ag NPs were 2-40 μg/plate, which is much lower than the limit of 5,000 μg/plate that is recommended for nontoxic test articles [17].

The Comet assay, also known as the single-cell gel electrophoresis assay, is a relatively simple and sensitive method for measuring DNA damage in individual eukaryotic cells [33]. Our literature review shows that 276 ENMs have been evaluated in 168 reports using the *in vitro* Comet assay. Thus, it is the most frequently used assay for ENM genotoxicity assessment (Table 1). The materials most tested with the Comet assay were TiO_2-, iron-, Ag-, and carbon-based ENMs. The majority of these tested ENMs (214 out of 276, 78%) induced DNA damage in various cell types in the standard or modified Comet assays. The high sensitivity of the assay may be ascribed to its ability to detect single- and double-strand breaks, cross-links, base damage, oxidative stress, DNA methylation, and apoptotic nuclei [33-35]. Some ENMs producing oxidative DNA damage were negative in the standard alkaline Comet assay, but were positive in the enzyme-modified Comet assay in which lesion-specific endonucleases were added to recognize particular oxidized nucleotides and create oxidized DNA-damage-specific breaks. The most commonly used modifying enzymes in these assays were formamidopyrimidine DNA glycosylase (FPG), followed by endonuclease III (EndoIII) from *Escherichia*

coli and human-derived oxoguanine DNA glycosylase (hOGG1) [36]. Oxidative DNA lesions in FPG-sensitive sites were found in Fe_3O_4 NP-treated A549 type II lung epithelial cells [37], and in SWCNT- and C60-treated FE1-Muta™ Mouse lung epithelial cells [38].

Assays	Publications[b]	ENMs[c]	Positive outcomes[d]	Negative outcomes[d]
Comet	168	276	214 (78%)	62 (22%)
MN	83	126	75 (60%)	51 (40%)
Ames	30	55	15 (27%)	40 (73%)
CA	25	36	16 (44%)	20 (56%)
Hprt	6	8	5 (63%)	3 (37%)
SCE	6	9	6 (67%)	3 (33%)
MLA	2	2	2 (100%)	0 (0%)

[a]Data represent a literature review on the *in vitro* genotoxicity of engineered nanomaterials. Literature was obtained from the PubMed online database using "nanomaterial", "comet", "micronuclei", "ames", "*hprt*", or "mouse lymphoma assay" as key words. [b]The number of papers published using each assay. [c]The number of various ENMs tested in current literature citations. [d]The number of positive or negative outcomes for genotoxicity testing on ENMs. The number in parentheses indicates the percentage of positive or negative outcomes for each assay. CA, chromosome aberration; *Hprt*, hypoxanthine phosphorybosyl transferase assay; MLA, the mouse lymphoma assay; MN, the micronucleus assay; SCE, sister chromatid exchange.

Table 1. Summary of *in vitro* genotoxicity outcomes of engineered nanomaterials (ENMs)[a]

The MN assay detects chromosome fragments and whole chromosomes in the cytoplasm of interphase cells resulting from the clastogenic and aneugenic activities of mutagens, indicating chemical-induced chromosome damage (OECD TG487) [39]. The MN assay was the second most used assay for the evaluation of ENM genotoxicity (Table 1) [12, 16, 40]. Two versions of the MN assay, with or without pretreatment with cytochalasin B (cytoB) which blocks cytokinesis and results in binucleated cells, were used for NM studies [2, 39]. Approximately 60% of the tested ENMs produced concentration-dependent micronucleus formation or a positive response at high concentrations, including TiO_2 [8, 41], silicon dioxide (SiO_2) [42], cerium oxide (CeO_2) [43], cobalt-chromium (Co-Cr) [44, 45], MWCNTs [46, 47], and Ag NPs [17]. Kim et al. [29] demonstrated that in the absence of S9 metabolic activation, 10 μg/ml Ag NPs with an average size of 59 nm induced significantly greater MN formation using the protocol without cytoB than that with cytoB. It was demonstrated that cytoB could inhibit the cellular uptake of particulate materials and may contribute to negative results in MN assays [40].

The chromosome aberration (CA) test identifies agents that cause structural chromosome alterations in cultured mammalian cells (OECD TG473) [48]. This labor-intensive assay is routinely used for screening possible mammalian mutagens and carcinogens [14]. The CA assay was the third most commonly used mammalian cell assay for ENM genotoxicity investigation in our literature search (Table 1). Thirty-six ENMs including MWCNTs, C_{60}

fullerenes, Ag, and TiO_2 NPs have been evaluated using the CA test in 25 publications. Less than half (44%) of the tested ENMs were positive. Impressively, Ag NPs induced significant chromosomal aberrations at concentrations as low as 0.1 μg/ml in human mesenchymal stem cells [49] and at a concentration of 0.1 $\mu g/cm^2$ in a nonmammalian fish cell line [50].

Another assay used for detecting chromosome damage is the sister chromatid exchange (SCE) assay. This assay detects reciprocal exchanges of DNA between two sister chromatids of a duplicating chromosome [8]. Only 9 ENMs have been investigated using the SCE assay. The results revealed a surprisingly high positive response rate (67%) for the tested ENMs. SiO_2 NPs (at different sizes of 6, 20, 50 nm), which is considered relatively less genotoxic than other metal ENMs, significantly increased the SCE frequency in peripheral blood lymphocytes while they were negative in the MN assay [51].

The MLA and the hypoxanthine phosphorybosyl transferase (*Hprt*) assay, using thymidine kinase (*Tk*) and *Hprt* genes as target genes, respectively, are the most commonly used assays for the determination of chemical-induced gene mutations [52]. Both assays are included in the guidelines for mammalian gene mutation tests (OECD 476) [53]. There were only two MLA and six *Hprt* studies found in the literature. In the MLA studies, 5 nm uncoated Ag NPs produced dose-dependent cytotoxicity and mutagenicity at doses of 3-6 μg/ml [34], and tungsten carbide-cobalt (WC-Co) NPs with a diameter of 20-160 nm induced significant increases in cytotoxicity and mutagenicity following both 4 h and 24 h treatments [54]. Six *Hprt* studies investigated the mutagenic effect of four ENMs, TiO_2, SiO_2, ultrafine quartz, and SWCNTs, with positive results for *Hprt* gene mutation found for TiO_2, SiO_2, and ultrafine quartz [41, 42, 55-58]. Manshian et al. [58] investigated the genotoxicity of three sizes of SWCNTs, with a diameter of 1-2 nm and a length of 400-800 nm, 1-3 μm, or 5-30 μm, using MCL-5 human B-lymphoblastoid cells. Only the 1-3 μm SWCNTs significantly increased *Hprt* point mutations at concentrations ≥25 μg/ml. A chronic exposure of Chinese hamster ovary (CHO-K1) cells with TiO_2 NPs at up to 40 μg/ml for 60 days produced negative results [57].

2.2. *In vivo* studies

In vivo responses reflect the systematic biodistribution of ENMs and evaluate the cytotoxicity/genotoxicity to different tissues and organs. Our literature search identified 73 publications on the *in vivo* genotoxicity of ENMs, with the number of publications increasing with time (Figure 1). As shown in Table 2, the Comet assay remains the most frequently used *in vivo* assay for investigating ENM genotoxicity, followed by the *in vivo* MN assay and then the CA assay. Both the *in vivo* MN and Comet assays are recommended by OECD (OECD TG 474 and 489) and ICH for regulatory decision-making [10, 59, 60]. Some ENMs, such as MWCNTs [47], carbon black [61], TiO_2 [8, 56, 62], CdSe quantum dots [63], and Ag NPs [64, 65], caused both DNA strand breaks and chromosomal damage in experimental animals (mainly mice and rats). However, in contrast to the high proportion of positive outcomes in *in vitro* studies, about half of the *in vivo* MN and Comet assay studies were negative for the tested ENMs (Table 2), probably due to the higher DNA repair capacity inherent to *in vivo* models as compared to *in vitro* models. It is worth noting that some of the positive ENMs were genotoxic only at the highest doses tested or in enzymatically modified Comet assays. In the liver of male B6C3F1

mice intravenously administered 15-100 nm PVP or 10-80 nm silicon-coated Ag NPs at a dose of 25 mg/kg/day for 3 consecutive days, no increase in DNA breaks was observed with the standard Comet assay. However, significant induction of oxidative DNA damage by the Ag NP treatment was detected with the EndoIII and hOOG1-modified Comet assay in the B6C3F1 mouse livers [65]. Interestingly, in the 8 publications using the *in vivo* CA assay, 75% of test articles were positive, which was much higher than the positive responses (44%) detected with *in vitro* CA assay testing of ENMs. This finding may be ascribed to the limited numbers of ENMs tested in the *in vivo* studies. The ENMs that did increase CA frequencies were CeO_2 [66, 67], TiO_2 [68], Ag [69], and MnO_2 NPs [70, 71]. Similar to the *in vitro* genotoxicity studies, inconsistent genotoxic outcomes were reported with *in vivo* models as well; however, there remains convincing evidence that ENMs can be genotoxic *in vivo*, depending on particle size, surface coating, exposure route, and exposure duration [72].

Assays	Publications[b]	ENMs[c]	Positive outcomes[d]	Negative outcomes[d]
Comet	60	87	49 (56%)	38 (44%)
MN	38	60	28 (47%)	32 (53%)
CA	8	8	6 (75%)	2 (25%)

[a-d] See Table 1 for notes.

Table 2. Summary of *in vivo* genotoxicity outcomes of engineered nanomaterials (ENMs)[a]

3. Possible mechanisms underlying genotoxicity of ENMs

ENMs are engineered to possess unique physicochemical properties that may have the potential to induce genotoxicity through different mechanisms [14]. Although these genotoxic mechanisms are still uncertain at present, studies indicate that ENMs can induce genotoxicity both directly and indirectly. Among these mechanisms, ENM-induced genotoxicity is most often attributed to oxidative stress.

3.1. Oxidative stress

A large number of studies suggest that oxidative stress plays a key role in ENM-induced genotoxicity [73, 74]. Induction of oxidative stress from ENM exposures could be the result of increased reactive oxygen species (ROS) or depletion of antioxidant defense molecules because of the high surface area of ENMs and their interaction with cells and cellular components [14, 73]. Increased ROS can modify DNA bases to induce oxidative DNA adducts, DNA single- and double-strand breaks, DNA cross-links, and DNA-protein cross-links [14, 75]. If ENM-induced DNA damage is not repaired, these DNA modifications and lesions can potentially cause mutations [76]. The correlation between oxidative stress and ENM-induced genotoxicity has been well documented in a number of studies using the Comet assay, γ-H2AX assay, and 8-hydroxy-2′-deoxyguanosine (8-OH-dG) assay [77].

To determine whether the mutagenicity of Ag NPs resulted from an oxidative stress mechanism [34], we conducted the standard Comet assay concurrent with the oxidative stress Comet assay. In the oxidative stress Comet assay, addition of FPG, EndoIII and hOGG1 lesion-specific endonucleases produces secondary DNA breaks by cutting at oxidative DNA adducts. While the Ag NP treatment of the cells did not increase DNA breaks in the standard assay, the FPG, EndoIII and hOGG1 modified Comet assays did detect oxidative DNA damages (Figure 3). These results suggest that Ag NP exposures induced oxidized nucleotides that could result in mutations.

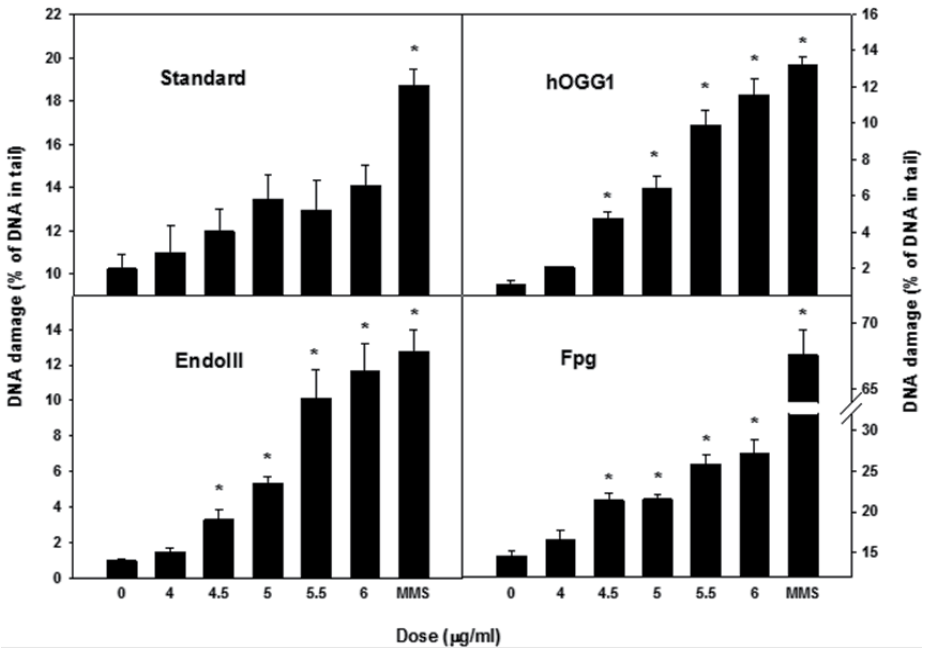

Figure 3. Silver nanoparticles induce DNA damage via oxidative stress. Mouse lymphoma cells were treated with 5nm Ag NPs for 4 hours. DNA damage was measured by the Comet assay. In the standard Comet assay, DNA breaks increased insignificantly with the increasing concentrations. In the oxidative stress Comet assay, however, addition of the different lesion-specific endonucleases (hOGG1, EndoIII, and Fpg) that cut different oxidative DNA adducts resulted in clear concentrations-dependent increases in DNA breaks. * indicates $p < 0.01$ when compared with the control group.

3.2. Direct interaction with DNA and nuclear protein

Due to their small size and charged surfaces, ENMs may be internalized through cellular membranes, reach the nucleus by diffusion across the nuclear membrane or by penetrating during mitosis. Thus, they can directly interact with DNA. During interphase, ENMs can chemically bind to DNA molecules and influence DNA replication that could result in DNA damage. It has been shown that NPs can dissociate double-stranded DNA [78] and cause clastogenic effects (breaks in chromosomes) or aneugenic effects (producing abnormal number of chromosomes) [12].

ENMs also can directly bind to DNA-related proteins leading to intranuclear protein aggregates that inhibit DNA replication, transcription, cell proliferation, and DNA repair [12, 14, 79]. It has been reported that SiO_2 NPs can enter the cell nucleus and cause aberrant clusters of topoisomerase I in the nucleoplasm [79]. *In silico* studies have identified a binding site for fullerene ENMs, on human DNA topoisomerase II alpha [80], and potential interactions between ENMs and proteins involved in the DNA mismatch repair pathway [81].

3.3. Ions released from ENM surfaces

Toxic metal ions can easily release from ENMs into their surrounding environment due to their relatively large surface area. These ions may exert genotoxic effects by the production of intracellular ROS [12], by binding to cellular macromolecules, or by activating mitogenic signaling pathways and inducing the expression of cellular proto-oncogenes [82]. For example, Co NPs can release Co^{2+} ions into the culture media [83], and Co^{2+} is a topoisomerase II poison that stimulates DNA cleavage in human MCF-7 cells [84] and induces micronuclei in the MN assay [85].

3.4. Inflammation

Inflammation is an important protective defense against tissue injury and infection. However, it can also induce genotoxicity in the form of DNA single- and double-strand breaks, chromosome fragmentation, point mutations, and DNA repair deficiency [14, 86]. Silica NP exposures induce genotoxic effects in male Wistar rats through an inflammatory reaction [87]. Many other ENMs, such as TiO_2, carbon black, magnetite iron, CeO_2, SWCNTs, and MWCNTs, can generate various degrees of inflammatory reactions, including increased expression of pro-inflammatory cytokines and inflammation-related genes, and formation of microgranulomas in treated animals [88, 89]. In addition, the association between ROS and inflammation has been demonstrated, where generation of inflammation and activated inflammatory cells can increase ROS production [90].

Chronic rat inhalation studies showed that TiO_2 NPs caused bronchoalveolar adenomas and cystic keratinizing squamous cell carcinomas, as well as alveolar/bronchiolar adenoma. Generation of ROS and induction of inflammation by TiO_2 NPs resulting in oxidative stress and genotoxicity were considered important factors in the initiation and progression stages of TiO_2 NP carcinogenesis [8, 91].

4. Approaches to the risk assessment of ENM genotoxicity

4.1. Suitability of current genotoxicity assays for evaluation of ENMs

A complete genotoxicity evaluation of a test agent required by regulatory agencies generally involves using a test battery that includes a bacterial gene mutation assay (e.g., the Ames test), an *in vitro* cytogenetic assay in mammalian cells and/or the mouse lymphoma mutation assay, and an *in vivo* cytogenetic assay (e.g., the *in vivo* rodent MN assay). However, these assays were developed for the evaluation of conventional chemicals and bulk materials. Whether or

not they are suitable for measuring ENM genotoxicity is still under investigation. ENM genotoxicity modes of action are not very clear and not always predictable. Thus, it remains a question as to whether the standard tests are appropriate and if they are sufficient.

Because bacterial mutation analysis is sometimes the only assay used for genotoxicity testing, it is very important to assess the utility of the Ames test for evaluating ENM mutagenicity. Most of the Ames test data for ENMs thus far reported are negative or only very weakly positive due to the inability of many ENMs to penetrate through the bacterial cell wall and the antimicrobial activity of some ENMs [16]. Our previous study indicated that TiO_2 NPs are not able to penetrate the cell wall of *Salmonella* tester strains [18]. Thus, there is a growing concern as to whether the Ames test is appropriate for evaluating ENM genotoxicity [92]. Since the Ames test is an important assay for measuring mutagenicity, if it is excluded from the genotoxicity test battery for ENMs, it may be necessary to include a mammalian cell gene mutation assay in the test battery [92].

Other standard genotoxicity assays used for evaluating NMs have shown inconsistent results. The most sensitive method for measuring ENM genotoxicity is the Comet assay. This assay produces the greatest number of positive results for ENMs both *in vitro* and *in vivo* (Table 1 and 2). The MN assay is another commonly used assay for detecting chromosome damage caused by ENMs. The MN data reveal that the *in vitro* assay is more sensitive than the *in vivo* assay. Mammalian gene mutation assays (*Hprt*, MLA, and transgenic mutation assays) and the CA assay are less frequently used than the Comet and MN assays. These genotoxicity assays are generally accepted for evaluation of ENMs with certain modifications. CytoB interferes with the uptake of ENMs and thus the binucleated MN assay should be used with caution. Also, the potential lack of uptake of agglomerated NMs by cells, and possible interference of NMs with endpoint measurement when measuring fluorescence should be considered, since these factors create a false positive or false negative result [92].

4.2. Regulatory approaches

For more than 40 years, the OECD has played an important regulatory role in ensuring the safe use of chemicals. In response to the fast-growing commercial applications for ENMs, the OECD established a project entitled "Manufactured Nanomaterials and Test Guidelines" in 2006 to ensure that the risk assessment of ENMs would be conducted in a suitable, science-based and internationally harmonized manner. After six years of work, the OECD concluded that it was unnecessary to develop completely new testing approaches for NMs and that most current test guidelines for assessment of traditional chemicals were in general applicable for ENMs. However, it was indicated that in some cases, modifications were needed to adapt current test guidelines for ENM specifications [93]. The OECD recently published a report on the genotoxicity testing of ENMs, in which some consensus statements were addressed [94]. Major recommendations were that the Ames test is not recommended for investigating the genotoxicity of ENMs; ENM characterization should be undertaken in the cell culture medium both at the beginning and after the treatment; the extent of cellular uptake is a critical factor to consider and cell lines that can take up ENMs are preferred for genotoxicity testing; cytoB should be added only postexposure or using a delayed cotreatment protocol for the *in vitro*

binucleated MN assay; pharmacokinetic investigations need to be conducted to determine if the ENMs reach the target tissue for *in vivo* studies; and the route most applicable to human exposure should be selected for ENM genotoxicity testing.

The U.S. Food and Drug Administration (FDA) has also made significant efforts to address the regulatory issues surrounding ENM products. The FDA Nanotechnology Task Force report addressed scientific and regulatory issues regarding to the safety and effectiveness of FDA-regulated products containing NMs. Also, the FDA issued a draft document on the use of nanotechnology in food for animals and three final guidance documents in 2014 related to nanotechnology application in regulated products, including cosmetics and food substances [95]. These documents assert that *in vitro* and *in vivo* mutagenicity/genotoxicity data are considered as one of the important factors for the safety assessment of ENMs. These guidance documents mainly focus on ENMs because materials manipulated on the nanoscale level may have altered biocompatibility and/or toxicity [96]. For example, some tea polyphenols in their bulk form have opposite effects on DNA damage in treated cells to those in their nano form [97].

4.3. Proposed tiered approaches for genotoxicity testing

Despite some discrepancies in the current literature, there is compelling evidence that some ENMs are genotoxic and potentially carcinogenic in living systems. Thus, multidisciplinary tiered toxicity testing approaches using different models and test methods are proposed for risk assessment of various ENMs [11, 98]. These proposals emphasize that a thorough characterization of the physicochemical properties of ENMs should be the first step in the evaluation of their genotoxicity. Then an *in silico* study should follow to simulate quantitative structure activity relationships between ENMs and their potential interaction with cellular macromolecules such as DNA and protein [98]. If positive, *in vitro* studies should be performed to assess the dose-response effects on cytotoxicity and genotoxicity of target cells, followed by mechanistic studies and *in vivo* studies to validate *in vitro* results. Positive outcomes for genotoxicity and mutagenicity may suggest a need for conducting further carcinogenicity and reproductive toxicity tests [11]. The proposed tiered approaches remain to be validated in the future.

5. Future perspectives

According to the current literature addressing ENM genotoxicity, a lack of physicochemical characterization, especially characterizing the ENMs in the testing medium, remains the biggest problem in most studies, and this may account for some of the conflicting test results. Inconsistency in dose metrics and the test systems also are important factors affecting the comparisons between studies [14]. Thus, the following should be taken into account for improving the genotoxicity evaluation of ENMs.

1. Comprehensively detailed physicochemical characterization of ENMs should be performed before and during any genotoxicity study. Important properties that can influence ENM-induced genotoxicity include size, coating, shape, chemical composition, crystal

structure, purity, surface area, surface chemistry, surface charge, solubility, and agglomeration. Measurements should include the stability of ENMs in the relevant test medium, such as aggregation status and ion release from metallic ENMs.

2. A battery of standard genotoxicity assays covering a wide range of mechanisms specifically tailored for ENMs is needed, since current studies generally use genotoxicity test batteries adapted for traditional chemicals. A mammalian mutation assay such as the MLA or an *Hprt* assay should be used in the battery given that the Ames test is not appropriate for testing the mutagenicity of ENMs. Integration of cytotoxicity assessment into genotoxicity evaluations will aid in avoiding false-positive results, especially in situations where genotoxicity can only be observed at excessively high concentrations with high cytotoxicity.

3. Appropriate controls, specifically ENM-related positive controls, need to be included in ENM genotoxicity tests. NMs may be different from their bulk materials in terms of uptake, absorption, transport into cells, and transport across barriers (e.g., blood-brain barrier) or have altered bioavailability or biological half-life [99]. Positive controls from bulk materials may or may not have the same tissue distributions as the corresponding nanoscale materials. If a soluble bulk material used as a positive control for a genotoxicity assay can reach a specific tissue for testing while insoluble ENMs cannot get into the target tissue, a false negative result could occur. Thus, ENM-related positive controls will benefit the genotoxicity evaluation of ENMs, and eventually ENM hazard identification and risk assessment.

4. Long-term impacts of ENM exposures need to be considered. To date, only a few studies are available describing the chronic and subchronic toxicity of ENMs *in vivo* or *in vitro*. Although no cytotoxicity or genotoxicity were observed for a chronic exposure of TiO_2 in Chinese hamster ovary cells [57], carbon-based ENMs could be visualized in the lung of mice following a 1-year pulmonary exposure, and SWCNT exposures increased the rate of K-*ras* mutations, MN formation, and nuclear protrusions in pulmonary epithelial cells [100].

5. Adopting high-throughput approaches, i.e., CometChip technology, for detection of DNA damage will facilitate screening a large number of ENMs. In addition, other endpoints and biomarkers may need to be considered for ENM genotoxicity assessment since a variety of molecular pathways, autophagy, and epigenetic alterations have been reported to be involved in ENM-induced genotoxic effects [101-105].

Acknowledgements

We thank Drs. Robert Heflich, Nan Mei, and Dayton Petibone for their critical review of this book chapter. The information in these materials is not a formal dissemination of information by the U.S. FDA and does not represent agency position or policy.

Author details

Xiaoqing Guo* and Tao Chen*

*Address all correspondence to: xiaoqing.guo@fda.hhs.gov; tao.chen@fda.hhs.gov

Division of Genetic and Molecular Toxicology, National Center for Toxicological Research, U.S. Food and Drug Administration, Jefferson, USA

References

[1] EU Commissions Delegated Regulation, No 1363/2013 amending Regulation (EU) No 1169/2011 of the European Parliament and of the Council on the provision of food information to consumers as regards the definition of 'engineered nanomaterials,' in *Off J EU*. 2013. p. L 343/26-28.

[2] Ng, C.T., et al. Current studies into the genotoxic effects of nanomaterials. *J Nucleic Acids*, 2010. 947859.

[3] Powell, M.C. and M.S. Kanarek. Nanomaterial health effects--part 1: background and current knowledge. *WMJ*, 2006. 105(2): p. 16-20.

[4] Wilson Center. Consumer Products Inventory. The project on emerging nanotechnologies. http://www.nanotechproject.org/cpi/about/analysis/, 2015.

[5] Ahamed, M., M.S. Alsalhi, and M.K. Siddiqui. Silver nanoparticle applications and human health. *Clin Chim Acta*, 2010. 411(23-24): p. 1841-8.

[6] Guo, X. and N. Mei. Assessment of the toxic potential of graphene family nanomaterials. *J Food Drug Anal*, 2014. 22(1): p. 105-15.

[7] Royal Society & The Royal Academy of Engineering report. *Nanoscience and nanotechnologies: opportunities and uncertainties.* http://www.nanotec.org.uk/report/Nano%20report%202004%20fin.pdf, 2004: p. 1-127.

[8] Chen, T., J. Yan, and Y. Li. Genotoxicity of titanium dioxide nanoparticles. *J Food Drug Anal*, 2014. 22(1): p. 95-104.

[9] FDA. *Toxicological Principles for the Safety Assessment of Food Ingredients*. Redbook 2000: IV.C.1 Short-Term Tests for Genetic Toxicity 2007 [cited 2014 september 16].

[10] ICH, *Guidance for Industry S2(R1) Genotoxicity Testing and Data Interpretation for Pharmaceuticals Intended for Human Use.* http://www.fda.gov/downloads/Drugs/Guidances/ucm074931.pdf, 2012: p. 1-28.

[11] Savolainen, K., et al. Risk assessment of engineered nanomaterials and nanotechnologies--a review. *Toxicology*, 2010. 269(2-3): p. 92-104.

[12] Magdolenova, Z., et al. Mechanisms of genotoxicity. A review of in vitro and in vivo studies with engineered nanoparticles. *Nanotoxicology*, 2014. 8(3): p. 233-78.

[13] Magaye, R., et al. Genotoxicity and carcinogenicity of cobalt-, nickel- and copper-based nanoparticles. *Exp Ther Med*, 2012. 4(4): p. 551-61.

[14] Singh, N., et al. NanoGenotoxicology: the DNA damaging potential of engineered nanomaterials. *Biomaterials*, 2009. 30(23-24): p. 3891-914.

[15] Claxton, L.D., et al. Guide for the Salmonella typhimurium/mammalian microsome tests for bacterial mutagenicity. *Mutat Res*, 1987. 189(2): p. 83-91.

[16] Landsiedel, R., et al. Genotoxicity investigations on nanomaterials: methods, preparation and characterization of test material, potential artifacts and limitations–many questions, some answers. *Mutat Res*, 2009. 681(2-3): p. 241-58.

[17] Li, Y., et al. Genotoxicity of silver nanoparticles evaluated using the Ames test and in vitro micronucleus assay. *Mutat Res*, 2012. 745(1-2): p. 4-10.

[18] Woodruff, R.S., et al. Genotoxicity evaluation of titanium dioxide nanoparticles using the Ames test and Comet assay. *J Appl Toxicol*, 2012. 32(11): p. 934-43.

[19] Di Sotto, A., et al. Multi-walled carbon nanotubes: Lack of mutagenic activity in the bacterial reverse mutation assay. *Toxicol Lett*, 2009. 184(3): p. 192-7.

[20] Gomaa, I.O., et al. Evaluation of in vitro mutagenicity and genotoxicity of magnetite nanoparticles. *Drug Discov Ther*, 2013. 7(3): p. 116-23.

[21] Han, D.W., et al. In-vivo and in-vitro biocompatibility evaluations of silver nanoparticles with antimicrobial activity. *J Nanosci Nanotechnol*, 2012. 12(7): p. 5205-9.

[22] Hu, P., et al. Genotoxicity evaluation of stearic acid grafted chitosan oligosaccharide nanomicelles. *Mutat Res*, 2013. 751(2): p. 116-26.

[23] Landsiedel, R., et al. Gene toxicity studies on titanium dioxide and zinc oxide nanomaterials used for UV-protection in cosmetic formulations. *Nanotoxicology*, 2010. 4: p. 364-81.

[24] Maenosono, S., Suzuki, T., and Saita, S. *Mutagenicity of water-soluble FePt nanoparticles in Ames test. J Toxicol Sci*, 2007. 32(5): p. 575-9.

[25] Naya, M., et al. Evaluation of the genotoxic potential of single-wall carbon nanotubes by using a battery of in vitro and in vivo genotoxicity assays. *Regul Toxicol Pharmacol*, 2011. 61(2): p. 192-8.

[26] Shinohara, N., et al. In vitro and in vivo genotoxicity tests on fullerene C60 nanoparticles. *Toxicol Lett*, 2009. 191(2-3): p. 289-96.

[27] Wirnitzer, U., et al. Studies on the in vitro genotoxicity of baytubes, agglomerates of engineered multi-walled carbon-nanotubes (MWCNT). *Toxicol Lett*, 2009. 186(3): p. 160-5.

[28] Hasegawa, G., Shimonaka, M., and Ishihara, Y. Differential genotoxicity of chemical properties and particle size of rare metal and metal oxide nanoparticles. *J Appl Toxicol*, 2012. 32(1): p. 72-80.

[29] Kim, H.R., et al. Appropriate in vitro methods for genotoxicity testing of silver nanoparticles. *Environ Health Toxicol*, 2013. 28: p. e2013003.

[30] Liu, Y., et al. Genotoxicity assessment of magnetic iron oxide nanoparticles with different particle sizes and surface coatings. *Nanotechnology*, 2014. 25(42): p. 425101.

[31] Jomini, S., et al. Modifications of the bacterial reverse mutation test reveals mutagenicity of TiO(2) nanoparticles and byproducts from a sunscreen TiO(2)-based nanocomposite. *Toxicol Lett*, 2012. 215(1): p. 54-61.

[32] Balasubramanyam, A., et al. In vitro mutagenicity assessment of aluminium oxide nanomaterials using the Salmonella/microsome assay. *Toxicol In Vitro*, 2010. 24(6): p. 1871-6.

[33] Tice, R.R., et al. Single cell gel/comet assay: guidelines for in vitro and in vivo genetic toxicology testing. *Environ Mol Mutagen*, 2000. 35(3): p. 206-21.

[34] Mei, N., et al. Silver nanoparticle-induced mutations and oxidative stress in mouse lymphoma cells. *Environ Mol Mutagen*, 2012. 53(6): p. 409-419.

[35] Olive, P.L., and Banath J. P. The comet assay: a method to measure DNA damage in individual cells. *Nat Protoc*, 2006. 1(1): p. 23-9.

[36] Moller, P., et al. Applications of the comet assay in particle toxicology: air pollution and engineered nanomaterials exposure. *Mutagenesis*, 2015. 30(1): p. 67-83.

[37] Karlsson, H.L., et al. Copper oxide nanoparticles are highly toxic: a comparison between metal oxide nanoparticles and carbon nanotubes. *Chem Res Toxicol*, 2008. 21(9): p. 1726-32.

[38] Jacobsen, N.R., et al. Genotoxicity, cytotoxicity, and reactive oxygen species induced by single-walled carbon nanotubes and C(60) fullerenes in the FE1-Mutatrade mark-Mouse lung epithelial cells. *Environ Mol Mutagen*, 2008. 49(6): p. 476-87.

[39] OECD. *In Vitro Mammalian Cell Micronucleus Test, OECD Guideline for Testing of Chemicals, No. 487.* http://www.oecd-ilibrary.org/docserver/download/9714561e.pdf?expires=1417033814&id=id&accname=guest&checksum=A77BB1B023EACFEF8C36FD865B6981D3, 2014.

[40] Oesch, F., and Landsiedel, R. Genotoxicity investigations on nanomaterials. *Arch Toxicol*, 2012. 86(7): p. 985-94.

[41] Wang, J.J., B.J. Sanderson, and Wang, H. Cyto- and genotoxicity of ultrafine TiO2 particles in cultured human lymphoblastoid cells. *Mutat Res*, 2007. 628(2): p. 99-106.

[42] Wang, J.J., B.J. Sanderson, and Wang, H. Cytotoxicity and genotoxicity of ultrafine crystalline SiO2 particulate in cultured human lymphoblastoid cells. *Environ Mol Mutagen*, 2007. 48(2): p. 151-7.

[43] Benameur, L., et al. DNA damage and oxidative stress induced by CeO nanoparticles in human dermal fibroblasts: Evidence of a clastogenic effect as a mechanism of genotoxicity. *Nanotoxicology*, 2014: p. 1-10.

[44] Papageorgiou, I., et al. The effect of nano- and micron-sized particles of cobalt-chromium alloy on human fibroblasts in vitro. *Biomaterials*, 2007. 28(19): p. 2946-58.

[45] Tsaousi, A., Jones, E., and Case, C.P. The in vitro genotoxicity of orthopaedic ceramic (Al2O3) and metal (CoCr alloy) particles. *Mutat Res*, 2010. 697(1-2): p. 1-9.

[46] Kato, T., et al. Genotoxicity of multi-walled carbon nanotubes in both in vitro and in vivo assay systems. *Nanotoxicology*, 2013. 7(4): p. 452-61.

[47] Muller, J., et al. Clastogenic and aneugenic effects of multi-wall carbon nanotubes in epithelial cells. *Carcinogenesis*, 2008. 29(2): p. 427-33.

[48] OECD. *In Vitro Mammalian Chromosome Aberration Test.* OECD Guideline for the Testing of Chemicals: TG473, 2014. http://www.oecd-ilibrary.org/docserver/download/9714531e.pdf?expires=1417033602&id=id&accname=guest&checksum=232CA39FC18225209745E6BAE3AFADB4.

[49] Hackenberg, S., et al. Silver nanoparticles: evaluation of DNA damage, toxicity and functional impairment in human mesenchymal stem cells. *Toxicol Lett*, 2011. 201(1): p. 27-33.

[50] Wise, J.P., Sr., et al. Silver nanospheres are cytotoxic and genotoxic to fish cells. *Aquat Toxicol*, 2010. 97(1): p. 34-41.

[51] Battal, D., et al. SiO Nanoparticule-induced size-dependent genotoxicity - an in vitro study using sister chromatid exchange, micronucleus and comet assay. *Drug Chem Toxicol*, 2014: p. 1-9.

[52] Johnson, G.E. Mammalian cell HPRT gene mutation assay: test methods. *Methods Mol Biol*, 2012. 817: p. 55-67.

[53] OECD. *In Vitro Mammalian Cell Gene Mutation Test.* OECD Guideline for the Testing of Chemicals, 1997. http://www.oecd.org/chemicalsafety/risk-assessment/1948426.pdf.

[54] Moche, H., et al. Tungsten carbide-cobalt as a nanoparticulate reference positive control in in vitro genotoxicity assays. *Toxicol Sci*, 2014. 137(1): p. 125-34.

[55] Wang, J.J., Wang, H., and Sanderson, B.J. Ultrafine Quartz-Induced Damage in Human Lymphoblastoid Cells in vitro Using Three Genetic Damage End-Points. *Toxicol Mech Methods*, 2007. 17(4): p. 223-32.

[56] Chen, Z., et al. Genotoxic evaluation of titanium dioxide nanoparticles in vivo and in vitro. *Toxicol Lett*, 2014. 226(3): p. 314-19.

[57] Wang, S., et al. Chronic exposure to nanosized, anatase titanium dioxide is not cyto- or genotoxic to Chinese hamster ovary cells. *Environ Mol Mutagen*, 2011. 52(8): p. 614-22.

[58] Manshian, B.B., et al. Single-walled carbon nanotubes: differential genotoxic potential associated with physico-chemical properties. *Nanotoxicology*, 2013. 7(2): p. 144-56.

[59] OECD. *In Vivo Mammalian Alkaline Comet assay.* OECD Guideline for Testing of Chemicals, No. 489, 2014. http://www.oecd-ilibrary.org/docserver/download/9714511e.pdf?expires=1417034151&id=id&accname=guest&checksum=B65AE67EDF756C95A5EC39B3A518DB0B.

[60] OECD. *Mammalian Erythrocyte Micronucleus Test.* OECD Guideline for THE Testing of Chemicals, No. 474, 2014. http://www.oecd-ilibrary.org/docserver/download/9714541e.pdf?expires=1417034451&id=id&accname=guest&checksum=8CAB5C07D1DEDD0CB07A7B9A3662157A.

[61] Bourdon, J.A., et al. Carbon black nanoparticle instillation induces sustained inflammation and genotoxicity in mouse lung and liver. *Part Fibre Toxicol*, 2012. 9: p. 5.

[62] El-Ghor, A.A., et al. Normalization of Nano-Sized TiO2-Induced Clastogenicity, Genotoxicity and Mutagenicity by Chlorophyllin Administration in Mice Brain, Liver, and Bone Marrow Cells. *Toxicol Sci*, 2014. 142(1): p. 21-32.

[63] Khalil, W.K., et al. Genotoxicity evaluation of nanomaterials: dna damage, micronuclei, and 8-hydroxy-2-deoxyguanosine induced by magnetic doped CdSe quantum dots in male mice. *Chem Res Toxicol*, 2011. 24(5): p. 640-50.

[64] Dobrzynska, M.M., et al. Genotoxicity of silver and titanium dioxide nanoparticles in bone marrow cells of rats in vivo. *Toxicology*, 2014. 315: p. 86-91.

[65] Li, Y., et al. Cytotoxicity and genotoxicity assessment of silver nanoparticles in mouse. *Nanotoxicology*, 2014. Suppl 1: p. 36-45.

[66] Kumari, M., Kumari, S.I., and Grover, P. Genotoxicity analysis of cerium oxide micro and nanoparticles in Wistar rats after 28 days of repeated oral administration. *Mutagenesis*, 2014. 29(6): p. 467-79.

[67] Kumari, M., et al. Genotoxicity assessment of cerium oxide nanoparticles in female Wistar rats after acute oral exposure. *Mutat Res Genet Toxicol Environ Mutagen*, 2014. 775-776: p. 7-19.

[68] Pakrashi, S., et al. In vivo genotoxicity assessment of titanium dioxide nanoparticles by Allium cepa root tip assay at high exposure concentrations. *PLoS One*, 2014. 9(2): p. e87789.

[69] Ghosh, M., et al. In vitro and in vivo genotoxicity of silver nanoparticles. *Mutat Res*, 2012. 749(1-2): p. 60-9.

[70] Singh, S.P., et al. Genotoxicity of nano- and micron-sized manganese oxide in rats after acute oral treatment. *Mutat Res*, 2013. 754(1-2): p. 39-50.

[71] Singh, S.P., et al. Toxicity assessment of manganese oxide micro and nanoparticles in Wistar rats after 28 days of repeated oral exposure. *J Appl Toxicol*, 2013. 33(10): p. 1165-79.

[72] Klien, K., and Godnic-Cvar, J. Genotoxicity of metal nanoparticles: focus on in vivo studies. *Arh Hig Rada Toksikol*, 2012. 63(2): p. 133-45.

[73] Kermanizadeh, A., et al. The role of intracellular redox imbalance in nanomaterial induced cellular damage and genotoxicity: A review. *Environ Mol Mutagen*, 2015. 56(2):p. 111-24.

[74] Fu, P.P., et al. Mechanisms of nanotoxicity: generation of reactive oxygen species. *J Food Drug Anal*, 2014. 22(1): p. 64-75.

[75] Schieber, M., and Chandel, N.S. ROS function in redox signaling and oxidative stress. *Curr Biol*, 2014. 24(10): p. R453-62.

[76] Toyokuni, S. Oxidative stress and cancer: the role of redox regulation. *Biotherapy*, 1998. 11(2-3): p. 147-54.

[77] Petersen, E.J., and Nelson, B.C. Mechanisms and measurements of nanomaterial-induced oxidative damage to DNA. *Anal Bioanal Chem*, 2010. 398(2): p. 613-50.

[78] Yang, J., et al. Dissociation of double-stranded DNA by small metal nanoparticles. *J Inorg Biochem*, 2007. 101(5): p. 824-30.

[79] Chen, M., and von Mikecz, A. Formation of nucleoplasmic protein aggregates impairs nuclear function in response to SiO2 nanoparticles. *Exp Cell Res*, 2005. 305(1): p. 51-62.

[80] Baweja, L., et al. C60-fullerene binds with the ATP binding domain of human DNA topoiosmerase II alpha. *J Biomed Nanotechnol*, 2011. 7(1): p. 177-8.

[81] Gupta, S.K., et al. Interaction of C60 fullerene with the proteins involved in DNA mismatch repair pathway. *J Biomed Nanotechnol*, 2011. 7(1): p. 179-80.

[82] Beyersmann, D., and Hartwig, A. Carcinogenic metal compounds: recent insight into molecular and cellular mechanisms. *Arch Toxicol*, 2008. 82(8): p. 493-512.

[83] Hahn, A., et al. Cytotoxicity and ion release of alloy nanoparticles. *J Nanopart Res*, 2012. 14(1): p. 1-10.

[84] Baldwin, E.L., J.A. Byl, and Osheroff, N. Cobalt enhances DNA cleavage mediated by human topoisomerase II alpha in vitro and in cultured cells. *Biochemistry*, 2004. 43(3): p. 728-35.

[85] Colognato, R., et al. Comparative genotoxicity of cobalt nanoparticles and ions on human peripheral leukocytes in vitro. *Mutagenesis*, 2008. 23(5): p. 377-82.

[86] Westbrook, A.M., et al. Intestinal inflammation induces genotoxicity to extraintestinal tissues and cell types in mice. *Int J Cancer*, 2011. 129(8): p. 1815-25.

[87] Downs, T.R., et al. Silica nanoparticles administered at the maximum tolerated dose induce genotoxic effects through an inflammatory reaction while gold nanoparticles do not. *Mutat Res*, 2012. 745(1-2): p. 38-50.

[88] Tsuda, H., et al. Toxicology of engineered nanomaterials - a review of carcinogenic potential. *Asian Pac J Cancer Prev*, 2009. 10(6): p. 975-80.

[89] Park, E.J., et al. Inflammatory responses may be induced by a single intratracheal instillation of iron nanoparticles in mice. *Toxicology*, 2010. 275(1-3): p. 65-71.

[90] Moller, P., et al. Oxidative stress and inflammation generated DNA damage by exposure to air pollution particles. *Mutat Res Rev Mutat Res*, 2014. 762C: p. 133-166.

[91] Shi, H., et al. Titanium dioxide nanoparticles: a review of current toxicological data. *Part Fibre Toxicol*, 2013. 10: p. 15.

[92] Pfuhler, S., et al. Genotoxicity of nanomaterials: refining strategies and tests for hazard identification. *Environ Mol Mutagen*, 2013. 54(4): p. 229-39.

[93] OECD. *Six years of OECD work on the safety of manfactured nanomaterials: Achievements and Future Opportunities.* 2012. http://www.oecd.org/science/nanosafety/Nano%20Brochure%20Sept%202012%20for%20Website%20%20(2).pdf.

[94] OECD. *Genotoxicity of Manufactured Nanomaterials : Report of the OECD expert meeting.* OECD Environment, Health and Safety Publications 2014. Series on the Safety of Manufactured Nanomaterials No. 43-ENV/JM/MONO(2014)34(http://www.oecd.org/officialdocuments/publicdisplaydocumentpdf/?cote=env/jm/mono(2014)34&doclanguage=en).

[95] FDA. *Nanotechnology*. Science & Research 2014; Available from: http://www.fda.gov/ScienceResearch/SpecialTopics/Nanotechnology/default.htm.

[96] FDA. *Use of Nanomaterials in Food for Animals (Draft Guidance).* Guidance for Industry #220, 2014. http://www.fda.gov/downloads/AnimalVeterinary/GuidanceComplianceEnforcement/GuidanceforIndustry/UCM401508.pdf.

[97] Alotaibi, A., et al. Tea phenols in bulk and nanoparticle form modify DNA damage in human lymphocytes from colon cancer patients and healthy individuals treated in vitro with platinum-based chemotherapeutic drugs. *Nanomedicine (Lond)*, 2013. 8(3): p. 389-401.

[98] Kumar, A., and Dhawan, A. Genotoxic and carcinogenic potential of engineered nanoparticles: an update. *Arch Toxicol*, 2013. 87(11): p. 1883-900.

[99] Lockman, P.R., et al. Nanoparticle surface charges alter blood-brain barrier integrity and permeability. *J Drug Target*, 2004. 12(9-10): p. 635-41.

[100] Shvedova, A.A., et al. Long-term effects of carbon containing engineered nanomaterials and asbestos in the lung: one year postexposure comparisons. *Am J Physiol Lung Cell Mol Physiol*, 2014. 306(2): p. L170-82.

[101] Boland, S., Hussain, S., and Baeza-Squiban, A., Carbon black and titanium dioxide nanoparticles induce distinct molecular mechanisms of toxicity. *Wiley Interdiscip Rev Nanomed Nanobiotechnol*, 2014. 6(6): p. 641-52.

[102] Demir, E., Creus, A., and Marcos, R. Genotoxicity and DNA repair processes of zinc oxide nanoparticles. *J Toxicol Environ Health A*, 2014. 77(21): p. 1292-303.

[103] Gong, C., et al. SiO(2) nanoparticles induce global genomic hypomethylation in HaCaT cells. *Biochem Biophys Res Commun*, 2010. 397(3): p. 397-400.

[104] Guo, D., et al. Zinc oxide nanoparticles induce rat retinal ganglion cell damage through bcl-2, caspase-9 and caspase-12 pathways. J Nanosci Nanotechnol, 2013. 13(6): p. 3769-77.

[105] Roy, R., et al. Zinc oxide nanoparticles induce apoptosis by enhancement of autophagy via PI3K/Akt/mTOR inhibition. Toxicol Lett, 2014. 227(1): p. 29-40.

Chapter 8

Medical Aspects of Nanomaterial Toxicity

Krzysztof Siemianowicz, Wirginia Likus and
Jarosław Markowski

Additional information is available at the end of the chapter

http://dx.doi.org/10.5772/60956

Abstract

Nanosilver is the most popular and most studied nanomaterial, however, a family of nanomaterials is rapidly enlarging. They are used in various branches of industry and everyday life. In medicine new nanomaterials can be used either alone or in combination with other "classical" drugs, e.g. cytostatic drugs or antibiotics. They can be also used as diagnostic agents. A development of nanoparticles has led to a new combination of diagnostic and therapy - theranostic. Size of a particle makes a difference not only between bulk material and nanomaterial, but also in their properties and toxicity. Nanomaterials can have beneficial properties, but can also be toxic. New issues concerning nanomaterials arise - an industrial exposure and environmental pollution. They can enter human body in various ways. Cellular mechanisms of nanomaterial toxicity comprise mainly a generation of reactive oxygen species and genotoxicity. The differences between toxicity of fine particles and nanoparticles have led to an origin of a new branch of science, nanotoxicology.

Keywords: nanomaterials, nanoparticles, medical use, toxicity

1. Introduction

Nanoparticles can be of various origin: natural, incidental, or manufactured. Natural nanoparticles can be met in fumes or smoke (e.g., carbon black). A fast-growing branch of science, nanotechnology has led to a development of a variety of newly engineered nanoparticles. As their use each day becomes broader, the proper evaluation of their toxicity becomes an urgent

must. Properties of nanomaterials change as their size goes down approaching a nanoscale. As properties of a bulk form and nanoparticles differ, so we must know if the toxicity also changes.

2. Nanomaterials used in medicine

When one says "nanoparticle" or "nanomaterial," the first association usually is nanosilver. It was the first nanomaterial introduced into medicine due to its antibacterial properties. Nanosilver has a broad spectrum of both medical and paramedical applications. It is used as an antibacterial addition to wound dressings and ointments used to protect from infection wounds, burns, ulcers, and pemphigus. Nanosilver is also applied to cover the surface of surgical threads, tools, and catheters introduced into veins. Medical protective clothes, gloves, bed clothes, mattresses, syringes, respiratory tubes, and masks also may contain nanosilver to reduce the risk of infection. Nanosilver is also used in orthopedics to cover the surface of various implants and as a component of bone cement to prevent a development of bacterial infection which in orthopedics may be very dangerous and difficult to treat. Nanosilver is also used in production of a variety of drug and food packings. Zinc oxide (ZnO) and magnesium oxide (MgO) nanoparticles also have antibacterial properties and are used as an additive to food packing [1-3].

Magnetic nanoparticles comprise a next group of medical applications. They are a well-known diagnostic tool used as magnetic resonance imaging contrast comprising iron oxide nanoparticles or nanoparticles with iron core. Calcium phosphate nanoparticles doped with a near-infrared dye for optical imaging, fluorophore, have been tested for in vivo diagnostic of human breast cancer.

A development of new nanoparticles has led to a development of a new combination of diagnostic and therapy, theranostic. The simplest explanation of this new term is an identification of diseased tissues or cells and delivery of a medicine or a therapy (e.g., heating) to this very site of pathology. A gold-silica nanoparticle system for optical imaging and photothermal ablation has been developed [4-6].

Superparamagnetic iron oxide nanoparticles (SPIONs) and ultra-small superparamagnetic iron oxide (USPIO) can be used for targeted drug delivery [7]. Another kind of intensively studied nanomaterials are mesoporous silica nanoparticles. They may be used for high drug or imaging agent loading. "Cornell dots" are the first silica-based diagnostic nanoparticles approved for human clinical trials. Gold nanoparticles can have various medical applications such as improving efficacy of high-resolution ultrasound imaging, photothermal therapy, and photothermal release of DNA cargo upon laser irradiation. They have been also shown to pose antibacterial activities. Quantum dots constitute another class of nanoparticles. They can be extremely small, typically having only few nanometers. They are usually composed of heavy metals such as lead or cadmium. Scientists hope to employ them in sophisticated multimodal imaging techniques [8]. Nanogels, dendrimers, and liposomes are the other classes of nano-

http://dx.doi.org/10.5772/60956

materials. They can be used for controlled drug delivery. Cell growth scaffolds may be another application of these classes of nanomaterials [8].

3. Entry portal of nanomaterials into the human body

Various nanomaterials can be used in different ways. Many nanomaterials are used as drug carriers or imaging agents with an intravenous entrance into the human body. This gateway for nanoparticles can be well controlled. This way of introducing nanoparticles into the human body allows for their easy distribution to all organs. The nanoparticles only have to be able to cross the barrier of blood vessel wall.

Absorption through the skin is another way in which nanoparticles can enter the human organism. The skin is the largest organ of the human body, reaching above 10 % body mass. It gives a large area of contact with the external environment, approximately 1,73 m^2. Skin contact with nanomaterials may be due to various reasons, occupational contact in industry, medical applications, and a still-growing amount of cosmetics containing nanoparticles and clothes with nanoparticles, e.g., sock containing nanosilver to reduce odors. Cosmetics and products for everyday hygiene like soaps, shampoos, gels, creams, and deodorants also may contain nanosilver. This nanoparticle is not the only one the skin may be exposed to. Sunscreens protecting the skin against UV radiation contain titanium dioxide (TiO_2) and ZnO nanoparticles. The nanoform of these two oxides is more often used due to its transparent form which is more acceptable by customers.

Often nanoparticles, mainly nanosilver, are used for treatment of burns, wounds, or ulcers. Although they are intended to be used topically to prevent infections, a damaged skin makes their penetration into the body easier. There are four pathways the chemical compounds can penetrate across the skin: intracellular, transcellular, and two of transappendageal through sweat glands and hair follicles. The way of penetration depends on physicochemical properties of nanoparticles. Many other factors can influence the extent of dermal uptake. They can be roughly divided into two groups, caused by a condition of the skin and by external factors. The anatomical side resulting in differences of epidermis thickness, a skin barrier integrity and the presence of wounds or scratches, and skin diseases like allergic or irritant contact dermatitis, atopic eczema, and psoriasis compose the first group. The external factors include the contaminated skin surface, irritant detergent and chemicals, mechanical flexion, and exposure to heat, infrared, or UV radiation. They can increase the skin absorption of nanoparticles [8].

Metallic nanoparticles smaller than 10 nm have been shown to penetrate epidermal layers [3, 9]. Most dermal exposure studies indicate that TiO_2 does not penetrate the stratum corneum [10]. Carbon nanoparticles comprising single-walled and multiwalled carbon nanotubes and fullerenes have a large variety of applications. Fullerenes have been shown to penetrate flexed but not unflexed skin [10]. Unrefined single-walled carbon nanotubes have been shown to exert negative effects on cultured skin cells, increasing generation of free radicals and causing ultrastructural and morphological changes in keratinocytes. These carbon nanoparticles induced also cellular apoptosis and necrosis response. The surface area of carbon nanotubes is the best predictor of their negative effects [10].

Quantum dots also can penetrate the intact skin. This fact is important in an aspect of occupationally relevant skin contact. A surface coating of quantum dots does not influence their penetration into the skin, but is responsible for a magnitude of toxic effects on skin cells including cytotoxicity and immunotoxicity [10]. Nanosilver which is contained in various dressings may influence both keratinocytes and fibroblasts. The latter are more sensitive to nanosilver than keratinocytes [10]. Gold nanoparticles can penetrate into the skin. This ability is size dependent. The smaller the nanoparticle, the deeper it can penetrate. Citrate/gold nanoparticles can be toxic to human dermal fibroblasts [11]. Iron oxide nanoparticles can penetrate into the skin. They can be rapidly endocytosed by cultured human fibroblasts and disrupt their function [10].

While discussing skin penetration of nanoparticles, another question arises. Can nanoparticles cross the skin barrier and be distributed by blood to other organs? Scientists mainly focus their attention on evaluation of nanoparticle penetration into either usually porcine skin or culture skin keratinocytes or fibroblasts. If some nanoparticles can penetrate into deeper layers of the skin, the abovementioned question requires an urgent answer.

Inhalation constitutes the next entry portal of nanomaterials into the human body. This gateway is very important in a case of occupational exposure to nanoparticles. Lansiedel et al. applied a new method for evaluation of toxicity of inhaled nanoparticles, a short-time inhalation study (STIS) instead of a 90-day rodent inhalation study. Nanoparticles and microscale zinc oxide were evaluated in this study. Among tested materials, only polyacrylate-coated silica and both forms of ZnO were found in extrapulmonary organs. The first was found in the spleen, whereas both forms of ZnO elicited necrosis on the olfactory epithelium. Five materials – coated nano TiO_2, nano-CeO_2, Al-doped nano-CeO_2, and both forms of ZnO – evoked transient, dose-dependent pulmonary inflammation. The results of this study enabled to classify studied materials into three groups. Nano-$BaSO_4$, nano-SiO_2, four types of surface coated silica – SiO_2-polyacrylate, SiO_2-PEG, SiO_2-phosphate, and SiO_2-amino – nano-ZrO_2, ZrO_2 TOTA, and ZrO_2-acrylate were of low toxic potency. The group of medium toxic potency had only one studied nanoparticle, non-coated amorphous silica (naked silica). The third group of higher toxic potency comprised coated nano-TiO_2, nano-CeO_2, Al-doped nano-CeO_2, microscale ZnO, and coated nano-ZnO [11]. ZnO nanoparticles induced collagen formation 4 weeks after instillation [12].

Titanium dioxide has gained much attention in recent years. It can be used in a form of either fine particles or nanoparticles. TiO_2 fine particles have been considered as poorly soluble, low-toxicity particles. Due to their properties, they have been used as a "negative control" in many toxicological studies. A long-term, 2 years, study with high-dosed TiO_2 revealed that fine particles of TiO_2 might cause lung tumors in rats. The International Agency for Research on Cancer (IARC) has classified TiO_2 as possibly carcinogenic to humans (carcinogen group 2B). With this fact arises a question: Can the results of studies of larger particles be automatically transferred to nanoparticles? Some studies have shown that TiO_2 are more toxic than TiO_2 fine particles. Although TiO_2 nanoparticles were shown not to penetrate through the skin, the effects of inhalation of these nanoparticles seem to require further studies [11].

Gastrointestinal absorption is another important route nanoparticles may enter the human body. This way is important for nanoparticles which are allowed as "food contact substances"

http://dx.doi.org/10.5772/60956

and which may come in contact with drinking water, e.g., nanosilver present in water filters or water purifiers.

The most common way of uptake for both microparticles and nanoparticles in gut is endocytosis by M-cell in Peyer's patches. Once nanoparticle enters the blood stream, they are distributed throughout the body. Nanoparticles can pass through barriers of the body and accumulate in certain organs. Small gold nanoparticles (10 nm) were found to accumulate in the liver, spleen, kidney, lungs, brain, and reproductive system, whereas larger ones (50–100 nm) and 250 nm were found only in the blood, liver, and spleen [13]. The size of nanoparticles is an important factor in determining their blood circulation time and places of deposition in an organism [14]. Nanoparticles entering the gastrointestinal tract are exposed to a wide range of pH. Hydrochloric acid secreted in the stomach has been shown to influence dissolution of silver nanoparticles. In these conditions, silver ions are generated from silver nanoparticles. As the ability of silver particles to cross the gut epithelium is limited, it seems that the main route of silver uptake from gastrointestinal tract is ion transport. Silver ions may be transported by mechanism responsible for transport of sodium and copper ions [1,15].

Biological fluids present a wide spectrum of chemical conditions. They can influence nanoparticles in various ways and can cause their agglomeration, changing their properties, penetration potency, and also toxicity. The fact that some in vivo conditions may change the particle size must be taken into consideration while evaluating the toxicity of nanomaterials. It may lead to a conclusion that in some conditions, not a particle size but a size of agglomerate may determine the properties of nanoparticles and consequently their toxicity [16].

Sometimes nanoparticles can be administered using the intraocular and intranasal routes which have not been widely studied. Nanosilver can be used in some intrauterine devices, creating another plausible gateway for nanoparticles.

Nanomaterials can be used as drug carriers and enhancers. The term "drugs" should be widely understood. They can be of classical chemical nature. Nanoparticles can improve dissolution and solubility of poorly soluble drugs and successful delivery of hydrophobic drugs, increasing their concentration at targeted tissues. Nanoparticles may also be used for delivery of drugs into specific cell compartment. This application of nanomaterials may comprise various routes of administration, not only intravenous.

Nanoscale changes structure-activity relationship of complex nanoparticles. The use of nanoformulations of drugs allows them to pass some biological barriers which for classical drug forms are not transferrable. The blood-brain barrier may be a prominent example. The complex of drug on a nanoporous silica gives a tool for controlling the release of drug at its side of destination and action [17]. As a progress of pharmacology and nanotechnology enables to create nanoparticles carrying various drugs, an important question arises. What is responsible for specific side effects, a carrier or a cargo? This approach creates the novel branch of science – nanotoxicology.

The efficacy of nanoparticles relies on a variety of their modifications and functionalities. This advantage creates a variety of tasks for nanotoxicology to evaluate the safety/toxicity profile of each modification. The study of Landsiedel et al. shows that modifications of nanoparticles

may change their toxicity. Those modifications can alter hydrophobicity and isoelectric points of particles. Various nanoparticles can have different abilities to agglomerate in specific biological conditions that may have an important influence on their toxicity [14,18].

4. Toxicity of nanoparticles

The size of nanoparticles of the same chemical compound or the same chemical element may vary in a wide range from a few nm to about 100 nm. Results of studies concerning nanoparticles of the same chemical nature can give various results depending on the size of used nanoparticles. A kind of exposure resulting in a specific way of possible absorption is another factor influencing the results of toxicological studies. TiO_2 which is thought not to cross the skin barrier in humans may induce lung tumors in rats when inhaled in high doses for a long time. TiO_2 nanoparticles may be absorbed both from the lungs and gastrointestinal tract. However, the rate of absorption appears to be low. Studies with intravenous administration of TiO_2 indicate that these nanoparticles can induce pathological lesions of the liver, spleen, kidney, and brain. These effects may be attributed to very high doses of TiO_2 nanoparticles used in this study [10]. The use of TiO_2 is widespread. It may be used even as a white color food additive. It is difficult to estimate how much of total TiO_2 used is the form of larger, fine particles and how much in the form of nanoparticles. The difference in toxicity of TiO_2 fine particles and nanoparticles is reflected in allowances of occupational exposure. In the USA, the threshold limit value of TiO_2 fine particles (total dust) is assigned as 10 mg/m^3 as time-weighted average (TWA) for an 8-hour daily work time 5 days per week. That value was established by the American Conference of Governmental Industrial Hygienists (ACGIH). The regulation of the Occupational Safety and Health Administration (OSHA) is 15 mg/m^3. The US National Institute for Occupational Safety and Health (NIOSH) proposed a recommended exposure limit (REL) for TiO_2 nanoparticles of 0.3 mg/m^3, being 10 times lower than REL for TiO_2 fine particles. In Japan, TWA for TiO_2 nanoparticles is 1.2 mg/m^3. The fact that the same recommendation in the USA and Japan differs four times indicates that further studies concerning safety limits of exposure to TiO_2 nanoparticles are required [10].

The skin is a site where the first side effect of nanomaterial was observed. Silver and nanosilver used as antibacterial agent when overdosed caused an irreversible pigmentation of skin termed argyria or argyrosis. In these patients, silver deposits form usually in skin regions exposed to light. The silver deposits are usually collocated with sulfur and selenium. Silver is usually bound to protein thiol groups or selenium in the case of selenoproteins. Both sulfides and selenides have a high binding affinity for silver, causing its uptake from biological fluids. Silver bound to these chemical groups is easily exchangeable and has significant biomolecular mobility. If silver complexes with thiol groups are located in the skin or near-skin region, silver can be easily reduced by visible or UV light to metallic nanosilver particles, resulting in an immobilization of silver nanoparticles in the skin. This process puts new light on a pathogenesis of a very old side effect of treatment with various drugs containing silver, argyria. It also explains why this side effect is usually located in skin regions exposed to light [15].

http://dx.doi.org/10.5772/60956

Animal experiments with topical administration of colloid nanosilver showed both acute and chronic dermal toxicity. It was also observed that nanosilver could penetrate from the skin to the blood and accumulate in the liver and spleen, causing their mild damage detected in histopathological examination [19]. The fact that nanosilver can cross the skin barrier makes us look closer and with a greater attention on results of in vitro studies showing nanosilver toxicity to various cultured cell lines. Nanosilver has been shown to be toxic to peripheral blood mononuclear cells, human alveolar epithelial cells and alveolar macrophages, rat hepatocytes, and mouse germline cells [17]. These results indicate that the safety of a still-increasing use of nanosilver should be better monitored.

In biological fluids, proteins can associate with nanoparticles. The competing of proteins for the nanoparticle surface leads to a generation of protein "corona" surrounding the nanoparticle. This process can take place in the blood. Not only albumins and fibrinogen can compete to create "corona" but also lipoproteins. Such an association alters nanoparticle characteristics and their biological properties. Some nanoparticles associated with apolipoprotein E can cross the blood-brain barrier. This modification giving some nanomaterials new important biological property has a potential significance for a development of new neurotherapies as well as for neurotoxicity [18,19].

In humans, nanosilver was shown to inhibit the extrinsic coagulation pathway evaluated by activated partial thromboplastin time (APTT) [20]. In animal experimental model, nanosilver decreased platelet activation [21]. Nanosilver can cross the blood-brain barrier and accumulate in the brain, causing necrosis and neuronal degeneration [22]. In a study of Ahamed et al. [23], nanosilver particles elicited genotoxicity on mouse embryonic fibroblasts. This was caused by both polysaccharide-coated and uncoated nanosilver particles. Nanosilver was also shown to accumulate in the testis [24].

Detailed nanotoxicological studies dealing with mammalian reproductive tissues and gametes have yet to be carried out. A very limited group of nanomaterials have been shown as biocompatible with mammalian sperm: magnetic iron nanoparticles, a specific type of CdSe/ZnS quantum dots, halloysite clay nanotubes, and commercial nanopolymer-based transfectants [25]. A group of nanomaterials biocompatible with mammalian embryo is smaller and comprises chitosan, CdSe/ZnS quantum dots, and externally applied polystyrene nanoparticles.

Results of studies of sperm toxicities of nanogold remain highly contradictory [25]. Some of them reported that nanogold elicited spermatoxicity [18].

Nanocopper was shown to reduce in a dose-depended manner cell viability of mouse testis Leydig cells. In vitro studies of TiO_2 nanoparticles and ZnO nanoparticles demonstrated a dose-dependent sperm DNA damage in human spermatozoa. Various studies evaluating the influence of TiO_2 nanoparticles on mammalian ovarian cells gave contradictory effects [26].

Various nanoparticles can also influence the endocrine system. In animal models, TiO_2 nanoparticles and CdTe/ZnTe quantum dots conjugated with transferrin could alter serum levels of sex hormones and gonadotropins [26].

Nanoparticles can easily cross the placental barrier and enter a fetus. The animal experiments showed that fullerene nanoparticles were traced in embryos and at higher doses caused significant toxicity and death [27]. TiO_2 was shown to transfer from pregnant mice to their offsprings, affecting the central nervous system and genitals [28]. The results of abovementioned studies raise a question about the risk of nanoparticle exposure to pregnant women.

Nanoparticles can influence the immune system. They were shown to induce inflammatory response. ZnO nanoparticles can exert their activity on immune cells through three mechanisms. Promoting antigen uptake by antigen-presenting cells is the first one. Targeting to specific cells like dendritic cells, Langerhans cells, or macrophages is the second mode. The third one is immunopotentation and modulation of activity of antigen-presenting cells through receptors of innate immune system [29]. ZnO nanoparticles have been found to induce toxicities particularly in the immune cells as these nanoparticles are specifically found to be internalized in these cells [29]. Nanoparticles can also act as haptens and modify protein structures, raising their potential for autoimmune effects [18].

5. Cellular mechanisms of nanoparticles toxicity

In this chapter, the cellular mechanisms of nanomaterials toxicity will be only very briefly mentioned as they are discussed in detail in other chapters of this book.

5.1. Reactive oxygen species production

Reactive oxygen species (ROS) constitute a pool of reactive species of molecular oxygen, previously termed free radicals, including superoxide anion ($O_2^{\cdot -}$), hydroxyl radical ($OH^{\cdot}$), hydrogen peroxide (H_2O_2), singlet oxygen ($^1O_2$), and hypochlorous acid (HOCl). Most of them are produced via electron transport chain in the mitochondria. ROS are generated intrinsically or extrinsically within the cell. ROS production is widely used in cell signaling, regulation, and homeostasis [14,30,31].

Nanoparticles entering the cell interact with mitochondria and other subcellular organelles increasing ROS production. Various nanomaterials of various sizes can disturb mitochondrial function. ZnO nanoparticles can generate Zn^{2+} ions interrupting charge balance in electron transport chain in the mitochondria and triggering ROS formation. Semiconductor nanomaterials can elicit an excited energy state, leading to the generation of $O_2^{\cdot -}$. This ROS is capable of damaging cellular macromolecules or interrupting cell signaling, leading to cell dysfunction. It also can cause further generation of other ROS. Some nanoparticles can interact between one another. Excited CdSe quantum dots are capable of injecting electrons into TiO_2 [32]. It was observed that photoactivation of TiO_2 could also generate $O_2^{\cdot -}$ and $OH^{\cdot}$ radicals [31]. This fact seems to be important considering the still-growing use of TiO_2 nanoparticles. An increased generation of ROS causes further intracellular disorders [31].

Nanosilver has been observed to significantly decrease incorporation of selenium into selenoproteins constituting enzymes engaged in antioxidant protection such as glutathione

peroxidase, thioredoxin reductase, or methionine sulfide reductase [1,21]. Nanomaterials via increased ROS generation lead to a glutathione depletion. Glutathione is a main intracellular antioxidant. This depletion may significantly affect cellular metabolism causing mitochondrial dysfunction and ATP depletion [30].

Generation of lipid peroxides is a next effect of increased ROS generation. Various nanomaterials have been reported to generate lipid peroxides and resultant cell membrane damage. Nanosilver can induce both mitochondrial damage and mitochondrial-dependent apoptotic pathway [30].

The destruction of cell membrane can cause a membrane leakage of lactate dehydrogenase. The assay for evaluating the extracellular activity of this enzyme is most commonly used for membrane leakage testing. Monitoring lactate dehydrogenase activity can be a useful tool for evaluation of toxicity of nanomaterials [30].

5.2. Genotoxicity

Genotoxicity is caused by agents interacting with DNA and other compounds controlling the integrity of the genetic material and includes DNA strand breaks, point mutations, adducts, and structural or numerical chromosomal changes. Nanosilver was the first nanomaterial reported to cause DNA damage. This effect was observed in various cells. Ma et al. [33] observed that nanosilver caused DNA damage accompanied by cell cycle arrest in human dermal fibroblasts. Hackenberg et al. [34] demonstrated genotoxic effect of nanosilver in human mesenchymal cells. However, to elucidate these effects, nanosilver had to be used at a significantly higher concentration as compared to antimicrobial effective levels. In mammalian cells, nanosilver caused an increase of p53 protein expression and Rad51 expression. The latter is a double-strand break repair protein. Nanosilver also induced apoptosis. The strength of this genotoxic influence of nanosilver depended on a kind of nanosilver particles used. Polysaccharide-coated nanosilver particles exhibited more severe DNA damage than uncoated [23].

Nanosilver can cause DNA damage mainly by two mechanisms. The augmentation of ROS generation by nanosilver may result in an oxidative damage of both proteins and DNA. Increased oxidation may lead to a transformation of nanosilver to silver ions Ag^{+} which can bind to guanine N7 atom. While increasing concentration, they can also bind to adenine N7 atom. Silver ions can also induce G1 phase cell cycle arrest and, at a higher concentration, a complete arrest in the S phase [35]. Nanosilver was also reported to induce formation of micronuclei due to the disruption of genetic material division. Formation of micronuclei is used to measure a potential of genotoxicity due to its sensitive response to various abnormalities in chromosomal segregation [36].

A study of Ivask et al. [36] revealed that nanosilver and graphene oxide nanoparticles shifted a melting point, triggering an early onset of DNA melting. These nanoparticles could also change a DNA hydrodynamic size. These observations may indicate novel mechanisms of nanoparticle genotoxicity. Very thin (1.4 nm) gold nanostructures can intercalate with DNA,

leading to cell death in human cancer cells [37]. SiO_2 nanoparticles can enter into the nucleus and localize in the nucleoplasm. However, they are not considered as carcinogenic [37,38].

Lan et al. observed that TiO_2 nanoparticles and carbon black nanoparticles could damage DNA via oxidative stress in human cells. These authors reported that eukaryotes, especially mammalian cells, were more sensitive to the genotoxicity than prokaryotes [39]. NIOSH has classified TiO_2 as carcinogenic. Interesting results were obtained by Darnes et al. who observed that genotoxicity of carbon nanotubes increased with their width [40].

CdS quantum dots are semiconductor nanocrystals with an increasing use. Their potential toxicity has become a health concern. A study of Munari et al. [41] indicated that this nanomaterial exhibited a concentration-independent genotoxicity in rainbow trout cell line RTG-2. In the same experiment, nanosized Ag_2S showed neither cytotoxicity nor genotoxicity.

While evaluating and comparing results of studies on genotoxicity of nanomaterials, an influence of several factors should be considered. The conflicting results of various studies may be caused by two groups of factors. The first one deals with nanoparticles and comprises variation of size of the nanoparticles, variations of size of distribution, various purities of the nanomaterials with the same average size of nanoparticles, differences of their coatings, differences of crystal structure of the types of nanomaterials, differences of size of aggregates in solution or medium, and different concentrations of nanomaterials used in assay test. The second group comprises testing conditions such as cell number, cell culture plate format and volume of treatment medium on the plate, and differences in assays [42,43].

5.3. Activation of inflammatory pathways

Nanoparticles can influence macrophages and neutrophils eliciting an inflammatory response. These cells try to destroy foreign objects, usually microbial pathogens, inducing enormous ROS generation. Nanoparticles are also treated by macrophages and neutrophils as something foreign and these cells try to get rid of them, increasing production of ROS. It leads to an induction of inflammation [20,31]. An augmented ROS generation can increase the inflammatory response by activation of expression of nuclear factor kappa B (NFκB). It is one of the major transcriptional factors. It plays an important role in cell survival, differentiation, and proliferation. It is also involved in growth and development of the immune system. NFκB is heavily involved in the initiation of inflammatory response [14].

Many nanoparticles have also been reported to induce inflammatory response through activation of expression of tumor necrosis factor alfa (TNF-α). Nanoparticles can also lead to an increased expression of other proinflammatory cytokines such as interleukins 2, 6, 8, and 10 (IL-2, IL-6, IL-8, and IL-10) [14,20].

ROS generated by nanoparticles can be either bound to the nanoparticle surface or generated as free entities in surrounding aqueous suspension. An antioxidant enzyme, glutathione reductase, can reduce metal nanoparticles into intermediates potentiating the ROS generation. In this way, nanoparticles can not only increase the generation of ROS but also interfere with the antioxidant protection mechanisms [31].

Macrophages and neutrophils can internalize nanoparticles. The consequence of this process is an activation of these cells, elucidation of inflammatory response, and even cytotoxic effects of nanoparticles on these cells [20,31].

Pulmonary inflammation seems to be the most prominent inflammatory response generated by nanoparticles. SiO_2 and TiO_2 nanoparticles have been reported to induce this response, whereas occupational exposure to metal nanoparticles such as Fe, Mn, Si, Cr, and Ni present in welding fumes may elicit both inflammation and fibrogenic response [31].

6. Conclusions

A family of nanomaterials is rapidly enlarging. The spectrum of the use of nanomaterials is getting wider, comprising medical, paramedical, and everyday use. In medicine, they can be used either alone or in combination with other "classical" compounds, e.g., cytostatic drugs or antibiotics. The latter situation uses their ability to penetrate to certain cells or intracellular compartments. Nanoparticles are also introduced as valuable tools improving existing diagnostic methods, e.g., MNR.

New issues concerning nanomaterials arise, an industrial exposure and environmental pollution. Nanoparticles are being discovered in already known pollutions like diesel exhaust or welding fumes. These "unwanted" nanoparticles put new light on the toxicological mechanisms of already known pollutions. It also makes us look at pollutions in macroscale, microscale, and nanoscale. A rapidly developing branch of electronics also creates new sources of possible occupational exposure hazard. This situation creates new challenges for both classical toxicology and nanotoxicology. Centuries ago, Paracelsus said, "everything is a poison and nothing is a poison, it is only a matter of a dose." In a case of nanomaterials, it is a case of both dose and particle size [1].

Author details

Krzysztof Siemianowicz[1], Wirginia Likus[2] and Jarosław Markowski[3]

1 Department of Biochemistry, School of Medicine in Katowice, Medical University of Silesia, Poland

2 Department of Human Anatomy, School of Medicine in Katowice, Medical University of Silesia, Poland

3 Department of Laryngology, School of Medicine in Katowice, Medical University of Silesia, Poland

References

[1] Likus W, Bajor G, Siemianowicz K: Nanosilver – does it have only one face? Acta Biochim Pol. 2013;60:495–501

[2] Chaloupka K, Malam Y, Seifalian AM: Nanosilver as a new generation of nanoproduct in biomedical applications. Trends Bioctechnol. 2010;28:580–588

[3] Mogharabi M, Abdollahi M, Faramarzi MA: Toxicity of nanomaterial; an undermined issue. Daru. 2014;22:59. doi: 10.1186/s40199-014-0059-4

[4] Altinoğlu EI, Russin TJ, Kaiser JM, Barth BM, Eklund PC, Kester M, Adair JH: Near-infrared emitting fluorophore-doped calcium phosphate nanoparticles for in vivo imaging of human breast cancer. ACS Nano. 2008;2:2075–2084

[5] Marchesan S, Prato M: Nanomaterials for (nano)medicine. ACS Med Chem Lett. 2012;4:147–149

[6] Study of the detection of lymphoblasts by a novel magnetic needle and nanoparticles in patients with leukemia. [Internet] Available from: https://www.clinicaltrials.gov/ct2/show/NCT01411904?term=detection±of±lymphoblasts±by±±novel±magnetic±needle&rank=1 [Accessed 2015-01-22]

[7] Francesca S: Nanotechnology and stem cell therapy for cardiovascular diseases: potential applications. Methodist Debakey Cardiovasc J. 2012;1:28–35

[8] Crosera M, Bovenzi M, Maina G, Adami G, Zanette C, Florio C, Larese FF: Nanoparticle dermal absorption and toxicity: a review. Int Arch Occup Environ Health. 2009;82:1043–1055

[9] Baroli B, Ennas MG, Loffredo F, Isola M, Pinna R, Lopez-Quintela MA: Penetration of metallic nanoparticles in human full-thickness skin. J Investig Dermatol. 2007;127:1701–1712

[10] Shi H, Magaye R, Castranova V, Zhao J: Titanium dioxide nanoparticles: a review of current toxicological data. Part Fibre Toxicol. 2013. doi: 10.1186/1743-8977-10-15

[11] Landsiedel R, Ma-Hock L, Hofmann T, Wiemann M, Strauss V, Treumann S, Wohlleben W, Gröters S, Wiench K, Ravenzwaay B: Application of short-term inhalation studies to assess the inhalation toxicity of nanomaterials. Part Fibre Toxicol. 2014. doi: 10.1186/1743-8977-11-16

[12] Lee KP, Trochimowicz HJ, Reinchardt CF: Pulmonary response of rats exposed to titanium dioxide (TiO_2) by inhalation for two years. Toxicol Appl Pharmacol. 1985;79:179–192

[13] Balasubramaniana S, Jittiwatb J, Manikandanc J, Ongd C, Yua L: Biodistribution of gold nanoparticles and gene expression changes in the liver and spleen after intravenous administration in rats. Biomaterials. 2010;31:2034–2042

[14] Sayed S, Zubair A, Frieri M: Immune response to nanomaterials: implications for medicine and literature review. Curr Allergy Asthma Rep. 2013;13:50–57

[15] Liu J, Wang Z, Liu FD, Kane AB, Hurt RH: Chemical transformations of nanosilver in biological environments. ACS Nano. 2012;6:9887–9899

[16] Korani M. Rezayat SM, Gilani K, Bidgoli AS, Adeli S: Acute and subchronic dermal toxicity of nanosilver in guinea pig. Int J Nanomedicine. 2011;6:855–862

[17] Ge l, Li Q, Wang M, Ouyang J, Li X, Xing MMQ: Nanosilver particles in medical applications: synthesis, performance, and toxicity. Int J Nanomedicine. 2014;9:2399–2407

[18] El-Ansary A, Al-Daihan S: On the toxicity of therapeutically used nanoparticles: an overview. J Toxicol. 2009;754810. doi: 10.1155/2009/754810

[19] Cedervall T, Lynch I, Lindman S, Berggård T, Thulin E, Nilsson H, Dawson KA, Linse S: Understanding the nanoparticle-protein corona using methods to quantify exchange rates and affinities of proteins for nanoparticles. PNAS. 2007;104:2050–2055

[20] Martínez-Gutierrez F, Thi EP, Silverman JM, de Oliveira CC, Svensson SL, Hoek AV et al: Antibacterial activity, inflammatory response, coagulation and cytotoxicity effects of silver nanoparticles. Nanomedicine. 2012;328–236

[21] Shrivastava S, Bera T, Singh G, Ramachandrarao P, Dash D: Characterization of antiplatelet properties of silver nanoparticles. ACS Nano. 2009;3:1357–1364

[22] Tang J, Xiong L, Wang S, Xiong L, Wang S, Wang J, Liu L, Li J, et al.: Influence of silver nanoparticles on neurons and blood-brain barrier via subcutaneous injection in rat. Appl Surf Sci. 2008;255:502–504

[23] Ahamed M, Karns M, Goodson M, Rowe J, Hussain SM, Schlager JJ, et al: DNA damage response to different surface chemistry of silver nanoparticles in mammalian cells. Toxicol Appl Pharmacol. 2008;233:404–410

[24] Kim YS, Kim JS, Cho HS, et al: Twenty-eight-day oral toxicity, genotoxicity. And gender-related tissue distribution of silver nanoparticles in Sprague-Dawley rats. Inhal Toxicol. 2008;20:575–583

[25] Barkalina N, Charalambous C, Jones C, Coward K: Nanotechnology in reproductive medicine: emerging applications of nanomaterials. Nanomedicine NBM. 2014;10:921–938

[26] Iavicoli I, Fontana L, Leso V, Bergamaschi A: The effects of nanomaterials as endocrine disruptors. Int J Mol Sci. 14:16732–16801

[27] Tsuchiya T, Oguri I, Yamakoshi YN, Miyata N: Novel harmful effects of [60] fullerene on mouse embryos in vitro and in vivo. FEBS Lett. 1996;393:139–145

[28] Takeda K, Suzuki KI, Ishihara A, Kubo-Irie M, Fujimoto R, Tabata M, Oshio S, Nihei Y, Ihara T, Sugamata M: Nanoparticles transferred from pregnant mice to their offspring can damage the genital and cranial nerve system. J Health Sci. 2009;55:95–102

[29] Roy R, Das M, Dwivedi PD: Toxicological mode of action of ZnO nanoparticles: impact on immune cells. Mol Immunol. 2015;63:184–192

[30] He X, Aker WG, Leszczynski J, Hwang HM: Using a holistic approach to assess the impact of engineered nanomaterials inducing toxicity in aquatic systems. J Food Drug Anal. 2014;22:128–146

[31] Manke A, Wang L, Rojanasakul Y: Mechanisms of nanoparticles-induced oxidative stress and toxicity. Biomed Res Int. 2013;2013:942916. doi: 10.1155/2013/942916

[32] Robel I, Kuno M, Kamat PV: Size-dependent electron injection from excited CdSe quantum dots into TiO_2 nanoparticles. J Am Chem Soc. 2007;129:4136–4137

[33] Ma J, Lü X, Huang Y: Genomic Analysis of cytotoxicity response to nanosilver in human dermal fibroblasts. Biomed Nanotechnol. 2011;7:263–275

[34] Hackenberg S, Scherzed A, Kessler M, Hummel S, Technau A, Froelich K et al.: Silver nanoparticles: evaluation of DNA damage, toxicity and functional impairment in human mesenchymal stem cells. Toxicol Lett. 2011;201:27–33

[35] You C, Han C, Wang X, Zheng Y, Li Q, Hu X, Sun H: The progress of silver nanoparticles in the antibacterial mechanism, clinical application and cytotoxicity. Mol Biol Rep. 2012;39:9193–9201

[36] Ivask A, Voelcker NH, Seabrook SA, Hor M, Kirby JK, Fenech M et al.: DNA melting and genotoxicity induced by silver nanoparticles and graphene. Chem Res Toxicol. 2015. doi: 10.1021/acs.chemrestox.5b00052

[37] De Stefano D, Carnuccio R, Maiuri MC: Nanomaterial toxicity and cell death modalities. J Drug Deliv. 2012;2012:167896. doi: 10.1155/2012/167896

[38] Becker H, Herzberg F, Schulte A, Kolossa-Gehring M: The carcinogenic potential of nanomaterials, their release from products and options for regulating them. Int J Hyg Environ Health. 2011;214:231–238

[39] Lan J, Gou N, Gao C, He M, Gu AZ: Comparative and mechanistic genotoxicity assessment of nanomaterials via a quantitative toxicogenomics approach across multiple species. Environ Sci Technol. 2014;48:12937–12945

[40] Darne C, Terzetti F, Coulais C, Fontana C, Binet S, Gaté L, Guichard Y: Cytotoxicity and genotoxicity of panel of single- and multiwalled carbon nanotubes: *in vitro* effects on normal Syrian hamster embryo and immortalized V79 hamster lung cells. J Toxicol. 2014; 872195. doi: 10.1155/2014/872195

[41] Munari M, Sturve J, Frenzilli G, Sanders MB, Brunelli A, Marcomini A, Nigro M, Lyons BP: Genotoxic effects of CdS quantum dots and Ag_2S nanoparticles in fish cell lines (RTG-2). Mutat Res Genet Toxicol Environ Mutagen. 2014;775–776:89–93

[42] Golbamaki N, Rasulev B, Cassano A, Marchese Robinson RL, Benfenati E, Leszczynski J, Cronin MT: Genotoxicity of metal oxide nanomaterials: review of recent data and discussion on possible mechanisms. Nanoscale. 2015;7:2154–2198

[43] Huk A, Collins AR, El Yamahi N, Porredon C, Azqueta A, de Lapuente J, Dusinska M: Critical factors to be considered when testing nanomaterials for genotoxicity with the comet assay. Mutagenesis. 2015;30:85–88

Chapter 9

Preparation and Self-assembly of Functionalized Nanocomposites and Nanomaterials – Relationship Between Structures and Properties

Tifeng Jiao, Jie Hu, Qingrui Zhang and Yong Xiao

Additional information is available at the end of the chapter

http://dx.doi.org/10.5772/60796

Abstract

The recent progress in nanocomposites and nanomaterials is varied and occupies various fields. Nanocomposites can be prepared with a variety of special physical, thermal, and other unique properties. On the other hand, self-assembly technique is playing an important role in preparing well-defined multilevel nanostructures and the functionalized surface with the designed and controlled properties. In this chapter, various kinds of nanocomposites including gold nanoparticles, inorganic-organic hybrid composites, graphene oxide nanocomposites, and supramolecular gels via functionalized imide amphiphiles/binary mixtures have all been investigated and analyzed. We summarize main research contributions in recent years in three sections: preparation and self-assembly of some functionalized hybrid nanostructures; preparation and self-assembly of some graphene oxide nanocomposites; preparation and self-assembly of supramolecular gels based on some functionalized imide amphiphiles/binary mixtures. The above work may give the potential perspective for the design and fabrication of nanomaterials and composites. New nanocomposites and nanomaterials are emerging as sensitive study platforms based on unique optical and electrical properties. Future research on preparation of nanocomposites and nanomaterials will depend on the less-expensive processes in order to produce low-cost nanomaterials and devices.

Keywords: nanocomposites, nanomaterials, self-assembly, nanostructures, properties

1. Introduction

The recent progress in nanocomposites and nanomaterials is varied and occupies various fields [1–5]. Nanocomposites can be prepared with a variety of special physical, thermal, and other unique properties. They have better properties than conventional microscale composites and can be synthesized using simple and inexpensive techniques. Now, in a broad sense the word "composite" means "made of two or more different parts" or "a composite is a combination of two or more different materials that are mixed in an effort to blend the best properties of both". A composite material consists of an assemblage of two materials of different natures completing and allowing us to obtain a material of which the set of performance characteristics is greater than that of the components taken separately. Mostly, composite material consists of one or more discontinuous phases distributed in one continuous phase. Hybrid components are that which are with several discontinuous phases of different natures. Discontinuous phase is usually harder and with superior mechanical properties than continuous phase. Nanomaterials and nanocomposites often have unique properties that could enable composite materials with multiple unique properties simultaneously; however, it is often challenging to achieve these properties in large-scale nanocomposite materials. Furthermore, it is important that nanomaterials have desirable properties that cannot be achieved through use of conventional chemicals and materials. To assess the potential value of nanocomposites, it is important to determine which nanomaterials can be effectively integrated into nanocomposites and what new or improved properties are enabled by this. Thus, models of the interactions within the nanocomposites are needed to enable development of effective rules of mixtures. This may require a combination of numerical modeling, characterization, and informatics to enable this nanocomposite with properties by design capability.

On the other hand, self-assembly technique is playing an important role in preparing well-defined multilevel nanostructures and the functionalized surface with the designed and controlled properties [6–8]. Unlike the conventional self-assemblies of amphiphilic compounds at various interfaces or in the bulk, the self-assembly process of the various nanoparticles, colloidal microspheres, metallo-supramolecular systems, inorganic-organic hybrids, and supramolecular nanostructures exhibits unusual advantages, especially in fabricating complicated nanomaterials and nanocomposites. The addition of nanocomposites to self-assembly has enabled new properties for the composite material, but results are highly dependent on the organized arrangement of the nanocomposites and the processing used. It is important to determine whether nanomaterials could be integrated into nanocomposites to enable multiple desirable properties required for a given application.

In our recent research, some functionalized nanocomposites and nanomaterials have been prepared and investigated. In addition, some of the analytical methods, theoretical treatments, and synthetic tools, which are being applied in the area of self-assembly and supramolecular chemistry, will be highlighted. In this chapter, we summarize our main research contributions in recent years in three sections: (1) preparation and self-assembly of some functionalized hybrid nanostructures; (2) preparation and self-assembly of some graphene oxide nanocomposites; (3) preparation and self-assembly of supramolecular gels based on some functionalized imide amphiphiles / binary mixtures.

http://dx.doi.org/10.5772/60796

2. Preparation and self-assembly of some functionalized hybrid nanostructures

In recent years, as a kind of important materials in nanoscience and nanotechnology, gold nanoparticles have been studied most [9–11]. As reported in previous literatures, many methods [12–14] and various kinds of capping agents [15–18] have been investigated to prepare functionalized gold nanoparticles with designed and tailored properties. The capacity to regulate size, shape, and surface functionalized groups to create certain surface properties as well as to manipulate the colloid stability of nanoparticle dispersions are important factors related to their practical applications [19–21]. On the other hand, since the self-assembled nanostructures are very sensitive to and dependent on the molecular skeletons in amphiphile compounds, the design and synthesis of amphiphilic molecules are of utmost importance. In this part, we have demonstrated some examples of such systems including preparation of gold nanoparticles by a series of amphiphiles with hydrophilic ethyleneamine spacers and aromatic headgroups at liquid–liquid interface. Interestingly, it was found that different gold nanostructures were obtained due to different substituted headgroups. The photocatalytic properties of as-made gold nanoparticles on the degradation of methyl orange were also investigated. At the same time, some amorphous nanocomposites were fabricated using chemical precipitation methods. All the results rendered us to believe that these nanocomposites are promising adsorbents for enhanced phosphate removal from contaminated waters.

Based on the research background, some gold nanoparticles were synthesized via a series of bolaform amphiphiles with hydrophilic ethyleneamine spacers and aromatic headgroups at a liquid–liquid interface [22]. By stirring the aqueous $AuCl_4^-$ ions solution with the chloroform solution of used Schiff base compounds, $AuCl_4^-$ ions were transferred into the chloroform phase and reduced to gold nanoparticles. Various gold nanoparticles and nanostructures have been gained depending on the different molecular skeletons and spacers, headgroups of bolaform Schiff base compounds, and the molar ratios of compounds to $AuCl_4^-$ ions. Morphological and spectral investigations suggested that used bolaform Schiff base compounds could act as both capping and reducing agents. For example, the selected-area electron diffraction (SAED) was done on a single nanostructure on a copper grid, as shown in Figure 1. From the SAED patterns, as for the gold nanostructures generated by NpN1 and NpN2 with amphiphile to chloroaurate ion ratio of 1:2, strong electron diffraction patterns were dominated, indicating the crystalline nature of these nanostructures. In addition, the photocatalytic properties of as-prepared gold nanoparticles on the degradation of dye (methyl orange as example) were investigated, demonstrating the effect of substituted groups and molecular skeletons in the compounds on the sizes of as-prepared gold nanoparticles and subsequent catalytic behaviors. The present research results indicated that gold nanostructures could be prepared and designed by bolaform Schiff base compounds and could be well regulated by changing various substituted skeletons and groups (headgroups and spacers).

In addition, some other gold nanoparticles were synthesized by two bolaform cholesteryl imide derivatives with different lengths of ethyleneamine spacers at a liquid–liquid interface [23]. Spectral and morphological measurements indicated that both bolaform amphiphiles

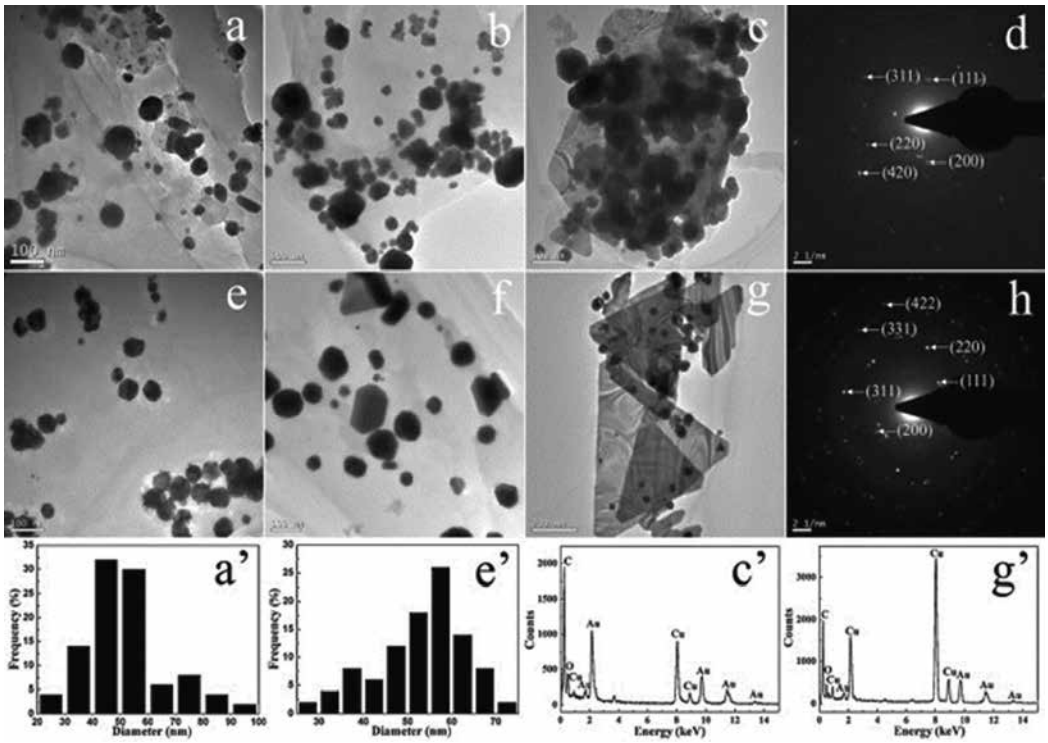

Figure 1. TEM images of gold nanoparticles using NpN1 and NpN2 with different amphiphile to chloroaurate ion ratio of 2:1 (a and e), 1:1 (b and f) and 1:2 (c and g) after 35 h, respectively. (d and h) SAED pattern and (c′ and g′) EDXS taken on the gold nanoparticle shown in (c and g), respectively. The Cu peaks originate from the TEM grid. (a′ and e′) Particle size distribution histograms of gold nanoparticles from TEM images (a and e), respectively.

could serve as both capping and reducing agents. Different gold nanostructures could be obtained depending on the different spacers and the molar ratios of amphiphile to $AuCl_4^-$ ions. In order to investigate the gold nanostructures, the chloroform solution was cast onto copper grid for TEM measurement, as shown in Figure 2. Two main results were obviously observed. One was the particle size distribution of gold nanostructures that changed distinctly depending on the different spacers in two bolaform amphiphiles. Another was the effect of molar ratio of the amphiphiles to $AuCl_4^-$ ions on the generation of gold nanostructures. In addition, we also researched the effect of molar ratio of the amphiphiles to $AuCl_4^-$ ions on the creation of gold nanostructures. The experimental results showed that, with the increase of molar ratio of the compounds to $AuCl_4^-$ ions from 2:1 to 1:2, different kinds of shapes and nanostructures were gained, including hexagonal, polygon nanoparticles and nanoplates with larger size, respectively. The obtained data demonstrated excess bolaform amide compounds could significantly increase the reducing ability, and the rapid reduction usually produced larger nanostructures and nanoparticles. In addition, the photocatalytic performances of as-prepared gold nanostructures on the degradation of dye (methyl orange as example) demonstrated that the spacers in the compounds skeletons indeed played an important role in regulating the sizes of obtained gold nanoparticles and subsequently changing relative catalytic behaviors. The

http://dx.doi.org/10.5772/60796

obtained research results would provide an exploratory investigation about the design and preparation of gold nanostructures by utilizing bolaform compounds with different skeletons and spacers.

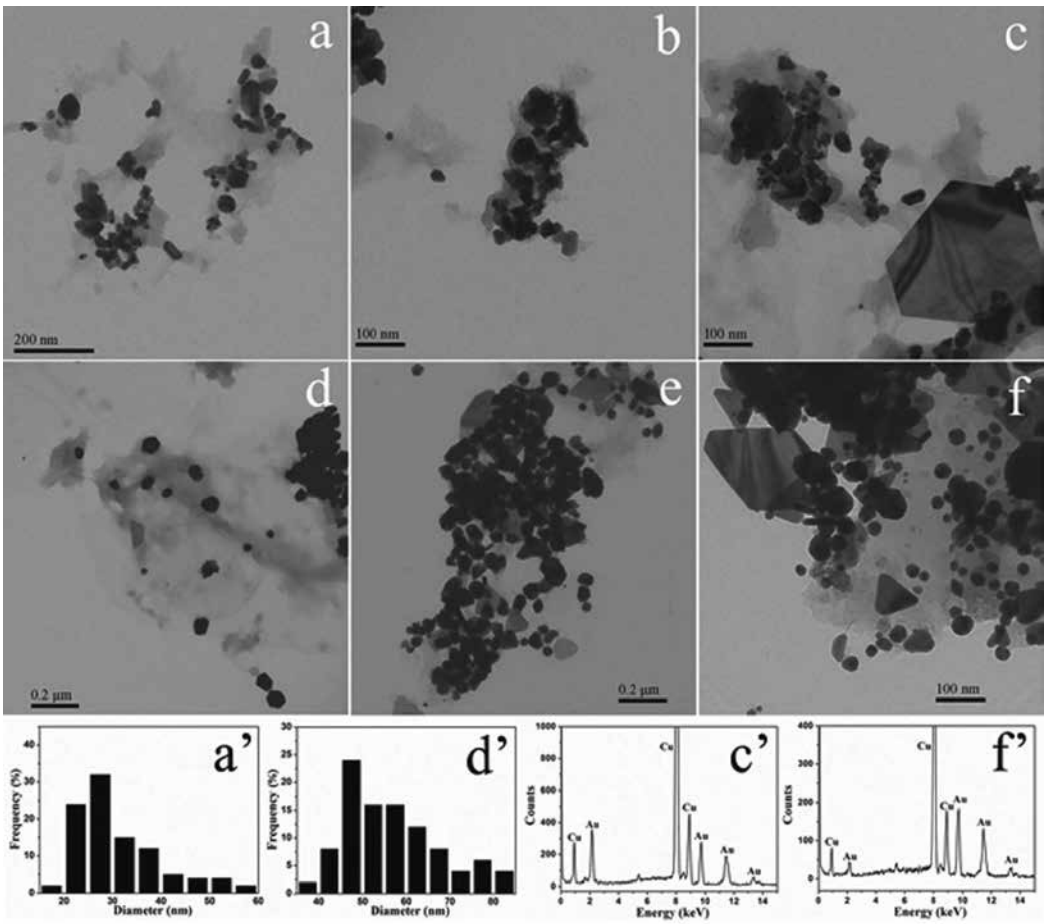

Figure 2. TEM images of gold nanoparticles using CH-N1 and CH-N2 with different amphiphile to chloroaurate ion ratio of 2:1 (a, d), 1:1 (b, e), and 1:2 (c, f) after 35 h, respectively. (c′, f′) EDXS were taken on the gold nanoparticle shown in (c and f), respectively. The Cu peaks originate from the TEM grid. (a′, d′) Particle size distribution histograms of gold nanoparticles from TEM images (a, d), respectively.

Moreover, composites of the nano-sized perovskite-type oxide of $LaMnO_3$ and multi-walled carbon nanotubes (MWCNTs) were synthesized in a single step using the sol–gel method [24]. Their photocatalytic activities for the degradation of various water-soluble dyes under visible light were evaluated. The prepared samples were characterized by thermogravimetry analysis, scanning electron microscopy, transmission electron microscopy, X-ray diffraction, photoluminescence spectroscopy, and UV–vis diffused spectroscopy. Results showed that $LaMnO_3$ nanoparticles grew on the surface of MWCNTs with a grain size of around 20 nm. Photoca-

talysis measurements revealed that the $LaMnO_3$/MWCNT nanocomposites had greater photocatalytic activities than pure $LaMnO_3$ nanoparticles, and the mass percentage of MWCNTs showed that 9.4% possessed the highest photocatalytic activity. These results can serve as a foundation for further research on developing MWCNTs-hybridized materials and improving the photocatalytic activity of the perovskite-type structure photocatalyst.

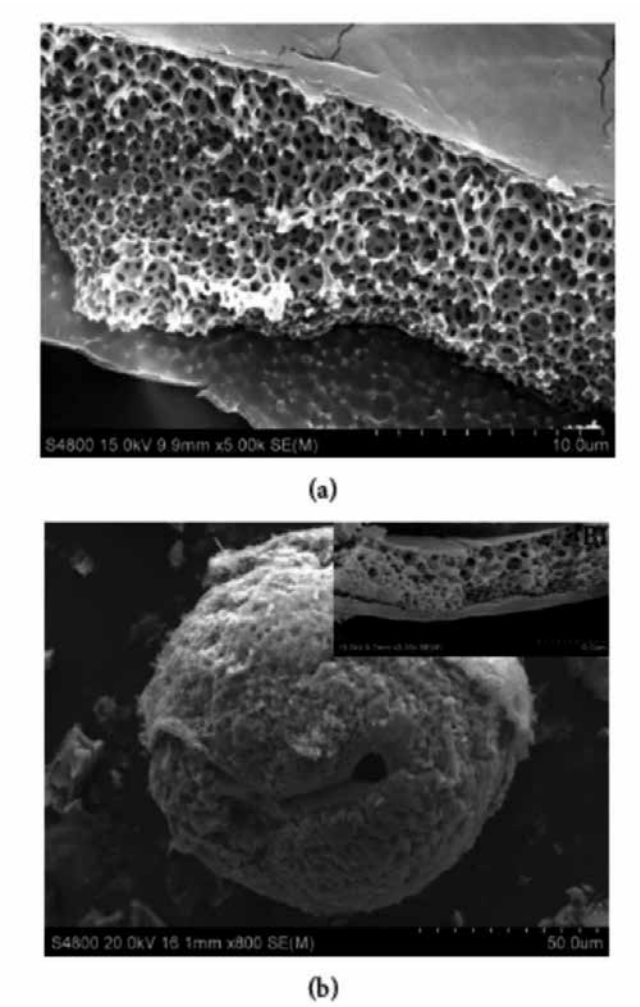

Figure 3. SEM images of (a) neat Artemia egg shell and (b) the shell–TiO2 composite material.

In another research system, some Artemia egg shell with asymptotic reduction pores (diameter: 500–2500 nm, shown in Figure 3) can be used as the carrier for nanocomposite materials [25]. The nanocomposite materials, Artemia egg shell-supported TiO_2, were in polycrystalline-like nanostructures and can be used for high-efficiency formaldehyde removal under visible light. Our results would suggest that iron, as one of the shell's natural components, should be

http://dx.doi.org/10.5772/60796

associated with the photocatalytic performance of shell–TiO_2 composites. Due to their interesting absorption and formaldehyde removal qualities, Artemia egg shell, as a novel naturally porous carrier for nanocomposite materials preparation, especially in the preparation of nanocatalysts, is worthy of further study.

In addition, a new hybrid nanocomposite was prepared by encapsulating ZrO_2 nanoparticles into spherical polystyrene beads (MPS) covalently linked with charged sulfonate groups ($-SO_3^-$) [26]. The obtained adsorbent material, Zr–MPS, demonstrated more preferential sorption performance toward Pb(II) than the simple equivalent mixture of MPS and ZrO_2. Such experimental data might be assigned to the hybrid of sulfonate groups in polymeric host spheres, which could increase nano-ZrO_2 dispersion and Pb(II) diffusion performances. In order to investigate the effect of surface functionalized groups, we composite nano-ZrO_2 with another two macroporous polystyrene host materials with different surface groups (i.e., $-N(CH_3)_3^+$/$-CH_2Cl$, respectively) and a conventional activated carbon, as shown in Figure 4. The three obtained nanocomposites were abbreviated as Zr–MPN, Zr–MPC, and Zr–GAC. The presence of $-SO_3^-$ and $-N(CH_3)_3^+$ was more favorable for nano-ZrO_2 dispersion than the neutral $-CH_2Cl$, resulting in the sequence of sorption capacities as Zr–MPS > Zr–MPN > Zr–GAC > Zr–MPC. Present study suggests that charged groups in the host resins improve the dispersion of embedded nanoparticles and enhance the reactivity and capacity for sorption of metal ions. In addition, selection of suitable surface groups is also a key factor related to the sorption kinetic enhancement and sorption performance for application.

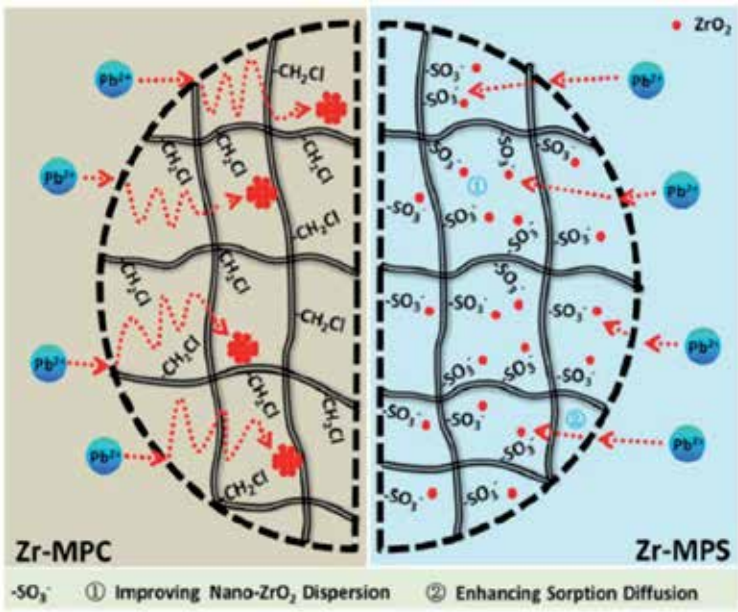

Figure 4. Schematic illustration of the role of charged sulfonate groups of polymeric host on the properties of Zr–MPS toward Pb(II) retention ($-CH_2Cl$ was involved for comparison purpose).

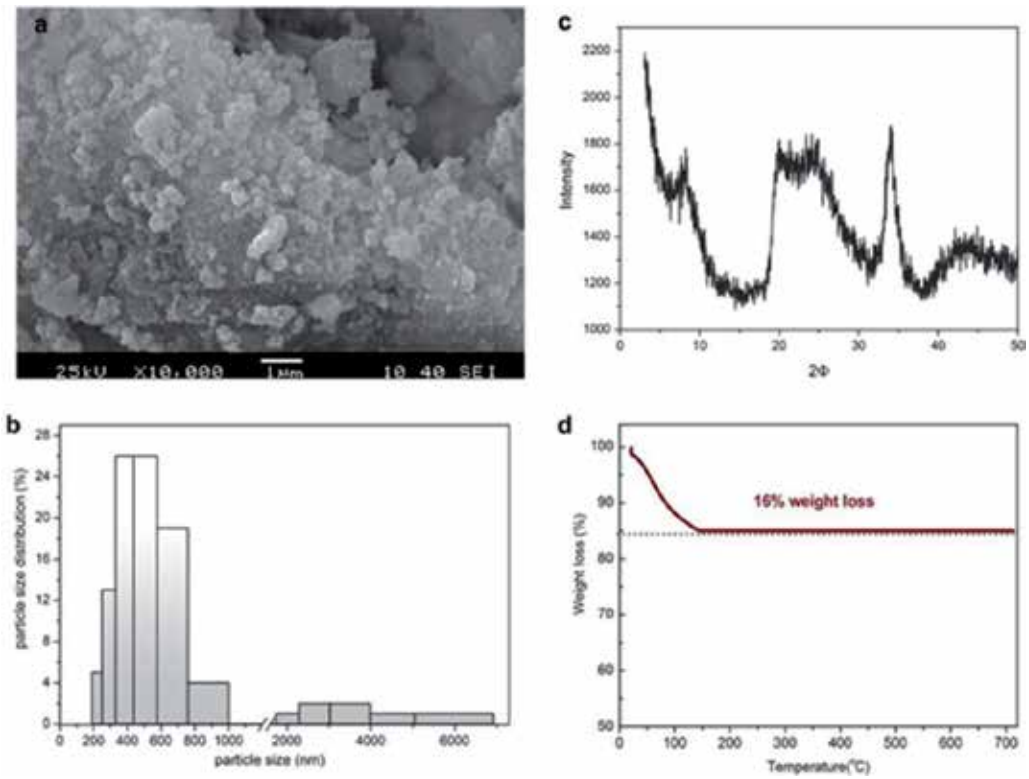

Figure 5. Characterization of ZrP particles (a) SEM of ZrP; (b) ZrP particles size distributions by DLS analysis; (c) XRD analysis of ZrP; (d) TGA curve of ZrP.

In another study, amorphous zirconium phosphate (ZrP) was prepared and the increased sorption performances toward anion-phosphate were investigated [27]. The uptake of phosphate onto ZrP was measured, and the common used anion-exchange resin (D201) and zirconium dioxide particles were introduced for references with coexistence of common anions, the results indicated that both ZrP and ZrO_2 exhibited more favorable sorption performances than D-201, which might be ascribed to the information of inner-sphere complex. Characterizations of ZrP particles were shown in Figure 5. Moreover, the exhausted ZrP particles were amenable to efficient regeneration by alkaline solution for repeated use. All the results rendered us to believe that ZrP is a promising adsorbent for enhanced phosphate removal from contaminated waters.

In addition, nano-ZrP supported by macroporous polystyrene beads with quaternary ammonium groups modification is fabricated based on Donnan membrane principles for efficient fluoride ion removal in waters [28]. The as-obtained materials exhibited favorable removal of fluoride ions from aqueous solution in the presence of common anions (SO_4^{2-}/NO_3^-/Cl^-) at high contents. Such satisfactory performances might be ascribed to the structural design of nanocomposite. Characterizations of the nanocomposite ZrP-MPN were shown in Figure 6. The $CH_2N^+(CH_3)_3Cl$ groups enhance sorption diffusion and preconcentration in sorbent phase

http://dx.doi.org/10.5772/60796

theoretically based on Donnan membrane principle. And the embedded ZrP nanoparticles also devote to the efficient adsorption capacities due to its size-dependent specific properties. Thus, ZrP-MPN was a promising material for fluoride retention in waters.

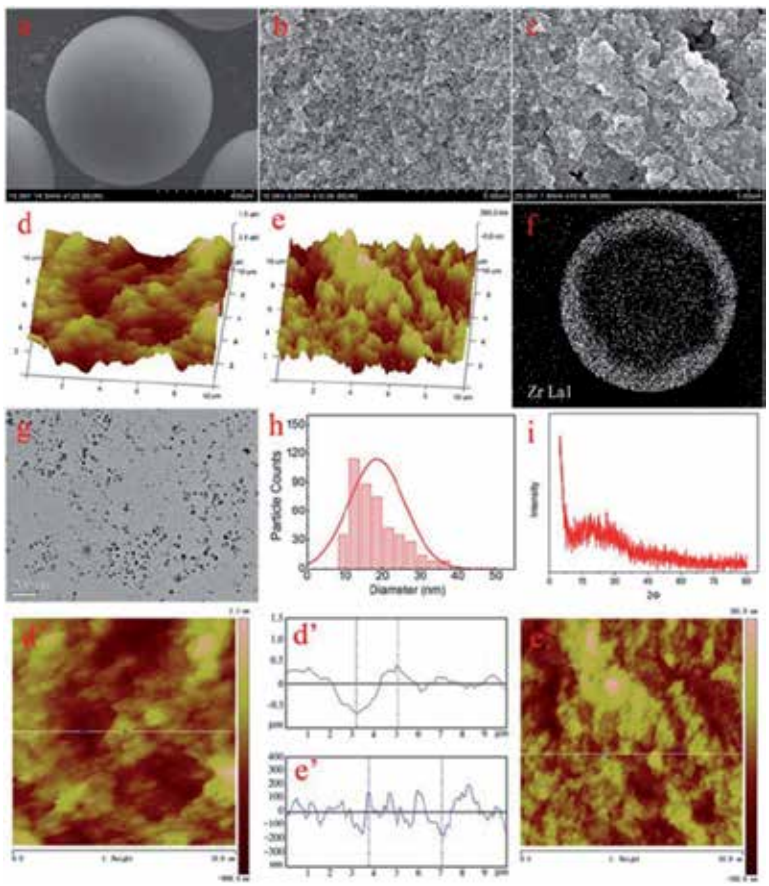

Figure 6. Morphological characterization of the obtained nanocomposites. SEM of (a) spherical bead Zr-MPN, (b) inner surfaces within the host material MPN, (c) inner surfaces within Zr-MPN, AFM 3D analysis onto the inner surface of MPN (d) and ZrP-MPN (e), (f) cross-section Zr distribution of ZrP-MPN by SEM–EDS, (g) TEM of Zr-MPS, (h) the encapsulated ZrP nanoparticle size distribution, (i) XRD spectrum of ZrP-MPN. (d′) AFM line profile analysis of MPN; (e ′) AFM line profile analysis of ZrP-MPN.

Recently, we present a new strategy for a one-step preparation of macroscopic peptide–inorganic hybrid supramolecular films with functionality [29]. The strategy is closely associated with supramolecular interactions of self-assembled starting materials. A mechanism regarding the morphological transition from hybrid nanospheres to visible macroscopic films is proposed, as shown in Figure 7. Firstly, cationic dipeptides and POM anions interact in bulk solution and form PECs as the basic building units mainly through electrostatic attraction. Subsequently, the preformed PECs further stack to form supramolecular networks through hydrophobic interactions, van der Waals forces, and aromatic stacking, finally leading to the

assembly of hybrid nanospheres in water. Depending on the NIR light irradiation, the morphological transition occurs from hybrid nanospheres to visible macroscopic films through a process involving disassembly in the aqueous solution and reorganization at air–water interfaces. Significantly, PECs as basic building blocks remain in the case of the film. The method presented in this study could be extended for preparation of macroscopic films involving weak intermolecular interactions suffering from environmental variations such as temperature and pH, etc.

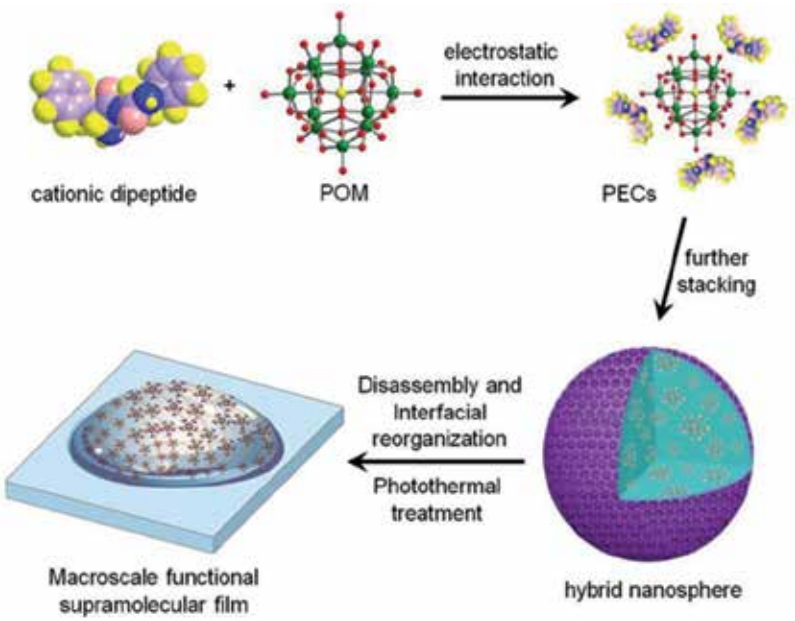

Figure 7. Schematic illustration of the formation of macroscale functional supramolecular films supported onto a solid substrate: hybrid nanospheres are initially self-assembled in aqueous solution mainly by strong electrostatic attraction of cationic dipeptide and polyanions; Structural transformation of a nanosphere solution into the macroscopic film occurs by photothermal treatment, presumably due to photothermally triggered disassembly, and interfacial enrichment and reorganization of PECs.

3. Preparation and self-assembly of some graphene oxide nanocomposites

Graphene, a single layer of sp^2-bonded carbon atoms, is now promising for enhancing photocatalytic activity because of its excellent adsorption capacity, high chemical stability, and large specific surface area [30]. Thus, compounding graphene with semiconductor photocatalysts to develop novel nanocomposites with enhanced photocatalytic performance has received increasing attention. Ullah and coworkers reported that Pt-graphene/TiO_2 nanocomposites were prepared by facile and fast microwave-assisted method and the photocatalytic activities were investigated by the degradation of rhodamine B (Rh.B) as a standard dye [31].

http://dx.doi.org/10.5772/60796

Bai et al. developed $ZnWO_4$/graphene hybrid (GZW-X) photocatalysts by an easy in situ reduction of graphene oxide and $ZnWO_4$ in water and high efficiency for the degradation of methylene blue under both UV and visible light [32]. Sun and coworkers prepared $ZnFe_2O_4$/ZnO nanocomposites immobilized on different content of graphene on the basis of an ultrasound-aided solution method [33]. The molar ratio of $ZnFe_2O_4$ to ZnO and the content of graphene could be controlled by adjusting the amount of zinc salts and graphene oxide dispersions. Xu et al. obtained reduced graphene oxide/Bi_2WO_6 (RGO–Bi_2WO_6) composite photocatalysts, and an enhancement in photocatalytic activities were observed in RGO–Bi_2WO_6 composites compared with pure Bi_2WO_6 [34]. To enhance the photocatalytic activity, efforts have been exerted to load photocatalysts on the structure of graphene [35–38]. In this part, we have demonstrated some examples of research systems including preparation of magnetite/reduced graphene oxide (MRGO) nanocomposites for removal of dye pollutants, as well as metal oxides–graphene composite for photocatalyst. These works not only provided important inspirations for developing graphene-hybridized materials but also opened new possibilities to improve the photocatalytic activity of photocatalyst.

Firstly, $LaMnO_3$-graphene nanocomposite photocatalysts were synthesized by a sol–gel method for the first time [39]. Pure $LaMnO_3$ perovskite phase was successfully anchored on the surface of graphene sheets and had good dispersion behavior, as shown in Figure 8. The photocatalytic activity of the $LaMnO_3$–graphene composite was higher than that of the pristine $LaMnO_3$. The enhancement of UV–vis photocatalytic light activity can be attributed to the high separation efficiency of photo-induced electron–hole pairs resulting from the excellent conductivity of graphene in $LaMnO_3$–graphene and the large surface contact between graphene and $LaMnO_3$, which can promote the adsorption of organic dyes and improve the transfer efficiency of the photocatalytic process. This work not only provided important inspirations for developing graphene-hybridized materials but also opened new possibilities to improve the photocatalytic activity of perovskite photocatalyst.

In another research work, $La_{1-x}Sr_xMnO_3$/graphene thin films were obtained using sol–gel and spin-coating methods on glass substrates [40]. A combination of chemical bonds between the thin films and substrates was achieved using a silane coupling agent (APTES), illustrated in Figure 9. In this method, the sol particles were adsorbed on the graphene surface by electrostatic adsorption in aging stage. The subsequent calcination process made the $LaMnO_3$ particles grow and crystallize on the graphene surface. The structure, grain size, and morphology were characterized by spectral and morphological methods. Results show that perovskite nanoparticles grew on graphene, and the size of the grain was about 40 nm. In the process of acid red 3GN photodegradation, $LaMnO_3$/graphene thin film had sound stability and better photocatalytic ability than $LaMnO_3$ thin film. Graphene accelerated the adsorption of the dye, which inhibited the reunion of light-induced e^-–h^+, and improved the photocatalytic efficiency. A red shift of the absorption edge, which enhanced the photocatalytic performance of the $LaMnO_3$/graphene thin film, was achieved by doping Sr. When $x = 0.1$, the decoloration rate reached 94.52%, and the TOC concentration of acid red 3GN was only 0.36 mg/L after illumination for 4 h.

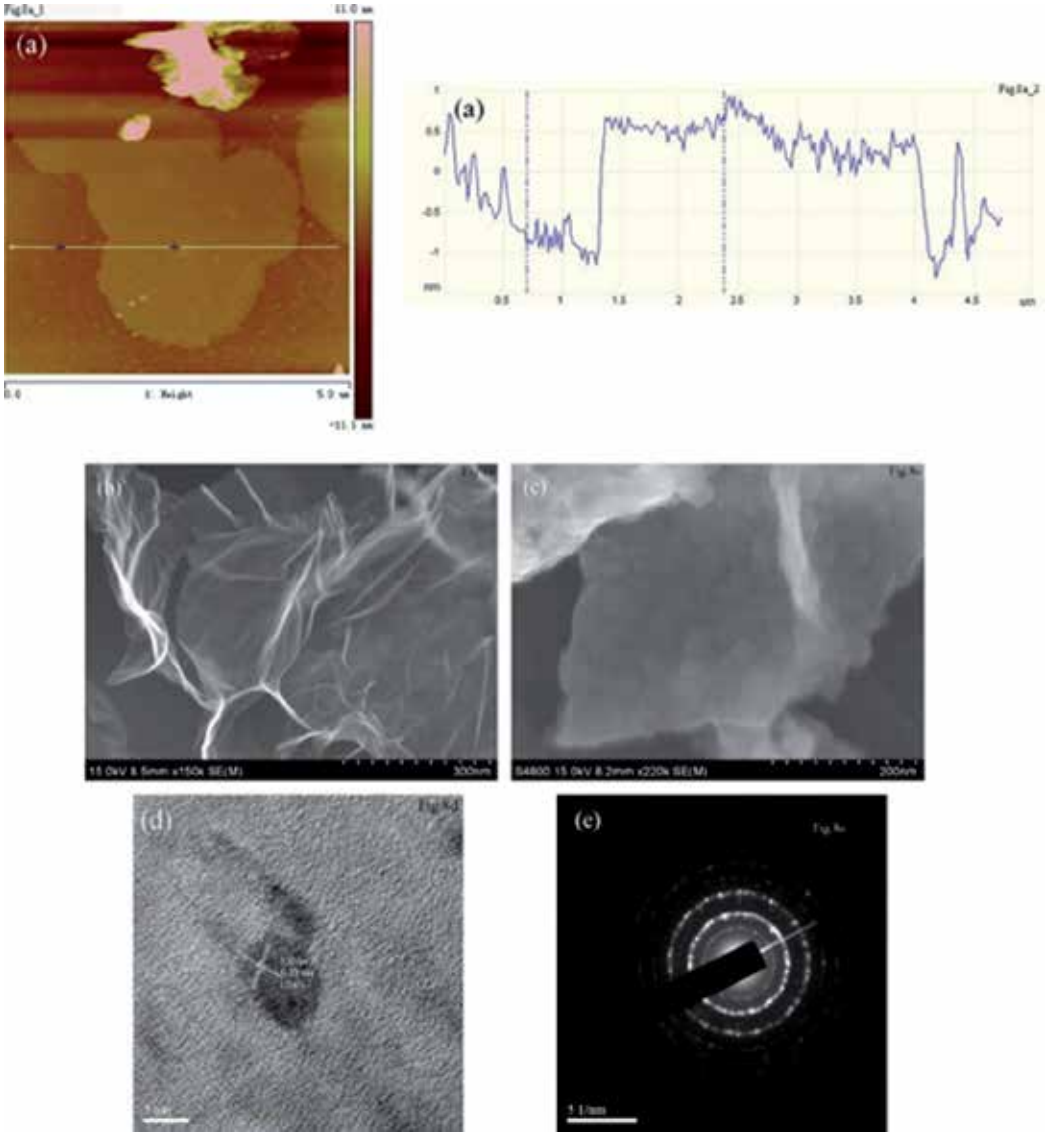

Figure 8. (a) AFM image of the as-synthesized graphene; (b) SEM image of graphene; (c, d, e) SEM, HRTEM and SAED images of $LaMnO_3$-graphene composites.

In addition, a novel photocatalyst of $LaMn_{1-x}Co_xO_3$/graphene composites had been synthesized by sol–gel process assisted with chelating effect of citric acid [41]. It was found that $LaMnO_3$ perovskite phase was successfully processed which anchored on the surface of graphene sheets, and doping Co did not change the perovskite structure. The UV–vis photocatalytic activity of the photocatalysts was evaluated by the degradation of diamine green B. In the photodegradation of diamine green B, after graphene was introduced to $LaMnO_3$ as a photocatalytic, it can accelerate the adsorption of the dye, while doping Co enhances the photoca-

http://dx.doi.org/10.5772/60796

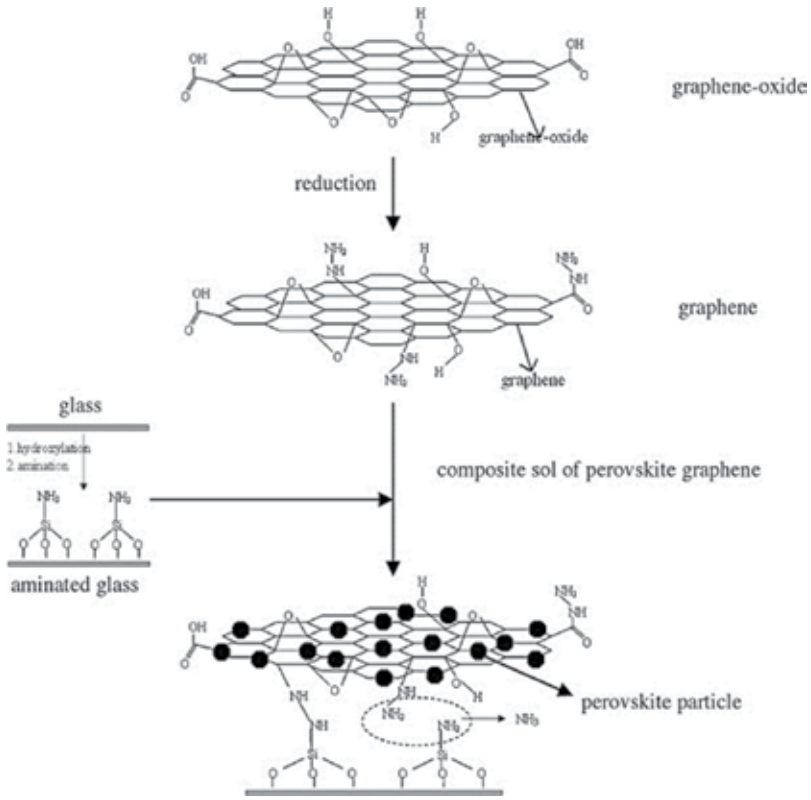

Figure 9. Preparation flow chart of the $LaMnO_3$/graphene thin film on glass substrate.

talytic performance of $LaMnO_3$/graphene composites and $LaMn_{0.85}Co_{0.15}O_3$/graphene composite has the best catalytic activity. The charge transfer mechanism that occurs in the $LaMnO_3$/graphene composite during photocatalytic process is shown in Figure 10. Diamine green B molecules could transfer from the solution to the composites' surface and be adsorbed with offset face-to-face orientation via π–π conjugation between diamine green B and aromatic regions of the graphene; therefore, due to its giant π-conjugation system and two-dimensional planar structure, the adsorptivity of dyes improved compared to the bare $LaMnO_3$. Due to these holes and electron transfers, charge recombination is suppressed in $LaMnO_3$/graphene composite and hence largely enhances the efficiency of photocatalytic properties.

Moreover, some graphene-based $LaNiO_3$ composite films were also prepared by using sol–gel method and spin coating technique on glass substrate [42]. The composite films were characterized by various techniques. The experimental data demonstrated that the size of $LaNiO_3$ crystalline grains is about 20 nm with uniform growth in graphene sheet. The photocatalytic performance of films had been investigated by degradation of Acid red A as an example. Comparing with $LaNiO_3$ films, the $LaNiO_3$/graphene composite films indicated better photocatalysis properties. When the content of graphene is changed as about 4%, the photocatalytic efficiency of the $LaNiO_3$/graphene composite films is double of the $LaNiO_3$ films.

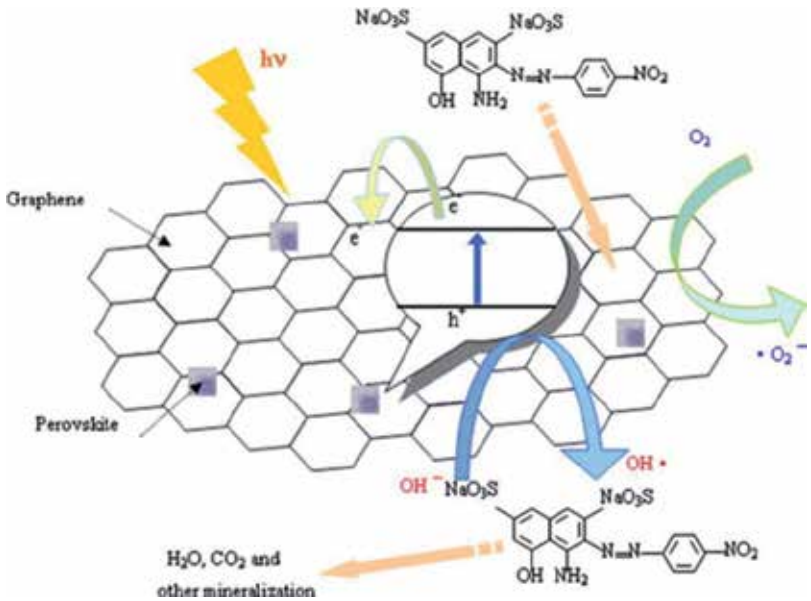

Figure 10. Proposed mechanism for photocatalytic degradation of diamine green B over graphene-based perovskite photocatalysts under light irradiation.

In another system, $La_{1-x}Ca_xMnO_3$ perovskite–graphene composites are synthesized as catalysts for Zn–air cell cathodes [43]. The results indicated that perovskite phase adhered on the surface of graphene sheets, and adding graphene significantly improved the electrochemical performance of $LaMnO_3$. FE-SEM analyses were carried out to observe the morphology of the as-synthesized material, as shown in Figure 11. The as-prepared graphene have gauze-shaped wrinkles and folds structure, which may be caused by oxygenic functional group and the resultant defects during the preparation of graphene oxide. As catalyst of air electrode, its porous structure could greatly increase the three-phase region, thereby improving the mass transfer process. The voltage plateau was superior when the ratio of graphene was 10 wt%. Ca doping not only maintained the perovskite structure but also significantly improved the electrocatalytic activity for the ORR, and $La_{0.6}Ca_{0.4}MnO_3$–graphene exhibited the best catalytic activity. The electron transfer number of $La_{0.6}Ca_{0.4}MnO_3$–graphene was 3.6, which was calculated from the RRDE measurement result. This finding indicated that the sample exhibited considerable catalytic activity for the ORR. These results indicate that the $La_{1-x}Ca_xMnO_3$–graphene composites are potential air electrodes catalysts.

Recently, a new photocatalyst of $LaMnO_3$/graphene thin films with the perovskite-type was synthesized by sol–gel process assisted with spin coating methods on glass substrates [44]. Results showed that after the introduction of graphene, the perovskite structure was unchanged and the size of $LaMnO_3$ particles was about 22 nm, with uniform growth in graphene sheet. Determination of contact angle indicated that the contact angle of glass substrate decreased and the hydrophilicity improved after treating with H_2SO_4 and APTES. The UV-vis photocatalytic activity of the photocatalysts was evaluated by the degradation of diamine

http://dx.doi.org/10.5772/60796

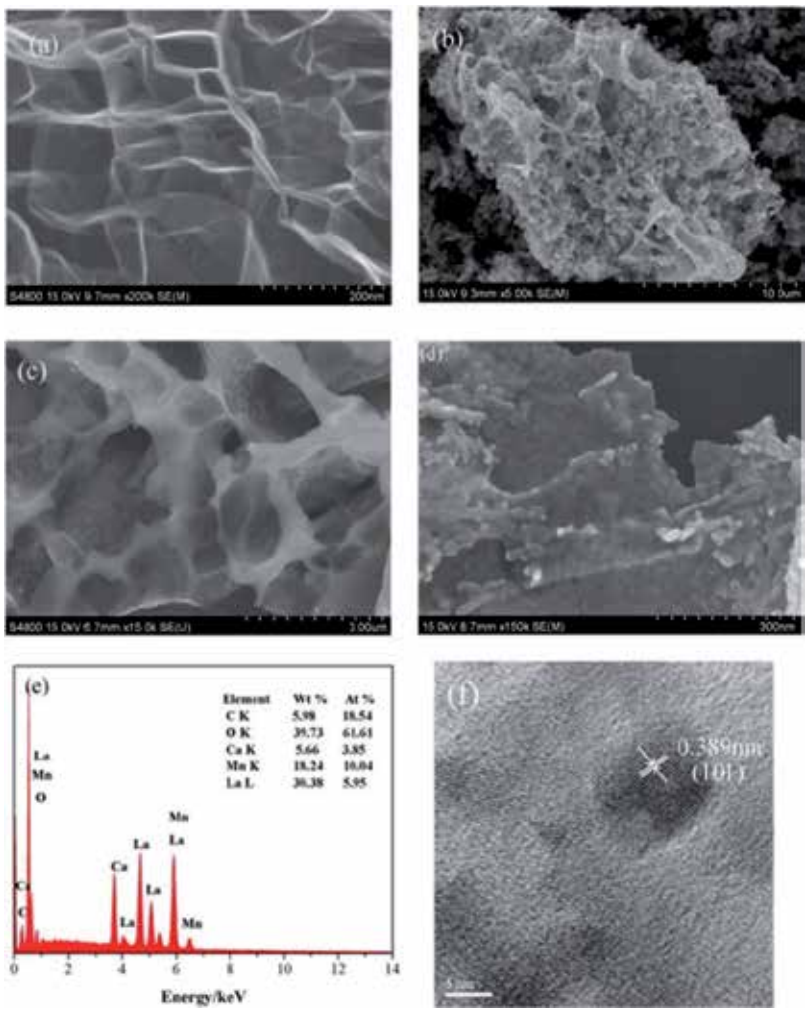

Figure 11. FESEM images of (a) graphene; (b, c, d) FE-SEM, (e) EDS, (f) HRTEM of $La_{0.6}Ca_{0.4}MnO_3$–graphene composite.

green B. $LaMnO_3$/graphene thin films had better photocatalytic ability than $LaMnO_3$ and TiO_2 films.

4. Preparation and self-assembly of supramolecular gels based on some functionalized imide amphiphiles/ binary mixtures

In recent years, supramolecular gels, which show different organized three-dimensional aggregates with micrometer-scale/nanometer-scale lengths and diameters immobilizing the flow of liquids (water or organic solvents), have been well known for wide applications on

drug delivery, functionalized materials, agents, and sensors as well as water purification [45–48]. The driving forces responsible for gel formations are mainly different noncovalent interactions, such as van der Waals forces, hydrogen bonding, dipole–dipole interaction, π–π stacking, and host–guest interaction [49–51]. On the other hand, gels are early investigated in macromolecular/polymer cases, but there has recently been an increasing attention in low molecular mass organic gelators (LMOGs) [52–54]. Such kind of organogels have some advantages over previous polymer-based gels: the molecular structure of the gelator is defined, and the gel process is usually reversible. Such properties can allow to design and prepare various functionalized gel systems and produce more complicated and controllable nanocomposites and/or nanostructures [55–57]. In this part, we have demonstrated some examples of such systems including supramolecular gels based on some functionalized imide amphiphiles or binary mixtures. The gelation properties of these organogels will be discussed to attempt to understand the stacking mechanism and assembly modes and thereby try to control multidirectional self-assembly in some content. The objective is to give some insight to design and character new versatile organogelators and soft materials with special molecular structures.

Firstly, two new cholesterol imide derivatives with azobenzene substituent groups have been synthesized. The difference in the headgroups of azobenzene segment can produce a dramatic change in the gelation behavior [58]. Upon UV irradiation on the as-formed gel, *trans–cis* photoisomerization of the azobenzene functionalized groups occurs, and the shift in molecular polarity leads to the collapsed breaking of van der Waals forces, resulting in the gel–sol transition. In addition, the formed gel can also be recovered by the reverse *cis–trans* photoisomerization after exposure to visible light, as shown in Figure 12. Morphological and spectral results indicate that the gelator molecules self-assemble into one-dimensional belts with diameters 50–80 nm, which further self-assemble to form regular nanobelts. The obtained experimental data give useful information for the development of new functionalized low molecular mass organogelators and nanomaterials.

In addition, new bolaform and trigonal cholesteryl amide derivatives with different aromatic spacers were designed and prepared [59]. The gelation behaviors of two cholesteryl derivatives with aromatic spacers in various organic solvents can be regulated by changing spacer size and molecular shapes, as shown in Figure 13. While the trigonal compound gels 3 of the 20 solvents investigated at a concentration more than 3.0%, the bolaform amide compound gels 2 of the solvents tested at a concentration more than 2.0%, respectively. In addition, morphological observations indicate that the size of the spacers and the identity of the solvents are the main factors affecting the organized stacking of the aggregates in the as-formed gels. After experimental investigation, a clear process about spacer effect on the organized nanostructures of the gels was proposed.

In another study, some new glutamic acid diethyl ester imide derivatives with different alkyl substituent chains were designed and synthesized [60]. The results indicated that the length of alkyl substituent chains linked to benzene ring in gelator compounds played an important role in the gelation performance of all compounds in various organic solvents. Longer alkyl chains in molecular skeletons in the present as-formed gelators are favorable for the gelation

http://dx.doi.org/10.5772/60796

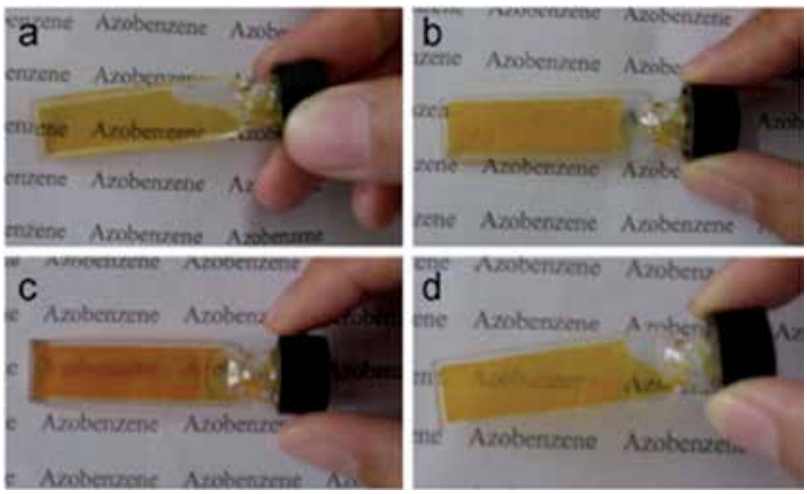

Figure 12. Photographs of Ch-azo (1.5% w/v, 0.1 cm path length) in hot DMF solution (a), formed gel in room temperature (b), after UV irradiation for 170 min (c), and subsequent visible irradiation for 40 min (d).

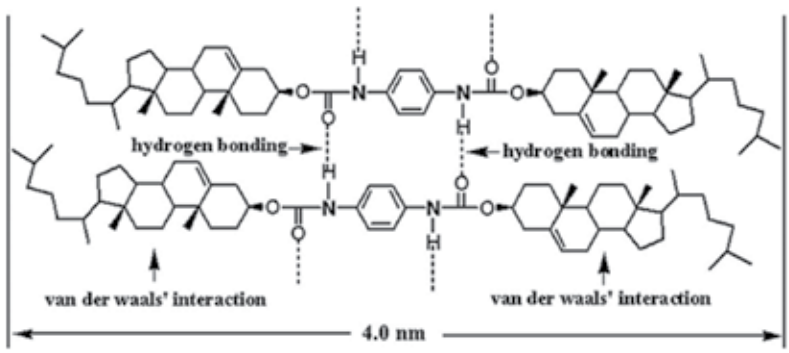

Figure 13. A possible aggregation mode of Ch-p-ben gel in aniline.

of organic solvents. SEM and AFM investigation demonstrated that the gelator molecules self-assemble into different aggregates from wrinkle, lamella, belt, to fiber with change of solvents. In addition, the xerogels in nitrobenzene of all compounds were characterized by AFM, as shown in Figure 14. From the pictures, it is wealthy to note that these big belt or lamella aggregates contained many little domains by stacking of the present imide compounds. Spectral studies indicated that there existed different H-bond formations and hydrophobic forces, depending on the alkyl substituent chains in molecular skeletons.

In addition, four azobenzene imide derivatives with different substituent groups were designed and synthesized. Their gelation behaviors in 21 solvents were tested as novel low-molecular-mass organic gelators [61]. It was shown that the substituent groups in azobenzene residue and benzoic acid derivatives can have a profound effect upon the gelation abilities of

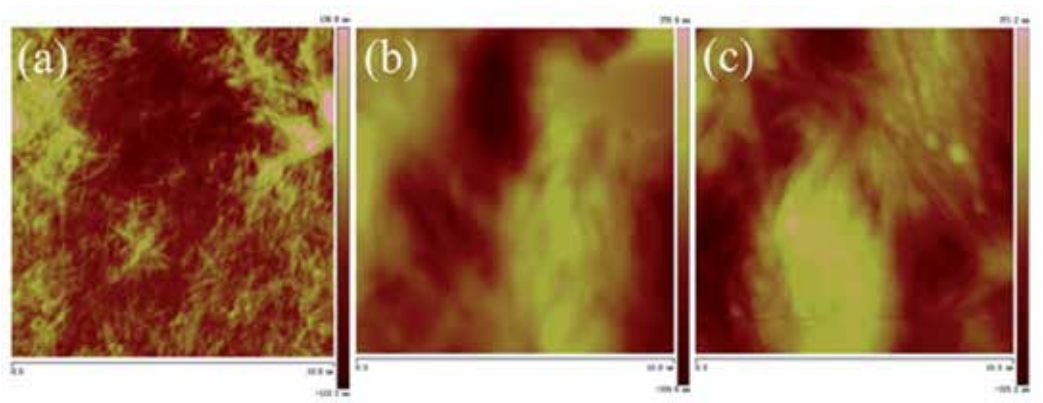

Figure 14. AFM images of xerogels from GC16 (a), GC14 (b), and GC12 (c) gels in nitrobenzene, respectively.

these studied compounds. The results indicated that more alkyl chains in compound skeletons in the present used gelators are favorable for the gelation of organic solvents. Morphological investigations suggested that the gelator molecules self-assemble into different shapes of aggregates, from wrinkle, lamella, and belt to fiber with the change of solvents, as shown in Figure 15. The present work may give some insight to the design and character of new organogelators and soft materials with special molecular structures.

It is well known that luminol is regarded as a famous and efficient case in electrochemiluminescence (ECL) investigations for the detection of hydrogen peroxide. In our previous reports, some novel luminol imide compounds with various substituent alkyl chains were designed and prepared. Their gelation performances in 26 solvents were measured as new low molecular mass organic gelators [62]. The experimental data indicated that the length and substituent number of alkyl chains connected with benzene ring in gelator skeletons played an important role in the gelation formation of all imide derivatives in different organic solvents. Longer alkyl chains in molecular structures in used gelator compounds are favorable for the gelation of present organic solvents. Morphological investigations suggested that the gelator molecules self-assemble into various micro/nanoscale aggregates from dot, flower, belt, rod, and lamella to wrinkle with solvents change, as shown in Figure 16. Considering the XRD results described above and the hydrogen bonding nature of the orderly aggregation of these imide compounds as confirmed by FT-IR, a possible assembly mode of TC18-Lu organogels was proposed. Now the ECL properties generated by the present xerogels of these luminol derivatives in the presence of hydrogen peroxide are under investigation to display the relationship between the molecular structures, as-formed nanostructures, and ECL sensors.

In addition, some functional cholesteryl compounds with various spacers were chosen and prepared. Their gelation performances in 23 solvents were tested, and some of them were investigated to be low molecular mass organic gelators [63]. The obtained data suggested that these as-prepared organogels can be changed by regulating the flexible/rigid parts in spacers and organic solvents. Suitable joint of flexible/rigid parts in molecular spacers in the used cholesteryl compounds is favorable for the gelation of organic solvents. To obtain a visual

http://dx.doi.org/10.5772/60796

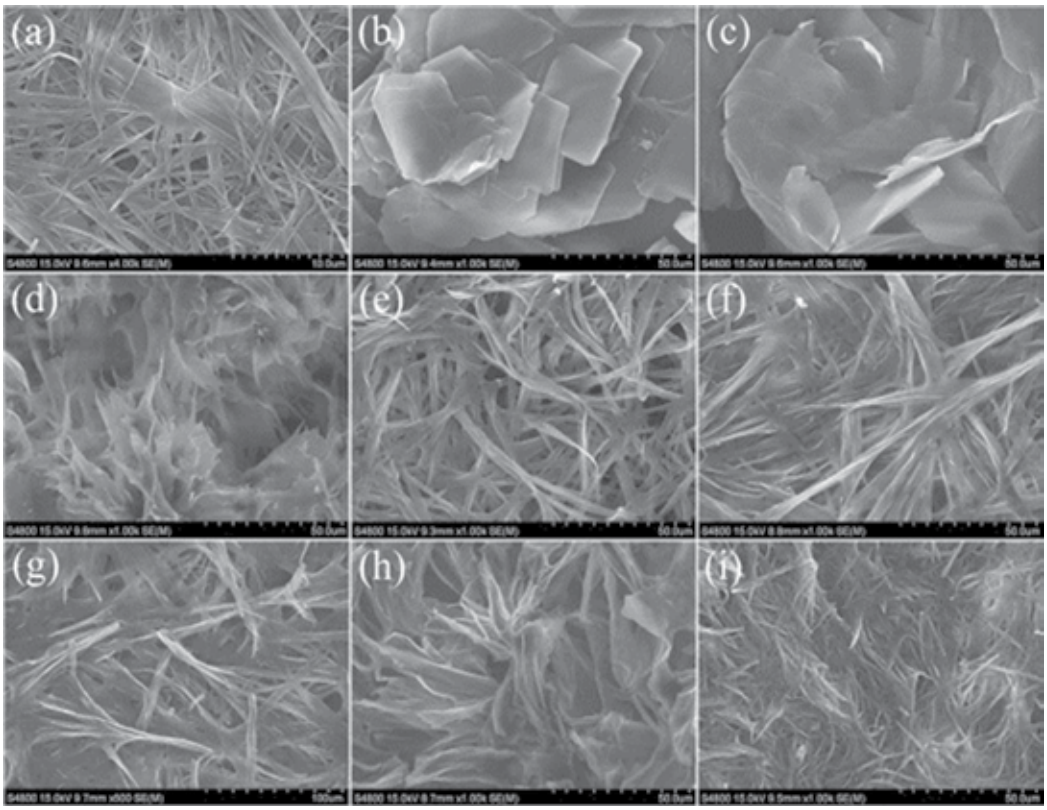

Figure 15. SEM images of xerogels. SC16-Azo gels ((a) benzene, (b) pyridine, and (c) DMF) and SC16-Azo-Me gels ((d) tetrachloromethane, (e) benzene, (f) nitrobenzene, (g) aniline, (h) DMF, and (i) 1,4-dioxane).

insight into the prepared gel nanostructures, the typical nanostructures of these gels were investigated by SEM technique, as shown in Figure 17. Considering the obtained results and the interaction nature about organized stacking in prepared organogels, some reasonable stacking modes in the formed gelators were proposed. As for CH-C1 xerogel from 1,4-dioxane, due to the flexibility of ether band in the molecular structures and various intermolecular forces with solvents, after the oriented hydrogen bonding and organized stacking in different solvents, various stacking units with various lengths were gained. As for CH-C3 with an additional diphenyl part connected with ether band in the spacer segment, the joint of a flexible ether band and a rigid diphenyl part in the molecular spacer with π–π stacking seemed more suitable to regulate molecular conformation to self-assemble and form organized self-assembly nanostructures. On the other hand, for the case of CH-C4 with a five-carbon alkyl substituent chain connected with phenoxy ether band in the molecular spacer, due to the addition of a flexible alkyl segment and a weak hydrophobic force between alkyl chains, it can also self-assemble to fabricate some belt-like domains. Moreover, for CH-C2 and CH-N1, the inefficient or poor gelation behaviors in used solvents may be mainly attributed to the too rigid or too flexible spacers in molecular skeletons, which cannot cause enough intermolecular forces to

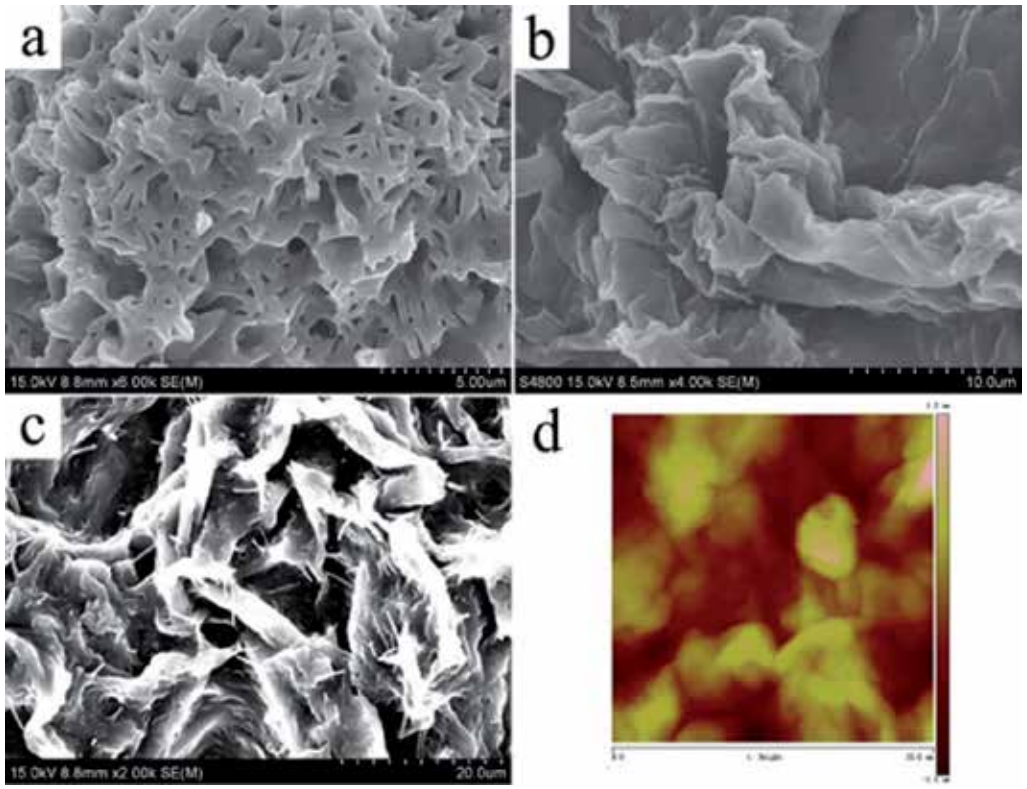

Figure 16. SEM and AFM images of xerogels. (a) TC18-Lu, (b,d) TC16-Lu, and (c) TC14-Lu in DMF gels.

make the molecules align and self-assemble in an organized way to form various nanostructures. Now, the drug release behaviors generated by the present xerogels in the mixture of Congo red are under investigation to display the relationship between the molecular structures of as-formed nanostructures and their properties.

Moreover, another bolaform cholesteryl imide derivative with conjugated aromatic spacer was designed and prepared. The gelation performances in 23 solvents were tested as efficient low-molecular-mass organic gelator [64]. The obtained data demonstrated that the morphologies and assembly modes of as-prepared organogels can be changed by regulating different kinds of organic solvents. Considering the described experimental results, some possible assembly mechanisms about the gelators were proposed and schematically shown in Figure 18. As for CH-PY xerogel from n-butyl acrylate, due to the rigidity of conjugated spacer in molecular structure and different intermolecular forces with solvents, after oriented hydrogen bonding and orderly π–π stacking, CH-PY molecules have a tendency to self-assemble in stretched mode. As for CH-PY xerogels from used other solvents, such as n-pentanol and cyclopentanone, in comparison with π–π stacking, the intermolecular forces with solvents seemed more obvious to adjust molecular conformation to self-assemble and form different twisted stacking nanostructures.

http://dx.doi.org/10.5772/60796

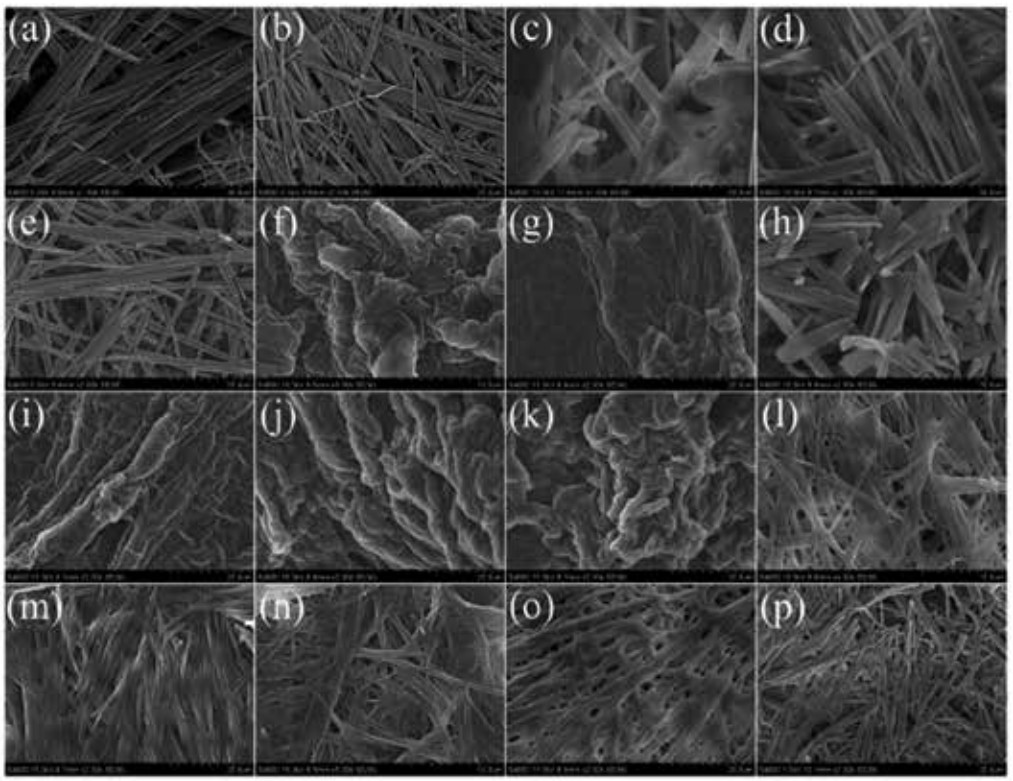

Figure 17. SEM images of xerogels. CH-C1 gels ((a) isooctanol, (b) n-hexane, (c) 1,4-dioxane, (d) nitrobenzene, (e) aniline), CH-C3 gels ((f) cyclohexanone, (g) 1,4-dioxane, (h) nitrobenzene, (i) ethyl acetate, (j) petroleum ether, (k) DMF), CH-C4 gels ((l) nitrobenzene, (m) aniline, (n) n-butyl acrylate, (o) DMF), and CH-N1 gels ((p) pyridine).

In another research work, the gelation behaviors of binary organogels composed of azobenzene amino derivatives and alkyloxybenzoic acids with different lengths of alkyl chains in various organic solvents were investigated and characterized [65]. The corresponding gelation performances in 20 solvents were characterized and shown as novel binary organic systems. It indicated that the lengths of substituent alkyl chains in compounds have played an important role in the gelation formation of gelator mixtures in present tested organic solvents. Longer methylene chains in molecular skeletons in these gelators seem more suitable for the gelation of present solvents. Morphological characterization showed that these gelator compounds have the tendency to self-assemble into various aggregates from lamella, wrinkle, and belt to dot with change of solvents and gelator mixtures, as shown in Figure 19. Meanwhile, these organogels can self-assemble to form monomolecular or multilayer nanostructures owing to the different lengths of alkyl substituent chains. Possible assembly modes for present xerogels were proposed. The present investigation is perspective to provide new clues for the design of new nanomaterials and functional textile materials with special microstructures.

In another continuous work, the gelation behaviors of binary organogels composed of azobenzene amino derivatives and fatty acids with different alkyl chains in various organic

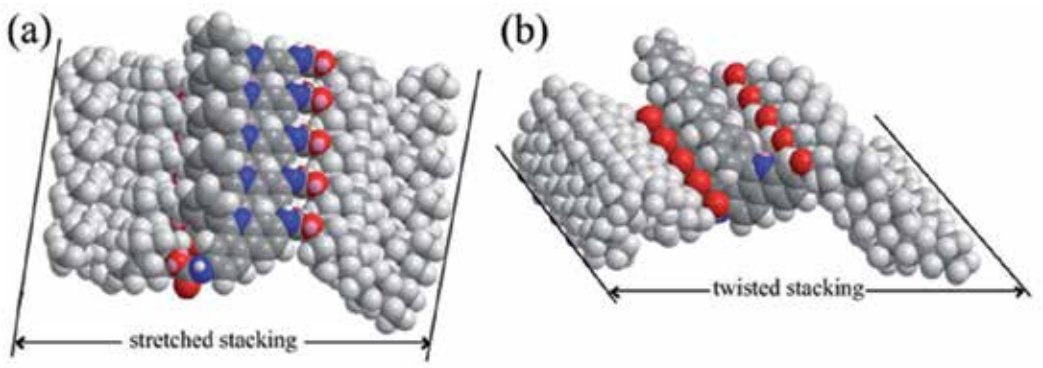

Figure 18. Rational assembly modes of CH-PY organogels in stretched stacking (a, 3.5 nm) and twisted stacking (b, 2.73 and 2.38 nm), respectively.

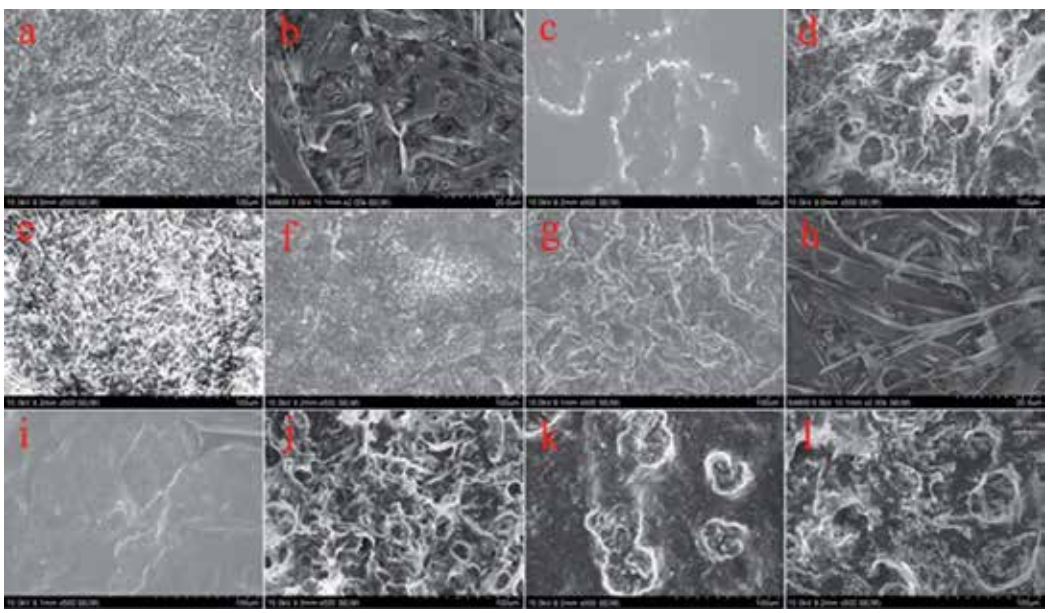

Figure 19. SEM images of xerogels. C16-Azo (a, b, c, d, e, and f) and C16-Azo-Me (g, h, i, j, k, and l) in toluene, nitrobenzene, ethanolamine, n-butyl acrylate, chloroform, and benzene, respectively.

solvents were designed and investigated [66]. The experimental results indicated that their gelation behaviors solvents can be regulated by changing the length of alkyl substituent chains and azobenzene segment. Longer alkyl chains in molecular skeletons in present gelators are favorable for the gelation of organic solvents. For the mixtures containing 4-aminoazobenzene, only C12-Azo cannot form any organogel in present solvents. While for the mixtures containing 2-aminoazotoluene, only C18-Azo-Me and C16-Azo-Me can form gel in ethanolamine, respectively. The prepared nanostructured materials have wide perspectives and many potential applications in nanoscience and material fields due to their scientific values.

http://dx.doi.org/10.5772/60796

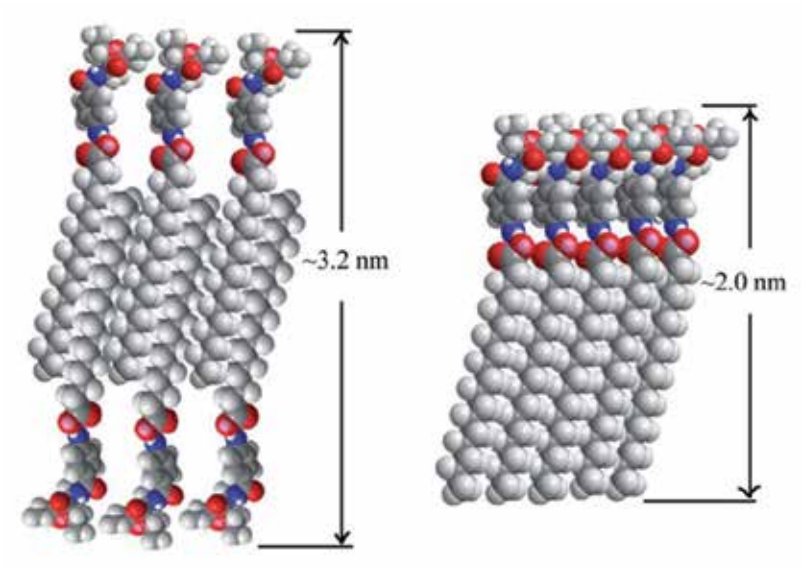

Figure 20. Two possible assembly modes for Glu-C18 organogels in different solvents.

In addition, the gelation behaviors of binary fatty acids with different length of alkyl chains and glutamic acid amino derivative in various organic solvents were designed and investigated [67]. The obtained data showed that the length of substituent chains has played an important role in the gelation properties of all gelator systems in different organic solvents. Longer alkyl chains in molecular structures in used gelator compounds are favorable for the gelation preparation of organic solvents. Considering the XRD results described and the hydrogen bonding interaction of these binary mixtures as confirmed by FT-IR measurements, two possible assembly modes of Glu-C18 were proposed and schematically shown in Figure 20. As for xerogels of Glu-C18 in different kinds of solvents (for example, toluene, isopropanol, n-butanol, and ethanolamine), the alkyl chains in neighboring molecules or stacking units will be able to penetrate easily into the empty room between the alkyl chains in another self-assembly unit. Under such self-assembly mode, the layer distance will increase to about 3.2 nm. For the xerogels of Glu-C18 in two other solvents, due to the chains parallel to the layer surface, the repeating stacking unit with length of about 2 nm was gained.

Moreover, some binary organogels based on glutamic acid derivatives and acids with different molecular skeletons were designed and prepared [68]. Their gelation behaviors in single or mixed solvents were tested as novel low molecular mass organic gelators. The experimental data showed that the solvents and molecular skeletons played a crucial role in regulating the gelation behaviors and fabrication of nanostructures. Suitable single solvents or volume ratios in ethanol/water mixed solvents seemed more favorable for the formation of supramolecular gels due to cooperation of multi-intermolecular weak forces, as shown in Figure 21. Rational assembly modes in organogels were proposed and discussed. In these gels systems, the strong π–π stacking of benzene ring and symmetrical assembly modes in molecular skeletons seemed

to have played an important role in regulating the intermolecular hydrogen bonding and orderly stacking in single/mixed solvents. In addition, the differences of gelation solvents can be mainly attributed to the variable molecular skeletons and assembly modes, which induced different types of intermolecular forces, such as π–πstacking in present cases.

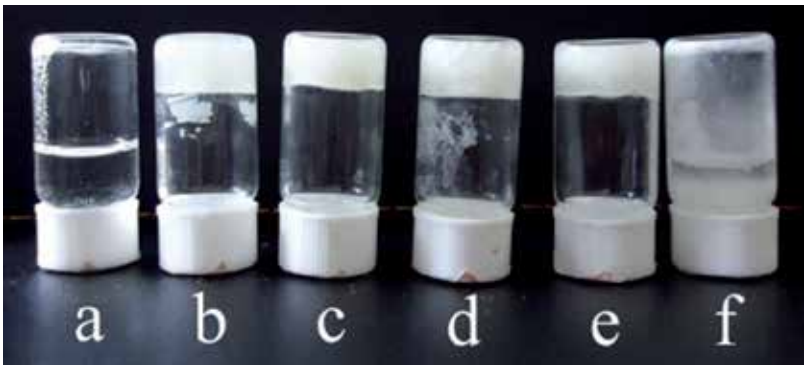

Figure 21. Photographs of GC2 organogels from ethanol/water mixed solvent with the volume ratios of 5:1, 2:1, 1:1, 1:2, 1:5, and 1:10 (a, b, c, d, e, f, respectively).

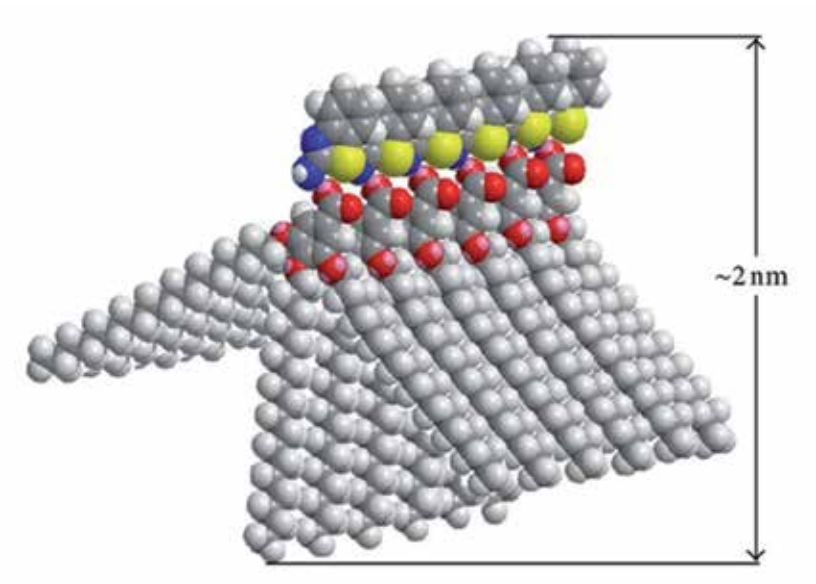

Figure 22. A reasonable self-assembly mode for S-TriC18 organogels.

In our recent study, the gelation behaviors of binary organogels composed of aminobenzimidazole/benzothiazole derivatives and benzoic acid with single/multi-alkyl substituent chain in various organic solvents were designed and investigated [69]. The experimental results

http://dx.doi.org/10.5772/60796

indicated that their gelation behaviors can be regulated by changing the number and length of alkyl substituent chains and benzimidazole/benzothiazole segment. The numbers of alkyl substituent chains linked to benzene rings in these acid derivatives have a profound effect upon the gelation abilities of these studied gelator mixtures. More alkyl chains in molecular skeletons in present gelators are favorable for the gelation of organic solvents. The length of alkyl substituent chains has also played an important role in changing the gelation behaviors and assembly states. Considering the obtained results and the interaction nature of the organized packing in prepared gelator system, a possible self-assembly mechanism of S-TriC18 was proposed and schematically shown in Figure 22. As for xerogels of S-TriC18, due to the S element position in benzothiazole ring, after the intermolecular hydrogen bonding and orderly stacking, the repeating unit with length of about 2 nm was obtained.

In another compared research work, some new benzimidazole/benzothiazole imide derivatives with different alkyl substituent chains were designed and synthesized. The experimental data demonstrated that the substituent alkyl chains and headgroups of benzimidazole/benzothiazole segments in gelators played an important role in the gelation properties of all derivative system in different organic solvents [70]. More alkyl chains in molecular structures in used gelator compounds are favorable for the gelation of used organic solvents. Morphological investigations indicated that the gelator molecules self-assemble into different aggregates domains from wrinkle, lamella, and belt to dot with solvent change. Spectral research suggested that there existed various H-bond between functional imide headgroups and hydrophobic force of substituent alkyl chains in molecular structures and skeletons. The present obtained results may provide new insights into preparing novel gelator systems and soft materials with special functions.

In another research system, we have investigated the preparation of organogels by self-assembly of cationic amphiphile-based GO composites [71]. Their gelation properties in different organic solvents can be changed by regulating functionalized headgroups in amphiphile compounds. Ammonium headgroup of molecular structures in the composites is more favorable for the gelation formation of different organic solvents in comparison with pyridinium headgroup. Headgroup effects of amphiphiles have been demonstrated to be an efficient means to manipulate the self-assembly of GO-based composites. Diversity of intermolecular packing between composites and solvents is presumably responsible for the presence of various nanostructures. Considering the obtained results data and the organized stacking modes in the prepared organogels, some reasonable self-assembly modes in cationic amphiphile–graphene oxide gels are proposed and schematically shown in Figure 23. As for CTAB-GO gel, due to the van der Waals force and flexibility of substituent chains in the molecular structures as well as the strong electrostatic force of ammonium headgroups with oxygen-containing functional groups at GO surface, after combination with GO, organized stacking units are gained in different solvents. As for C16Py-GO and BPy-GO nanocomposites with additional functionalized pyridinium headgroups, the π–π stacking between carbon net in GO plane and pyridine ring suggest being competitive with the electrostatic interaction and van der Waals force. So the self-assembly stacking units in nanostructures between amphiphile compounds and GO in present two systems are not organized sufficiently in comparison with

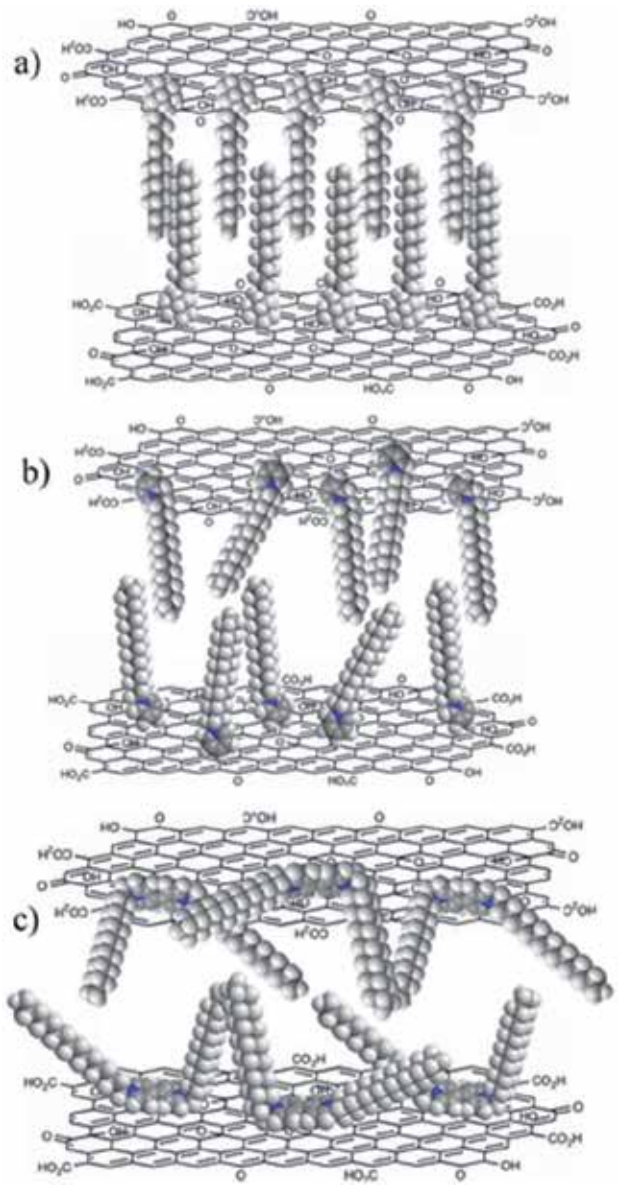

Figure 23. Scheme of different assembly modes in cationic amphiphiles–graphene oxide gels. CTAB-GO (a), C16Py-GO (b), and BPy-GO (c).

that of CTAB-GO gel due to the joint of many kinds of forces. Therefore, the present research work might renew interest and provide useful exploration in the design of self-assembled GO composites and soft matters in the future.

In addition, we have also demonstrated the formation of organogels by self-assembly of cationic gemini amphiphile–GO composites [72]. Their gelation behaviors in various organic

http://dx.doi.org/10.5772/60796

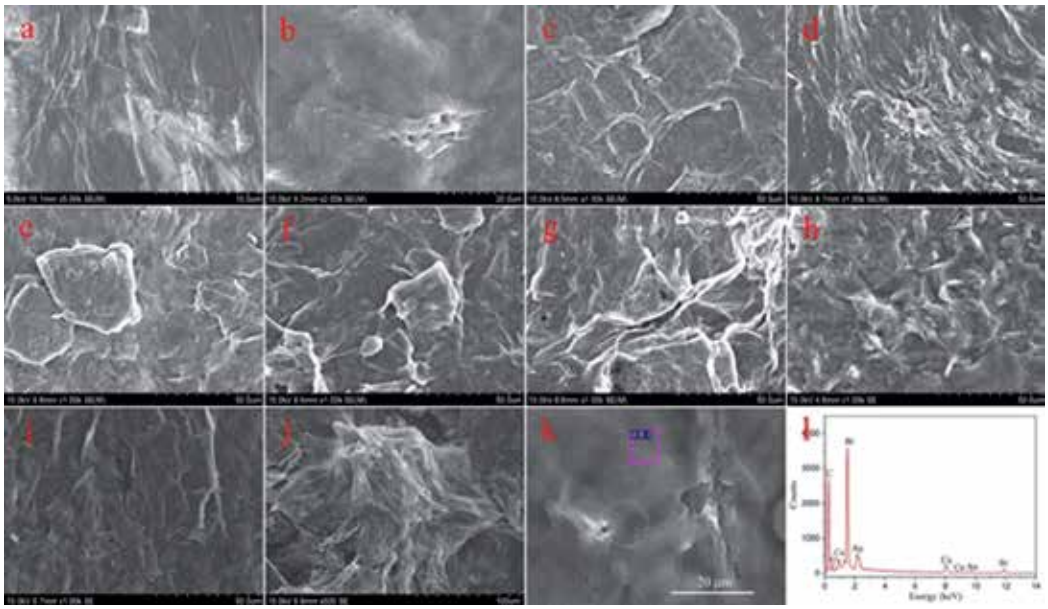

Figure 24. SEM images of xerogels. GO powder (a), C18-6-6/GO gels ((b) DMF), C18-6-12/GO gels ((c) DMF, (d) benzene, (e) toluene, (f) 1,4-dioxane, and (g) THF), and C18-6-18/GO gels ((h) cyclohexanone, (i) THF, and (j) pyridine). Typical EDXS (l) of xerogels originate from C18-6-6/GO gels in DMF (k). The Cu and Au peaks originate from the substrate of copper foil and the coated gold nanoparticles.

solvents can be regulated by changing symmetry in skeletons of amphiphiles. The substituent groups or symmetry in molecular skeletons can regulate the stacking and self-assembled nanostructures upon distinct intermolecular forces. Longer alkyl chains and symmetric structures in molecular skeletons helped to increase hydrophobic force and flexibility in self-assembly process. Diversity of intermolecular packing between composites and solvents is presumably responsible for the presence of various nanostructures, as shown in Figure 24. It is clearly investigated that the nanostructures of the as-formed xerogels of all composites in various solvents are significantly different from each other, and the morphologies and nanostructures of the self-assembled aggregates change from wrinkle and lamella to belt with the change of solvents. The difference of morphologies can be mainly attributed to the different stacking mechanisms and self-assembly modes upon interactive forces between gelators and solvent molecules. A possible mechanism for symmetry effects on self-assembly and as-prepared nanostructures is proposed. It is believed that the present amphiphile-GO self-assembled system will provide an alternative exploration for the design of new GO composite nanomaterials and soft matters.

5. Conclusion and perspectives

We are working on the design, preparation, and self-assembly of functionalized nanocomposites and nanomaterials. In this chapter, various kinds of nanocomposites including gold

nanoparticles, inorganic–organic hybrid composites, graphene oxide nanocomposites, and supramolecular gels via functionalized imide amphiphiles/binary mixtures have all been investigated and analyzed. The above work may give the potential perspective for the design and fabrication of nanomaterials and composites. In closing, new nanocomposites and nanomaterials are emerging as sensitive study platforms based on unique optical and electrical properties. In addition, supramolecular self-assembly is a key physical chemistry subject due to its close relationship to many fundamental and application scientific questions like catalysis, chirality, electron and energy transfer, single molecule science, and organic electronics. The results mentioned here only provide a cursory browse of some progress. Future research on preparation of nanocomposites and nanomaterials will depend on the less-expensive processes in order to produce low-cost nanomaterials and devices. The development in this area has been fascinating. It can be predicted that as the growth of understandings of the rules in the nanoscale, our dream to prepare functionalized nanocomposites and nanomaterials with self-assembly and organized nanostructures could be realized in future.

Acknowledgements

The authors would like to extend their thanks to the National Natural Science Foundation of China (Nos. 21473153, 21207112, and 51402253); the Natural Science Foundation of Hebei Province (No. B2013203108); the Science Foundation for the Excellent Youth Scholars from Universities and Colleges of Hebei Province (Nos. Y2011113 and YQ2013026); the Support Program for the Top Young Talents of Hebei Province; and Open Foundation of National Key Laboratory of Biochemical Engineering (Institute of Process Engineering, Chinese Academy of Sciences) for providing funds for this research.

Author details

Tifeng Jiao[1,2*], Jie Hu[1], Qingrui Zhang[1] and Yong Xiao[3]

*Address all correspondence to: tfjiao@ysu.edu.cn

1 Hebei Key Laboratory of Applied Chemistry, School of Environmental and Chemical Engineering, Yanshan University, Qinhuangdao, P. R. China

2 National Key Laboratory of Biochemical Engineering, Institute of Process Engineering, Chinese Academy of Sciences, Beijing, P. R. China

3 Qinhuangdao Environmental Protection Science Research Institute, Qinhuangdao, P. R. China

http://dx.doi.org/10.5772/60796

References

[1] Vashist SK, Luong JHT. Recent advances in electrochemical biosensing schemes using graphene and graphene-based nanocomposites. Carbon 2015;84:519–50.

[2] Hu K, Kulkarni DD, Choi I, Tsukruk VV. Graphene-polymer nanocomposites for structural and functional applications. Prog Polymer Sci 2014;39(11):1934–72.

[3] Mutiso RM, Winey KI. Electrical properties of polymer nanocomposites containing rod-like nanofillers. Prog Polymer Sci 2015;40:63–84.

[4] Zhu S, Segura T. Hydrogel-based nanocomposites of therapeutic proteins for tissue repair. Curr Opin Chem Eng 2014;4:128–36.

[5] Campbell TA, Ivanova OS. 3D printing of multifunctional nanocomposites. Nano Today 2013;8(2):119–20.

[6] Lee YS. Self-Assembly and Nanotechnology Systems: Design, Characterization, and Applications. New Jersey: John Wiley & Sons, Inc.; 2011.

[7] Pelesko JA. Self Assembly: The Science of Things That Put Themselves Together. London: Chapman and Hall/CRC Press; 2007.

[8] Jiao T, Wang S, Zhou J. Molecular design and supramolecular assemblies of novel amphiphiles with special molecular structures in organized molecular films. In: Rahman M. (ed.) Nanomaterials. Rijeka: InTech; 2011, pp.315–46.

[9] Ghosh SK, Pal T. Interparticle coupling effect on the surface plasmon resonance of gold nanoparticles: from theory to applications. Chem Rev 2007;107:4797–862.

[10] Katz E, Willner I. Integrated nanoparticle-biomolecule hybrid systems: synthesis, properties, and applications. Angewandte Chemie International Edition 2004;43(45): 6042–108.

[11] Daniel MC, Astruc D. Gold nanoparticles: assembly, supramolecular chemistry, quantum-size-related properties, and applications toward biology, catalysis, and nanotechnology. Chem Rev 2004;104:293–346.

[12] Liao J, Bernard L, Langer M, Schoenberger C, Calame M. Reversible formation of molecular junctions in 2D nanoparticle arrays. Adv Mater 2006;18(18):2444–7.

[13] Klajn R, Bishop KJM, Grzybowski BA. Light-controlled self-assembly of reversible and irreversible nanoparticle suprastructures. Proc Nat Acad Sci USA 2007;104:10305–9.

[14] Koplin E, Niemeyer CM, Simon U. Formation of electrically conducting DNA-assembled gold nanoparticle monolayers. J Mater Chem 2006;16:1338–44.

[15] Meister A, Drescher S, Mey I, Wahab M, Graf G, Garamus VM, Hause G, Mo1gel HJ, Janshoff A, Dobner B, Blume A. Helical nanofibers of self-assembled bipolar phospholipids as template for gold nanoparticles. J Phys Chem B 2008;112:4506–11.

[16] Jadzinsky PD, Calero G, Ackerson CJ, Bushnell DA, Kornberg RD. Structure of a thiol monolayer-protected gold nanoparticle at 1.1 Å resolution. Science 2007;318:430–3.

[17] Wen Y, Jiang X, Yin G, Yin J. Multi-responsive amphiphilic gold nanoparticles (AuNPs) protected by poly(ether amine) (PEA). Chem Commun 2009;43:6595–7.

[18] Song WJ, Du JZ, Sun TM, Zhang PZ, Wang J. Gold nanoparticles capped with polyethyleneimine for enhanced siRNA delivery. Small 2010;6:239–46.

[19] Ko S, Park TJ, Kim HS, Kim JH, Cho YJ. Directed self-assembly of gold binding polypeptide-protein: a fusion proteins for development of gold nanoparticle-based SPR immunosensors. Biosens Bioelectron 2009;24:2592–7.

[20] George J, Thomas KG. Surface plasmon coupled circular dichroism of Au nanoparticles on peptide nanotubes. J Am Chem Soc 2010;132:2502–3.

[21] Cho EC, Au L, Zhang Q, Xia Y. The effects of size, shape, and surface functional group of gold nanostructures on their adsorption and internalization by cells. Small 2010;6:517–22.

[22] Jiao T, Wang Y, Guo W, Zhang Q, Yan X, Chen J, Wang L, Xie D, Gao F. Synthesis and photocatalytic property of gold nanoparticles by using a series of bolaform Schiff base amphiphiles. Mater Res Bull 2012;47(12):4203–9.

[23] Jiao T, Wang Y, Zhang Q, Yan X, Chen J, Zhou J, Gao F. Preparation and photocatalytic property of gold nanoparticles by using two bolaform cholesteryl imide derivatives. J Dispers Sci Technol 2013;34(12):1675–82.

[24] Huang H, Sun G, Hu J, Jiao T. Single-step synthesis of $LaMnO_3$/MWCNT nanocomposites and their photocatalytic activities. Nanomater Nanotechnol 2014;4:27.

[25] Wang S, Lv F, Jiao T, Ao J, Zhang X, Jin F. A novel porous carrier found in nature for nanocomposite materials preparation: a case study of Artemia Egg shell-supported TiO_2 for formaldehyde removal. J Nanomater 2014;2014:963012.

[26] Zhang Q, Du Q, Hua M, Jiao T, Gao F, Pan B. Sorption enhancement of lead ions from water by surface charged polystyrene-supported nano-zirconium oxide composites. Environ Sci Technol 2013;47(12):6536–44.

[27] Zhang Q, Du Q, Jiao T, Pan B, Zhang Z, Sun Q, Wang S, Wang T, Gao F. Selective removal of phosphate in waters using a novel of cation adsorbent: Zirconium phosphate (ZrP) behavior and mechanism. Chem Eng J 2013;221:315–21.

[28] Zhang Q, Du Q, Jiao T, Zhang Z, Wang S, Sun Q, Gao F. Rationally designed porous polystyrene encapsulated zirconium phosphate nanocomposite for highly efficient fluoride uptake in waters. Scientific Rep 2013;3:2551.

[29] Xing R, Jiao T, Feng L, Zhang Q, Zou Q, Yan X, Zhou J, Gao F. Photothermally-induced molecular self-assembly of macroscopic peptide-inorganic hybrid films. Sci Adv Mater 2015;7:in press.

[30] Liang D, Cui C, Hu H, Wang Y, Xu S, Ying B, Li P, Lu B, Shen H. One-step hydrothermal synthesis of anatase TiO_2/reduced graphene oxide nanocomposites with enhanced photocatalytic activity. J Alloys Compd 2014;582:236–40.

[31] Ullah K, Zhu L, Meng ZD, Ye S, Sun Q, Oh WC. A facile and fast synthesis of novel composite Pt-graphene/TiO_2 with enhanced photocatalytic activity under UV/Visible light. Chem Eng J 2013;231:76–83.

[32] Bai XJ, Wang L, Zhu YF. Visible photocatalytic activity enhancement of $ZnWO_4$ by graphene hybridization. ACS Catal 2012;2:2769–78.

[33] Sun L, Shao R, Tang LQ, Chen ZD. Synthesis of $ZnFe_2O_4$/ZnO nanocomposites immobilized on graphene with enhanced photocatalytic activity under solar light irradiation. J Alloys Compd 2013;564:55–62.

[34] Xu JJ, Ao YH, Chen MD. A simple method for the preparation of Bi_2WO_6-reduced graphene oxide with enhanced photocatalytic activity under visible light irradiation. Mater Lett 2013;92:126–8.

[35] Li T, Shen JF, Li N, Ye MX. Hydrothermal preparation, characterization and enhanced properties of reduced graphene-$BiFeO_3$ nanocomposite. Mater Lett 2013;91:42–4.

[36] Lv T, Pan LK, Liu XJ, Lu T, Zhu G, Sun Z. Enhanced photocatalytic degradation of methylene blue by ZnO-reduced graphene oxide composite synthesized via microwave-assisted reaction. J Alloys Compd 2011;509:10086–91.

[37] Jiang LX, Li KX, Yan LS, Dai YH, Huang ZM. Preparation of Ag(Au)/graphene-TiO_2 composite photocatalysts and their catalytic performance under simulated sunlight irradiation. Chinese J Catal 2012;33(12):1974–81.

[38] Zhang DF, Pu XP, Ding GQ, Shao X, Gao YY, Liu JX, Gao MC, Li Y. Two-phase hydrothermal synthesis of TiO_2-graphene hybrids with improved photocatalytic activity. J Alloys Compd 2013;572:199–204.

[39] Hu J, Ma J, Wang L, Huang H. Synthesis and photocatalytic properties of $LaMnO_3$-graphene nanocomposites. J Alloys Compd 2014;583:539–45.

[40] Hu J, Ma J, Wang L, Huang H. Preparation of $La_{1-x}Sr_xMnO_3$ /graphene thin films and their photocatalytic activity. Mater Sci Eng B 2014;180:46–53.

[41] Hu J, Ma J, Wang L, Huang H, Ma L. Preparation, characterization and photocatalytic activity of Co-doped $LaMnO_3$/graphene composites, Powder Technol 2014;254:556–62.

[42] Hu J, Wang L, Ma J, Huang H. Study on the preparation and photocatalytic performance of the $LaNiO_3$/graphene composite film. Rare Metal Mater Eng 2014;43(7):1736–41.

[43] Hu J, Wang L, Shi L, Huang H. Preparation of $La_{1-x}Ca_xMnO_3$ perovskite-graphene composites as oxygen reduction reaction electrocatalyst in alkaline medium. J Power Sources 2014;269:144–51.

[44] Hu J, Men J, Ma J, Huang H. Preparation of $LaMnO_3$/graphene thin films and their photocatalytic activity. J Rare Earths 2014;32(12):1127–35.

[45] Basrur VR, Guo J, Wang C, Raghavan SR. Synergistic gelation of silica nanoparticles and a sorbitol-based molecular gelator to yield highly-conductive free-standing gel electrolytes. ACS Appl Mater Interfaces 2013;5:262–7.

[46] van der Laan S, Feringa BL, Kellogg RM, van Esch J. Remarkable polymorphism in gels of new azobenzene bis-urea gelators. Langmuir 2002;18:7136–40.

[47] Oh H, Jung BM, Lee HP, Chang JY. Dispersion of single walled carbon nanotubes in organogels by incorporation into organogel fibers. J Colloid Interface Sci 2010;352:121–7.

[48] Delbecq F, Tsujimoto K, Ogue Y, Endo H, Kawai T. N-stearoyl amino acid derivatives: potent biomimetic hydro/organogelators as templates for preparation of gold nanoparticles. J Colloid Interface Sci 2013;390:17–24.

[49] George SJ, Ajayaghosh A. Self-assembled nanotapes of oligo (p-phenylene vinylene)s: sol-gel-controlled optical properties in fluorescent π-electronic gels. Chemistry-A European Journal 2005; 11: 3217-3227.

[50] Kuroiwa K, Shibata T, Takada A, Nemoto N, Kimizuka N. Heat-set gel-like networks of lipophilic Co(II) triazole complexes in organic media and their thermochromic structural transitions. Journal of the American Chemical Society 2004; 126: 2016-2021.

[51] Ajayaghosh A, Chithra P, Varghese R. Self-assembly of tripodal squaraines: cation-assisted expression of molecular chirality and change from spherical to helical morphology. Angewandte Chemie International Edition 2007; 46: 230-233.

[52] Xin F, Zhang H, Hao B, Sun T, Kong L, Li Y, Hou Y, Li S, Zhang Y, Hao A. Controllable transformation from sensitive and reversible heat-set organogel to stable gel induced by sodium acetate. Colloids and Surfaces A: Physicochem Eng Aspects 2012;410:18–22.

[53] Iwanaga K, Sumizawa T, Miyazaki M, Kakemi M. Characterization of organogel as a novel oral controlled release formulation for lipophilic compounds. Int J Pharmaceut 2010;388:123–8.

[54] Lofman M, Koivukorpi J, Noponen V, Salo H, Sievanen E. Bile acid alkylamide derivatives as low molecular weight organogelators: systematic gelation studies and qualitative structural analysis of the systems. J Colloid Interface Sci 2011;360:633–44.

[55] Bastiat G, Plourde F, Motulsky A, Furtos A, Dumont Y, Quirion R, Fuhrmann G, Leroux JC. Tyrosine-based rivastigmine-loaded organogels in the treatment of Alzheimer's disease. Biomaterials 2010;31:6031–8.

[56] Tao ZG, Zhao X, Jiang XK, Li ZT. A hexaazatriphenylene-based organogel that responds to silver(I) with high selectivity under aqueous condition. Tetrahedron Lett 2012;53:1840–2.

[57] Miyamoto K, Jintoku H, Sawada T, Takafuji M, Sagawa T, Ihara H. Informative secondary chiroptics in binary molecular organogel systems for donor-acceptor energy transfer. Tetrahedron Lett 2011;52:4030–5.

[58] Jiao T, Wang Y, Gao FQ, Zhou J, Gao FM. Photoresponsive organogel and organized nanostructures of cholesterol imide derivatives with azobenzene substituent groups. Prog Nat Sci: Mater Int 2012;22(1):64–70.

[59] Jiao T, Gao FQ, Wang Y, Zhou J, Gao FM, Luo X. Supramolecular gel and nanostructures of bolaform and trigonal cholesteryl derivatives with different aromatic spacers. Curr Nanosci 2012;8(1):111–6.

[60] Jiao T, Wang R, Zhang Q, Yan X, Zhou J, Gao F. Nanostructures and substituent alkyl chains effect on assembly of organogels based on some glutamic acid diethyl ester imide derivatives. Curr Nanosci 2013;9(4):536–42.

[61] Jiao T, Wang Y, Zhang Q, Zhou J, Gao F. Regulation of substituent groups on morphologies and self-assembly of organogels based on some azobenzene imide derivatives. Nanoscale Res Lett 2013;8:160.

[62] Jiao T, Huang Q, Zhang Q, Xiao D, Zhou J, Gao F. Self-assembly of organogels via new luminol imide derivatives: diverse nanostructures and substituent chain effect. Nanoscale Res Lett 2013;8:278.

[63] Jiao T, Gao F, Zhang Q, Zhou J, Gao F. Spacer effect on nanostructures and self-assembly in organogels via some bolaform cholesteryl imide derivatives with different spacers. Nanoscale Res Lett 2013;8:406.

[64] Jiao TF, Gao FQ, Shen XH, Zhang QR, Zhang XF, Zhou JX, Gao FM. Self-assembly and nanostructures in organogels based on a bolaform cholesteryl imide compound with conjugated aromatic spacer. Materials 2013;6(12):5893–906.

[65] Hu Y, Li Q, Hong W, Jiao T, Xing G, Jiang Q. Characterization of binary organogels based on some azobenzene compounds and alkyloxybenzoic acids with different chain lengths. J Spectrosc 2014;2014:970827.

[66] Guo H, Jiao T, Shen X, Zhang Q, Li A, Gao F. Preparation and characterization of binary organogels via some azobenzene amino derivatives and different fatty acids: self-assembly and nanostructures. J Spectrosc 2014;2014:758765.

[67] Jiao T, Xing R, Shen X, Zhang Q, Zhou J, Gao F. Investigation of orderly nanostructures and assembly modes of binary organogels via glutamic acid amino derivative and different fatty acids. Integr Ferroelect: Int J 2014;151(1):31–41.

[68] Guo H, Jiao T, Shen X, Zhang Q, Li A, Zhou J, Gao F. Binary organogels based on glutamic acid derivatives and different acids: solvent effect and molecular skeletons on self-assembly and nanostructures. Colloids Surfaces A: Physicochem Eng Aspects 2014;447:88–96.

[69] Jiao T, Ma K, Shen X, Zhang Q, Li X, Zhou J, Gao F. Self-assembly and soft material preparation of binary organogels via aminobenzimidazole/benzothiazole and acids with different alkyl substituent chains. J Nanomater 2013;2013:762732.

[70] Shen X, Jiao T, Zhang Q, Guo H, Lv Y, Zhou J, Gao F. Nanostructures and self-assembly of organogels via benzimidazole/benzothiazole imide derivatives with different alkyl substituent chains. J Nanomater 2013;2013:409087.

[71] Jiao T, Wang Y, Zhang Q, Yan X, Zhao X, Zhou J, Gao F. Self-assembly and headgroup effect in nanostructured organogels via cationic amphiphile-graphene oxide composites. PLoS ONE 2014;9(7):e101620.

[72] Jiao T, Wang Y, Zhang Q, Yan X, Zhao X, Huo Q, Zhou J, Gao F. Organogels via gemini amphiphile-graphene oxide composites: self-assembly and symmetry effect. Sci Adv Mater 2015;7:in press.

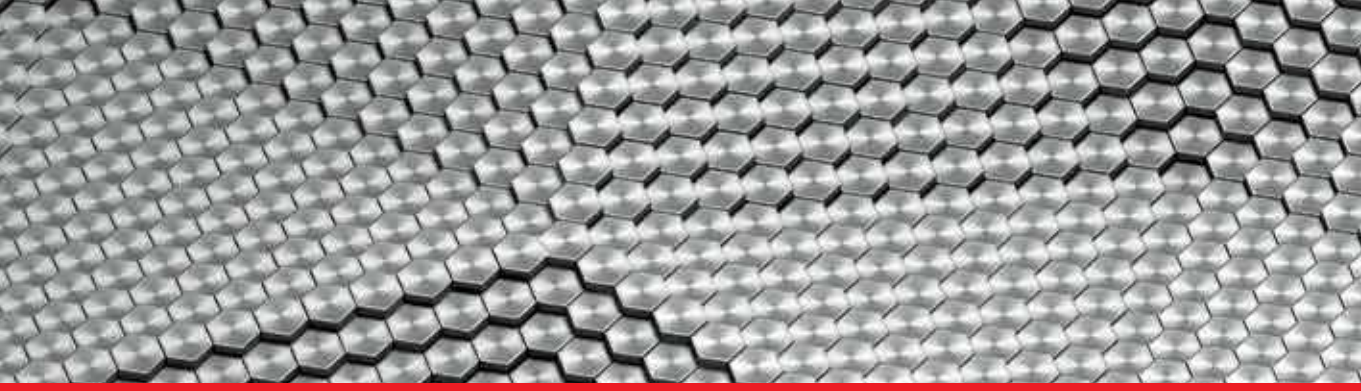

Edited by Sonia Soloneski and Marcelo L. Larramendy

This edited book, Nanomaterials - Toxicity and Risk Assessment, is a collection of current research and information on numerous advances on the toxicity and hazardous effects of nanomaterials, including theoretical and experimental approaches as well as nanotechnology applications in the field of medicine, pharmacology, and the manufacture of nanoscale materials. Based on the large number of nanomaterial applications, a careful understanding of the associated systemic and local toxicity is critically required.

ISBN 978-953-51-4219-5

Photo by whitehoune / iStock

IntechOpen